1-1-2016

Abelian Gauge Symmetries in F-Theory and Dual Theories

Peng Song
University of Pennsylvania, songpengphysics@qq.com

Abelian Gauge Symmetries in F-Theory and Dual Theories

Abstract
In this dissertation, we focus on important physical and mathematical aspects, especially abelian gauge symmetries, of F-theory compactifications and its dual formulations within type IIB and heterotic string theory.

F-theory is a non-perturbative formulation of type IIB string theory which enjoys important dualities with other string theories such as M-theory and E8 × E8 heterotic string theory. One of the main strengths of F-theory is its geometrization of many physical problems in the dual string theories. In particular, its study requires a lot of mathematical tools such as advanced techniques in algebraic geometry. Thus, it has also received a lot of interests among mathematicians, and is a vivid area of research within both the physics and the mathematics community.

Although F-theory has been a long-standing theory, abelian gauge symmetry in Ftheory has been rarely studied, until recently. Within the mathematics community, in 2009, Grassi and Perduca first discovered the possibility of constructing elliptically fibered varieties with non-trivial toric Mordell-Weil group. In the physics community, in 2012, Morrison and Park first made a major advancement by constructing general F-theory compactifications with $U(1)$ abelian gauge symmetry. They found that in such cases, the ellipticallyfibered Calabi-Yau manifold that F-theory needs to be compactified on has its fiber being a generic elliptic curve in the blow-up of the weighted projective space $P(1;1;2)$ at one point.

Subsequent developments have been made by Cveti˘c, Klevers and Piragua extended the works of Morrison and Park and constructed general F-theory compactifications with $U(1)$ $U(1)$ abelian gauge symmetry. They found that in the $U(1) \times U(1)$ abelian gauge symmetry case, the elliptically-fibered Calabi-Yau manifold that F-theory needs to be compactified on has its fiber being a generic elliptic curve in the del Pezzo surface dP2. In chapter 2 of this dissertation, I bring this a step further by constructing general F-theory compactifications with $U(1) \times U(1) \times U(1)$ abelian gauge symmetry. I showed that in the case with three $U(1)$ factors, the general elliptic fiber is a complete intersection of two quadrics in P3, and

the general elliptic fiber in the fully resolved elliptic fibration is embedded as the generic Calabi-Yau complete intersection into Bl3P3, the blow-up of P3 at three generic points. This eventually leads to our analysis of representations of massless matter at codimension two singularities of these compactifications. Interestingly, we obtained a tri-fundamental representation which is unexpected from perturbative Type II compactifications, further illustrating the power of F-theory.

In chapter 1 of this dissertation, I proved finiteness of a region of the string landscape in Type IIB compactifications. String compactifications give rise to a collection of effective low energy theories, known as the string landscape. However, it is not known whether the number of physical theories we can derive from the string landscape is finite. The vastness of the string landscape also poses a serious challenge to attempts of studying it. A breakthrough was made by Douglas and Taylor in 2007 when they studied the landscape of intersecting brane models in Type IIA compactifications on a particular Z2× Z2 orientifold. They found that two consistency conditions, namely the D6-brane tadpole cancellation condition, and the conditions on D6-branes that were required for N = 1 supersymmetry in four dimensions, only permitted a finite number of D6-brane configurations. These finite number of allowed D6-brane configurations thus result in only a finite number of gauge sectors in a 4D supergravity theory, allowing them to be studied explicitly. Douglas and Taylor also believed that the phenomenon of using tadpole cancellation and supersymmetry consistency conditions to restrict the possible number of allowed configurations to a finite one is not a mere coincidence unique to their construction; they conjectured that this phenomenon also holds for theories with magnetised D9- or D5-branes compactified on elliptically fibered Calabi-Yau threefolds. Indeed, this was what my collaborators and I also felt. To this end, I showed, using a mathematical proof, that their conjecture is indeed true for elliptically fibered Calabi-Yau threefolds p X B whose base B satisfy a few easily-checked conditions (summarized in chapter 1 of this dissertation). In particular, these conditions are satisfied by, although not limited to, the almost Fano twofold bases B given by the toric varieties associated to all 16 reflexive two-dimensional polytopes and

the del Pezzo surfaces dPn for n = 0;1; :::; 8. This list, in particular, also includes the Hirzebruch surfaces F0 = P1 ×P1;F1 = dP1;F2. My proof also allowed us to derive the explicit and computable bounds on all flux quanta and on the number of D5-branes. These bounds only depends on the topology of the base B and are independent on the continuous moduli of the compactification, in particular the Kahler moduli, as long as the supergravity approximation is valid. Physically, my proof showed that these compactifications only give rise to a finite number of four-dimensional N = 1 supergravity theories, and that these theories only have finitely many gauge sectors with finitely many chiral spectra. Such finiteness properties are not observed in generic quantum field theories, further fortifying superstring theory as a more promising theory.

In chapter 3 of this dissertation, I study abelian gauge symmetries in the duality between F-theory and E8 × E8 heterotic string theory. It is conjectured that F-theory, when compactified on an elliptic K3-fibered $(n + 1)$-dimensional Calabi-Yau manifold X B, and heterotic string theory when compactified on an elliptically fibered n-dimensional Calabi-Yau manifold Z B with the same base B, are dual to each other. Thus under such duality, in particular, if the F-theory compactification admits abelian gauge symmetries, the dual heterotic string theory must admit the same abelian gauge symmetry as well. However, how abelian gauge symmetries can arise in the dual heterotic string theory has never been studied. The main goal of this chapter is to study exactly this. We start with F-theory compactifications with abelian gauge symmetry. With the help of a mathematical lemma as well as a computer code that I came up with, I was able to construct a rich list of specialized examples with specific abelian and nonabelian gauge groups on the F-theory side. The computer code also directly computes spectral cover data for each example constructed, allowing us to further analyze how abelian gauge symmetries arise on heterotic side. Eventually, we found that in general, there are three ways in which $U(1)$-s can arise on the heterotic side: the case where the heterotic theory admits vector bundles with $S(U(1) \times U(m))$ structure group, the case where the heterotic theory admits vector bundles with $SU(m)\times Zn$ structure group, as well as the case where the heterotic theory

admits vector bundles with structure groups having a centralizer in E8 which contains a U(1) factor. Another important achievement was my discovery of the non-commutativity of the semi-stable degeneration map which splits a K3 surface into two half K3 surfaces, and the map to Weierstrass form, which was not previously known in the literature.

Degree Type
Dissertation

Degree Name
Doctor of Philosophy (PhD)

Graduate Group
Physics & Astronomy

First Advisor
Mirjam Cvetic

Keywords
abelian gauge theory, algebraic geometry, F-theory, string compactification, string landscape

Subject Categories
Mathematics | Physics

ABELIAN GAUGE SYMMETRIES IN F-THEORY AND DUAL THEORIES

Peng Song

A DISSERTATION

in

Physics and Astronomy

Presented to the Faculties of the University of Pennsylvania

in

Partial Fulfillment of the Requirements for the

Degree of Doctor of Philosophy

2016

_____

Mirjam Cvetič, Professor of Physics and Astronomy
Supervisor of Dissertation

_____

Philip Nelson, Professor of Physics and Astronomy
Graduate Group Chairperson

Dissertation Committee

Mirjam Cvetič, Professor of Physics and Astronomy

Antonella Grassi, Professor of Mathematics

Elliot Lipeles, Professor of Physics and Astronomy

Philip Nelson, Professor of Physics and Astronomy

Evelyn Thomson, Professor of Physics and Astronomy

ABELIAN GAUGE SYMMETRIES IN F-THEORY

AND DUAL THEORIES

ACKNOWLEDGMENTS

This dissertation would not have been possible without the support of my family, my advisor, my research group and my good friends.

First and foremost, I want to thank my family for being so supportive and understanding. It is their morale support that fuelled me to move on throughout these years.

Next, I would like to thank my advisor Mirjam Cvetič, for her constant guidance in my pursuit of physics and mathematics. Her keen insights and intuitions have always shed light on the obscurities I encountered during my research works. There were many occasions in which Professor Cvetič have successfully solved problems using innovative and creative approaches that no one else in my group thought of, creating important breakthroughs. I am extremely grateful to the great mathematician Ron Donagi, from whom I learnt a great deal of mathematics and physics. His deep understanding about physics from a mathematical point of view had always been a great help to both me and my entire research group. I have attended a lot of his classes, in which he masterfully interwove physics and mathematics seamlessly into a single art piece. I am extremely grateful to professor Donagi's teachings, from which I learnt physics from a rigorous mathematical viewpoint, as well as his patience with my naive questions. I am also much indebted to the great mathematician Antonella Grassi, with whom I have the honor to collaborate with. Her deep knowledge in algebraic geometry are crucial to solve many key problems in my research works. She is willing to patiently and skillfully simplify her mathematical language to a level that even a physics student could understand, and I benefited tremendously by attending her classes. Throughout my years of research, I have always reviewed materials from Professor Grassi's classes over and over again, which are always helpful in one way or another.

I wish to express my gratitude to my collaborators, James Halverson, Denis Klevers, Hernan Piragua, and Maximilian Poretschkin for all the enjoyable times when writing papers together. I would also like to thank all the professors in the High Energy group,

especially Burt Ovrut and Mark Trodden, for their teachings and guidance, from whom I learnt a great deal of physics. I am also thankful to my friends Steven Gilhoon, Hirnan Piragua, Zain Saleem, and James Stokes for all their help and support in all areas, academic and non-academic alike, over all these years.

Of course, last but not least, I would also like to thank Millicent Minnick for solving all my administrative related problems efficiently and masterfully.

ABSTRACT

ABELIAN GAUGE SYMMETRIES IN F-THEORY

AND DUAL THEORIES

Peng Song

Mirjam Cvetič

In this dissertation, we focus on important physical and mathematical aspects, especially abelian gauge symmetries, of F-theory compactifications and its dual formulations within type IIB and heterotic string theory.

F-theory is a non-perturbative formulation of type IIB string theory which enjoys important dualities with other string theories such as M-theory and $E_8 \times E_8$ heterotic string theory. One of the main strengths of F-theory is its geometrization of many physical problems in the dual string theories. In particular, its study requires a lot of mathematical tools such as advanced techniques in algebraic geometry. Thus, it has also received a lot of interests among mathematicians, and is a vivid area of research within both the physics and the mathematics community.

Although F-theory has been a long-standing theory, abelian gauge symmetry in F-theory has been rarely studied, until recently. Within the mathematics community, in 2009, Grassi and Perduca first discovered the possibility of constructing elliptically fibered varieties with non-trivial toric Mordell-Weil group. In the physics community, in 2012, Morrison and Park first made a major advancement by constructing general F-theory compactifications with U(1) abelian gauge symmetry. They found that in such cases, the elliptically-fibered Calabi-Yau manifold that F-theory needs to be compactified on has its fiber being a generic elliptic curve in the blow-up of the weighted projective space $\mathbb{P}^{(1,1,2)}$ at one point. Subsequent developments have been made by Cvetič, Klevers and Piragua extended the

works of Morrison and Park and constructed general F-theory compactifications with U(1) $\times$ U(1) abelian gauge symmetry. They found that in the U(1) $\times$ U(1) abelian gauge symmetry case, the elliptically-fibered Calabi-Yau manifold that F-theory needs to be compactified on has its fiber being a generic elliptic curve in the del Pezzo surface dP_2. In chapter 2 of this dissertation, I bring this a step further by constructing general F-theory compactifications with U(1) $\times$ U(1) $\times$ U(1) abelian gauge symmetry. I showed that in the case with three U(1) factors, the general elliptic fiber is a complete intersection of two quadrics in $\mathbb{P}^3$, and the general elliptic fiber in the fully resolved elliptic fibration is embedded as the generic Calabi-Yau complete intersection into $\mathrm{Bl}_3\mathbb{P}^3$, the blow-up of $\mathbb{P}^3$ at three generic points. This eventually leads to our analysis of representations of massless matter at codimension two singularities of these compactifications. Interestingly, we obtained a tri-fundamental representation which is unexpected from perturbative Type II compactifications, further illustrating the power of F-theory.

In chapter 1 of this dissertation, I proved finiteness of a region of the string landscape in Type IIB compactifications. String compactifications give rise to a collection of effective low energy theories, known as the string landscape. However, it is not known whether the number of physical theories we can derive from the string landscape is finite. The vastness of the string landscape also poses a serious challenge to attempts of studying it. A breakthrough was made by Douglas and Taylor in 2007 when they studied the landscape of intersecting brane models in Type IIA compactifications on a particular $\mathbb{Z}_2 \times \mathbb{Z}_2$ orientifold. They found that two consistency conditions, namely the D6-brane tadpole cancellation condition, and the conditions on D6-branes that were required for $N = 1$ supersymmetry in four dimensions, only permitted a finite number of D6-brane configurations. These finite number of allowed D6-brane configurations thus result in only a finite number of gauge sectors in a 4D supergravity theory, allowing them to be studied explicitly. Douglas and Taylor also believed that the phenomenon of using tadpole cancellation and supersymme-

try consistency conditions to restrict the possible number of allowed configurations to a finite one is not a mere coincidence unique to their construction; they conjectured that this phenomenon also holds for theories with magnetised D9- or D5-branes compactified on elliptically fibered Calabi-Yau threefolds. Indeed, this was what my collaborators and I also felt. To this end, I showed, using a mathematical proof, that their conjecture is indeed true for elliptically fibered Calabi-Yau threefolds $\pi : X \to B$ whose base B satisfy a few easily-checked conditions (summarized in chapter 1 of this dissertation). In particular, these conditions are satisfied by, although not limited to, the almost Fano twofold bases B given by the toric varieties associated to all 16 reflexive two-dimensional polytopes and the del Pezzo surfaces dP_n for $n = 0, 1, ..., 8$. This list, in particular, also includes the Hirzebruch surfaces $\mathbb{F}_0 = \mathbb{P}^1 \times \mathbb{P}^1, \mathbb{F}_1 = dP_1, \mathbb{F}_2$. My proof also allowed us to derive the explicit and computable bounds on all flux quanta and on the number of D5-branes. These bounds only depends on the topology of the base B and are independent on the continuous moduli of the compactification, in particular the Kähler moduli, as long as the supergravity approximation is valid. Physically, my proof showed that these compactifications only give rise to a finite number of four-dimensional $N = 1$ supergravity theories, and that these theories only have finitely many gauge sectors with finitely many chiral spectra. Such finiteness properties are not observed in generic quantum field theories, further fortifying superstring theory as a more promising theory.

In chapter 3 of this dissertation, I study abelian gauge symmetries in the duality between F-theory and $\mathrm{E}_8 \times \mathrm{E}_8$ heterotic string theory. It is conjectured that F-theory, when compactified on an elliptic K3-fibered $(n+1)$-dimensional Calabi-Yau manifold $X \to B$, and heterotic string theory when compactified on an elliptically fibered n-dimensional Calabi-Yau manifold $Z \to B$ with the same base B, are dual to each other. Thus under such duality, in particular, if the F-theory compactification admits abelian gauge symmetries, the dual heterotic string theory must admit the same abelian gauge symmetry as well.

However, how abelian gauge symmetries can arise in the dual heterotic string theory has never been studied. The main goal of this chapter is to study exactly this. We start with F-theory compactifications with abelian gauge symmetry. With the help of a mathematical lemma as well as a computer code that I came up with, I was able to construct a rich list of specialized examples with specific abelian and nonabelian gauge groups on the F-theory side. The computer code also directly computes spectral cover data for each example constructed, allowing us to further analyze how abelian gauge symmetries arise on heterotic side. Eventually, we found that in general, there are three ways in which U(1)-s can arise on the heterotic side: the case where the heterotic theory admits vector bundles with $S(U(1)\times U(m))$ structure group, the case where the heterotic theory admits vector bundles with $SU(m)\times\mathbb{Z}_n$ structure group, as well as the case where the heterotic theory admits vector bundles with structure groups having a centralizer in E_8 which contains a U(1) factor. Another important achievement was my discovery of the non-commutativity of the semi-stable degeneration map which splits a K3 surface into two half K3 surfaces, and the map to Weierstrass form, which was not previously known in the literature.

Contents

List of Tables

List of Figures

Chapter 1

On finiteness of Type IIB compactifications: Magnetized branes on elliptic Calabi-Yau threefolds

1.1 Introduction

M-theory or superstring compactification to four dimensions remains the most promising framework for the unification of the fundamental forces in Nature. The set of associated low energy effective theories which can arise in consistent compactifications is known as the string landscape. There have been many efforts to quantify this space, with the hope of uncovering observable properties shared by large classes of vacua which lead to novel insights in particle physics or cosmology. However, this has proven to be a very difficult problem deserving a multi-faceted approach.

The traditional one is to study the effective scalar potential on moduli space and to ex-

amine its associated vacua; in general a variety of perturbative and non-perturbative effects are utilized to this end. For example, in the much studied moduli stabilization scenarios of Type IIB compactifications [1, 2], these effects include superpotential contributions from background Ramond-Ramond flux and D-instanton effects. Increasingly more detailed realizations of these constructions have been studied in recent years; for progress on vacua with explicit complex structure moduli stabilization, see [3, 4], and on constructing explicit de Sitter flux vacua with a chiral spectrum, see the recent [5]. While this progress is significant and provides excellent proofs of principle, a clear caveat to the explicit construction of vacua is the enormity of the landscape.

Another approach is to study properties of the landscape more broadly. In Type IIB flux compactifications this has included, for example, the importance of four-form fluxes in obtaining the observed value of the cosmological constant [6]; issues of computational complexity, including finding vacua in agreement with cosmological data [7] and the systematic computation of non-perturbative effective potentials [8]; and the distribution and number of various types of supersymmetric and non-supersymmetric vacua [9, 10]. Progress has also been made in understanding vacua in strongly coupled corners of the landscape. For example there has been much progress in F-theory, beginning with [71, 72].

A final approach, which will be the one utilized in this paper, is to understand how consistency conditions and properties of the landscape differ from those of generic quantum field theories. The former case is motivated in part by the existence of a swampland [13] of consistent effective theories which do not admit a string embedding. There are a number of examples of limitations on gauge theories in the landscape not present in generic gauge theories. In weakly coupled theories with D-branes, Ramond-Ramond tadpole cancellation places stronger constraints [14, 15, 16, 17] on low energy gauge theories than anomaly cancellation, which include additional anomaly nucleation constraints [18] on $\mathrm{SU}(2)$ gauge theories; see also [120] for a recent analysis of anomalies at strong coupling in F-theory;

ranks of gauge groups are often bounded [20, 21]; and the matter representations are limited by the fact that open strings have precisely two ends. While more matter representations are possible at strong coupling, the possibilities are still limited. For example, in F-theory the possible non-Abelian [89, 23, 24, 188, 26, 93, 28, 29, 30] and Abelian [154, 155, 156, 129, 123, 157, 158, 159, 160] matter representations are limited by the structure of holomorphic curves in the geometry.

In [40], Douglas and Taylor studied the landscape of intersecting brane models[1] in Type IIA compactifications on a particular $\mathbb{Z}_2 \times \mathbb{Z}_2$-orientifold[2]. They found that the conditions on D6-branes necessary for $\mathcal{N} = 1$ supersymmetry in four dimensions, together with the D6-brane tadpole cancellation condition required for consistency of the theory, allow only a finite number of such D6-brane configurations[3]. In each configuration, the four-dimensional gauge group and matter spectrum can be determined explicitly. Thus, the finite number of D6-brane configurations gives a finite number of gauge sectors in a 4D supergravity theory that arise from these compactifications, and their statistics were studied explicitly. It is expected that the finiteness result which they obtained is a much more general consequence of supersymmetry and tadpole cancellation conditions, rather than a phenomenon specific to their construction. In fact, they proposed a potential generalization of their result to theories with magnetized D9- and D5-branes on smooth elliptically fibered Calabi-Yau threefolds, which can also be motivated by mirror symmetry, for example.

In this paper, we demonstrate that finiteness results are indeed much more general phenomena, providing further evidence that the string landscape itself is finite. Specifically, in large volume Type IIB compactifications on many smooth elliptically fibered Calabi-Yau threefolds $\pi : X \to B$, we prove that there are finitely many configurations of magnetized D9-

[1] See [41, 42, 43] for reviews of these compactifications and their implications for particle physics.

[2] See [44, 21] for a finiteness proof of the number of supersymmetric D-branes for fixed complex structures of this orientifold and [45, 17] for a first construction of chiral $\mathcal{N} = 1$ supersymmetric three-family models.

[3] See [46] for a counting of three family vacua, that yields eleven such vacua.

and D5-branes satisfying Ramond-Ramond tadpole cancellation and the conditions necessary for $\mathcal{N} = 1$ supersymmetry in four dimensions. We formulate a general, mathematical proof showing the existence of computable, explicit bounds on the number of magnetic flux quanta on the D9-branes and on the number of D5-branes, which only depends on the topology of the manifold B and is in particular independent of its Kähler moduli, as long as they are in the large volume regime of X. These bounds involve simple geometric quantities of the twofold base B of X and the proof applies to any base B that satisfies certain geometric conditions, that are easy to check and summarized in this paper. Furthermore, we show that these conditions are met by the almost Fano twofold bases B given by the toric varieties associated to all 16 reflexive two-dimensional polytopes and the generic del Pezzo surfaces dP_n for $n = 0, \ldots, 8$. This list in particular includes also the Hirzebruch surfaces $\mathbb{F}_0 = \mathbb{P}^1 \times \mathbb{P}^1$, $\mathbb{F}_1 = dP_1$, and $\mathbb{F}_2$. In this work, we focus on the finiteness question only, leaving the analysis of gauge group and matter spectra for this finite set of configurations to future work.

This paper is organized is follows. In section 1.2 we provide the relevant background on Type IIB compactifications with magnetized D9- and D5-branes and elliptically fibered Calabi-Yau threefolds at large volume. We first discuss the tadpole and supersymmetry conditions of general such setups, then present a basic account on elliptically fibered Calabi-Yau threefolds and end with a detailed discussion of the geometries of the twofold bases $B = \mathbb{F}_k$, dP_n and the 16 toric twofolds. In section 1.3 we prove the finiteness of such D-brane configurations. We begin by rewriting the tadpole and supersymmetry constraints in a useful form for the proof and make some definitions, then show the power of these definitions by proving finiteness on $\mathbb{P}^2$. Finally, we prove the existence of explicit bounds on the number of fluxes and D5-branes, that apply certain geometric conditions on B are satisfied. In section 1.4 we conclude and discuss possibilities for future work. In appendix 1.5 we discuss the detailed structure of the Kähler cone of generic del Pezzo surfaces dP_n

and give the proof of positive semi-definiteness of certain intersection matrices on these Kähler cones, which is essential for the proof. In appendix 1.6 we summarize the geometrical data of the considered almost Fano twofolds which is necessary to explicitly compute the bounds derived in this work.

While finishing this manuscript we learned about the related work [47] in which heterotic compactifications and their F-theory duals are constructed systematically.

1.2 Magnetized Branes on Elliptically Fibered Calabi-Yau Manifolds

We consider an $\mathcal{N} = 1$ compactification of Type IIB string theory on a Calabi-Yau threefold X with spacetime-filling D5-branes, magnetized D9-branes, i.e. D9-branes with magnetic fluxes[4], and an O9-plane. We group the D9-branes into stacks of N^α branes and their orientifold image branes. The corresponding line bundle magnetic fluxes in $H^{(1,1)}(X,\mathbb{Z})$ are denoted by F^α, respectively, $-F^\alpha$ for the image brane. In addition, we add stacks of D5-branes wrapping a curve Σ^{D5}.

In the following discussion of these models[5] we mainly follow the notations and conventions of [40], to which we also refer for more details. For a concise review see [42].

1.2.1 Tadpole Cancellation and SUSY Conditions

D-branes carry Ramond-Ramond charge and source flux lines that must be cancelled in the compact extra dimensions, in accord with Gauss' law. These give rise to the so-called tadpole cancellation conditions. The D5-brane tadpole cancellation conditions are

$$n_I^{D5} - T_I = \sum_\alpha N^\alpha \mathcal{K}(F^\alpha, F^\alpha, D_I)\,, \qquad \forall\, D_I \in H^{(1,1)}(X) \tag{1.1}$$

(we note a sign difference between the D5-tadpoles[6] in [40] and [42]; here, we use the sign in [42]) where D_I is a basis of divisors on X, $\mathcal{K}(\cdot,\cdot,\cdot)$ is the classical triple intersection of three two-forms or their dual divisors, where we denote, by abuse of notation, a divisor D_I

[4] For the generic case of gauge bundles with non-Abelian structure groups, see [48].

[5] These models were first proposed for model-building in [49].

[6] We thank Washington Taylor and Michael Douglas for helpful correspondence related to this issue.

and its Poincaré dual by the same symbol. Furthermore, we define the curvature terms

$$T_I = \int_{D_I} c_2(X)\,, \qquad n_I^{\mathrm{D5}} = \Sigma^{\mathrm{D5}} \cdot D_I\,, \tag{1.2}$$

where $c_2(X)$ is the second Chern-class on X and Σ^{D5} is the curve wrapped by all D5-branes. The integral wrapping numbers n_I^{D5} are positive if Σ^{D5} is a holomorphic curve and the D_I are effective divisors. Following [42], the D9-brane tadpole cancellation condition reads

$$16 = \sum_\alpha N^\alpha\,. \tag{1.3}$$

Compactification of Type IIB string theory on a Calabi-Yau manifold gives rise to a four-dimensional $\mathcal{N} = 2$ supergravity theory. An O9-orientifold breaks half of these supersymmetries and give rise to an $\mathcal{N} = 1$ supergravity theory at low energies. Only D9- and D5-branes can be added in a supersymmetric way to this orientifold. However, this requires aligning the central charges $Z(F^\alpha)$ of the branes appropriately with the O9-plane. For consistency with the supergravity approximation, we have to assume that the Kähler parameters of the Calabi-Yau threefold X are at large volume. In this case, the conditions on the central charges[7] necessary for $\mathcal{N} = 1$ supersymmetry, with J denoting the Kähler form on X, reduce to

$$3\mathcal{K}(J,J,F^\alpha) = \mathcal{K}(F^\alpha,F^\alpha,F^\alpha)\,, \qquad \mathcal{K}(J,J,J) > 3\mathcal{K}(J,F^\alpha,F^\alpha)\,, \tag{1.4}$$

to which we will refer in the following as the SUSY equality and the SUSY inequality respectively.

[7] In general, the central charge (and also the Kähler potential on the Kähler moduli space) receives perturbative and non-perturbative α' corrections. Recently it has been understood [50, 51, 52, 53] that these corrections are captured by the so-called Gamma class $\hat{\Gamma}_X$ on X rather than $\sqrt{Td_X}$. Since we study compactifications at large volume, these corrections can be neglected.

1.2.2 Smooth Elliptic Calabi-Yau Threefolds

We study compactifications where X is a smooth elliptically fibered Calabi-Yau threefold over a complex two-dimensional base B, $\pi : X \to B$, with a single section $\sigma : B \to X$, the zero-section. The class of the section σ is the base B. By the adjunction formula and the Calabi-Yau condition, the section σ obeys the relation

$$\sigma^2 = -c_1 \sigma \,, \tag{1.5}$$

where c_1 denotes the first Chern class of the base B. For a smooth threefold the second cohomology is given by $H^{(1,1)}(X) = \sigma H^0(B) \oplus \pi^* H^{(1,1)}(B)$. A basis of $H^{(1,1)}(X)$ generating the Kähler cone of X is given by

$$D_I = (D_0, D_i) \,, \qquad D_0 = \sigma + \pi^* c_1 \,, \qquad I = 0, 1, \ldots, p \equiv h^{(1,1)}(B) \tag{1.6}$$

with Poincaré duality implied when discussing divisors. The divisors D_i, $i = 1, \ldots, p$, are inherited from generators of the Kähler cone of the base, by abuse of notation denoted by the same symbol as their counterparts in B. The divisor D_0 is dual to the elliptic fiber $\mathcal{E}$ in the sense that it does not intersect any curve in B, i.e. $D_0 \cdot \sigma \cdot D_i = 0$ by (1.5), and obeys $D_0 \cdot \mathcal{E} = 1$. We note that $\mathcal{E}$ is an effective curve.

We emphasize that the requirement of a smooth elliptically fibered X, which means that the fibration can at most have I_1-fibers, restricts the choice of two-dimensional bases B. The bases we consider here are smooth almost Fano twofolds, which are the nine del Pezzo surfaces dP_n, $n = 0, \ldots, 8$, that are the blow-ups of $\mathbb{P}^2$ at up to eight generic points, the Hirzebruch surfaces $\mathbb{F}_k$, $k = 0, 1, 2$ and the toric surfaces described by the 16 reflexive two-dimensional polytopes. For these bases, the elliptic fibration X is smooth.

We abbreviate the triple intersections of three divisors on X as $\mathcal{K}_{IJK} = \mathcal{K}(D_I, D_J, D_K)$.

In the particular basis (1.6), we obtain the following structure of the triple intersections,

$$\mathcal{K}_{ijk} = 0\,, \quad \mathcal{K}_{00i} = \sum_j^p b_j \mathcal{K}_{0ij}\,, \quad \mathcal{K}_{000} = \sum_{i,j}^p b_i b_j \mathcal{K}_{0ij} = \sum_i^p b_i \mathcal{K}_{00i}\,, \tag{1.7}$$

where the first equation is a property of the fibration and the second and third relations can be derived using (1.5). We also introduce the $p \times p$-matrix

$$(C)_{ij} := \mathcal{K}(D_0, D_i, D_j) = \mathcal{K}_{0ij}\,, \tag{1.8}$$

which defines a bilinear pairing on divisors on the base B. For the cases we consider here its signature is $(1, p-1)$ for $\mathbb{F}_k$ and dP_n, $n = 1, \ldots, 8$, and $C = 1$ for $\mathbb{P}^2 = dP_0$. Note that it will be convenient at some places in this work to view $H^{(1,1)}(B)$ as a p-dimensional vector space equipped with an inner product (1.8). We denote the inner product of two vectors v, w in $H^{(1,1)}(B)$ simply by $C(v, w)$. In addition, we view the first Chern class c_1 of B, the fluxes F^α and the Kähler form J as column vectors

$$j = \begin{pmatrix} j_1 \\ . \\ . \\ . \\ j_p \end{pmatrix} \qquad m^\alpha = \begin{pmatrix} m_1^\alpha \\ . \\ . \\ . \\ m_p^\alpha \end{pmatrix} \qquad b = \begin{pmatrix} b_1 \\ . \\ . \\ . \\ b_p \end{pmatrix}. \tag{1.9}$$

Here the components of these vectors are defined via the expansion w.r.t. the D_I in (1.6),

$$\pi^* c_1 = \sum_{i=1}^p b_i D_i\,, \quad F^\alpha = m_0^\alpha D_0 + \sum_{i=1}^p m_i^\alpha D_i\,, \quad J = j_0 D_0 + \sum_{i=1}^p j_i D_i\,, \tag{1.10}$$

where $b_i \in \mathbb{Q}^+$, $m_I^\alpha \in \mathbb{Q}$ and $j_I \in \mathbb{R}^+$.[8]

We emphasize that the flux quantization condition $F^\alpha \in H^{(1,1)}(X,\mathbb{Z})$ can be equivalently written as

$$\int_C F^\alpha \in \mathbb{Z}, \qquad \forall\, C \in H_2(X,\mathbb{Z}), \tag{1.11}$$

where C is any curve in X. Noting that the elliptic fiber $\mathcal{E}$ and the Kähler generators D_i of B are integral curves in X, this implies, using (1.10),

$$\int_{\mathcal{E}} F^\alpha = m_0^\alpha \in \mathbb{Z}, \qquad \int_{D_i} F^\alpha = \sum_j^p C_{ij} m_j^\alpha \in \mathbb{Z}. \tag{1.12}$$

We conclude by noting that for smooth elliptically fibered Calabi-Yau threefolds, the second Chern class $c_2(X)$ can be computed explicitly, see e.g. [139] for a derivation. By adjunction one obtains $c_2(X) = 12\sigma\cdot c_1 + \pi^*(c_2 + 11c_1^2)$ with c_2 the second Chern class on B, employing the relation (1.5). Using this and (1.7) we evaluate the curvature terms in (1.2) as

$$T_0 = \int_B (c_2 + 11c_1^2), \qquad T_i = 12\int_{D_i} c_1 = 12\mathcal{K}_{00i}, \tag{1.13}$$

which is straightforward to evaluate for concrete bases B.

1.2.3 Basic Geometry of Almost Fano Twofolds

In this section we briefly discuss the geometrical properties of the almost Fano twofolds $B = \mathbb{F}_k$, dP_n and the toric surfaces. The discussion in this section is supplemented by the explicit computations of the Kähler cones of dP_n in appendix 1.5 and the summary of the key geometric data of $\mathbb{F}_k$, dP_n in Appendix 1.6, which is critical for the proof in Section 1.3.

[8] We allow here for rational coefficients m_I^α, b_i in the expansion of F^α, $\pi^* c_1$ that are in the integral homology $H^{(1,1)}(X,\mathbb{Z})$ in order to account for the possibility of Kähler generators D_I that only span a sublattice of $H^{(1,1)}(X,\mathbb{Z})$ of index greater than one. This can happen for non-simplicial Kähler cones.

Hirzebruch Surfaces

The Hirzebruch surfaces $\mathbb{F}_k$ are $\mathbb{P}^1$-bundles over $\mathbb{P}^1$ of the form $\mathbb{F}_k = \mathbb{P}(\mathcal{O} \oplus \mathcal{O}(k))$. There is an infinite family of such bundles for every positive $k \in \mathbb{Z}_{\geq 0}$.

The isolated section of this bundle, S, and the fiber F are effective curves generating the Mori cone and spanning the entire second homology

$$H_2(\mathbb{F}_k, \mathbb{Z}) = \langle S, F \rangle . \tag{1.14}$$

Their intersections read

$$S^2 = -k , \qquad S \cdot F = 1 , \qquad F^2 = 0 . \tag{1.15}$$

From this we deduce that the generators D_i, $i = 1,2$, of the Kähler cone, which are defined to be dual to the generators in (1.14), read

$$D_1 = F , \qquad D_2 = S + kF . \tag{1.16}$$

The Chern classes on $\mathbb{F}_k$ read

$$c_1(\mathbb{F}_k) = 2S + (2+k)F = (2-k)D_1 + 2D_2 , \qquad c_2(\mathbb{F}_k) = 4 , \tag{1.17}$$

which implies that the vector b in (1.9) is $b = (2-k, 2)^T$.

Using (1.15), we compute the triple intersections in (1.7), in particular (1.8), as

$$C = \begin{pmatrix} 0 & 1 \\ 1 & k \end{pmatrix} , \qquad \mathcal{K}_{001} = 2 , \qquad \mathcal{K}_{002} = 2 + k , \qquad \mathcal{K}_{000} = 8 , \tag{1.18}$$

from which the curvature terms in (1.13) immediately follow as

$$T_0 = 92\,, \qquad T_1 = 24\,, \qquad T_2 = 24 + 12k \tag{1.19}$$

We emphasize that $\mathbb{F}_k$ by means of (1.17) is Fano for $k < 2$ and almost Fano for $k = 2$, since the coefficient $b_1 = 2 - k \geq 0$. The general elliptic Calabi-Yau fibration X over F_k with $k = 0, 1, 2$ is smooth and develops I_3-singularities for $k = 3$ up to II^*-singularities for $k = 12$, before terminal singularities occur for $k > 12$ [136]. Thus, we focus on the Hirzebruch surfaces with $k = 0, 1, 2$.

Del Pezzo Surfaces

The Fano del Pezzo surfaces dP_n are the blow-up of $\mathbb{P}^2$ at up to eight generic points.[9]

Their second homology group is spanned by the pullback of the hyperplane on $\mathbb{P}^2$, denoted by H, and the classes of the exceptional divisors, denoted as E_i, $i = 1, \ldots, n$,

$$H_2(dP_n, \mathbb{Z}) = \langle H, E_{i=1,\ldots,n} \rangle\,. \tag{1.20}$$

The intersections of these classes read

$$H^2 = 1\,, \qquad H \cdot E_i = 0\,, \qquad E_i \cdot E_j = -\delta_{ij}\,. \tag{1.21}$$

The Chern classes on dP_n read

$$c_1(dP_n) = 3H - \sum_{i=1}^{n} E_i\,, \qquad c_2(dP_n) = 3 + n\,. \tag{1.22}$$

[9] See [94, 57] for recent computations of refined BPS invariants on del Pezzo surfaces as well as their interpretation in M-/F-theory.

The Mori cone of dP_n for $n > 1$ is spanned by the curves Σ obeying [58, 59]

$$\Sigma^2 = -1\,, \qquad \Sigma\cdot[K_{dP_n}^{-1}] = 1\,, \tag{1.23}$$

where $[K_{dP_n}^{-1}]$ is the anti-canonical divisor in dP_n, which is dual to $c_1(dP_n)$. By adjunction, we see that the curves obeying (1.23) obey the necessary condition for being $\mathbb{P}^1$'s. By solving the conditions (1.23) with the ansatz $a_0 H + \sum_{i=1}^n a_i E_i$ for $a_0, a_i \in \mathbb{Z}$, we obtain a cone that is simplicial, i.e. generated by $h^{(1,1,)}(B) = 1 + n$ generators, for $n = 0, 1, 2$ and non-simplicial for $n > 2$. The number of generators, beginning with dP_2, furnish irreducible representations of A_1, $A_1 \times A_2$, A_4, D_5, E_n, for $n = 6, 7, 8$, which concretely are **3**, $\mathbf{2}\otimes\mathbf{3}$, **10**, **16**, **27**, **56**, **248**.[10] For the simplicial cases the Mori cone reads

$$\mathbb{P}^2 : \langle H\rangle\,, \qquad dP_1 : \langle E_1, H - E_1\rangle\,, \qquad dP_2 : \langle E_1, E_2, H - E_1 - E_2\rangle \tag{1.24}$$

and we refer to appendix 1.5 for more details on the non-simplicial cases.

Consequently, also the Kähler cones of the dP_n, which are the dual of the Mori cones defined by (1.23), are non-simplicial for $n > 2$. The Kähler cone is spanned by rational curves Σ obeying

$$\Sigma^2 = 0\,, \quad \Sigma\cdot[K_{dP_n}^{-1}] = 2 \qquad \text{or} \qquad \Sigma^2 = 1\,, \quad \Sigma\cdot[K_{dP_n}^{-1}] = 3\,, \tag{1.25}$$

which again implies by adjunction that $\Sigma = \mathbb{P}^1$. The solutions over the integers of these conditions yield the generators of the Kähler cone of dP_n which again follow the representation theory of the above mentioned Lie algebras. The number of generators, starting with dP_0, is 1, 2, 3, 5, 10, 26, 99, 702 and 19440, see appendix 1.5. In the simplicial cases, the

[10] The genuine roots in $H_2(dP_n)$ are the -2-curves orthogonal to $[K_{dP_n}^{-1}]$, i.e. $\alpha_i = E_i - E_{i+1}$, $i = 1, \ldots, n-1$, $\alpha_n = H - E_1 - E_2 - E_3$ for $n > 2$. These act on $H_2(dP_n)$ by means of the Weyl group, cf. [58].

Kähler cone generators read

$$\mathbb{P}^2 : D_1 = H\,, \quad dP_1 : D_1 = H - E_1, D_2 = H\,, \quad dP_2 : D_1 = H - E_1, D_2 = H - E_2, D_3 = H \quad (1.26)$$

Generically, for $n \geq 2$ the vector $c_1(dP_n)$ is the center both of the Kähler and Mori cone. This implies that for all del Pezzo surfaces, the coefficients b_i are positive. For the simplicial Kähler cones, this can be computed explicitly. For the non-simplicial cases we will argue in appendix 1.5, that a covering of the Kähler cone by simplicial subcones, i.e. subcones with $h^{(1,1)}$ generators, with all $b_i \geq 0$ always exists. We note that for all dP_n, the defining property of the Kähler cone (1.25), together with (1.7), implies the intersections

$$\mathcal{K}_{00i} = 2, 3\,, \qquad \mathcal{K}_{000} = 9 - n\,. \quad (1.27)$$

In addition, by explicit computations we check in general that all $C_{ij} \geq 0$ for all pairs of Kähler cone generators. The intersections (1.27) together with (1.21), (1.22) further imply that the curvature terms in (1.13) read

$$T_0 = 102 - 10n\,, \qquad T_i = 24, 36 \quad (1.28)$$

For the three simplicial cases of $\mathbb{P}^2$, dP_1 and dP_2, we compute the matrices (1.8) in the basis (1.26) as

$$C_{\mathbb{P}^2} = 1\,, \qquad C_{dP_1} = \begin{pmatrix} 0 & 1 \\ 1 & 1 \end{pmatrix}, \qquad C_{dP_2} = \begin{pmatrix} 0 & 1 & 1 \\ 1 & 0 & 1 \\ 1 & 1 & 1 \end{pmatrix}. \quad (1.29)$$

We emphasize that the del Pezzos dP_n by means of (1.27) are Fano for $n < 9$ and almost Fano for $n = 9$, since $c_1^2 = 0$. The surface dP_9 is the rational elliptic surface. Its Mori cone is the Mordell-Weil group of rational sections by (1.23). Thus, it as well as its dual Kähler

cone is infinite dimensional. We will only consider the Fano del Pezzo surfaces dP_n, $n < 9$.

Toric Surfaces from Reflexive Polytopes

Toric surfaces obtained from fine star triangulations of reflexive polytopes are smooth almost Fano twofolds.[11] There are 16 such polytopes in two dimensions, which are displayed in Figure 1.1.

A number of these twofolds are simply toric descriptions of previously described surfaces. Specifically, these are $\mathbb{P}^2$, dP_1, dP_2, dP_3, $\mathbb{F}_0$ and $\mathbb{F}_2$ which are described by polytopes 1, 3, 5, 7, 2 and 4, respectively. From the form of some of the other polytopes it is clear that they can be obtained from $\mathbb{P}^2, dP_1, dP_2$, or dP_3 via toric blow-up. For example, reflecting polytope 7 through the vertical axis going through its center and performing a toric blow-up associated to the point $(-1,1)$, one obtains polytope 12. Thus, the smooth Fano surface associated to polytope 12 is a toric realization of dP_4 at a non-generic point in its complex structure moduli space.

The toric varieties associated to all these 16 reflexive polytopes can be constructed explicitly using the software package Sage [61]. The intersections (1.7), (1.8) are readily constructed in a given fine star triangulation and the Kähler cone can be obtained. We summarize the geometric data necessary for the computation of the bounds derived below in the proof in Appendix 1.6.

[11] See the recent [60] for a systematic study of the quantum geometry of the elliptically fibered Calabi-Yau manifolds over these bases.

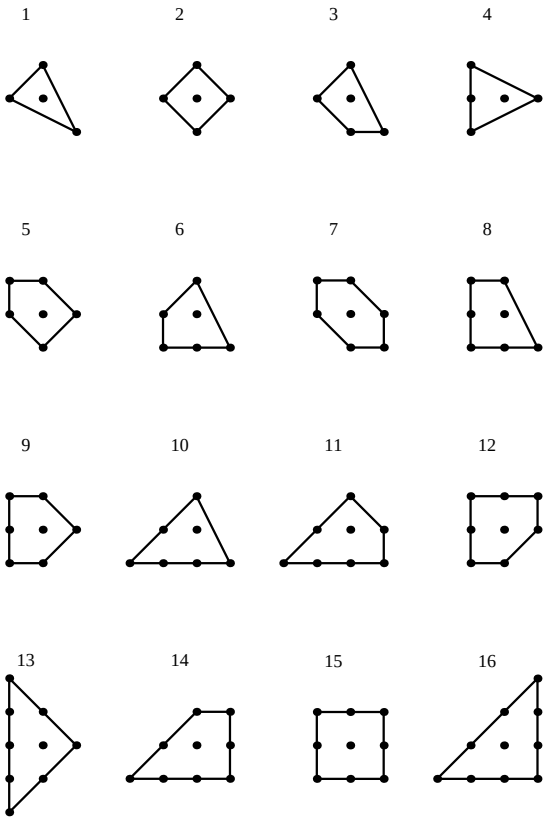

Figure 1.1: The sixteen two-dimensional reflexive polytopes which define the almost Fano toric surfaces via their fine star triangulations.

1.3 Finiteness of Magnetized D9- & D5-brane Configurations

In this section we bound the number of possible gauge sectors arising in the considered compactifications of Type IIB string theory.

As emphasized in section 1.2, the number N^α of branes in a stack and their associated magnetic fluxes F^α are subject to the consistency conditions imposed by tadpole cancellation conditions (1.1), (1.3) and the SUSY conditions (1.4). Since the numbers N^α of D9-branes are bounded by (1.3), it is therefore the goal of this proof to bound the flux quanta F^α and the number of D5-branes in Σ^{D5}.

Most of the proofs in this work have the same basic structure. The key point is to find a bound on the number of different flux configurations F^α and D5-branes Σ^{D5} at an arbitrary point in the large volume regions of Kähler moduli space, i.e. a bound that is independent of the Kähler moduli. As we will see, proving this requires an intriguing interplay between both the tadpole conditions (1.1), (1.3) and the SUSY conditions (1.4), a general rubic which was also used in the proof of [40][12]. In addition, the following proof applies if a list of geometrical properties, listed at the beginning of Section 1.3.3, are satisfied. These are obeyed for the considered examples $B = \mathbb{F}_k$, dP_n and the toric surfaces.

Before delving into the details of the proof, let us introduce a very important notation. Because of their fundamentally different contributions to (1.1), (1.3) and (1.4) it is useful to split D9-brane stacks into to qualitatively different types according to their flux quanta. We denote D9-brane stacks with $m_0^\alpha \neq 0$ as $\underline{\beta\text{-branes}}$, and those with $m_0^\alpha = 0$ as $\underline{\gamma\text{-branes}}$:

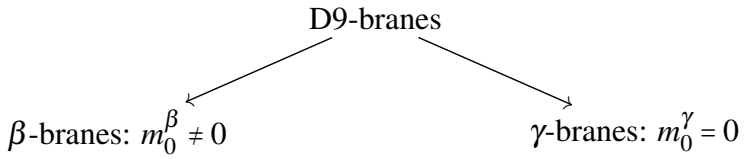

(1.30)

In addition, in the rest of this section we label fluxes of a β- and γ-brane by m_I^β and m_I^γ, respectively.

We begin in Section 1.3.1 by preparing for the general finiteness proof by writing out the tadpoles and SUSY conditions of Section 1.2 for elliptically fibered Calabi-Yau threefolds X. We also make certain definitions and deduce a number of simple inequalities and bounds, that will be essential for the later discussion. Then, in Section 1.3.2 we prove finiteness for the special base $B = \mathbb{P}^2$, which will demonstrate the usefulness of the definitions of the previous section and serve as a warm-up for the general proof in Section

[12]The interplay between SUSY and tadpole conditions has also been used in [44, 21] for rigid $\mathbb{Z}_2 \times \mathbb{Z}_2$-orientifolds and for other models in [62, 63].

1.3.3.

1.3.1 Prerequisites: Definitions & Basic Inequalities

In this section we make some general definitions and observations necessary to formulate and organize the proof in Section 1.3.3.

As a starting point, we observe that the SUSY conditions (1.4) must be satisfied by each brane stack, but only involve the direction along the Kähler class j, whereas the tadpole conditions (1.1) have to be obeyed for each divisor D_I, but are summed across brane stacks. Thus, in order to bound each component m_I^α of every flux vector m^α, labelled by the brane stack α, it is crucial to identify quantities, that enter both types of constraints, when rewritten in a particular form.

To this end, we write out the tadpole conditions explicitly in the basis of divisors (1.6). The conditions (1.1) for $I = 0$, to which we will refer in the future as the 0^{th}-tadpole, reads

$$0^{\text{th}}\text{-tadpole}: \; n_0^{D5} - T_0 = \underbrace{\sum_\beta N^\beta C\left(b + \frac{m^\beta}{m_0^\beta}, b + \frac{m^\beta}{m_0^\beta}\right)(m_0^\beta)^2}_{\beta \text{ brane contributions}} + \underbrace{\sum_\gamma N^\gamma C(m^\gamma, m^\gamma)}_{\gamma \text{ brane contributions}} \tag{1.31}$$

where we used (1.8) and (1.9) and emphasized the respective contributions from β-branes and γ-branes. For $I = i$, to which we will refer as the i^{th}-tadpole, the tadpole (1.1) reads

$$i^{\text{th}}\text{-tadpole}: \; n_i^{D5} - T_i = \underbrace{\sum_\beta N^\beta t_i^\beta (m_0^\beta)^2}_{\beta \text{ brane contributions}} \qquad \text{with} \qquad t_i^\beta \equiv 2\sum_{j=1}^{p} C_{ij}\left(\frac{b_j}{2} + \frac{m_j^\beta}{m_0^\beta}\right). \tag{1.32}$$

We note that the first term in t_k^β can be written as $\sum_j b_j C_{ij} = \mathcal{K}_{00i}$ which is an integer by (1.18), (1.27) and Table 1.5. The quantities t_i^β can be defined for β-branes and play an important in the proof, because they naturally appear in the SUSY constraints. We

emphasize that while both β-branes and γ-branes contribute to the 0^{th}-tadpole condition, only β-branes contribute to the i^{th}-tadpole as is indicated by the braces in (1.31), (1.32).

We note that one can immediately deduce a lower bound on the left hand side of (1.31) and (1.32) by setting the positive numbers $n_I^{\text{D5}} = 0$:

$$-T_0 \leq \sum_\beta N^\beta C\left(b+\frac{m^\beta}{m_0^\beta}, b+\frac{m^\beta}{m_0^\beta}\right)(m_0^\beta)^2 + \sum_\gamma N^\gamma C(m^\gamma, m^\gamma), \quad -T_i \leq \sum_\beta N^\beta t_i^\beta (m_0^\beta)^2. \quad (1.33)$$

These lower bounds on the i^{th}-tadpoles imply, as we will see, that if the t_i^β are bounded above, then they are automatically bounded below. This can be seen by bringing the bounded positive contribution to the left hand side of (1.33).

For β-branes, which have $m_0^\beta \neq 0$, it useful to divide the SUSY equality (1.4) by m_0^β. Using again (1.8) and (1.9), we write the first condition in (1.4) to obtain

$$\left[3C\left(\frac{j}{j_0}, \frac{j}{j_0}\right) + 6C\left(\frac{b}{2}+\frac{j}{j_0}, b+\frac{m^\beta}{m_0^\beta}\right)\right] j_0^2 = \left[\frac{1}{4}\mathcal{K}_{000} + 3C\left(\frac{b}{2}+\frac{m^\beta}{m_0^\beta}, \frac{b}{2}+\frac{m^\beta}{m_0^\beta}\right)\right](m_0^\beta)^2. \quad (1.34)$$

The SUSY inequality in (1.4) for β-branes can be combined with the SUSY equality (1.34) as follows. By dividing the SUSY inequality in (1.4) by j_0 and subtracting the SUSY equality (1.34), we obtain after a few lines of algebra the following inequality:

$$0 > \frac{1}{2}\mathcal{K}_{000} + 6C\left(\frac{b}{2}+\frac{m^\beta}{m_0^\beta}, \frac{b}{2}+\frac{j}{j_0}\right). \quad (1.35)$$

This can equivalently be written in the form

$$0 > \frac{1}{2}\mathcal{K}_{000} + 3\sum_i^p t_i^\beta \left(\frac{b_i}{2}+\frac{j_i}{j_0}\right) \quad (1.36)$$

and we see that the expression t_i^β, which explicitly appears in the i^{th}-tadpole conditions in (1.13), appears also in this manipulation of the SUSY constraints.

We note that (1.36) can be related to the tadpole conditions. By multiplying (1.36) by $N^\beta (m_0^\beta)^2$ and summing over β, we employ the right hand side of (1.32) to obtain

$$0 > \frac{1}{2}\mathcal{K}_{000}\sum_\beta N^\beta (m_0^\beta)^2 + 3\sum_{i=1}^{p}(n_i^{\mathrm{D5}} - T_i)\Big(\frac{b_i}{2}+\frac{j_i}{j_0}\Big) \geq \frac{1}{2}\mathcal{K}_{000}\sum_\beta N^\beta (m_0^\beta)^2 - 3\sum_{i=1}^{p} T_i\Big(\frac{b_i}{2}+\frac{j_i}{j_0}\Big), \tag{1.37}$$

where we set $n_i^{\mathrm{D5}} = 0$ in the last inequality. This condition is used throughout the proof.

Next, we demonstrate that it is possible to also rewrite the SUSY equality (1.34) and the 0^{th}-tadpole (1.31) in a form that manifestly contains the quantities t_i^β. To this end, we first define for each distinct pair of indices $\{i,k\}$, $i \neq k$, the matrix $M_{\{i,k\}}$ whose (j,l)-th entry in the basis D_i is:

$$\big(M_{\{i,k\}}\big)_{jl} = x_{\{i,k\}} C_{ij} C_{kl} + x_{\{i,k\}} C_{il} C_{kj} - C_{jl} \tag{1.38}$$

where $x_{\{i,k\}} \in \mathbb{Q}^+$ is a non-negative rational number. This number has to be chosen such that its corresponding $M_{\{i,k\}}$ is positive semi-definite. We note, that the matrices $M_{\{i,k\}}$ resemble the stress energy tensor of a system of free particles, c.f. Appendix 1.7. We use this to show that, if the first condition in Section 1.3.3 is met, there always exists an $x_{\{i,k\}}$ so that these matrices are positive semi-definite, see Appendices 1.5 and 1.7. Thus, throughout the rest of this proof we assume that all matrices $M_{\{i,k\}}$ are positive semi-definite.

With this definition, the SUSY equality (1.34) and 0^{th}-tadpole (1.31) can be written as

$$\Big[3C\Big(\tfrac{j}{j_0},\tfrac{j}{j_0}\Big)+6C\Big(\tfrac{b}{2}+\tfrac{j}{j_0},b+\tfrac{m^\beta}{m_0^\beta}\Big)\Big]j_0^2 = \Big[\tfrac{1}{4}\mathcal{K}_{000}+\tfrac{3}{2}x_{\{i,k\}}t_i^\beta t_k^\beta - 3M_{\{i,k\}}\Big(\tfrac{b}{2}+\tfrac{m^\beta}{m_0^\beta},\tfrac{b}{2}+\tfrac{m^\beta}{m_0^\beta}\Big)\Big](m_0^\beta)^2$$

and

$$n_0^{D5} - T_0 = \underbrace{\sum_\beta N^\beta \left[\frac{1}{2} x_{\{i,k\}} \tilde{t}_i^\beta \tilde{t}_k^\beta - M_{\{i,k\}} \left(b + \frac{m^\beta}{m_0^\beta}, b + \frac{m^\beta}{m_0^\beta} \right) \right] (m_0^\beta)^2}_{\beta-\text{ brane contributions}} + \underbrace{\sum_\gamma N^\gamma C(m^\gamma, m^\gamma)}_{\gamma-\text{ brane contributions}} , \tag{1.39}$$

respectively, where we indicated the contributions from $\beta-$ and γ-branes by braces and used the short hand notation

$$\tilde{t}_i^\beta = \mathcal{K}_{00i} + t_i^\beta . \tag{1.40}$$

As we will see, the proof of Section 1.3.3 applies whenever the M-matrices in (1.38) are all positive semi-definite. In fact, for all the bases B of the threefold X considered, this matrix is positive semi-definite. For $\mathbb{P}^2, \mathbb{P}^1 \times \mathbb{P}^1, dP_1, dP_2$, and $\mathbb{F}_2$ the M-matrix can be readily computed in the Kähler cone basis, and indeed, it is positive semi-definite. However, for dP_n with $n \geq 3$ there exists a significant complication since in these examples, the Kähler cone is non-simplicial, as mentioned in Section 1.2. In these cases, we cover the Kähler cone by simplicial subcones consisting of $h^{(1,1)}$ generators and compute the M-matrix (1.38) for this choice. As demonstrated in Appendix 1.5, for dP_n, $n < 9$, the M-matrices are positive semi-definite for all such subcones. For the toric surfaces, we refer to Appendix 1.6 for positive semi-definiteness of the matrices (1.38). Thus, for the rest of the paper we can assume that all $M_{\{i,k\}}$ are positive semi-definite for these bases.

1.3.2 Warm Up: Finiteness for Elliptic Fibrations over $\mathbb{P}^2$

Before proceeding on to more difficult examples, let us prove finiteness in the simplest example of $B = \mathbb{P}^2$. In particular, in this example we will demonstrate the usefulness of the derived inequality (1.35) and (1.37).

For an elliptically fibered Calabi-Yau threefold X over $B = \mathbb{P}^2$, the relevant geometrical

data following from (1.22), (1.27), (1.28) and (1.29) is:

$$\mathcal{K}_{000} = 9\,, \quad \mathcal{K}_{001} = 3\,, \quad \mathcal{K}_{011} \equiv C_{11} = 1\,, \quad b_1 = 3\,, \quad T_1 = 36\,. \tag{1.41}$$

Using this the inequality (1.35) reduces to

$$0 > \mathcal{K}_{001}(m_0^\beta)^2 + 2\mathcal{K}_{011} m_0^\beta m_1^\beta\,. \tag{1.42}$$

The tadpole for D_1 reads

$$n_1^{D5} - T_1 = \sum_\beta N^\beta \left[\mathcal{K}_{001}\,(m_0^\beta)^2 + 2\,\mathcal{K}_{011}\, m_0^\beta m_1^\beta\right]. \tag{1.43}$$

By (1.42), the right hand side of (1.43) must be negative. Thus we have a bound for $n_1^{\rm D5}$, given by

$$n_1^{\rm D5} < T_1\,. \tag{1.44}$$

In addition, for each β-brane we deduce from (1.42) that

$$\begin{aligned} 0 \;&<\; |m_0^\beta|\,|\mathcal{K}_{001} m_0^\beta + 2\mathcal{K}_{011} m_1^\beta| = |\mathcal{K}_{001}(m_0^\beta)^2 + 2\mathcal{K}_{011} m_0^\beta m_1^\beta| \\ &\le\; \sum_\beta N^\beta\, |\mathcal{K}_{001}(m_0^\beta)^2 + 2\mathcal{K}_{011} m_0^\beta m_1^\beta| \le T_1\,. \end{aligned} \tag{1.45}$$

Notice that $|\mathcal{K}_{001} m_0^\beta + 2\mathcal{K}_{011} m_1^\beta|$ is a non-zero integer by virtue of the strict inequality (1.42). This implies the bound

$$|m_0^\beta| \le T_1\,. \tag{1.46}$$

Next, since $|\mathcal{K}_{001}m_0^\beta + 2\mathcal{K}_{011}m_1^\beta| \leq T_1/|m_0^\beta|$ and $|m_0^\beta|$ is bounded, m_1^β is also bounded as

$$|m_1^\beta| \leq \frac{1}{2\mathcal{K}_{011}}\Big(\frac{T_1}{|m_0^\beta|} + \mathcal{K}_{001}|m_0^\beta|\Big). \tag{1.47}$$

Thus we have shown that the magnetic flux quanta m^β associated to β-branes are bounded.

A bound on the flux quanta of γ-branes is straightforward to obtain. The SUSY equality in (1.4) for each γ-brane is $\mathcal{K}_{011}\left(\frac{b_1}{2} + \frac{j_1}{j_0}\right)m_1^\gamma = 0$. Since $\mathcal{K}_{011} \neq 0$ and $\left(\frac{b_1}{2} + \frac{j_1}{j_0}\right)$ is strictly positive, we must have $m_1^\gamma = 0$. Since a γ-brane by definition has $m_0^\gamma = 0$, the flux quanta of γ-branes are trivially bounded. This completes the proof for $B = \mathbb{P}^2$.

1.3.3 Proving Finiteness for Two-Dimensional Almost Fano Bases

In this section we present the general proof of the finiteness of the number of consistent Type IIB compactification with magnetized D9-branes on smooth elliptically fibered Calabi-Yau threefolds. As discussed before the bases B for which the presented proof has been developed are the two-dimensional almost Fano varieties. These are the del Pezzo surfaces dP_n, $n = 0, \ldots, 8$, with the case of $dP_0 = \mathbb{P}^2$ discussed in the previous section 1.3.2, the Hirzebruch surfaces $\mathbb{F}_k$, $k = 0, 1$, including the almost Fano $\mathbb{F}_2$, as well as the toric surfaces.

The geometrical properties that are essential for the following proof are the smoothness of the generic elliptic Calabi-Yau fibration over them, as well as the following list of properties:

(1) all Kähler cone generators of B are time- or light-like vectors in the same light-cone.

(2) positivity of the coefficients b_i in (1.10), i.e. $b_i \geq 0$ for all i.

(3) positivity and integrality of $\mathcal{K}_{00i}$ as defined in (1.7), i.e. $\mathcal{K}_{00i} \in \mathbb{Z}_{\geq 0}$ for all i.

(4) the signature of the matrix C_{ij} defined in (1.8) is $(1, n)$, where $n + 1 = h^{(1,1)}(B)$, i.e. has one positive and n negative eigenvalues.

(5) positivity of the Kähler parameters j_i and validity of the large volume approximation, i.e. $j_i \gg 1$ for all i.

We claim that the proof presented below applies to all bases B that obey these conditions.

We note that properties (4) and (5) are automatically satisfied for all the surfaces we consider: the signature of the matrix C_{ij} defined in (1.8) is $(1,n)$, cf. Section 1.2.3, and $j_i \gg 1$ always holds in the Kähler cone basis at large volume for any B. The validity of properties (1)-(3) for the considered bases is shown in the Appendices 1.5 and 1.6. As discussed there, the only subtlety arises for the higher del Pezzos dP_n, $n > 2$, which have non-simplicial Kähler cones. In this case, the indices i refer to the generators of a suitably chosen simplicial subcone, such that properties (1)-(3) hold. As argued in appendix 1.5 there always exists a covering of the Kähler cones of the dP_n by simplicial subcones, such that for each subcone in the covering properties (1)-(3) hold.

The following proof is organized as follows. We already introduced the two types of branes, denoted β- and γ-branes, to distinguish between branes with and without fluxes along the fiber $\mathcal{E}$, i.e. $\int_{\mathcal{E}} F^\beta \neq 0$ and $\int_{\mathcal{E}} F^\gamma = 0$, respectively. First we prove in Section 1.3.3 that there is only a finite number of flux configurations on β-branes. Then in Section 1.3.3 we show finiteness of the numbers of D5-branes n_I^{D5}. Finally, we conclude the proof in Section 1.3.3 by showing finiteness of the number of flux configurations on γ-branes.

Bounds on β-branes

Bounds on m_0^β

In the following we obtain a bound on the flux component m_0^β for all β-branes. The result is

$$|m_0^\beta| \leq \max(T_i)\,, \tag{1.48}$$

where the maximum is taken over all generators of the specific subcone of the Kähler cone. We note that here and in the rest of the paper, all minima and maxima on T_i and $x_{\{i,k\}}$ are taken across generators of the specific subcone we are in. However, except the minimum on T_i in theorem 4, the reader is free to take all other maxima and minima across all generators of the entire Kähler cone, for easy computation purposes. For del Pezzo surfaces this yields $\max(T_i) = 36$, for the Hirzebruch surfaces $\mathbb{F}_k$ it is $\max(T_i) = 24 + 12k$ and for the toric surfaces we can read off this bound from Table 1.5.

We begin by considering inequality (1.36). In fact, since $\mathcal{K}_{000} \geq 0$, (1.36) implies

$$0 > \sum_i^p t_i^\beta \left(\frac{b_i}{2} + \frac{j_i}{j_0}\right) \tag{1.49}$$

Next we multiply this by $N^\beta (m_0^\beta)^2$ and sum over β to obtain, using (1.32),

$$0 > \sum_\beta \sum_i^p N^\beta t_i^\beta (m_0^\beta)^2 \left(\frac{b_i}{2} + \frac{j_i}{j_0}\right) = \sum_i^p \left(n_i^{\mathrm{D5}} - T_i\right)\left(\frac{b_i}{2} + \frac{j_i}{j_0}\right) \geq \sum_i^p (-T_i)\left(\frac{b_i}{2} + \frac{j_i}{j_0}\right) \tag{1.50}$$

where we set the positive $n_i^{\mathrm{D5}} = 0$ for all i in the last inequality. This lower bound on the sum over β also implies

$$0 > \sum_{i=1}^p N_\beta t_i^\beta (m_0^\beta)^2 \left(\frac{b_i}{2} + \frac{j_i}{j_0}\right) \geq \sum_{i=1}^p (-T_i)\left(\frac{b_i}{2} + \frac{j_i}{j_0}\right). \tag{1.51}$$

because by (1.49) all summands are negative. This motivates the following definition:

Definition 1. *A **special brane** is a β-brane with $t_i^\beta < 0$ for all i. A **mixed brane** is a β-brane which is not a special brane (i.e. there exists an i such that $t_i^\beta \geq 0$).*

Remark 1. By (1.49), there does not exist a mixed brane with $t_i \geq 0 \ \forall i$, since $b_i, j_i \geq 0$. Hence for a mixed brane, we cannot have t_i of the same sign $\forall i$, they must be of mixed signs. This motivates its name.

For special branes, we immediately conclude from (1.51) that

$$\begin{aligned}\max(T_i)\sum_{i=1}^{p}\left(\frac{b_i}{2}+\frac{j_i}{j_0}\right) &\geq \sum_{i=1}^{p}T_i\left(\frac{b_i}{2}+\frac{j_i}{j_0}\right)\geq\sum_{i=1}^{p}N_\beta|t_i^\beta|(m_0^\beta)^2\left(\frac{b_i}{2}+\frac{j_i}{j_0}\right) \\ &= \sum_{i=1}^{p}\underbrace{N_\beta|t_i^\beta m_0^\beta|}_{\in\mathbb{N},\geq 1}|m_0^\beta|\left(\frac{b_i}{2}+\frac{j_i}{j_0}\right)\geq|m_0^\beta|\sum_{i=1}^{p}\left(\frac{b_i}{2}+\frac{j_i}{j_0}\right).\end{aligned} \tag{1.52}$$

Here we have used (1.51) in the second inequality, and that $t_i^\beta m_0^\beta = \sum_j C_{ij}(b_j m_0^\beta + 2m_j^\beta)$ is a non-zero positive integer, cf. (1.32) in the last inequality: it is an integer because both its first term, $\mathcal{K}_{00i}m_0^\beta$, and the second term, the flux F^β integrated over the integral class D_i, are integers by (1.12). It is non-zero because t_i^β is non-zero by the definition of special branes, and m_0^β is non-zero by the definition of β-branes. Thus for special branes, the flux quantum m_0^β is bounded as

$$|m_0^\beta|\leq\max(T_i). \tag{1.53}$$

We will show that mixed branes have a even smaller bound for their $|m_0^\beta|$.

Let us first make an observation that will facilitate the identification of special branes.

Lemma 1. *A β-brane which satisfies $0\leq C\left(\frac{b}{2}+\frac{j}{j_0},b+\frac{m^\beta}{m_0^\beta}\right)$ is a special brane.*

Proof. For any β brane with $0\leq C\left(\frac{b}{2}+\frac{j}{j_0},b+\frac{m^\beta}{m_0^\beta}\right)$, consider its SUSY equality (1.39). Then

$$\text{LHS of (1.39)}\geq 3C\left(\frac{j}{j_0},\frac{j}{j_0}\right)j_0^2. \tag{1.54}$$

Suppose it is not a special brane. Then by definition we cannot have $t_i^\beta<0\ \forall i$. Remark 1 also forbids $t_i^\beta\geq 0\ \forall i$. Thus there exists a pair of i,k such that t_i^β and t_k^β are of opposite signs (the following argument still applies if one of them is zero). Writing the RHS of

(1.39) in terms of this particular pair of t_i^β, t_k^β, we observe that

$$\text{RHS of (1.39)} \leq \frac{1}{4}\mathcal{K}_{000}(m_0^\beta)^2 \leq \frac{1}{4}\mathcal{K}_{000}\sum_\beta N^\beta (m_0^\beta)^2 < \frac{3}{2}\sum_{i=1}^{p}(T_i)\left(\frac{b_i}{2}+\frac{j_i}{j_0}\right) \tag{1.55}$$

where in the first inequality we dropped all negative terms on the RHS of (1.39) and in the last inequality we employed the lower bound on (1.37). Now (1.54) shows that the LHS of (1.39) is at least quadratic in the j_i's and grows as the Kähler volume of B. However, inequality (1.55) implies that the RHS of (1.39) is at most on the order of j_i/j_0. In the limit of all j_I large, which in particular implies large volume of B, the LHS of (1.39) has to be greater than the RHS of (1.39). Thus, the SUSY equality (1.39) is violated. Our initial assumption that this β-brane is not a special brane must be wrong; it must be a special brane. □

Remark 2. The argument in Lemma 1 about the growth of the two sides of the SUSY equality (1.39) can be further substantiated for concrete bases B. For all $\mathbb{F}_k$, we can check that we have LHS of (1.39)> RHS of (1.39) when $j_I \geq 3\ \forall I$. This is clearly the case if the supergravity approximation is supposed to be valid. For dP_n, the matrix $C(\cdot,\cdot)$ has signature $(1,n)$, i.e. we can have $C(j,j) = 0$ for $j \neq 0$ and the above argument might be invalidated. However, we can only have $C(j,j) = 0$ if the Kähler form $j_B = \sum_i j_i D_i$ on B is on the boundary of the Kähler cone. This means that the Kähler volume of B is zero or cycles in B have shrunk to zero which clearly invalidates the supergravity approximation.

Thus, it remains to bound m_0^β for β-branes satisfying $0 \geq C\left(\frac{b}{2}+\frac{j}{j_0}, b+\frac{m^\beta}{m_0^\beta}\right)$. For such β-branes, we observe

$$0 \geq C\left(\frac{b}{2}+\frac{j}{j_0}, b+\frac{m^\beta}{m_0^\beta}\right) = \frac{1}{2}\sum_{i=1}^{p}\mathcal{K}_{00i}\left(\frac{b_i}{2}+\frac{j_i}{j_0}\right) + \underbrace{\frac{1}{2}\sum_{i=1}^{p} t_i^\beta\left(\frac{b_i}{2}+\frac{j_i}{j_0}\right)}_{<0 \text{ by (1.49)}} \tag{1.56}$$

using (1.7) and the definition of t_i^β (1.32). Next, label all β-branes with $0 \geq C\left(\frac{b}{2}+\frac{j}{j_0}, b+\frac{m^\beta}{m_0^\beta}\right)$ by β', multiply the above inequality by $N^{\beta'}(m_0^{\beta'})^2$ and sum over β':

$$\begin{aligned}
0 &\geq \frac{1}{2}\sum_{i=1}^{p}\mathcal{K}_{00i}\left(\frac{b_i}{2}+\frac{j_i}{j_0}\right)\sum_{\beta'}N^{\beta'}(m_0^{\beta'})^2+\frac{1}{2}\sum_{\beta'}N^{\beta'}(m_0^{\beta'})^2\sum_{i=1}^{p}t_i^{\beta'}\left(\frac{b_i}{2}+\frac{j_i}{j_0}\right)\\
&\geq \frac{1}{2}\sum_{i=1}^{p}\mathcal{K}_{00i}\left(\frac{b_i}{2}+\frac{j_i}{j_0}\right)\sum_{\beta'}N^{\beta'}(m_0^{\beta'})^2+\frac{1}{2}\sum_{\beta}N^{\beta}(m_0^{\beta})^2\sum_{i=1}^{p}t_i^{\beta}\left(\frac{b_i}{2}+\frac{j_i}{j_0}\right)\\
&= \frac{1}{2}\sum_{i=1}^{p}\mathcal{K}_{00i}\left(\frac{b_i}{2}+\frac{j_i}{j_0}\right)\sum_{\beta'}N^{\beta'}(m_0^{\beta'})^2+\frac{1}{2}\sum_{i=1}^{p}(n_i^{D5}-T_i)\left(\frac{b_i}{2}+\frac{j_i}{j_0}\right)\\
&\geq \frac{1}{2}\sum_{i=1}^{p}\mathcal{K}_{00i}\left(\frac{b_i}{2}+\frac{j_i}{j_0}\right)\sum_{\beta'}N^{\beta'}(m_0^{\beta'})^2+\frac{1}{2}\sum_{i=1}^{p}(-T_i)\left(\frac{b_i}{2}+\frac{j_i}{j_0}\right).
\end{aligned} \tag{1.57}$$

Here in the second line we extended the sum over β' to the sum over all β-branes; by (1.49) each summand is negative, thus, extending the sum only decreases it. In the third line we have used (1.32). With (1.13) and the last line of the above inequality we obtain

$$12\sum_{i=1}^{p}\mathcal{K}_{00i}\left(\frac{b_i}{2}+\frac{j_i}{j_0}\right)\geq\sum_{\beta'}N^{\beta'}(m_0^{\beta'})^2\sum_{i=1}^{p}\mathcal{K}_{00i}\left(\frac{b_i}{2}+\frac{j_i}{j_0}\right) \tag{1.58}$$

Comparing coefficients, we see $\sum_{\beta'}N^{\beta'}(m_0^{\beta'})^2\leq 12$ which implies the bound

$$|m_0^{\beta'}|\leq 3\,. \tag{1.59}$$

This is an even smaller bound than (1.53) derived previously for special branes satisfying $0\leq C\left(\frac{b}{2}+\frac{j}{j_0}, b+\frac{m^\beta}{m_0^\beta}\right)$ because each $T_i = 12\mathcal{K}_{00i}$ is a integer multiple of 12. Thus, the overall bound on m_0^β for a β-brane is still $|m_0^\beta|\leq\max(T_i)$.

Recall γ branes by definition have $m_0^\gamma = 0$. Thus we are done bounding m_0^α, where (1.48) is the concrete, computable bound. In summary, we have found the precise bounds in Table 1.1.

Branes	Special branes with $0 \leq C\left(\frac{b}{2}+\frac{j}{j_0}, b+\frac{m^\beta}{m_0^\beta}\right)$	Special branes with $0 \geq C\left(\frac{b}{2}+\frac{j}{j_0}, b+\frac{m^\beta}{m_0^\beta}\right)$	Mixed branes	γ-branes
m_0^α-bound	$\lvert m_0^\beta\rvert \leq \max(T_i)$	$\lvert m_0^\beta\rvert \leq 3$	$\lvert m_0^\beta\rvert \leq 3$	$m_0^\gamma = 0$

Table 1.1: Summary of bounds on m_0^α.

Bounds on the number of Solutions to the Vector m^β

We begin by noting that (1.32) can be viewed as the following matrix multiplication equation

$$t^\beta := \begin{pmatrix} t_1^\beta \\ . \\ . \\ . \\ t_p^\beta \end{pmatrix} = 2C \cdot \left(\frac{b}{2}+\frac{m^\beta}{m_0^\beta}\right). \tag{1.60}$$

The invertible matrix $2C$ gives a 1-1 correspondence between the vector m^β and the vector t^β. Thus, in order to show that there are finitely many solutions for the vector m^β, we can equivalently show that there are finitely many solutions for the vector t^β.

We can accomplish this by showing each component t_i^β is bounded. We recall that it suffices to prove each t_i^β is bounded above: since $(m_0^\beta)^2$ is bounded as we have just shown, an upper bound also implies a lower bound by the second inequality in (1.33). Since the t_i^β of special branes are by definition bounded above by 0, see Definition 1, we only have to bound the t_i^β of mixed branes.

It is important for finding this upper bound on the t_i^β, to first analyze how each type of branes contribute to the sign of a tadpole. We obtain the table 1.2, where we have indicated in parenthesis where the corresponding result will be proven in this work.

Next, we proceed with proving the results of this table. We begin with the following

	Special branes		Mixed branes	γ-branes
0^{th}-tadpole	positive ($\Rightarrow \forall\, \tilde{t}_i^{\beta} < 0$ by Cor. 1)	negative	negative (by Prop. 2)	negative (by Prop. 1)
i^{th}-tadpole	negative (by (1.32) and Def. 1)		$\text{sign}(t_i^{\beta})$ (by (1.32))	0

Table 1.2: Summary of the contributions of the different types of branes to the different tadpoles.

Proposition 1. *γ-branes only contribute negatively to the 0^{th}-tadpole (1.31). Furthermore, any γ-brane contributing zero to the 0^{th}-tadpole is the trivial brane, i.e. $m_I^{\gamma} = 0$ for all I.*

Proof. A γ-brane's contribution to the 0^{th}-tadpole is proportional to $C(m^{\gamma}, m^{\gamma})$ by (1.31). In addition, for γ-branes, the SUSY equality in (1.4) reads

$$C\left(\left(\frac{b}{2} + \frac{j}{j_0}\right), m^{\gamma}\right) = 0\,, \tag{1.61}$$

as can be seen by setting $m_0^{\gamma} = 0$ and using the intersection relations (1.7).

We recall that C has Minkowski signature $(1,1)$ for $\mathbb{F}_k$ and $(1,n)$ for dP_n and the toric surfaces. The vector $\frac{b}{2} + \frac{j}{j_0}$ is time-like, since

$$C\left(\left(\frac{b}{2} + \frac{j}{j_0}\right), \left(\frac{b}{2} + \frac{j}{j_0}\right)\right) = \frac{1}{4}\mathcal{K}_{000} + \sum_{i=1}^{p} \mathcal{K}_{00i}\frac{j_i}{j_0} + C\left(\frac{j}{j_0}, \frac{j}{j_0}\right) > 0\,. \tag{1.62}$$

Here, the first term on the RHS of (1.62) is positive because $\mathcal{K}_{000} = 8$ for $\mathbb{F}_n$, $9-n$ for dP_n and Table 1.5 applies for toric surfaces. The second term is positive because $j_I > 0$ and for $\mathbb{F}_k$, $\mathcal{K}_{001} = 2$, $\mathcal{K}_{002} = 2+k$; for dP_n, $\mathcal{K}_{00i} = 2, 3$; for toric surfaces, all relevant entries in Table 1.5 are positive. Finally, the third term is positive because it is proportional to the volume of B. By (1.61) the vector m^{γ} is orthogonal to a time-like vector, thus, it is space-like, i.e. $0 > C(m^{\gamma}, m^{\gamma})$, unless it is the zero vector, which trivially has $C(m^{\gamma}, m^{\gamma}) = 0$.

□

Proposition 2. *Only special branes contribute positively to the* 0^{th}*-tadpole. This is equivalent to the fact, that mixed branes only contribute negatively to the* 0^{th}*-tadpole.*

Proof. We recall that the 0^{th}-tadpole can be written in the form (1.39) for arbitrary choices of $\{i,k\}$, $i \neq k$. Focusing on its RHS, we note that the second term is always negative by the positive semi-definiteness of the matrices $M_{\{i,k\}}$. Furthermore, the third term is always negative by Proposition 1. Thus, the RHS of (1.39) can only be positive, if the first term on the RHS is positive. This implies that all $\tilde{t}_i^\beta = \mathcal{K}_{00i} + t_i^\beta$, cf. (1.40), have to be of the same sign: if not, there exists a pair $\tilde{t}_i^\beta$, $\tilde{t}_k^\beta$ of opposite sign. Writing the RHS of (1.39) in terms of this pair, the first term is negative and the entire RHS of (1.39) would be negative.

If all $\tilde{t}_i^\beta$ are negative, all t_i^β have to be strictly negative since each $\mathcal{K}_{00i}$ are strictly positive. By Definition 1, a β-brane with this property is a special brane. If the $\tilde{t}_i^\beta$ are all positive, then we have $\frac{1}{2}\sum_{i=1}^p \tilde{t}_i^\beta \left(\frac{b_i}{2} + \frac{j_i}{j_0}\right) = C\left(\frac{b}{2} + \frac{j}{j_0}, b + \frac{m^\beta}{m_0^\beta}\right) \geq 0$, and by Lemma 1 it is also a special brane. □

Corollary 1. *A special brane that contributes positively to the* 0^{th}*-tadpole must have* $\tilde{t}_i^\beta < 0$ *for all i.*

Proof. Recall from the proof of Proposition 1 that a special brane which contributes positively to the 0^{th}-tadpole must have all $\tilde{t}_i^\beta$ of the same sign. If they are all negative, we are done. Thus, assume all $\tilde{t}_i^\beta \geq 0$. We prove this is not possible using a similar argument as in the proof of Lemma 1.

Since $\mathcal{K}_{00i} > 0 \ \ \forall i$ and we are considering a special brane, i.e. all $t_i^\beta < 0$, having $\tilde{t}_i^\beta = (\mathcal{K}_{00i} + t_i^\beta) \geq 0 \ \ \forall i$ means $|t_i^\beta| \leq \mathcal{K}_{00i} \ \ \forall i$. Now consider the SUSY equality (1.39). Since the M-matrix is positive semi-definite, the RHS of (1.39) is at most $\left[\frac{1}{4}\mathcal{K}_{000} + \frac{3}{2}x^{\{i,k\}}\mathcal{K}_{00i}\mathcal{K}_{00k}\right](m_0^\beta)^2$. Also, by the last inequality in (1.37), we have

$$6\sum_{i=1}^{p} T_i\left(\frac{b_i}{2} + \frac{j_i}{j_0}\right) > \mathcal{K}_{000}\sum_{\beta} N_\beta (m_0^\beta)^2, \tag{1.63}$$

i.e. $(m_0^\beta)^2$ is smaller than a linear combination of j_i/j_0, so is $\left[\frac{1}{4}\mathcal{K}_{000}+\frac{3}{2}x^{\{i,k\}}\mathcal{K}_{00i}\mathcal{K}_{00k}\right](m_0^\beta)^2$, since the prefactor $\left[\frac{1}{4}\mathcal{K}_{000}+\frac{3}{2}x^{\{i,k\}}\mathcal{K}_{00i}\mathcal{K}_{00k}\right] \sim \mathcal{K}_{000}$. However, $\tilde{t}_i^\beta > 0$ for all i means $\frac{1}{2}\sum_{i=1}^p \tilde{t}_i^\beta\left(\frac{b_i}{2}+\frac{j_i}{j_0}\right) = C\left(\frac{b}{2}+\frac{j}{j_0}, b+\frac{m^\beta}{m_0^\beta}\right) \geq 0$, which implies that the LHS of (1.39) is at least $3C(j,j)$ which is quadratic in the j_i.

Thus, in the limit that all j_I are large, the LHS of (1.39) will always be greater than its RHS, thus violating the SUSY equality.[13] □

This concludes the proof of the results in Table 1.2. We prove three more important Lemmas before we finally derive the bounds on t_i^β.

For the rest of the proof, we will label special branes that contribute positively to the 0^{th}-tadpole by β_s, and mixed branes by β_m. We also use the simplified notation

$$\sum_{\beta_m,+} \equiv \sum_{\beta_m,\tilde{t}_i^{\beta_m}\geq 0} . \tag{1.64}$$

The index i is omitted in this simplified notation when it is clear from the context to which i we are referring.

Lemma 2. *For any index i, we have the following inequality:*

$$\sum_{\beta_s} N^{\beta_s}\left|\tilde{t}_i^{\beta_s}\right|(m_0^{\beta_s})^2 < \sum_{\beta_m,+} N^{\beta_m}\tilde{t}_i^{\beta_m}(m_0^{\beta_m})^2 + T_i . \tag{1.65}$$

Proof. By (1.33), we have a lower bound for the i^{th}-tadpole. Thus, we have the following

[13] The precise value of the j_I at which the SUSY equality is violated can be computed as mentioned in Remark 2. For example, for $\mathbb{F}_k$, we find that the SUSY equality is violated for $j_I \geq 10\ \forall I$.

inequality for the i^{th}-tadpole:

$$
\begin{aligned}
T_i &\geq \sum_{\beta, t_i^\beta<0} N^\beta \left|t_i^\beta\right| (m_0^\beta)^2 - \sum_{\beta_m, t_i^{\beta_m}\geq 0} N^{\beta_m} t_i^{\beta_m} (m_0^{\beta_m})^2 \geq \sum_{\beta_s} N^{\beta_s} \left|t_i^{\beta_s}\right| (m_0^{\beta_s})^2 - \sum_{\beta_m, t_i^{\beta_m}\geq 0} N^{\beta_m} t_i^{\beta_m} (m_0^{\beta_m})^2 \\
&> \sum_{\beta_s} N^{\beta_s} \left|t_i^{\beta_s}\right| (m_0^{\beta_s})^2 - \sum_{\beta_m, t_i^{\beta_m}\geq 0} N^{\beta_m} t_i^{\beta_m} (m_0^{\beta_m})^2 - \sum_{\beta_s} N^{\beta_s} \mathcal{K}_{00i} (m_0^{\beta_s})^2 - \sum_{\beta_m, t_i^{\beta_m}\geq 0} N^{\beta_m} \mathcal{K}_{00i} (m_0^{\beta_m})^2 \\
&\quad - \sum_{\beta_m, t_i^{\beta_m}<0, \tilde{t}_i^{\beta_m}\geq 0} N^{\beta_m} \tilde{t}_i^{\beta_m} (m_0^{\beta_m})^2 \\
&= \sum_{\beta_s} N^{\beta_s} \left|\tilde{t}_i^{\beta_s}\right| (m_0^{\beta_s})^2 - \sum_{\beta_m, t_i^{\beta_m}\geq 0} N^{\beta_m} \tilde{t}_i^{\beta_m} (m_0^{\beta_m})^2 - \sum_{\beta_m, t_i^{\beta_m}<0, \tilde{t}_i^{\beta_m}\geq 0} N^{\beta_m} \tilde{t}_i^{\beta_m} (m_0^{\beta_m})^2 \\
&= \sum_{\beta_s} N^{\beta_s} \left|\tilde{t}_i^{\beta_s}\right| (m_0^{\beta_s})^2 - \sum_{\beta_m, +} N^{\beta_m} \tilde{t}_i^{\beta_m} (m_0^{\beta_m})^2 ,
\end{aligned}
\tag{1.66}
$$

where in the first inequality, we split terms in the sum of (1.33) into positive and negative contributions, as indicated in the summation by $t_i^{\beta_m} \geq 0$ and $t_i^{\beta_m} < 0$. In the second inequality, in the first term, we only kept those special branes in the sum that contribute positively to the 0^{th}-tadpole, which are labelled by β_s. In the second line, we added three more negative terms and in the next equality, we combined them into three sums using (1.40), that yield the two sums in the last line. □

Lemma 3. *For any pair of a special brane that contributes positively to the* 0^{th}*-tadpole and a mixed brane, there exists an index k such that* $\tilde{t}_k^{\beta_m}$ *is strictly negative and* $|\tilde{t}_k^{\beta_m}| > |\tilde{t}_k^{\beta_s}|$. *In particular*

$$
|\tilde{t}_k^{\beta_m}| - |\tilde{t}_k^{\beta_s}| \geq \frac{1}{3} . \tag{1.67}
$$

Proof. Suppose the converse is true, i.e. for some pair of a special brane that contributes positively to the 0^{th}-tadpole and a mixed brane, there does not exist an index k such that $\tilde{t}_k^{\beta_m}$ is strictly negative and $|\tilde{t}_k^{\beta_m}| > |\tilde{t}_k^{\beta_s}|$. Then, consider the difference of the SUSY equality

(1.39) for the mixed brane and for the special brane:

$$\begin{aligned} & \text{LHS of (1.39) for the mixed brane - LHS of (1.39) for the special brane} \\ = \; & \text{RHS of (1.39) for the mixed brane - RHS of (1.39) for the special brane} \end{aligned} \tag{1.68}$$

We will show that (1.68) will be violated. To simplify our notation, we will in the following denote the difference of the LHS and RHS in (1.68) by Δ_{LHS} and Δ_{RHS}, respectively. First consider the difference Δ_{LHS}. The first term, $3C\left(\frac{j}{j_0}, \frac{j}{j_0}\right) j_0^2$, is the same for both branes. Thus, by expanding everything out and using (1.32) and (1.40), we obtain

$$\begin{aligned} \Delta_{\text{LHS}} &= 6C\left(\frac{b}{2}+\frac{j}{j_0}, b+\frac{m^{\beta_m}}{m_0^{\beta_m}}\right) j_0^2 - 6C\left(\frac{b}{2}+\frac{j}{j_0}, b+\frac{m^{\beta_s}}{m_0^{\beta_s}}\right) j_0^2 \\ &= 3\sum_{i=1}^{p} \tilde{t}_i^{\beta_m}\left(\frac{b_i}{2}+\frac{j_i}{j_0}\right) j_0^2 - 3\sum_{i=1}^{p} \tilde{t}_i^{\beta_s}\left(\frac{b_i}{2}+\frac{j_i}{j_0}\right) j_0^2 . \end{aligned} \tag{1.69}$$

By Corollary 1, since the special brane contributes positively to the 0^{th}-tadpole, $\tilde{t}_i^{\beta_s} < 0$ for all i. Also notice that the mixed brane must have at least one i for which $\tilde{t}_i^{\beta_m} > 0$, because by definition, a mixed brane must have at least one i for which $t_i^{\beta_m} \geq 0$, and for this i, by (1.40) and the positivity of $\mathcal{K}_{00i}$, $\tilde{t}_i^{\beta_m} > 0$. Labelling those i for which $\tilde{t}_i^{\beta_m} > 0$ as $i+$, and those i for which $\tilde{t}_i^{\beta_m} \leq 0$ as $i-$, (1.69) becomes

$$\begin{aligned} \Delta_{\text{LHS}} =& 3j_0^2\Big[\sum_{i+}\tilde{t}_{i+}^{\beta_m}\Big(\frac{b_{i+}}{2}+\frac{j_{i+}}{j_0}\Big)+\sum_{i-}(|\tilde{t}_{i-}^{\beta_s}|-|\tilde{t}_{i-}^{\beta_m}|)\Big(\frac{b_{i-}}{2}+\frac{j_{i-}}{j_0}\Big)+\sum_{i+}|\tilde{t}_{i+}^{\beta_s}|\Big(\frac{b_{i+}}{2}+\frac{j_{i+}}{j_0}\Big)\Big] \\ \geq& 3j_0^2\left[\sum_{i+}\tilde{t}_{i+}^{\beta_m}\left(\frac{b_{i+}}{2}+\frac{j_{i+}}{j_0}\right)+\sum_{i+}|\tilde{t}_{i+}^{\beta_s}|\left(\frac{b_{i+}}{2}+\frac{j_{i+}}{j_0}\right)\right]. \end{aligned} \tag{1.70}$$

Here in the last step we dropped the second sum, which is positive, because by assumption there does not exist an index k such that $\tilde{t}_k^{\beta_m}$ is strictly negative and $|\tilde{t}_k^{\beta_m}| > |\tilde{t}_k^{\beta_s}|$.

Notice, by (1.32), $\tilde{t}_i^{\beta_s}, \tilde{t}_i^{\beta_m}$ are rational numbers $\frac{a}{m_0^{\beta_s}}, \frac{b}{m_0^{\beta_m}}$ with $a, b \in 2\mathbb{Z}$.[14] By Table 1.1, we have $|m_0^{\beta_m}| \leq 3$. For the special brane, since $\tilde{t}_i^{\beta_s} < 0$ for all i, we have

$$0 > \frac{1}{2}\sum_{i=1}^{p} \tilde{t}_i^{\beta_s}\left(\frac{b_i}{2} + \frac{j_i}{j_0}\right) = C\left(\frac{b}{2} + \frac{j}{j_0}, b + \frac{m^{\beta_s}}{m_0^{\beta_s}}\right). \tag{1.71}$$

Thus, the bound $|m_0^{\beta_s}| \leq 3$ in the third column of Table 1.1 applies. This implies both $|\tilde{t}_i^{\beta_s}| > 0$, $\tilde{t}_{i+}^{\beta_m} > 0$ are either integers or a third of integers:

$$3\tilde{t}_{i+}^{\beta_m} > 1\,, \qquad 3|\tilde{t}_i^{\beta_s}| > 1\,. \tag{1.72}$$

Hence, (1.70) becomes

$$\begin{aligned} \Delta_{\text{LHS}} &\geq \sum_{i+} 3\tilde{t}_{i+}^{\beta_m}\left(\frac{b_{i+}}{2} + \frac{j_{i+}}{j_0}\right) j_0^2 + \sum_{i+} 3|\tilde{t}_{i+}^{\beta_s}|\left(\frac{b_{i+}}{2} + \frac{j_{i+}}{j_0}\right) j_0^2 \geq 2\sum_{i+}\left(\frac{b_{i+}}{2} + \frac{j_{i+}}{j_0}\right) j_0^2 \\ &\geq 2\sum_{i+} j_{i+} j_0\,, \end{aligned} \tag{1.73}$$

where in the last step we dropped the term containing the positive b_i. We have discussed that at least one index $i+$ exists. With $j_I \gg 1$ for all I, (1.73) shows that the difference between the LHS of (1.39) for the two branes is large.

Next, we show that the difference Δ_{RHS} between the RHS of (1.39) for the two branes is much smaller. Starting from the RHS of (1.39) for the special brane we note the identity

$$\begin{aligned} &3\left[\tfrac{1}{2}x_{\{i,k\}}\tilde{t}_i^{\beta}\tilde{t}_k^{\beta} - M_{\{i,k\}}\left(b + \tfrac{m^{\beta}}{m_0^{\beta}}, b + \tfrac{m^{\beta}}{m_0^{\beta}}\right)\right](m_0^{\beta})^2 \\ =&\left[\tfrac{1}{4}\mathcal{K}_{000} + \tfrac{3}{2}x_{\{i,k\}}t_i^{\beta}t_k^{\beta} - 3M_{\{i,k\}}\left(\tfrac{b}{2} + \tfrac{m^{\beta}}{m_0^{\beta}}, \tfrac{b}{2} + \tfrac{m^{\beta}}{m_0^{\beta}}\right)\right](m_0^{\beta})^2 + \tfrac{3}{2}\sum_{i=1}^{p} b_i\tilde{t}_i^{\beta}(m_0^{\beta})^2 - \mathcal{K}_{000}(m_0^{\beta})^2\,. \end{aligned} \tag{1.74}$$

Since the special brane contributes positively to the 0^{th}-tadpole, the LHS of (1.74) is pos-

[14] By (1.32), we have $\tilde{t}_k^{\beta_s} = 2\mathcal{K}_{00k} + 2\sum_j C_{kj}\frac{m_j^{\beta_s}}{m_0^{\beta_s}} = \frac{a}{m_0^{\beta_s}}$, $\tilde{t}_k^{\beta_m} = 2\mathcal{K}_{00k} + 2\sum_j C_{kj}\frac{m_j^{\beta_m}}{m_0^{\beta_m}} = \frac{b}{m_0^{\beta_m}}$ for $a, b \in 2\mathbb{Z}$.

itive. We also recall that $\tilde{t}_i^{\beta} < 0$ for all i by Corollary 1, which implies that the second last term on the RHS of (1.74) is strictly negative, as $b_i \geq 0$. In addition, the last term on the RHS is always negative for the bases B we consider. Thus, the term in square brackets on the RHS of (1.74), which is the RHS of (1.39), must be strictly positive. In particular, it must have a bigger magnitude than that of (the next to last term and) the last term:

$$\text{RHS of (1.39) for the special brane} > \mathcal{K}_{000}(m_0^{\beta_s})^2.$$

Next, consider the RHS of (1.39) for the mixed brane. Since it is a mixed brane, we can pick a pair of $t_i^{\beta_m}$, $t_k^{\beta_m}$ of opposite signs to make the second term of the RHS of (1.39) negative. By the positive semi-definiteness of the M-matrix, the third term of the RHS of (1.39) is always negative. Thus

$$\text{RHS of (1.39) for the mixed brane} \leq \frac{1}{4}\mathcal{K}_{000}(m_0^{\beta_m})^2.$$

Hence, we obtain, using again the bounds on m_0^{β} from Table 1.1,

$$\Delta_{\text{RHS}} < \frac{1}{4}\mathcal{K}_{000}(m_0^{\beta_m})^2 - \mathcal{K}_{000}(m_0^{\beta_s})^2 \leq \frac{1}{4}\mathcal{K}_{000}(3)^2 - \mathcal{K}_{000}(1)^2 = \frac{5}{4}\mathcal{K}_{000}\,. \tag{1.75}$$

By comparison of (1.73) and (1.75), using the property $j_I \gg 1$ for all I, we see that we will always have

$$\Delta_{\text{LHS}} > \Delta_{\text{RHS}}\,, \tag{1.76}$$

which clearly violates (1.68).

Finally we prove (1.67). Recall both $\tilde{t}_k^{\beta_s}$, $\tilde{t}_k^{\beta_m}$ are either integers or a third of an integer. Since $|\tilde{t}_k^{\beta_m}| > |\tilde{t}_k^{\beta_s}|$, their difference is at least a non-zero integer divided by their common denominator, which is 3, i.e. (1.67) applies. □

We make two useful definitions for the next lemma before stating it. Recall that the contribution of a mixed brane to the 0^{th}-tadpole is negative, cf. Table 1.2, and is given by the first term in (1.39):

$$0 \geq R^{\beta_m} \equiv N^{\beta_m}\left[\frac{1}{2}x_{\{i,k\}}\tilde{t}_i^{\beta_m}\tilde{t}_k^{\beta_m} - M_{\{i,k\}}\left(b+\frac{m^{\beta_m}}{m_0^{\beta_m}}, b+\frac{m^{\beta_m}}{m_0^{\beta_m}}\right)\right](m_0^{\beta_m})^2\,. \tag{1.77}$$

Similarly, for a special brane that contributes positively to the 0^{th}-tadpole, its contribution is also given by the first term in (1.39):

$$0 \leq S^{\beta_s} \equiv N^{\beta_s}\left[\frac{1}{2}x_{\{i,k\}}\tilde{t}_i^{\beta_s}\tilde{t}_k^{\beta_s} - M_{\{i,k\}}\left(b+\frac{m^{\beta_s}}{m_0^{\beta_s}}, b+\frac{m^{\beta_s}}{m_0^{\beta_s}}\right)\right](m_0^{\beta_s})^2\,. \tag{1.78}$$

Thus, the total positive contribution to the 0^{th}-tadpole, and part of the total negative contributions to the 0^{th}- tadpole from mixed branes with $\tilde{t}_i^{\beta_m} \geq 0$ are

$$\sum_{\beta_s} S^{\beta_s} \geq 0\,, \qquad\qquad \sum_{\beta_m,+} R^{\beta_m} \leq 0\,. \tag{1.79}$$

Lemma 4. *Given $h_1, h_2 \in \mathbb{Q}^+$, $0 < h_1, h_2 \leq 1$, so that for some index i*

$$h_1 \sum_{\beta_m,+} N^{\beta_m}\tilde{t}_i^{\beta_m}(m_0^{\beta_m})^2 \;= h_2 \sum_{\beta_s} N^{\beta_s}\left|\tilde{t}_i^{\beta_s}\right|(m_0^{\beta_s})^2 \tag{1.80}$$

holds, then $h_1\sum_{\beta_m,+}|R^{\beta_m}| > h_2\sum_{\beta_s}S^{\beta_s}$. In particular,

$$h_1 \sum_{\beta_m,+}|R^{\beta_m}| - h_2\sum_{\beta_s}S^{\beta_s} \geq \frac{1}{6}\min\Big(x_{\{i,k\}}\Big)h_1\sum_{\beta_m,+}N^{\beta_m}\tilde{t}_i^{\beta_m}(m_0^{\beta_m})^2\,, \tag{1.81}$$

where the minimum and maximum is taken over all pairs $\{i,k\}$ of indices of Kähler cone generators in the subcone, but can also be taken across the entire Kähler cone.

Proof. We introduce a partition of unity $\{f^{\beta_s}\}_{\beta_s}$, and, for every index β_s, a partition of

unity $\{g^{\beta_s,\beta_m}\}_{\beta_m,+}$,[15] i.e.

$$\sum_{\beta_s} f^{\beta_s} = 1\,, \qquad \sum_{\beta_m,+} g^{\beta_s,\beta_m} = 1\,, \qquad f^{\beta_s},\, g^{\beta_s,\beta_m} \in \mathbb{Q}^+\,, \qquad 0 < f^{\beta_s}, g^{\beta_s,\beta_m} \leq 1\,, \tag{1.82}$$

defined by the property

$$f^{\beta_s} h_1 N^{\beta_m} \tilde{t}_i^{\beta_m} (m_0^{\beta_m})^2 = g^{\beta_s,\beta_m} h_2 N^{\beta_s} \left|\tilde{t}_i^{\beta_s}\right| (m_0^{\beta_s})^2\,. \tag{1.83}$$

Inserting unity as $1 = \sum_{\beta_s} f^{\beta_s} = \sum_{\beta_m,+}, g^{\beta_s,\beta_m}$, we obtain the obvious identity

$$\begin{aligned} & h_1 \sum_{\beta_m,+} |R^{\beta_m}| - h_2 \sum_{\beta_s} S^{\beta_s} = \Big(\sum_{\beta_s} f^{\beta_s}\Big) h_1 \sum_{\beta_m,+} |R^{\beta_m}| - h_2 \sum_{\beta_s} \Big(\sum_{\beta_m,+} g^{\beta_s,\beta_m}\Big) S^{\beta_s} \\ = & \sum_{\beta_s} \sum_{\beta_m,+} \left(f^{\beta_s} h_1 |R^{\beta_m}| - g^{\beta_s,\beta_m} h_2 S^{\beta_s} \right). \end{aligned} \tag{1.84}$$

For each summand in the sum of the last line of (1.84), we have

$$\begin{aligned} f^{\beta_s} h_1 |R^{\beta_m}| - g^{\beta_s,\beta_m} h_2 S^{\beta_s} = & f^{\beta_s} h_1 N^{\beta_m} \Big| \tfrac{1}{2} x_{\{i,k\}} \underbrace{\tilde{t}_i^{\beta_m}}_{\geq 0} \underbrace{\tilde{t}_k^{\beta_m}}_{<0} - M_{\{i,k\}} \Big(b + \frac{m^{\beta_m}}{m_0^{\beta_m}}, b + \frac{m^{\beta_m}}{m_0^{\beta_m}}\Big) \Big| (m_0^{\beta_m})^2 \\ & - g^{\beta_s,\beta_m} h_2 N^{\beta_s} \Big[\frac{1}{2} x_{\{i,k\}} \underbrace{\tilde{t}_i^{\beta_s}}_{<0} \underbrace{\tilde{t}_k^{\beta_s}}_{<0} - M_{\{i,k\}} \Big(b + \frac{m^{\beta_s}}{m_0^{\beta_s}}, b + \frac{m^{\beta_s}}{m_0^{\beta_s}}\Big) \Big] (m_0^{\beta_s})^2. \end{aligned} \tag{1.85}$$

Here, the pair $\{i,k\}$ is chosen so that the index i is the one for which (1.80) holds, and the index k is chosen such that the inequality $|\tilde{t}_k^{\beta_m}| - |\tilde{t}_k^{\beta_s}| \geq \frac{1}{3}$ of Lemma 3 holds for the pair (β_s, β_m) of special and mixed brane in (1.85). We emphasize that the choice of this index k depends on the brane pair (β_s, β_m) and thus might be different for each summand in (1.84).

[15] We emphasize that the index β_m on g^{β_s,β_m} is only limited to mixed branes with $\tilde{t}_i^{\beta_m} \geq 0$.

Next, we drop the positive semi-definite M-matrix terms in (1.85) to get

$$\begin{aligned} f^{\beta_s} h_1 |R^{\beta_m}| - g^{\beta_s,\beta_m} h_2 S^{\beta_s} &\geq \frac{1}{2} x_{\{i,k\}} \Big[f^{\beta_s} h_1 N^{\beta_m} \tilde{t}_i^{\beta_m} (m_0^{\beta_m})^2 \Big| \tilde{t}_k^{\beta_m} \Big| - g^{\beta_s,\beta_m} h_2 N^{\beta_s} \Big| \tilde{t}_i^{\beta_s} \Big| (m_0^{\beta_s})^2 \Big| \tilde{t}_k^{\beta_s} \Big| \Big] \\ &= \frac{1}{2} x_{\{i,k\}} \left(f^{\beta_s} h_1 N^{\beta_m} \tilde{t}_i^{\beta_m} (m_0^{\beta_m})^2 \right) \underbrace{\left(\Big| \tilde{t}_k^{\beta_m} \Big| - \Big| \tilde{t}_k^{\beta_s} \Big| \right)}_{\geq 1/3} \\ &\geq \frac{1}{6} \min(x_{\{i,k\}}) f^{\beta_s} h_1 N^{\beta_m} \tilde{t}_i^{\beta_m} (m_0^{\beta_m})^2 , \end{aligned} \tag{1.86}$$

where we have used that the coefficients of $|\tilde{t}_k^{\beta_m}|$, $|\tilde{t}_k^{\beta_s}|$ in the first line are equal by (1.83). In addition, we have removed the aforementioned implicit dependence of the index k on (β_s, β_m) by taking the minimum over all $\{i,k\}$.

Thus, plugging (1.86) into (1.84) we obtain

$$h_1 \sum_{\beta_m,+} |R^{\beta_m}| - h_2 \sum_{\beta_s} S^{\beta_s} \geq \frac{1}{6} \min\Big(x_{\{i,k\}} \Big) h_1 \sum_{\beta_m,+} N^{\beta_m} \tilde{t}_i^{\beta_m} (m_0^{\beta_m})^2 , \tag{1.87}$$

where we performed the sum over β_s and used $\sum_{\beta_s} f^{\beta_s} = 1$, cf. (1.82). □

Now we are finally ready to show that every t_i^β has an upper bound.

Theorem 2. *For all i and β, t_i^β are bounded from above as*

$$t_i^\beta \leq \frac{6T_0 + 3T_i \cdot \max(x_{\{i,k\}}) \cdot \max(T_l)}{\min(x_{\{i,k\}})} , \tag{1.88}$$

where the minimum and maximum is taken over all pairs $\{i,k\}$ of indices of Kähler cone generators in the subcone, but can also be taken across the entire Kähler cone.

Proof. We derive the above bound for t_i^β for an arbitrary index i. By Lemma 2, we either have $\sum_{\beta_s} N^{\beta_s} \Big| \tilde{t}_i^{\beta_s} \Big| (m_0^{\beta_s})^2 \leq \sum_{\beta_m,+} N^{\beta_m} \tilde{t}_i^{\beta_m} (m_0^{\beta_m})^2$, or $\sum_{\beta_m,+} N^{\beta_m} \tilde{t}_i^{\beta_m} (m_0^{\beta_m})^2 < \sum_{\beta_s} N^{\beta_s} \Big| \tilde{t}_i^{\beta_s} \Big| (m_0^{\beta_s})^2 < \sum_{\beta_m,+} N^{\beta_m} \tilde{t}_i^{\beta_m} (m_0^{\beta_m})^2 + T_i$. We consider each case separately:
Case 1: $\sum_{\beta_s} N^{\beta_s} \Big| \tilde{t}_i^{\beta_s} \Big| (m_0^{\beta_s})^2 \leq \sum_{\beta_m,+} N^{\beta_m} \tilde{t}_i^{\beta_m} (m_0^{\beta_m})^2$.

In other words, we have a relation as in (1.80) with $h_1 \leq 1$, $h_2 = 1$,

$$h_1 \sum_{\beta_m,+} N^{\beta_m} \tilde{t}_i^{\beta_m} (m_0^{\beta_m})^2 \; = \sum_{\beta_s} N^{\beta_s} \left| \tilde{t}_i^{\beta_s} \right| (m_0^{\beta_s})^2 \,. \tag{1.89}$$

Starting with the first inequality in (1.33) and employing (1.77), (1.78), we obtain

$$\begin{aligned}
T_0 \geq & \sum_{\beta_m,+} |R^{\beta_m}| - \sum_{\beta_s} S^{\beta_s} = (1-h_1) \sum_{\beta_m,+} |R^{\beta_m}| + h_1 \sum_{\beta_m,+} |R^{\beta_m}| - \sum_{\beta_s} S^{\beta_s} \\
\geq & (1-h_1) \sum_{\beta_m,+} |R^{\beta_m}| + \frac{1}{6} \min(x_{\{i,k\}}) h_1 \sum_{\beta_m,+} N^{\beta_m} \tilde{t}_i^{\beta_m} (m_0^{\beta_m})^2 \\
\geq & (1-h_1) \sum_{\beta_m,+} N^{\beta_m} \frac{1}{2} x_{\{i,k\}} \tilde{t}_i^{\beta_m} \underbrace{|\tilde{t}_k^{\beta_m}|}_{\geq 1/3} (m_0^{\beta_m})^2 + \frac{1}{6} \min(x_{\{i,k\}}) h_1 \sum_{\beta_m,+} N^{\beta_m} \tilde{t}_i^{\beta_m} (m_0^{\beta_m})^2 \\
\geq & (1-h_1) \frac{1}{6} \min(x_{\{i,k\}}) \sum_{\beta_m,+} N^{\beta_m} \tilde{t}_i^{\beta_m} (m_0^{\beta_m})^2 + h_1 \frac{1}{6} \min(x_{\{i,k\}}) \sum_{\beta_m,+} N^{\beta_m} \tilde{t}_i^{\beta_m} (m_0^{\beta_m})^2 \\
= & \frac{1}{6} \min(x_{\{i,k\}}) \sum_{\beta_m,+} N^{\beta_m} \tilde{t}_i^{\beta_m} (m_0^{\beta_m})^2 \,,
\end{aligned} \tag{1.90}$$

where in the first inequality we only kept negative contributions to the 0^{th}-tadpole from mixed branes with $\tilde{t}_i^{\beta_m} \geq 0$ (see Table 1.2). In the second line we used Lemma 4. In the third line we plugged in the definition (1.77) of R^{β_m}, where we picked our choice of the pair $\{i,k\}$ so that i is the same index i that we want to derive a bound for t_i^{β}, and k such that $|\tilde{t}_k^{\beta_m}| \geq \frac{1}{3}$ [16], and dropped the M-matrix term. The remaining two lines of (1.90) are just algebra. Thus, we have the following bound on t_i:

$$T_0 \geq \frac{1}{6} \min(x_{\{i,k\}}) \sum_{\beta_m,+} N^{\beta_m} \tilde{t}_i^{\beta_m} (m_0^{\beta_m})^2, \implies t_i^{\beta} < \sum_{\beta_m,+} N^{\beta_m} \tilde{t}_i^{\beta_m} (m_0^{\beta_m})^2 \leq \frac{6T_0}{\min(x_{\{i,k\}})} \,. \tag{1.91}$$

[16] Indeed, since a non-zero $\tilde{t}_k^{\beta_m}$ is at least a third of an integer, we only have to argue that a k with a non-zero $\tilde{t}_k^{\beta_m}$ exists. But this is true since otherwise $C\left(\frac{b}{2} + \frac{j}{j_0}, b + \frac{m^{\beta_m}}{m_0^{\beta_m}}\right) = \frac{1}{2} \sum_{i=1}^{p} \tilde{t}_i^{\beta_m} \left(\frac{b_i}{2} + \frac{j_i}{j_0}\right) \geq 0$, which by Lemma 1 implies that this brane would be a special, not a mixed brane.

Case 2: $\sum_{\beta_m,+} N^{\beta_m}\tilde{t}_i^{\beta_m}(m_0^{\beta_m})^2 < \sum_{\beta_s} N^{\beta_s}\left|\tilde{t}_i^{\beta_s}\right|(m_0^{\beta_s})^2 < \sum_{\beta_m,+} N^{\beta_m}\tilde{t}_i^{\beta_m}(m_0^{\beta_m})^2 + T_i$.

In this case we are in a special case of (1.80) with $h_1 = 1$, $h_2 \leq 1$ and

$$\sum_{\beta_m,+} N^{\beta_m}\tilde{t}_i^{\beta_m}(m_0^{\beta_m})^2 \;= h_2 \sum_{\beta_s} N^{\beta_s}\left|\tilde{t}_i^{\beta_s}\right|(m_0^{\beta_s})^2 \qquad (1-h_2)\sum_{\beta_s} N^{\beta_s}\left|\tilde{t}_i^{\beta_s}\right|(m_0^{\beta_s})^2 < T_i\,. \tag{1.92}$$

Analogous to (1.90) of Case 1, we obtain

$$\begin{aligned} T_0 &\geq \sum_{\beta_m,+} |R^{\beta_m}| - \sum_{\beta_s} S^{\beta_s} = \sum_{\beta_m,+} |R^{\beta_m}| - h_2 \sum_{\beta_s} S^{\beta_s} - (1-h_2)\sum_{\beta_s} S^{\beta_s} \\ &\geq \frac{1}{6}\min\left(x_{\{i,k\}}\right) \sum_{\beta_m,+} N^{\beta_m}\tilde{t}_i^{\beta_m}(m_0^{\beta_m})^2 - (1-h_2)\sum_{\beta_s} S^{\beta_s}\,. \end{aligned} \tag{1.93}$$

We digress to consider the following inequality:

$$\begin{aligned} &\sum_{i}^{p}\sum_{\beta_s} N^{\beta_s}\tilde{t}_i^{\beta_s}(m_0^{\beta_s})^2\left(\frac{b_i}{2}+\frac{j_i}{j_0}\right) = \sum_{\beta_s}\sum_{i}^{p} N^{\beta_s}\left(t_i^{\beta_s}+\mathcal{K}_{00i}\right)(m_0^{\beta_s})^2\left(\frac{b_i}{2}+\frac{j_i}{j_0}\right) \\ &\geq \sum_{\beta_s}\sum_{i}^{p} N^{\beta_s}t_i^{\beta_s}(m_0^{\beta_s})^2\left(\frac{b_i}{2}+\frac{j_i}{j_0}\right) \geq \sum_{\beta}\sum_{i}^{p} N^{\beta}t_i^{\beta}(m_0^{\beta})^2\left(\frac{b_i}{2}+\frac{j_i}{j_0}\right) \geq \sum_{i}^{p}(-T_i)\left(\frac{b_i}{2}+\frac{j_i}{j_0}\right), \end{aligned} \tag{1.94}$$

where in the first equality we used (1.40), in the second inequality, we extended the sum across β_s to the sum across all β because each summand is negative by (1.51), and in the last inequality we used (1.50). Comparing coefficients of $\frac{b_i}{2}+\frac{j_i}{j_0}$ between the first and last term in (1.94), we note that there has to exist an index k such that

$$T_k \geq \sum_{\beta_s} N^{\beta_s}\left|\tilde{t}_k^{\beta_s}\right|(m_0^{\beta_s})^2 \geq \left|\tilde{t}_k^{\beta_s}\right|. \tag{1.95}$$

If the index i for which we want to bound t_i^{β} coincides with such an index k, we have an obvious bound on t_i^{β}

$$T_i \geq \sum_{\beta_s} N^{\beta_s}\left|\tilde{t}_i^{\beta_s}\right|(m_0^{\beta_s})^2 > \sum_{\beta_m,+} N^{\beta_m}\tilde{t}_i^{\beta_m}(m_0^{\beta_m})^2 > t_i^{\beta}\,, \tag{1.96}$$

where in the first inequality, we used (1.95) with $k = i$, and in the second inequality we used the assumption that $\sum_{\beta_s} N^{\beta_s} \left|\tilde{t}_i^{\beta_s}\right| (m_0^{\beta_s})^2 > \sum_{\beta_m,+} N^{\beta_m} \tilde{t}_i^{\beta_m} (m_0^{\beta_m})^2$.

Thus we only need to consider $i \neq k$ with k satisfying (1.95). Then, the last term on the second line of (1.93) becomes

$$\begin{aligned}(1-h_2)\sum_{\beta_s} S^{\beta_s} &\leq (1-h_2)\sum_{\beta_s} N^{\beta_s}\frac{1}{2}x_{\{i,k\}}\left|\tilde{t}_i^{\beta_s}\right|(m_0^{\beta_s})^2\left|\tilde{t}_k^{\beta_s}\right| \\ \leq \frac{1}{2}x_{\{i,k\}} \underbrace{(1-h_2)\sum_{\beta_s} N^{\beta_s}\left|\tilde{t}_i^{\beta_s}\right|(m_0^{\beta_s})^2}_{<T_i}\cdot T_k &< \frac{1}{2}\max(x_{\{i,k\}})\cdot T_i \cdot T_k \end{aligned} \tag{1.97}$$

where in the first inequality we plugged in the definition (1.78) of S^{β_s} and picked the pair $\{i,k\}$ such that i is the index for which we want to show boundedness for t_i^{β}, k is the index such that (1.95) is satisfied and dropped the negative M-matrix term. In the second inequality we used (1.95) for $\tilde{t}_k^{\beta_s}$, as well as the second inequality in (1.92). Combining (1.93) and (1.97), we obtain

$$T_0 > \sum_{\beta_m,+}|R^{\beta_m}| - \sum_{\beta_s} S^{\beta_s} \geq \frac{1}{6}\min(x_{\{i,k\}})\sum_{\beta_m,+} N^{\beta_m}\tilde{t}_i^{\beta_m}(m_0^{\beta_m})^2 - \frac{1}{2}\max\left(x_{\{i,k\}}\right)T_i\cdot \underbrace{T_k}_{\leq \max(T_l)} \tag{1.98}$$

and arrive at the final bound

$$t_i^{\beta} < \sum_{\beta_m,+} N^{\beta_m}\tilde{t}_i^{\beta_m}(m_0^{\beta_m})^2 < \frac{6T_0 + 3T_i\cdot\max(x_{\{i,k\}})\cdot\max(T_l)}{\min(x_{\{i,k\}})}. \tag{1.99}$$

□

Bounds on n_I^{D5}

In this section, we employ the results from the previous Section 1.3.3 to derive bounds on the numbers n_I^{D5} of D5-branes. These bounds are formulated in two theorems.

Theorem 3. *For all i we have the following bound on* n_i^{D5}*:*

$$n_i^{D5} < \frac{6T_0}{\min(x_{\{i,k\}})} + T_i\,, \tag{1.100}$$

where the minimum is taken over all pairs $\{i,k\}$ *of indices of Kähler cone generators in the subcone, but can also be taken across the entire Kähler cone.*

Proof. From (1.32), we obtain

$$n_i^{D5} = \sum_\beta N^\beta t_i^\beta (m_0^\beta)^2 + T_i < \sum_\beta N^\beta t_i^\beta (m_0^\beta)^2 + T_i + \sum_\beta N^\beta \mathcal{K}_{00i} (m_0^\beta)^2 = \sum_\beta N^\beta \tilde{t}_i^\beta (m_0^\beta)^2 + T_i\,, \tag{1.101}$$

where in the last equality we used (1.40). If $\sum_\beta N^\beta \tilde{t}_i^\beta (m_0^\beta)^2 \le 0$, then we have the obvious bound $n_i^{D5} < T_i$. Conversely if $0 < \sum_\beta N^\beta \tilde{t}_i^\beta (m_0^\beta)^2$, we have

$$0 < \sum_\beta N^\beta \tilde{t}_i^\beta (m_0^\beta)^2 \le \sum_{\beta_m,+} N^{\beta_m} \tilde{t}_i^{\beta_m} (m_0^{\beta_m})^2 - \sum_{\beta_s} N^{\beta_s} |\tilde{t}_i^{\beta_s}| (m_0^{\beta_s})^2\,, \tag{1.102}$$

where we dropped negative terms in the last inequality. Thus, we are in case 1 in the proof of Theorem 2, i.e. $\sum_{\beta_s} N^{\beta_s} \left|\tilde{t}_i^{\beta_s}\right| (m_0^{\beta_s})^2 \le \sum_{\beta_m,+} N^{\beta_m} \tilde{t}_i^{\beta_m} (m_0^{\beta_m})^2$, and can use results derived previously for that case. Using the fraction h_1 defined in (1.89), (1.102) becomes

$$\sum_\beta N^\beta \tilde{t}_i^\beta (m_0^\beta)^2 \le \sum_{\beta_m,+} N^{\beta_m} \tilde{t}_i^{\beta_m} (m_0^{\beta_m})^2 - \sum_{\beta_s} N^{\beta_s} |\tilde{t}_i^{\beta_s}| (m_0^{\beta_s})^2 = (1-h_1) \sum_{\beta_m,+} N^{\beta_m} \tilde{t}_i^{\beta_m} (m_0^{\beta_m})^2\,. \tag{1.103}$$

By the third line of (1.90), we obtain

$$\begin{aligned} T_0 \ge & (1-h_1) \sum_{\beta_m,+} N^{\beta_m} \frac{1}{2} x^{\{i,k\}} \tilde{t}_i^{\beta_m} \underbrace{\frac{|\tilde{t}_k^{\beta_m}|}{\ge 1/3}} (m_0^{\beta_m})^2 + \frac{1}{6} \min\left(x_{\{i,k\}}\right) h_1 \sum_{\beta_m,+} N^{\beta_m} \tilde{t}_i^{\beta_m} (m_0^{\beta_m})^2 \\ \ge & \frac{1}{6} \min(x_{\{i,k\}}) (1-h_1) \sum_{\beta_m,+} N^{\beta_m} \tilde{t}_i^{\beta_m} (m_0^{\beta_m})^2 \end{aligned} \tag{1.104}$$

by dropping the second term on the RHS of the first line. By rearranging and combining with (1.103), we arrive at

$$\sum_{\beta} N^{\beta} \tilde{t}_i^{\beta} (m_0^{\beta})^2 \leq (1-h) \sum_{\beta_m,+} N^{\beta_m} \tilde{t}_i^{\beta_m} (m_0^{\beta_m})^2 \leq \frac{6T_0}{\min(x_{\{i,k\}})}, \tag{1.105}$$

which in combination with (1.101) gives the desired bound (1.100). □

Remark 3. We note also, that the first inequality of (1.37) forbids $(n_i^{D5} - T_i) \geq 0$ for all i, i.e. although each n_i^{D5} is bounded above by (1.100), together they are further constrained by this condition.

Theorem 4. *We have the following bound on* n_0^{D5}*:*

$$n_0^{D5} \leq \frac{1}{2} \max(x_{\{i,k\}}) \cdot \min(T_i) \cdot \max(T_i) + T_0, \tag{1.106}$$

where the minimum and maximum is taken over all pairs $\{i,k\}$ *of indices of Kähler cone generators in the subcone. The maximum can also be taken across the entire Kähler cone.*

Proof. Using (1.39), we obtain

$$\begin{aligned} n_0^{D5} &= \sum_{\beta} N^{\beta} \left[\frac{1}{2} x_{\{i,k\}} \tilde{t}_i^{\beta} \tilde{t}_k^{\beta} - M_{\{i,k\}} \left(b + \frac{m^{\beta}}{m_0^{\beta}}, b + \frac{m^{\beta}}{m_0^{\beta}} \right) \right] (m_0^{\beta})^2 + \sum_{\gamma} N^{\gamma} C(m^{\gamma}, m^{\gamma}) + T_0 \\ &\leq \sum_{\beta_s} S^{\beta_s} - \sum_{\beta_m,+} |R^{\beta_m}| + T_0 \end{aligned} \tag{1.107}$$

where we dropped some negative contributions of the first term on the RHS of the first line as well the negative γ-brane contribution and used S^{β_s}, R^{β_m} as defined in (1.78), (1.77), respectively. We see that the coarsest bound on n_0^{D5} occurs when $\sum_{\beta_s} S^{\beta_s} - \sum_{\beta_m,+} |R^{\beta_m}|$ is maximized. By (1.90), since its last line is positive, this expression is always negative in case 1 of Theorem 2. To maximize it, we look at case 2 of Theorem 2. Starting from (1.93) in case 2 of Theorem 2, we obtain

$$
\begin{aligned}
&\sum_{\beta_m,+} |R^{\beta_m}| - \sum_{\beta_s} S^{\beta_s} \geq \frac{1}{6}\min\Big(x_{\{i,k\}}\Big) \sum_{\beta_m,+} N^{\beta_m} \tilde{t}_i^{\beta_m} (m_0^{\beta_m})^2 - (1-h_2) \sum_{\beta_s} S^{\beta_s} \\
&\geq -(1-h_2) \sum_{\beta_s} S^{\beta_s} \geq -(1-h_2) \sum_{\beta_s} N^{\beta_s} \frac{1}{2} x_{\{i,k\}} \left|\tilde{t}_i^{\beta_s}\right| (m_0^{\beta_s})^2 \left|\tilde{t}_k^{\beta_s}\right| \\
&\geq -\frac{1}{2}\max(x_{\{i,k\}}) \underbrace{(1-h_2) \sum_{\beta_s} N^{\beta_s} \left|\tilde{t}_i^{\beta_s}\right| (m_0^{\beta_s})^2}_{<T_i} \cdot T_k > -\frac{1}{2}\max(x_{\{i,k\}}) \cdot T_i \cdot T_k \\
&\geq -\frac{1}{2}\max(x_{\{i,k\}}) \cdot \min(T_l) \cdot \max(T_l)\,,
\end{aligned}
\tag{1.108}
$$

where in the second inequality, we dropped the positive first term. In the third inequality, we plugged in the definition (1.78) of S^{β_s} and picked the pair $\{i,k\}$ such that k is an index so that (1.95) is satisfied, and i is the particular index such that $T_i = \min(T_l)$ if this $i \neq k$. If $i = k$, pick any other index as i, and drop the M-matrix term. In the fourth inequality we used the second inequality in (1.92). In the last inequality, we note that if we have used the first way of choosing the pair $\{i,k\}$, then $T_i = \min(T_l)$ and $T_k \leq \max(T_l)$; if we have used the second way of choosing the pair $\{i,k\}$, then $T_i \leq \max(T_l)$ and $T_k = \min(T_l)$. Combining this result with (1.107), we get the desired bound (1.106) on n_0^{D5}. □

Bounds on γ-branes

Finally, we derive a bound on the number of γ-brane configurations, i.e. we bound the flux quanta m^γ.

The contribution of γ-branes to the 0^{th}-tadpole is fixed by (1.39) as

$$
-\sum_\gamma N^\gamma C(m^\gamma, m^\gamma) = T_0 - n_0^{\text{D5}} + \sum_\beta N^\beta \left[\frac{1}{2} x_{\{i,k\}} \tilde{t}_i^\beta \tilde{t}_k^\beta - M_{\{i,k\}}\left(b + \frac{m^\beta}{m_0^\beta}, b + \frac{m^\beta}{m_0^\beta}\right)\right] (m_0^\beta)^2 \,. \tag{1.109}
$$

As by Proposition 1, the LHS of this equation is positive, a solution to it only exists if the

right hand side is also positive. Thus, this is the equation of an ellipsoid and the vector m^γ of discrete flux quanta is given by the finite number of integral points on this ellipsoid. We denote the positive RHS of (1.109) by r^2 with $r \in \mathbb{R}$.

Consequently, the question of boundedness of m^γ translates into showing boundedness of r^2. By (1.109) we have

$$\begin{aligned} r^2 &= -\sum_\gamma N^\gamma C(m^\gamma, m^\gamma) = T_0 - n_0^{\mathrm{D5}} + \sum_\beta N^\beta \left[\tfrac{1}{2} x_{\{i,k\}} \tilde{\imath}_i^\beta \tilde{\imath}_k^\beta - M_{\{i,k\}}\left(b + \tfrac{m^\beta}{m_0^\beta}, b + \tfrac{m^\beta}{m_0^\beta}\right)\right](m_0^\beta)^2 \\ &\leq T_0 + \sum_{\beta_s} S^{\beta_s} - \sum_{\beta_m,+} |R^{\beta_m}| \leq T_0 + \frac{1}{2}\max\left(x_{\{i,k\}}\right) \cdot \min(T_i) \cdot \max(T_i)\,, \end{aligned} \tag{1.110}$$

where we set $n_0^{\mathrm{D5}} = 0$ and dropped some negative terms in the sum over β to obtain the second line and used (1.108) for the last inequality.

This argument and also Proposition 1 require that the matrix C is of negative signature $(0,n)$ when restricted to the subspace of vectors obeying (1.61). As we have argued before, for the bases $B = \mathbb{F}_k$, dP_n, $n > 1$ and the toric surfaces the matrix C is of Minkowski signature and the vector $\frac{b}{2} + \frac{j}{j_0}$ is time-like. Thus, the above argument applies.

1.4 Conclusions

We have studied Type IIB compactifications on smooth Calabi-Yau elliptic fibrations over almost Fano twofold bases B with magnetized D9-branes and D5-branes. We have proven that the tadpole cancellation and SUSY conditions imply that there are only finitely many such configurations. We have derived explicit and calculable bounds on all flux quanta (Table 1.1, Theorem 2, Section 1.3.3) as well as the number of D5-branes (Theorem 3, Theorem 4), which are independent on the continuous moduli of the compactification, in particular the Kähler moduli, as long as the supergravity approximation is valid.

The presented proof applies for any geometry that meets the geometric conditions listed

at the beginning of Section 1.3.3. We have shown explicitly in Section 1.2.3 and Appendix 1.5 that these geometric conditions are obeyed for the twofold bases B given by the Hirzebruch surfaces $\mathbf{F}_k$, $k = 0, 1, 2$, the generic del Pezzos dP_n, $n = 0, \ldots, 8$ as well all toric varieties associated to the 16 reflexive two-dimensional polytopes. This in particular required showing the positive semi-definiteness of the matrices $M_{\{i,k\}}$ defined in (1.38). To this end we studied the Kähler cones of the generic dP_n and explicitly constructed their Kähler cone generators, which are listed in Table 1.3 and reveal useful geometric properties of these Kähler cones.

Physically, we have proven that there exists a finite number of four-dimensional $\mathcal{N} = 1$ supergravity theories realized by these compactifications. Most notably, there arise only finitely many gauge sectors in these theories with finitely many different chiral spectra. The details of these gauge sectors are determined by the bounded number of branes in a stack and the bounded magnetic flux quanta. Concretely, this means that the ranks of the gauge groups are bounded, that only certain matter representations with certain chiral indices exist (which is always true in weakly coupled Type IIB) and that for fixed gauge group there exist only a finite set of possible multiplicities for the matter fields. These finiteness properties, and more broadly similar results elsewhere in the landscape, are particularly interesting when contrasted to generic quantum field theories.

While we have shown finiteness of these compactifications and provided explicit bounds, we have not explicitly constructed all of these compactifications. It would be interesting to systematically construct this finite set of configurations and extract generic features of the four-dimensional effective theories in this corner of the landscape. In addition, we have not systematically explored the bases B for which the proof applies, i.e. there may exist additional algebraic surfaces satisfying the geometric conditions of Section 1.3.3. Other points of interest would be to determine whether a simple modification of our proof exists for blow-ups of singular elliptic fibrations or elliptically fibered Calabi-Yau

manifolds which do not satisfy the supergravity approximation; in the latter case the supersymmetry conditions receive corrections of various types. Of most interest would be to find a general proof for a general Calabi-Yau threefold X. It seems plausible that there are even more general proof techniques which utilize SUSY and tadpole cancellation conditions to prove finiteness for a general X. For example, some of the arguments in the proof presented here, e.g. the ones used to eliminate the dependence of the SUSY conditions (1.4) on the Kähler moduli, should still apply for general Calabi-Yau manifolds X. In addition, string dualities of the considered Type IIB configurations extend our finiteness proof to the dual theories, for example to the heterotic string on certain elliptic fibrations with specific vector bundles and to F-theory on certain elliptic $K3$-fibered fourfolds. It is very important to work out the details of the duality maps and the analogs of the bounds we found in the dual theories.

The presented proof is based on tadpole and supersymmetry conditions at weak coupling and large volume of X. It is crucial for a better understanding of the string landscape to understand string consistency conditions away from large volume and weak coupling. This requires the understanding of perturbative and non-perturbative corrections[17] both in α' and in g_S; for example, the supersymmetry conditions receive α'-corrections from worldsheet instantons. Avenues towards a better understanding might be provided by applications of $\mathcal{N} = 1$ mirror symmetry, i.e. mirror symmetry, and S-duality.

It is particularly interesting that the finiteness results we have proven and similar results elsewhere in the landscape do not have known analogs in generic quantum field theories. Such differences are one of the hallmarks of string compactifications, and it seems reasonable to expect that similar finiteness results can be proven for even the most general string compactifications, in particular those at small volume and strong coupling. This

[17] See [64, 65, 66, 67] for recent computations of corrections to $\mathcal{N} = 1$ couplings in M-/F-theory compactifications.

would have profound implications for our picture of the landscape: while it is larger than originally thought, our results provide further evidence that it may, in fact, be finite.

We thank Mike Douglas, Antonella Grassi, Albrecht Klemm, Dave Morrison, Hernan Piragua and Wati Taylor for useful conversations and correspondence. This research is supported in part supported by the DOE grant DE-SC0007901 (M.C. and D.K.), Dean's Funds for Faculty Working Group (M.C. and D.K.), the Fay R. and Eugene L. Langberg Endowed Chair (M.C.), the Slovenian Research Agency (ARRS) (M.C.) and the NSF grant PHY11-25915 (J.H.). J.H. thanks J.L. Halverson for her encouragement.

1.5 Kähler Cones of del Pezzo Surfaces & their $M_{\{i,k\}}$-Matrices

In this Appendix we discuss in detail the structure of the Kähler cone of the del Pezzo surfaces dP_n for $n \leq 8$. We are interested in the extremal rays, i.e. the generators, of these in general non-simplicial cones, and the existence of coverings of these cones by simplicial subcones so that conditions (1)-(3) listed at the beginning of Section 1.3.3 are obeyed.

First, we expand the Kähler cone generators D_i of dP_n in the basis (1.20) of $H^2(dP_n, \mathbb{Z})$

$$D_i = (v_i)^1 H + \sum_{j=1}^{n} (v_i)^j E_j \,, \tag{1.111}$$

which maps every D_i to a vector v_i in $\mathbb{Z}^{n+1}$. With this definition, we obtain the matrices (1.38) in this basis as

$$M_{\{i,k\}} = \eta \cdot [x_{\{i,k\}}(v_i \cdot v_k^T + v_k \cdot v_i^T) - \eta] \cdot \eta \,, \tag{1.112}$$

where $i \neq k$, v^T denotes the transpose of a vector, '$\cdot$' denotes the matrix product and η =

$\mathrm{diag}(1,-1,\ldots,-1)$ is the standard Minkowski matrix in $n+1$ dimensions. We note that in order to check positive semi-definiteness of the matrices in (1.112), it suffices to prove it for the matrices $\eta \cdot M_{\{i,k\}} \cdot \eta$, which is the matrix in the square brackets in (1.112).

Next, we need the explicit form for the Kähler generators of dP_n. We present these by listing the corresponding vectors v_i defined via (1.111). We explicitly solve (1.25) over the integers to obtain the Kähler cone generators. For the simplicial cases dP_0, dP_1, dP_2 we obtain (1.26) as discussed earlier. In the non-simplicial cases dP_n, $n > 2$, we summarize the generators in Table 1.3.

Here, the second column contains the schematic form of the vectors v_i, with each row containing all vectors of the same particular form. In each row, the explicit expressions for the v_i are obtained by inserting the values listed in the third column for the place holder variables in the entries of v_i in that row and by permuting the underlined entries of the vector v_i. The number of different vectors in each row is given in the fourth column, where the two factors are given by the number of elements in the list in the third column and the number of permutations of the entries, respectively. The fifth column contains a list of the Minkowski length of all vectors in a given row. We note that this column precisely contains the self-intersection of the curves associated to the D_i. All are either 0 or 1 and it can be checked that the intersections of the v_i with $c_1(dP_n) = 3H - \sum_i E_i \equiv (3,-1,\ldots,-1)$ are precisely 2 or 3, respectively, as required by (1.25).

For example, in the second row of Table 1.3, all vectors v_i are of the form $v_i = (a,b,b,b)$ by the second column. By the third column, there are two different vectors of this type, namely $v_1 = (2,-1,-1,-1)$ and $v_2 = (1,0,0,0)$. Thus, there are precisely 2 vectors as indicated in the fourth column and the Minkowski length of the two vectors is 1, 1, respectively, as in the last column of the second row.

We note that the Kähler cone generators and their grouping as in Table 1.3 can be understood by representation theory, recalling that the Weyl group naturally acts on $H_2(dP_n,\mathbb{Z})$.

	Kähler cone generators v_i		#	$\eta(v_i,v_i)$
dP_3	(a,b,b,b)	$(a,b)\in\{(2,-1),(1,0)\}$	$2\cdot1$	$\{1,1\}$
	$(c,\underline{d,e,e})$	$(c,d,e)\in\{(1,-1,0)\}$	3	0
	Total number of Kähler generators =		5	
dP_4	(a,b,b,b,b)	$(a,b)\in\{(2,-1),(1,0)\}$	$2\cdot1$	$\{0,1\}$
	$(c,\underline{d,e,e,e})$	$(c,d,e)\in\{(2,0,-1),(1,-1,0)\}$	$2\cdot4$	$\{1,0\}$
	Total number of Kähler generators =		10	
dP_5	(a,b,b,b,b,b)	$(a,b)\in\{(1,0)\}$	1	1
	$(c,\underline{d,e,e,e,e})$	$(c,d,e)\in\{(3,-2,-1),(2,0,-1),(1,-1,0)\}$	$3\cdot5$	$\{0,0,1\}$
	$(f,\underline{g,g,g,h,h})$	$(f,g,h)\in\{(2,-1,0)\}$	10	0
	Total number of Kähler generators =		26	
dP_6	(a,b,b,b,b,b,b)	$(a,b)\in\{(1,0),(5,-2)\}$	$2\cdot1$	$\{1,1\}$
	$(c,\underline{d,e,e,e,e,e})$	$(c,d,e)\in\{(1,-1,0),(3,-2,-1)\}$	$2\cdot6$	$\{0,0\}$
	$(f,\underline{g,g,g,g,h,h})$	$(f,g,h)\in\{(2,-1,0)\}$	15	0
	$(i,\underline{j,j,j,k,k,k})$	$(i,j,k)\in\{(2,-1,0),(4,-2,-1)\}$	$2\cdot20$	$\{1,1\}$
	$(l,\underline{m,n,n,n,n,o})$	$(l,m,n,o)\in\{(3,-2,-1,0)\}$	30	1
	Total number of Kähler generators =		99	
dP_7	(a,b,b,b,b,b,b,b)	$(a,b)\in\{(8,-3),(1,0)\}$	$2\cdot1$	$\{1,1\}$
	$(c,\underline{d,e,e,e,e,e,e})$	$(c,d,e)\in\{(5,0,-2),(5,-1,-2),(4,-3,-1),(1,-1,0)\}$	$4\cdot7$	$\{1,0,1,0\}$
	$(f,\underline{g,g,g,h,h,h,h})$	$(f,g,h)\in\{(7,-2,-3),(4,-2,-1),(2,0,-1),(2,-1,0)\}$	$4\cdot35$	$\{1,0,0,1\}$
	$(i,\underline{j,k,l,l,l,l,l})$	$(i,j,k,l)\in\{(3,0,-2,-1)\}$	42	0
	$(m,\underline{n,o,o,p,p,p,p})$	$(m,n,o,p)\in\{(6,-1,-3,-2),(3,-2,0,-1)\}$	$2\cdot105$	$\{1,1\}$
	$(q,\underline{r,s,s,s,t,t,t})$	$(q,r,s,t)\in\{(5,-3,-2,-1),(4,0,-2,-1)\}$	$2\cdot140$	$\{1,1\}$
	Total number of Kähler generators =		702	
dP_8	(a,b,b,b,b,b,b,b,b)	$(a,b)\in\{(17,-6),(1,0)\}$	$2\cdot1$	$\{1,1\}$
	$(c,\underline{d,e,e,e,e,e,e,e})$	$(c,d,e)\in\{(11,-3,-4),(10,-6,-3),(8,-1,-3),(8,0,-3),$ $(4,-3,-1),(1,-1,0)\}$	$6\cdot8$	$\{0,1,0,1,0,0\}$
	$(f,\underline{g,g,h,h,h,h,h,h})$	$(f,g,h)\in\{(13,-6,-4),(5,0,-2)\}$	$2\cdot28$	$\{1,1\}$
	$(i,\underline{j,j,j,k,k,k,k,k})$	$(i,j,k)\in\{(16,-5,-6),(2,-1,0)\}$	$2\cdot56$	$\{1,1\}$
	$(l,\underline{m,n,o,o,o,o,o,o})$	$(l,m,n,o)\in\{(14,-3,-6,-5),(7,-4,-3,-2),(5,-1,0,-2),$ $(4,-3,0,-1)\}$	$4\cdot56$	$\{1,0,0,1\}$
	$(p,\underline{q,q,q,q,r,r,r,r})$	$(p,q,r)\in\{(10,-4,-3),(9,-4,-2),(2,-1,0)\}$	$3\cdot70$	$\{0,1,0\}$
	$(s,\underline{t,u,u,v,v,v,v,v})$	$(s,t,u,v)\in\{(10,-2,-5,-3),(10,-1,-3,-4),(9,-2,-4,-3),$ $(8,-5,-3,-2),(8,-4,-1,-3),(3,-2,0,-1)\}$	$6\cdot168$	$\{1,1,0,1,1,0\}$
	$(w,\underline{x,y,y,y,z,z,z,z})$	$(w,x,y,z)\in\{(15,-4,-6,-5),(12,-4,-3,-5),$ $(12,-2,-5,-4),(11,-6,-4,-3),$ $(8,-4,-2,-3),(7,-1,-2,-3),(7,0,-2,-3),$ $(6,-4,-1,-2),(6,-2,-3,-1),(5,-3,-2,-1),$ $(4,0,-2,-1),(3,-2,0,-1)\}$	$12\cdot280$	$\{1,1,1,1,0,0,$ $1,1,1,0,0,1\}$
	$(\tilde{a},\underline{\tilde{b},\tilde{b},\tilde{c},\tilde{c},\tilde{d},\tilde{d},\tilde{d},\tilde{d}})$	$(\tilde{a},\tilde{b},\tilde{c},\tilde{d})\in\{(6,-1,-3,-2)\}$	420	0
	$(\tilde{e},\underline{\tilde{f},\tilde{f},\tilde{g},\tilde{g},\tilde{g},\tilde{h},\tilde{h},\tilde{h}})$	$(\tilde{e},\tilde{f},\tilde{g},\tilde{h})\in\{(14,-6,-5,-4),(4,0,-1,-2)\}$	$2\cdot560$	$\{1,1\}$
	$(\tilde{i},\underline{\tilde{j},\tilde{k},\tilde{l},\tilde{l},\tilde{m},\tilde{m},\tilde{m},\tilde{m}})$	$(\tilde{i},\tilde{j},\tilde{k},\tilde{l},\tilde{m})\in\{(12,-6,-5,-3,-4),(6,0,-1,-3,-2)\}$	$2\cdot840$	$\{1,1\}$
	$(\tilde{n},\underline{\tilde{o},\tilde{p},\tilde{q},\tilde{q},\tilde{q},\tilde{r},\tilde{r},\tilde{r}})$	$(\tilde{n},\tilde{o},\tilde{p},\tilde{q},\tilde{r})\in\{(13,-3,-6,-5,-4),(9,-5,-4,-3,-2),$ $(9,-2,-1,-4,-3),(5,-3,0,-2,-1)\}$	$4\cdot1120$	$\{1,1,1,1\}$
	$(\tilde{s},\underline{\tilde{t},\tilde{u},\tilde{u},\tilde{v},\tilde{v},\tilde{w},\tilde{w},\tilde{w}})$	$(\tilde{s},\tilde{t},\tilde{u},\tilde{v},\tilde{w})\in\{(11,-2,-3,-5,-4),(10,-5,-2,-3,-4),$ $(8,-1,-4,-3,-2),(7,-4,-3,-1,-2)\}$	$4\cdot1680$	$\{1,1,1,1\}$
	Total number of Kähler generators =		19440	

Table 1.3: Kähler cone generators for dP_n. The underlined entries of the v_i are permuted.

For instance the Kähler cone generators of dP_n, $n=2,\ldots,6$ form the representations **3**,

$(\bar{\mathbf{3}} \otimes \mathbf{1}) \oplus (\mathbf{1} \otimes \mathbf{2})$, $\mathbf{5} \oplus \bar{\mathbf{5}}$, $\mathbf{16} \oplus \mathbf{10}$ and $\mathbf{78} \oplus \mathbf{27}$ under the corresponding groups A_1, $A_2 \times A_1$, A_4, D_5 and E_6, respectively. Here the first representation in all direct sums is formed by all generators with Minkowski length 1 and the second one is formed by generators with Minkowski length 0. These results can be worked out explicitly by computing the Dynkin labels of the generators in Table 1.3 for the canonical roots α_i, which are the -2-curves in $H_2(dP_n, \mathbb{Z})$ orthogonal to $c_1(dP_n)$. Thus, the zero weight vector is identified with $c_1(dP_n)$. For dP_7 only the union of the generators of the Kähler and Mori cone have a representation theoretical decomposition as $\mathbf{912} \oplus \mathbf{133}$ (some of the weights of the $\mathbf{912}$ have higher multiplicities yielding only 576 different weights), where the first representation contains the length 1 and the second one the length 0 Kähler cone generators.

Next, we make one important observation. As one can check explicitly from Table 1.3 and (1.26), for every del Pezzo dP_n with $n > 1$, the first Chern class $c_1(dP_n) \equiv (3, -1, \ldots, -1)$ is proportional to the sum of all Kähler cone generators v_i

$$c_1(dP_n) \equiv (3, -1, \ldots, -1) = \frac{1}{A_n \cdot N} \sum_{i=1}^{N} v_i \tag{1.113}$$

where N denotes the total number of Kähler cone generators of dP_n, cf. Table 1.3. The positive proportionality factor A_n depends on n and reads

$$A_3 = \frac{2}{5}, \quad A_4 = \frac{1}{2}, \quad A_5 = \frac{17}{26}, \quad A_6 = \frac{10}{11}, \quad A_7 = \frac{55}{39}, \quad A_8 = \frac{26}{9} \tag{1.114}$$

for dP_3, dP_4, dP_5, dP_6, dP_7 and dP_8, respectively. This means that $c_1(dP_n)$ is in the center of the Kähler cone of all del Pezzo surfaces with $n > 1$.

This implies that we can find a cover of the Kähler cone by simplicial subcones so that properties (1)-(3) at the beginning of section 1.3.3 are satisfied. We present two such covers:

Cover 1: Intersect the Kähler cone with a hyperplane that is normal to $c_1(dP_n)$ and passes through $c_1(dP_n)$. This yields an n-dimensional polytope with vertices corresponding to the generators of the Kähler cone. Triangulate this polytope with star being $c_1(dP_n)$. This triangulation induces a decomposition of the Kähler cone into simplicial subcones. As the generators of one simplicial subcone, take $c_1(dP_n)$ and those generators v_i of the Kähler cone that go through the vertices of an n-dimensional cone of the triangulated polytope.

In this covering of the Kähler cone, properties (2) and (3) are satisfied: we obviously have b_i all positive, because $c_1(dP_n)$ is one of the generators in every simplicial subcone. From (1.10) we get $b_i = 0$ for all $D_i \neq c_1(dP_n)$ and $b_K = 1$, where K denotes the index such that $D_K = c_1(dP_n)$. In addition, we have $C_{KK} = \mathcal{K}_{000} = 9 - n$ and $C_{iK} = \mathcal{K}_{00i} = 2, 3$ for $i \neq K$ by (1.7) and (1.27) and $T_K = 12 \int_B c_1^2 = 12\mathcal{K}_{000} = 12(9-n)$ by (1.13) and (1.27). We discuss why property (1) is satisfied later.

Cover 2: Although the above cover 1 obeys all the required properties listed at the beginning of Section 1.3.3, it slightly increases the bounds because it increases $\max(T_i)$ for $n \leq 6$ in which case $\max(T_i) = T_K = 12(9-n)$ is larger than the T_i found in (1.28).

Thus, we provide the following alternative cover which exists if the Kähler cone is sufficiently symmetric, in addition to $c_1(dP_n)$ being its center. Take a vertex of the polytope constructed in cover 1. Construct the line through that vertex and the star, i.e. $c_1(dP_n)$. This line has to intersect the boundary of the polytope at another point. This point lies on a certain facet of this polytope. Take the vertices of this facet together with the original vertex we have started with to define a simplicial subcone of the Kähler cone. Notice that this subcone contains $c_1(dP_n)$ and the cone formed by the vertices of this facet and $c_1(dP_n)$, i.e. a subcone in cover 1. Repeat this procedure for all vertices of the polytope. If the Kähler cone is sufficiently symmetric, each facet will be hit exactly once. Thus, each subcone in cover 1 is contained in a corresponding subcone defined in this way. Consequently, since

cover 1 covers the Kähler cone completely, so does cover 2.

This cover also satisfies conditions (1)-(3) at the beginning of Section 1.3.3. We again leave the discussion of condition (1) for later. Conditions (2) and (3) are satisfied since $c_1(dP_n)$ is contained in each subcone, which implies $b_i \geq 0$ for all i, and by (1.27) all $\mathcal{K}_{00i}$ are positive integers. In addition, the advantage of this cover is that all generators of all simplicial subcones are generators of the Kähler cone. Thus in all bounds derived in this work, we have that $\max(T_i)$ is given precisely by (1.28). Given the fact that the generators of the Kähler cone sit in representations of Lie algebras, which implies that the Kähler cone is symmetric, and that $c_1(dP_n)$ lies in its center, we expected this cover 2 to exist.

Finally, we discuss why condition (1), i.e. the positive semi-definiteness of the matrices $M_{\{i,k\}}$ in (1.38), is satisfied in both Cover 1 and Cover 2. We notice the following fact: for both covers, in order to show that the matrices (1.38) are positive semi-definite, we only have to prove that these matrices written in the form (1.112) are positive semi-definite for all possible choices of two vectors v_i, v_j of Table 1.3. This is clear for Cover 2, because the generators of all simplicial subcones are generators of the Kähler cone. For Cover 1, in every simplicial subcone, all matrices $M_{\{i,j\}}$ with $i, j \neq K$ involve only the generators v_i, v_j. Thus, we only have to consider the matrices $M_{\{i,K\}}$ with $i \neq K$ (recall that we only have to show positive semi-definiteness of the matrices $M_{\{i,j\}}$ for $i \neq j$). For these we use

Lemma 5. *In Cover 1, let K be the index corresponding to $c_1(dP_n)$, then the matrices $M_{\{i,K\}}$ for all $i \neq K$ are positive semi-definite, if all matrices $M_{\{i,j\}}$ for all pairs of generators v_i, v_j of the Kähler cone are positive semi-definite.*

Proof. Using the first Chern class $c_1(dP_n) \equiv (3,-1,\ldots,-1)$ and $\lambda_j = \frac{1}{A_n \cdot N}$, we obtain

$$M_{\{i,K\}} = x_{\{i,K\}}(v_i \cdot c_1(dP_n)^t + c_1(dP_n) \cdot v_i^t) - \eta = \sum_{j=1}^{N} \lambda_j x_{\{i,K\}}(v_i \cdot v_j^t + v_j \cdot v_i^t) - \eta\,, \quad (1.115)$$

where we used (1.113). Choose $x_{\{i,K\}}$ for every i so that the following equality is satisfied

$$\sum_{j=1}^{N} \lambda_j \frac{x_{\{i,K\}}}{x_{\{i,j\}}} = x_{\{i,K\}} \sum_{j=1}^{N} \frac{\lambda_j}{x_{\{i,j\}}} = x_{\{i,K\}} \frac{1}{A_n} \left\langle \frac{1}{x_{\{i,j\}}} \right\rangle_j \stackrel{!}{=} 1\,, \tag{1.116}$$

where $\left\langle \frac{1}{x_{\{i,j\}}} \right\rangle_j$ denotes the average of $\frac{1}{x_{\{i,j\}}}$ with i kept fixed and j varied over all Kähler cone generators. Then, (1.115) can be written as

$$\begin{aligned} M_{\{i,K\}} &= \sum_{j=1}^{N} \lambda_j \frac{x_{\{i,K\}}}{x_{\{i,j\}}} x_{\{i,j\}} (v_i \cdot v_j^t + v_j \cdot v_i^t) - \eta = \sum_{j=1}^{N} \lambda_j \frac{x_{\{i,K\}}}{x_{\{i,j\}}} (x_{\{i,j\}} (v_i \cdot v_j^t + v_j \cdot v_i^t) - \eta) \\ &= \sum_{j=1}^{N} \lambda'_j (x_{\{i,j\}} (v_i \cdot v_j^t + v_j \cdot v_i^t) - \eta) = \sum_{j=1}^{N} \lambda'_j M_{\{i,j\}}\,, \end{aligned} \tag{1.117}$$

where we set $\lambda'_j = \lambda_j \frac{x_{\{i,K\}}}{x_{\{i,j\}}}$. We note that $M_{\{i,K\}}$ is defined in terms of generators of the Kähler cone and $\lambda'_j \geq 0$ for all $j = 1, \ldots, N$. Thus, if all the $M_{\{i,j\}}$ are positive semi-definite, then $M_{\{i,K\}}$ will be automatically positive semi-definite because it is just a positive linear combination of the $M_{\{i,j\}}$ by (1.117). A positive linear combination of positive semi-definite matrices is again positive semi-definite. □

Thus, it only remains to show positive semi-definiteness of the matrices $M_{\{i,k\}}$ defined in (1.112) for any choice of two Kähler cone generators of dP_n from Table 1.3. We note that the Kähler cone generators of dP_n are obtained by permutations of the vectors in Table 1.3. Most of these permutations simply interchange the rows and columns of the matrices (1.112), which does not affect their eigenvalues. Thus, we only have to consider matrices (1.112) that do not differ only by such a permutation. We provide an efficient algorithm making use of this permutation symmetry to generate all matrices (1.112) with different sets of eigenvalues. Recall that to check positive-semi-definiteness for any $M_{\{i,k\}}$, it suffices to check positive-semi-definiteness for $\tilde{M}_{\{i,k\}}$, defined as

$$\tilde{M}_{\{i,k\}} = x_{\{i,k\}} (v_i \cdot v_k^T + v_k \cdot v_i^T) - \eta\,. \tag{1.118}$$

For each $\tilde{M}_{\{i,k\}}$ define (v_i, v_k) as the pair of Kähler cone generators in its definition (1.118). By definition of $M_{\{i,k\}}$, we have $i \neq k$ in (v_i, v_k). For each dP_n, we define an equivalence relation on the set of all pairs (v_i, v_k) and show if $(v_i, v_k) \sim (v_i', v_k')$ and $x_{\{i,k\}} = x'_{\{i,k\}}$, the corresponding matrices $\tilde{M}_{\{i,k\}}$ and $\tilde{M'}_{\{i,k\}}$ have the same sets of eigenvalues.

Definition 2. *For each dP_n, let $\{(v_i, v_k)\}$, $i \neq k$, be the set of all pairs of its Kähler cone generators. The symmetric group S_n of degree n acts on the Kähler cone generator $v_i \in \mathbb{Z}^{1+n}$ by permuting its last n components, cf. the second column of Table 1.3. Define an equivalence relation $\sim$ on $\{(v_i, v_k)\}$ by $(v_i, v_k) \sim (v_i', v_k')$ if $(v_i', v_k') = (\sigma(v_i), \sigma(v_k))$, for some $\sigma \in S_n$.*

Lemma 6. *Suppose $(v_i, v_k) \sim (v_i', v_k')$. Let $\tilde{M}_{\{i,k\}}$ and $\tilde{M'}_{\{i,k\}}$ be the matrix defined by (v_i, v_k) and (v_i', v_k'), respectively, with $x_{\{i,k\}} = x'_{\{i,k\}}$, in* (1.118)*. Then $\tilde{M}_{\{i,k\}}$ and $\tilde{M'}_{\{i,k\}}$ have the same set of eigenvalues.*

Proof. Let $\sigma \in S_n$ so that $(v_i', v_k') = (\sigma(v_i), \sigma(v_k))$. Denote the permutation matrix that permutes the j^{th} and l^{th} rows/columns by P_{jl}. Since any $\sigma \in S_n$ can be written as a product of such permutation matrices, we can WLOG assume $\sigma = P_{jl}$. Then we have

$$\begin{aligned}\tilde{M'}_{\{i,k\}} &= x_{\{i,k\}}(P_{jl} v_i v_k^T P_{jl}^T + P_{jl} v_k v_i^T P_{jl}^T) - \eta = x_{\{i,k\}}(P_{jl} v_i v_k^T P_{jl}^T + P_{jl} v_k v_i^T P_{jl}^T) - P_{jl}\eta P_{jl}^T \\ &= P_{jl}[x_{\{i,k\}}(v_i v_k^T + v_k v_i^T) - \eta] P_{jl}^T = P_{jl} \tilde{M}_{\{i,k\}} P_{jl}^T . \end{aligned} \tag{1.119}$$

This implies that the characteristic polynomials of $\tilde{M}_{\{i,k\}}$ and $\tilde{M'}_{\{i,k\}}$ are the same,

$$\begin{aligned}\det\left(\tilde{M'}_{\{i,k\}} - \lambda I\right) &= \det\left(P_{jl} \tilde{M}_{\{i,k\}} P_{jl}^T - \lambda P_{jl} I P_{jl}^T\right) = \det\left(P_{jl}\left(\tilde{M}_{\{i,k\}} - \lambda I\right) P_{jl}^T\right) \\ &= \det(P_{jl}) \det\left(\tilde{M}_{\{i,k\}} - \lambda I\right) \det(P_{jl}^T) = \det\left(\tilde{M}_{\{i,k\}} - \lambda I\right). \end{aligned} \tag{1.120}$$

□

Lemma 6 shows that for each equivalence class $[(v_i, v_k)]$, we just need to pick any representative (v_i, v_k) and check if there exists an $x_{\{i,k\}} \in \mathbb{Q}^+$ such that (v_i, v_k) and $x_{\{i,k\}}$ defines a positive semi-definite matrix $\tilde{M}_{\{i,k\}}$ according to (1.118). If such an $x_{\{i,k\}}$ exists, any $\tilde{M'}_{\{i,k\}}$ with $(v_i', v_k') \sim (v_i, v_k)$ will be automatically positive semi-definite for $x'_{\{i,k\}} = x_{\{i,k\}}$. For each dP_n, in order to find all different equivalence classes, we start by picking an arbitrary pair (v_i, v_k) from Table 1.3 and carry out the following algorithm:

(1) Fix v_i and only permute the entries of v_k. Indeed, if $v_i' = \sigma(v_i), v_k' = \tau(v_k)$, then $(v_i', v_k') \sim (v_i, \sigma^{-1}\tau(v_k))$. Let $\tau' = \sigma^{-1}\tau$, then we have $[(v_i', v_k')] = [(v_i, \tau'(v_k))]$.

(2) Only permute those entries in v_k for which the corresponding entries in v_i are different from each other. Permuting two entries in v_k when the corresponding two entries in the fixed vector v_i are the same is equivalent to the action of permuting these two entries for both vectors. Thus, the resulting pair of vectors $(v_i, v_k') \sim (v_i, v_k)$.

Pick a different pair (w_i, w_k) of Kähler cone generators from Table 1.3 and repeat (1), (2).

For example, consider dP_8. Suppose we begin by picking $v_i = (a, b, b, b, b, b, b, b, b)$ and $v_k = (s, t, u, u, v, v, v, v, v)$ from the second column of Table 1.3. By (1) above, we can fix v_i and only consider permutations in the last eight entries of v_k. By (2), however, we do not need to consider any permutation in the last eight entries in v_k, because the last eight entries in the fixed vector v_i are the same; they are all equal to b. Thus, there is only one equivalence class $[(v_i, v_k)]$. From the third column of Table 1.3, there are two sets of different values for $v_i = (a, b, b, b, b, b, b, b, b)$, and six sets of different values for $v_k = (s, t, u, u, v, v, v, v, v)$. Thus there will be $2 \cdot 6 = 12$ different $\tilde{M}'_{\{i,k\}}$ matrices to check for positive semi-definiteness. Next pick a different pair of (w_i, w_k) and repeat this process.

We obtain that the matrices (1.112) are positive semi-definite for any choice of two

Kähler cone generators in Table 1.3 and $x_{\{i,k\}}$ of the form

$$x_{\{i,k\}} = \frac{1}{a} \qquad \text{for} \qquad a \in \{1,2,\ldots,19\}\,. \tag{1.121}$$

More precisely, for dP_2 and dP_3 all $x_{\{i,k\}} = 1$, for dP_4 and dP_5 we have $x_{\{i,k\}} = 1, \frac{1}{2}$, for dP_6 we have $x_{\{i,k\}} = \frac{1}{a}$ with $a \in \{1,2,\ldots,4\}$, for dP_7 we find $x_{\{i,k\}} = \frac{1}{a}$ with $a \in \{1,2,\ldots,7\}$ and for dP_8 all values in (1.121) are assumed.

1.6 Geometric Data of almost Fano Twofolds for computing Explicit Bounds

In this appendix, we summarize the geometric data of Hirzebruch surfaces $\mathbb{F}_k$, $k = 0,1,2$, the del Pezzo surfaces dP_n, $n = 2,\ldots,8$, and the toric varieties associated to the 16 reflexive polytopes that is necessary to explicitly compute the various bounds derived in this paper.

We begin with the bases $\mathbb{F}_k$ and dP_n. The following results in Table 1.4 are derived employing (1.19), (1.28), the two covers of the Kähler cones of dP_n constructed in Appendix 1.5, (1.114) and the values of $x_{\{i,k\}}$ listed below (1.121).

First, we list the maximal and minimal values of $x_{\{i,k\}}$ and T_i for the bases $\mathbb{F}_k$ and dP_2 that have a simplicial Kähler cone. For the non-simplicial Kähler cones, we obtain different results for the two different covers of their Kähler cones. We note that for both cover 1 and 2 the values below (1.121) apply. Indeed, this is precisely what we get in the second and third column under cover 2. However, for cover 1, these numbers have to be multiplied by appropriate A_n in (1.114). Indeed, by (1.116) we have $x_{\{i,K\}} = A_n(\langle x_{\{i,k\}} \rangle_j)^{-1}$. By (1.114), we have $A_n \leq 1$ for $n \leq 6$, i.e. the minimum value of $x_{\{i,K\}}$ is bounded by $A_n \cdot \min(x_{\{i,K\}})$, but the maximum is unaffected, as indicated in the first four rows of the second and third column in Table 1.4 under cover 1. For dP_7 and dP_8, we have $A_n > 1$, thus

$x_{\{i,K\}} \leq A_n \max(x_{\{i,k\}}) = A_n$ and the minimum is unaffected, as displayed in the last two rows of the second and third column in Table 1.4 for cover 1.

	$\max(x_{\{i,k\}})$	$\min(x_{\{i,k\}})$	$\max(T_i)$	$\min(T_i)$
$\mathbb{F}_k$	1	1	$24+12k$	24
dP_2	1	1	36	24
	Cover 1 of Kähler cone of dP_n			
dP_3	1	$A_3 \leq$	72	24, 36
dP_4	1	$\frac{1}{2}A_4 \leq$	60	24, 36
dP_5	1	$\frac{1}{2}A_5 \leq$	48	24, 36
dP_6	1	$\frac{1}{4}A_6 \leq$	36	24, 36
dP_7	$A_7 \geq$	$\frac{1}{7}$	36	24
dP_8	$A_8 \geq$	$\frac{1}{19}$	36	12
	Cover 2 of Kähler cone of dP_n			
dP_3	1	1	36	24, 36
dP_4	1	$\frac{1}{2}$	36	24, 36
dP_5	1	$\frac{1}{2}$	36	24, 36
dP_6	1	$\frac{1}{4}$	36	24, 36
dP_7	1	$\frac{1}{7}$	36	24, 36
dP_8	1	$\frac{1}{19}$	36	24, 36

Table 1.4: Key geometrical data for the computation of the explicit bounds derived in the proof.

In addition, without knowing every simplicial subcone in the two covers explicitly, we can not determine the explicit value $\min(T_i)$ for both covers. Therefore, depending on the chosen subcone, employing (1.28), we either obtain 24 or 36 as indicated in the last

Polytope	$\int c_2$	$\int c_1^2$	|K.C. Gens|	List of $T_i = 12 \int_{D_i} c_1$
2	4	8	2	(24,24)
3	4	8	2	(24,36)
4	4	8	2	(24,48)
5	5	7	3	(24,24,36)
6	5	7	3	(24,36,48)
7	6	6	5	(24,24,24,36,36)
8	6	6	4	(24,36,24,48)
9	6	6	5	(24,36,24,48,36)
10	6	6	4	(24,48,72,36)
11	7	5	7	(24,36,48,24,36,72,48)
12	7	5	8	(24,24,36,36,48,48,24,36)
13	8	4	10	(24,48,36,72,48,36,24,72,48,48)
14	8	4	13	(24,24,36,48,36,48,24,72,36,48,72,48,36)
15	8	4	12	(24,36,24,48,36,48,36,48,48,24,24,36)
16	9	3	21	(24,24,36,72,48,36,48,36,48,36,48,72,72,72,36,48,24,36,72,48,72)

Table 1.5: Displayed are some of the relevant data for the smooth almost Fano toric surfaces obtained from fine star triangulations of the two-dimensional reflexive polytopes in Figure 1.1.

column of Table 1.4. However, in the case of cover 1 we have $T_K = 24$, 12 for dP_7 and dP_8, respectively. Since by construction, the first Chern class $c_1(dP_n)$ is in every subcone, we know that $\min(T_i) = T_K = 24$, 12 for dP_7 and dP_8, respectively.

Finally, in Table 1.5 we display the relevant topological data of the toric varieties constructed from the 16 reflexive two-dimensional polytopes which is relevant to our finiteness proof in section 1.3.3. We confirmed that the first Chern class $c_1(B)$ is inside the Kähler cone in all these cases, i.e. Cover 1 constructed in Appendix 1.5 exists for these non-simplicial Kähler cones. As explained there, in this cover the conditions (2) and (3) listed at the beginning of Section 1.3.3 are obeyed. We also checked that the matrices (1.112) are all positive semi-definite for $x_{\{i,k\}}$ of the form $x_{\{i,k\}} = \frac{1}{a}$ with $a \in \{1,\ldots,6\}$, i.e. condition (1) listed in Section 1.3.3 is also satisfied.

1.7 An analytic proof of positive semi-definiteness of the $M_{\{i,k\}}$-Matrices

In this section we provide an alternative general proof of positive semi-definiteness of the $M_{\{i,k\}}$-matrices, in comparison to the numerical proof given in Appendix 1.5 for specific B.

We recall that to check positive-semi-definiteness for any $M_{\{i,k\}}$ defined in (1.112) it suffices to check positive semi-definiteness for the matrix $\tilde{M}_{\{i,k\}}$ defined in (1.118). The advantage of the following general proof is that it predicts a precise value of $x_{\{i,k\}}$ for which each $M_{\{i,k\}}$ is positive semi-definite. Thus, we do not have to search for the existence of such an $x_{\{i,k\}}$ numerically. To be precise, we will show that we can always choose

$$x_{\{i,k\}} = \frac{1}{C_{ik}} \tag{1.122}$$

to make each $M_{\{i,k\}}$ positive semi-definite. We note, however, that such a choice may not produce the best bounds (since the various bounds derived depend on $x_{\{i,k\}}$). Hence, in order to minimize the various bounds we may still want to numerically find alternative values for $x_{\{i,k\}}$, for which the matrices (1.112), (1.118) are also positive semi-definite.

The correctness of the value (1.122) can be motivated physically as follows. Consider a system of two particles with masses $m = 1$ with the Lorentz-invariant Lagrangian

$$L^{i,k} = p^i \cdot p^k\,, \qquad i \neq k\,, \tag{1.123}$$

where p^i for every $i,k = 1,\ldots,N$ are the particle momenta. Due to space-time invariance, the respective Noether currents are stress-energy tensors,

$$T^{i,k}_{\mu,\nu} = p^i_\mu\, p^k_\nu + p^k_\mu\, p^i_\nu - L^{i,k}\eta_{\mu\nu}\,, \qquad i \neq k\,. \tag{1.124}$$

With the identification $\frac{1}{x^{i,k}} \equiv L^{i,k}$, these stress-energy tensors are precisely the matrices (1.118) multiplied by $\frac{1}{x^{i,k}}$. By the positive energy theorem in general relativity the $T^{i,k}_{\mu,\nu}$ are positive semi-definite for every chosen pair of time- or light-like $(n+1)$-vectors p^i, p^k.

In the following, we prove explicitly that the the matrices in (1.118), i.e. the stress energy tensors (1.124), are indeed positive semi-definite for time- or light-like $(n+1)$-vectors p^i, p^k. To this end, we will need the following general fact:

Lemma 7. *For any $n \times n$ matrix M and any invertible $n \times n$ matrix A, M is positive semi-definite if and only if $A^T M A$ is positive semi-definite.*

Using of Lemma 7, we can prove positive semi-definiteness of $\tilde{M}_{\{i,k\}}$ by instead proving positive semi-definiteness of $A^T \tilde{M}_{\{i,k\}} A$, where A is a suitably chosen invertible matrix so that $A^T \tilde{M}_{\{i,k\}} A$ takes a simpler form than $\tilde{M}_{\{i,k\}}$. We will discuss how to choose A shortly. First, recall from Table 1.3 that each Kähler cone generator v_i is either time-like or light-like with Minkowski inner product $\eta(v_i, v_i)$ either 1 or 0, and all the Kähler cone generators belong to the same light cone (the future-directed light cone). We choose A as follows:

Case 1. Suppose $\tilde{M}_{\{i,k\}}$, defined in (1.118), has at least one of its v_i, v_k with Minkowski inner product 1. WLOG say $\eta(v_i, v_i) = 1$. Then there is a matrix $A \in O(1,n)$ such that

$$A^T v_i = (1, 0, ..., 0)^T . \tag{1.125}$$

We note that this is just a Lorentz transformation to the rest frame. Pick this matrix as the invertible matrix A in Lemma 7.

Case 2. Suppose $\tilde{M}_{\{i,k\}}$, defined in (1.118), has both of its v_i, v_k with Minkowski inner product 0. Then there exists a Lorentz transformation $A' \in O(1,n)$ such that

$$A'^{T} v_i = (a_0, a_0, 0, ..., 0)^T, \qquad v_k^T A' = (b_0, b_1, b_2, 0, ..., 0), \tag{1.126}$$

where $a_0, b_0, b_1, b_2 \in \mathbb{Q}$ and $b_0^2 - b_1^2 - b_2^2 = 0$. Pick A' as the invertible matrix in Lemma 7.

The above mentioned matrices in $O(1,n)$ exist because of the following general lemma:

Lemma 8. *For any vector $v \in \mathbb{R}^{1,n}$ which Minkowski inner product $\eta(v,v) = 1$, there exists a matrix $A \in O(1,n)$ such that $A^T v = (1,0,...,0)^T$. For any pair of vector $v_i, v_k \in \mathbb{R}^{1,n}$ both with Minkowski inner product $\eta(v_i,v_i) = \eta(v_k,v_k) = 0$, there exists a matrix $A' \in O(1,n)$ such that $A'^{T} v_i = (a_0, a_0, 0, ..., 0)^T$, $v_k^T A' = (b_0, b_1, b_2, 0, ..., 0)$ where $a_0, b_0, b_1, b_2 \in \mathbb{R}$ and $b_0^2 - b_1^2 - b_2^2 = 0$.*

Proof. First consider any $v \in \mathbb{R}^{1,n}$ with Minkowski inner product $\eta(v,v) = 1$. Since $\eta(v,v) = 1 \neq 0$, we can carry out the Gram-Schmidt process starting with v as the first vector to generate an orthonormal basis $\{e_1 = v, e_2, ..., e_{n+1}\}$ for $\mathbb{R}^{1,n}$. Define the $(1+n) \times (1+n)$ matrix B whose i-th column is e_i, and define $A = \eta B$. Then $A^T v = (1,0,...,0)^T$ by orthonormality. Both B and η are in $O(1,n)$ because each has its columns orthonormal to one another under the $(1,n)$ Minkowski metric. Thus $A = \eta B \in O(1,n)$.

Next consider any pair of vector $v_i, v_k \in \mathbb{R}^{1,n}$, both with Minkowski inner product $\eta(v_i,v_i) = \eta(v_k,v_k) = 0$. If both are equal to the trivial vector $(0,...,0)^T$, let A' be any matrix in $O(1,n)$ and we are done with $a_0 = b_0 = b_1 = b_2 = 0$. Thus assume at least one of them, WLOG say v_i, is not the trivial vector. Let $v_i = (a_0, \mathbf{a})^T$ where $\mathbf{a} = (a_1, ..., a_n)^T \in \mathbb{R}^n$. Since $\eta(v_i,v_i) = 0$ and v_i is not the trivial vector, the Euclidean norm of $\mathbf{a}$, $|\mathbf{a}| = a_0 \neq 0$ (a_0 is positive because v_i is in the positive light cone). We can thus use $\mathbf{a}/|\mathbf{a}|$ as the first vector in the Gram-Schmidt process on $\mathbb{R}^n$ to generate an orthonormal basis $\{e_1 = \mathbf{a}/|\mathbf{a}|, e_2, ..., e_n\}$ for $\mathbb{R}^n$. Define the $n \times n$ matrix B' whose i-th column is e_i. Then define the $(1+n) \times (1+n)$ block diagonal matrix B'' by

$$B'' = \begin{pmatrix} 1 & 0 \\ 0 & B' \end{pmatrix}. \tag{1.127}$$

$B'' \in O(1,n)$ because its columns are orthonormal. Also $B''^T v_i = (a_0, a_0, 0, ..., 0)^T$. Let $v_k^T B'' = (b_0, b_1, \mathbf{b}')$ where $\mathbf{b}' = (b_2', ..., b_n') \in \mathbb{R}^{n-1}$. If $\mathbf{b}'$ is the trivial vector in $\mathbb{R}^{n-1}$, we are done by setting $A' = B''$ and $b_2 = 0$. If $\mathbf{b}'$ is not the trivial vector, we can again use $\mathbf{b}'/|\mathbf{b}'|$ as the first vector in the Gram-Schmidt process on $\mathbb{R}^{n-1}$ to generate an orthonormal basis $\{e_1 = \mathbf{b}'/|\mathbf{b}'|, e_2, ..., e_{n-1}\}$ for $\mathbb{R}^{n-1}$. Define the $(n-1)\times(n-1)$ matrix C' whose i-th column is e_i. Then define the $(1+n)\times(1+n)$ block diagonal matrix C'' by

$$C'' = \begin{pmatrix} 1 & 0 & 0 \\ 0 & 1 & 0 \\ 0 & 0 & C' \end{pmatrix}. \tag{1.128}$$

$C'' \in O(1,n)$ because its columns are orthonormal. Let $A' = B''C''$. $A' \in O(1,n)$ because B'', C'' are. We also have $A'^T v_i = (a_0, a_0, 0, ..., 0)^T$, $v_k^T A' = (b_0, b_1, b_2, 0, ..., 0)$ where $b_2 = |\mathbf{b}'|$. Notice that $b_0^2 - b_1^2 - b_2^2 = \eta(A'^T v_k, A'^T v_k) = \eta(v_k, v_k) = 0$, where in the second equality we used the facts that $O(1,n)$ is closed under transposition, so $A'^T \in O(1,n)$, and that the Lorentz group $O(1,n)$ preserves $\eta(\cdot,\cdot)$. □

Before justifying the choice $x_{\{i,k\}} = 1/C_{ik}$, we need to show $C_{ik} \neq 0$ for $i \neq k$ (by definition we always have $i \neq k$ in $x_{\{i,k\}}$ and $M_{\{i,k\}}$). Also recall that in (1.38), we require $x_{\{i,k\}} \in \mathbb{Q}^+$. Thus a prerequisite for the choice $x_{\{i,k\}} = 1/C_{ik}$ to make sense is that $C_{ik} > 0$ for $i \neq k$ (C_{ik} is already an integer since it is an intersection number). We have the following lemma:

Lemma 9. *$C_{ik} \geq 0$. Furthermore, $C_{ik} > 0$ if $i \neq k$; $C_{ii} = 0$ if and only if v_i is lightlike; i.e. $\eta(v_i, v_i) = 0$.*

Proof. Recall we have

$$C_{ik} = \eta(v_i, v_k). \tag{1.129}$$

Also, by Table 1.3, all the Kähler cone generators v_i, v_k are either time-like or light-like vectors belonging to the same light cone. In addition, of course neither of them is the trivial vector $\mathbf{0}$, because they generate the Kähler cone. This means all their inner products are non-negative, i.e. $C_{ik} = \eta(v_i, v_k) \geq 0$, where equality $C_{ik} = \eta(v_i, v_k) = 0$ holds only when v_i and v_k are parallel light-like vectors. This implies that v_i and v_k are not independent, so they must be the same Kähler cone generator $v_i = v_k$. □

With this, we can prove the following theorem:

Theorem 5. *Let $x_{\{i,k\}} = 1/C_{ik}$. Then $M_{\{i,k\}}$ is positive semi-definite.*

Proof. It is equivalent to prove that with $x_{\{i,k\}} = 1/C_{ik}$, $A^T \tilde{M}_{\{i,k\}} A$ or $A'^T \tilde{M}_{\{i,k\}} A'$, depending on which case above we are refering to is positive semi-definite, where A (or A') is the appropriately chosen matrix in $O(1,n)$ discussed above.

Case 1. Suppose $\tilde{M}_{\{i,k\}}$, defined in (1.118), has at least one of its v_i, v_k with Minkowski inner product 1. WLOG say $\eta(v_i, v_i) = 1$. Then

$$\begin{aligned} A^T \tilde{M}_{\{i,k\}} A &= x_{\{i,k\}} A^T (v_i \cdot v_k^T + v_k \cdot v_i^T) A - \eta \\ &= \frac{1}{c_0} \Big((1,0,...,0)^T (c_0, c_1, ..., c_n) + (c_0, c_1, ..., c_n)^T (1,0,...,0) \Big) - \eta \\ &= \begin{pmatrix} 1 & \frac{c_1}{c_0} & \frac{c_2}{c_0} & \frac{c_3}{c_0} & ... & \frac{c_n}{c_0} \\ \frac{c_1}{c_0} & 1 & 0 & 0 & ... & 0 \\ \frac{c_2}{c_0} & 0 & 1 & 0 & ... & 0 \\ . & . & . & . & . & . \\ \frac{c_n}{c_0} & 0 & 0 & . & . & 1 \end{pmatrix}, \end{aligned} \tag{1.130}$$

where in the first equality, we used the fact that $A \in O(1,n)$ if and only if $A^T \eta A = \eta$. In the second equality, we used (1.125) and let $A^T v_k = (c_0, c_1, ..., c_n)^T$, so $C_{ik} = \eta(v_i, v_k) = \eta(A^T v_i, A^T v_k) = \eta((1,0,...,0)^T, (c_0, c_1, ..., c_n)^T) = c_0$ (notice that $O(1,n)$ is closed under transposition, so $A^T \in O(1,n)$ and thus A^T preserves the inner product $\eta(\cdot,\cdot)$). It is not hard to see that the characteristic equation of $A^T \tilde{M}_{\{i,k\}} A$ is

$$\det\left(A^T \tilde{M}_{\{i,k\}} A - \lambda I\right) = (1-\lambda)^{n-1}\left(\lambda^2 - 2\lambda + 1 - \frac{1}{c_0^2}\sum_{j=1}^{n} c_j^2\right) = 0, \tag{1.131}$$

so the eigenvalues are

$$\lambda = \left\{\underbrace{1, ...1}_{n-1}, \left(1 \pm \sqrt{\sum_{j=1}^{n} \frac{c_j^2}{c_0^2}}\right)\right\}. \tag{1.132}$$

Since

$$0 \le 0 \text{ or } 1 = \eta(v_k, v_k) = \eta(A^T v_k, A^T v_k) = \eta((c_0, c_1, ..., c_n)^T, (c_0, c_1, ..., c_n)^T) = c_0^2 - \sum_{j=1}^{n} c_j^2, \tag{1.133}$$

we must have

$$1 \ge \sqrt{\sum_{j=1}^{n} \frac{c_j^2}{c_0^2}}, \tag{1.134}$$

so all the eigenvalues in (1.132) are non-negative. In particular, if $\eta(v_k, v_k) = c_0^2 - \sum_{j=1}^{n} c_j^2 = 1$, the eigenvalues will be

$$\lambda = \left\{\underbrace{1, ...1}_{n-1}, \left(1 \pm \sqrt{1 - \frac{1}{c_0^2}}\right)\right\}. \tag{1.135}$$

If $\eta(v_k, v_k) = c_0^2 - \sum_{j=1}^{n} c_j^2 = 0$, the eigenvalues will be

$$\lambda = \left\{\underbrace{1, ...1}_{n-1}, 0, 2\right\}. \tag{1.136}$$

Case 2. Suppose $\tilde{M}_{\{i,k\}}$, defined in (1.118), has both of its v_i, v_k with Minkowski inner product 0. Then

$$
\begin{aligned}
&A'^{T}\tilde{M}_{\{i,k\}}A' = x_{\{i,k\}}A'^{T}(v_i\cdot v_k^T + v_k\cdot v_i^T)A' - \eta \\
&= \frac{1}{b_0-b_1}\left((1,1,0,...,0)^T(b_0,b_1,b_2,0...,0) + (b_0,b_1,b_2,0,...,0)^T(1,1,0,...,0)\right) - \eta \\
&= \begin{pmatrix}
\frac{b_0+b_1}{b_0-b_1} & \frac{b_0+b_1}{b_0-b_1} & \frac{b_2}{b_0-b_1} & 0 & ... & 0 \\
\frac{b_0+b_1}{b_0-b_1} & \frac{b_0+b_1}{b_0-b_1} & \frac{b_2}{b_0-b_1} & 0 & ... & 0 \\
\frac{b_2}{b_0-b_1} & \frac{b_2}{b_0-b_1} & 1 & 0 & ... & 0 \\
0 & . & 0 & 1 & . & . \\
. & . & . & . & . & . \\
0 & . & 0 & . & . & 1
\end{pmatrix},
\end{aligned}
\tag{1.137}
$$

where in the second equality we used (1.126) and $C_{ik} = \eta(v_i, v_k) = \eta(A'^{T}v_i, A'^{T}v_k) = \eta((a_0,a_0,0,...,0)^T, (b_0,b_1,b_2,0,...,0)^T) = a_0(b_0-b_1)$. Letting

$$
s \equiv \frac{b_0+b_1}{b_0-b_1} \qquad \sqrt{s} = \frac{b_2}{b_0-b_1}, \tag{1.138}
$$

where in the second equation we used the relationship $b_0^2 - b_1^2 - b_2^2 = 0$, it is not hard to see that the characteristic equation of $A'^{T}\tilde{M}_{\{i,k\}}A'$ is

$$
\det\left(A'^{T}\tilde{M}_{\{i,k\}}A' - \lambda I\right) = (1-\lambda)^{n-2}\lambda^2(2s+1-\lambda) = 0, \tag{1.139}
$$

so the eigenvalues are

$$
\lambda = \left\{\underbrace{1,...1}_{n-2}, 0, 0, \frac{3b_0+b_1}{b_0-b_1}\right\}. \tag{1.140}
$$

The last eigenvalue $\frac{3b_0+b_1}{b_0-b_1}$ is positive because $b_0^2 - b_1^2 - b_2^2 = 0$, so $|b_0| > |b_1|$. □

Notice that the only required condition for this general proof is that all the Kähler cone generators v_i, v_k are either time-like or light-like, and belong to the same light cone. This light cone does not need to be the positive one. Indeed, it is not hard to see that if all the Kähler cone generators were to belong to the negative light cone, the proof still holds with slight modifications at the relevant parts. Also, the time-like Kähler cone generators can always be rescaled to have Minkowski inner product $\eta(v_i, v_i) = 1$. In summary, we have the following corollary:

Corollary 6. *If all the Kähler cone generators v_i, v_k are either time-like or light-like, and belong to the same light cone, then each matrix $M_{\{i,k\}}$ will be positive semi-definite by setting $x_{\{i,k\}} = 1/C_{ik}$.*

Chapter 2

Elliptic fibrations with rank three Mordell-Weil group: F-theory with U(1) × U(1) × U(1) gauge symmetry

2.1 Introduction and Summary of Results

Compactifications of F-theory [135, 137, 136] are a very interesting and broad class of string vacua, because they are on the one hand non-perturbative, but still controllable, and on the other hand realize promising particle physics. In particular, F-theory GUTs have drawn a lot of attention in the recent years, first in the context of local models following [71, 72, 73, 74] and later also in compact Calabi-Yau manifolds [167, 76, 77, 78, 79], see e.g. [80, 81, 82] for reviews. Both of these approaches rely on the well-understood realization of non-Abelian gauge symmetries that are engineered by constructing codimension one singularities of elliptic fibrations [135, 137, 136, 173] that have been classified in [174, 180].[1] In addition, the structure of these codimension one singularities governs the

[1] A toolbox to construct examples of compact Calabi-Yau manifolds with a certain non-Abelian gauge group is provided by toric geometry, see [142, 87, 88].

pattern of matter that is localized at codimension two singularities of the fibration [89], with some subtleties of higher codimension singularities uncovered recently in [90, 91, 92].[2]

Abelian gauge symmetries are crucial ingredients for extensions both of the standard model as well as of GUTs. However, the concrete construction of Abelian gauge symmetries as well as their matter content has only recently been addressed systematically in global F-theory compactifications. This is due to the fact that U(1) gauge symmetries in F-theory are not related to local codimension one singularities but to the global properties of the elliptic fibration of the Calabi-Yau manifold. Concretely, the number of U(1)-factors in an F-theory compactification is given by the rank of the Mordell-Weil group of the elliptic fibration[3] [137, 136], see [97, 98, 99, 100, 101] for a mathematical background. The explicit compact Calabi-Yau manifolds with rank one [154] and the most general rank two [155, 156] Abelian sector have been constructed recently. In the rank two case, the general elliptic fiber is the generic elliptic curve in dP_2 and its Mordell-Weil group is rank two with the two generators induced from the ambient space dP_2. The full six-dimensional spectrum of the Calabi-Yau elliptic fibrations with elliptic fiber in dP_2 has been determined in [156, 159] and chiral compactifications to four dimensions on Calabi-Yau fourfolds with G_4-flux were constructed in [157, 158]. We note, that certain aspects of Abelian sectors in F-theory could be addressed in local models [108, 166, 76, 110, 111, 112, 113, 114, 115]. In addition, special Calabi-Yau geometries realizing one U(1)-factor have been studied in [168, 117, 118, 119, 120, 121].[4]

In this work we follow the systematic approach initiated in [154, 156] to construct elliptic curves with higher rank Mordell-Weil groups and their resolved elliptic fibrations, that aims at a complete classification of all possible Abelian sectors in F-theory. We con-

[2]For a recent approach based on deformations, cf. [93]. See also [94] for a determination of BPS-states, including matter states, of (p,q)-strings using the refined topological string.

[3]See also [169, 96] for the interpretation of the torsion subgroup of the Mordell-Weil group as inducing non-simply connected non-Abelian group in F-theory.

[4]For a systematic study of rational sections on toric K3-surfaces we refer to [164].

struct the most general F-theory compactifications with $\mathrm{U}(1)\times\mathrm{U}(1)\times\mathrm{U}(1)$ gauge symmetry by building elliptically fibered Calabi-Yau manifolds with rank three Mordell-Weil group. Most notably, we show that this forces us to leave the regime of hypersurfaces to represent these Calabi-Yau manifolds explicitly. In fact, the general elliptic fiber in the fully resolved elliptic fibration is naturally embedded as the generic Calabi-Yau complete intersection into $\mathrm{Bl}_3\mathbb{P}^3$, the blow-up of $\mathbb{P}^3$ at three generic points. We show that this is the general elliptic curve $\mathcal{E}$ with three rational points and a zero point. We determine the birational map to its Tate and Weierstrass form. All generic Calabi-Yau elliptic fibrations of $\mathcal{E}$ over a given base B are completely fixed by the choice of three divisors in the base B. Furthermore, we show that every such F-theory vacuum corresponds to an integral in certain reflexive polytopes[5], that we construct explicitly.

As a next step, we determine the representations of massless matter in four- and six-dimensional F-theory compactifications by thoroughly analyzing the generic codimension two singularities of these elliptic Calabi-Yau manifolds. We find 14 different matter representations, cf. table 2.1, with various $\mathrm{U}(1)^3$-charges. Note, that the construction leads to representations that are symmetric under permutations of the first two U(1) factors, but not the third one. Interestingly, we obtain three representations charged under all

$\mathrm{U}(1)\times\mathrm{U}(1)\times\mathrm{U}(1)$-charged matter
$(1,1,1)$, $(1,1,0)$, $(1,0,1)$, $(0,1,1)$, $(1,0,0)$, $(0,1,0)$, $(0,0,1)$,
$(1,1,-1)$, $(-1,-1,-2)$, $(0,1,2)$, $(1,0,2)$, $(-1,0,1)$, $(0,-1,1)$, $(0,0,2)$

Table 2.1: Matter representation for F-theory compactifications with a general rank-three Mordell-Weil group, labeled by their U(1)-charges (q_1,q_2,q_3).

three U(1)-factors, most notably a tri-fundamental representation. Matter in these rep-

[5]The correspondence between F-theory compactifications and (integral) points in a polytope has been noted in the toric case [123] and in elliptic fibrations with a general rank two Mordell-Weil group [157].

resentations is unexpected in perturbative Type II compactifications and might have interesting phenomenological implications. These results, in particular the appearance of a tri-fundamental representation, indicate an intriguing structure of the codimension two singularities of elliptic fibration with rank three Mordell Weil group.

Furthermore, we geometrically derive closed formulas for all matter multiplicities of charged hypermultiplets in six dimensions for F-theory compactifications on elliptically fibered Calabi-Yau threefolds over a general base B. As a consistency check, we show that the spectrum is anomaly-free. Technically, the analysis of codimension two singularities requires the study of degenerations of the complete intersection $\mathcal{E}$ in $\mathrm{Bl}_3\mathbb{P}^3$ and the computation of the homology classes of the determinantal varieties describing certain matter loci.

Along the course of this work we have encountered and advanced a number of technical issues. Specifically, we discovered three birational maps of the generic elliptic curve $\mathcal{E}$ in $\mathrm{Bl}_3\mathbb{P}^3$ to a non-generic form of the elliptic curve of [155, 156] in dP_2. These maps are isomorphisms if the elliptic curve $\mathcal{E}$ does not degenerate in a particular way. The dP_2-elliptic curves we obtain are non-generic since one of the generators of the Mordell-Weil group of $\mathcal{E}$, with all its rational points being toric, i.e. induced from the ambient space $\mathrm{Bl}_3\mathbb{P}^3$, maps to a non-toric rational point. It would be interesting to investigate, whether any non-toric rational point on dP_2 can be mapped to a toric point of $\mathcal{E}$ in $\mathrm{Bl}_3\mathbb{P}^3$. In addition, we see directly from this map that the elliptic curve in dP_3 can be obtained as a special case of the curve $\mathcal{E}$ in $\mathrm{Bl}_3\mathbb{P}^3$.

This work is organized as follows. In section 2.2 we construct the general elliptic curve $\mathcal{E}$. From the existence of the three rational points alone, we derive that $\mathcal{E}$ is naturally represented as the complete intersection of two non-generic quadrics in $\mathbb{P}^3$, see section 2.2.1. The resolved elliptic curve $\mathcal{E}$ is obtained in section 2.2.2 as the generic Calabi-Yau complete intersection in $\mathrm{Bl}_3\mathbb{P}^3$, where all its rational points are toric, i.e. induced from the

ambient space. In section 2.2.3 we construct three canonical maps of this elliptic curve to the non-generic elliptic curves in dP_2. In section 2.2.4 we find the Weierstrass form of the curve $\mathcal{E}$ along with the Weierstrass coordinates of all its rational points. We proceed with the construction of elliptically fibered Calabi-Yau manifolds $\hat{X}$ with general elliptic fiber in $\mathrm{Bl}_3\mathbb{P}^3$ over a general base B in section 2.3. First, we determine the ambient space and all bundles on B relevant for the construction of $\hat{X}$ in section 2.3.1. We discuss the basic general intersections of $\hat{X}$ in section 2.3.2 and classify all Calabi-Yau fibrations for a given base B in section 2.3.3. In section 2.4 we analyze explicitly the codimension two singularities of $\hat{X}$, which determine the matter representations of F-theory compactifications to six and four dimensions. We follow a two-step strategy to obtain the charges and codimension two loci of the 14 different matter representations of $\hat{X}$ in sections 2.4.1 and 2.4.2, respectively. We also determine the explicit expressions for the corresponding matter multiplicities of charged hypermultiplets of a six-dimensional F-theory compactification on a threefold $\hat{X}_3$ with general base B. Our conclusions and a brief outlook can be found in 2.5. This work contains two appendices: in appendix 2.6 we present explicit formulae for the Weierstrass form of $\mathcal{E}$, and in appendix 2.7 we give a short account on nef-partitions, that have been omitted in the main text.

2.2 Three Ways to the Elliptic Curve with Three Rational Points

In this section we construct explicitly the general elliptic curve $\mathcal{E}$ with a rank three Mordell-Weil group of rational points, denoted Q, R and S.

We find three different, but equivalent representations of $\mathcal{E}$. First, in section 2.2.1 we find that $\mathcal{E}$ is naturally embedded into $\mathbb{P}^3$ as the complete intersection of two non-generic quadrics, i.e. two homogeneous equations of degree two. Equivalently, we embed $\mathcal{E}$ in sec-

tion 2.2.2 as the generic complete intersection Calabi-Yau into the blow-up $\mathrm{Bl}_3\mathbb{P}^3$ of $\mathbb{P}^3$ at three generic points, which is effectively described via a nef-partition of the corresponding 3D toric polytope. In this representation the three rational points of $\mathcal{E}$ and the zero point P descend from the four inequivalent divisors of the ambient space $\mathrm{Bl}_3\mathbb{P}^3$. Thus, the Mordell-Weil group of $\mathcal{E}$ is *toric*. Finally, we show in section 2.2.3 that $\mathcal{E}$ can also be represented as a non-generic Calabi-Yau hypersurface in dP_2. In contrast to the generic elliptic curve in dP_2 that has a rank two Mordell-Weil group [155, 156] which is toric, the onefold in dP_2 we find here exhibits a third rational point, say S, and has a rank three Mordell-Weil group. This third rational point, however, is *non-toric* in the presentation of $\mathcal{E}$ in dP_2. We note that there are three different maps of the quadric intersection in $\mathrm{Bl}_3\mathbb{P}^3$ to an elliptic curve in dP_2 corresponding to the different morphisms from $\mathrm{Bl}_3\mathbb{P}^3$ to dP_2.

We emphasize that in the presentation of $\mathcal{E}$ as a complete intersection in $\mathrm{Bl}_3\mathbb{P}^3$ the rank four Mordell-Weil group is toric. Thus, as we will demonstrate in section 2.3 this representation is appropriate for the construction of resolved elliptic fibrations of $\mathcal{E}$ over a base B.

2.2.1 The Elliptic Curve as Intersection of Two Quadrics in $\mathbb{P}^3$

In this section we derive the embedding of $\mathcal{E}$ with a zero point P and the rational points Q, R and S into $\mathbb{P}^3$ as the intersection of two non-generic quadrics. We follow the methods described in [154, 156] used for the derivation of the general elliptic curves with rank one and two Mordell-Weil groups.

We note that the presence of the four points on $\mathcal{E}$ defines a degree four line bundle $\mathcal{O}(P+Q+R+S)$ over $\mathcal{E}$. Let us first consider a general degree four line bundle $\mathcal{M}$ over $\mathcal{E}$. Then the following holds, as we see by employing the Riemann-Roch theorem:

1. $H^0(\mathcal{E},\mathcal{M})$ is generated by four sections, that we denote by u', v', w', t'.

2. $H^0(\mathcal{E}, \mathcal{M}^2)$ is generated by eight sections. However we know ten sections of M^2, the quadratic monomials in $[u' : v' : w' : t']$, i.e. u'^2, v'^2, w'^2, t'^2, $u'v'$, $u'w'$, $u't'$, $v'w'$, $v't'$, $w't'$.

The above first bullet point shows that $[u' : v' : w' : t']$ are of equal weight one and can be viewed as homogeneous coordinates on $\mathbb{P}^3$. The second bullet point implies that $H^0(2\mathcal{M})$ is generated by sections we already know and that there have to be two relations between the ten quadratic monomials in $[u' : v' : w' : t']$, that we write as

$$s_1 t'^2 + s_2 u'^2 + s_3 v'^2 + s_4 w'^2 + s_5 t'u' + s_6 u'v' + s_7 u'w' + s_8 v'w' = s_9 v't' + s_{10} w't' \,, \qquad (2.1)$$
$$s_{11} t'^2 + s_{12} u'^2 + s_{13} v'^2 + s_{14} w'^2 + s_{15} u't' + s_{16} u'v' + s_{17} u'w' + s_{18} v'w' = s_{19} v't' + s_{20} w't' \,,$$

Now specialize to $\mathcal{M} = \mathcal{O}(P+Q+R+S)$ and assume u' to vanish at all points P, Q, R, S. By inserting $u' = 0$ into (2.1) we should then get four rational solutions corresponding to the four points, i.e. other words (2.1) should factorize accordingly. However, this is not true for generic s_i taking values e.g. in the ring of functions of the base B of an elliptic fibration[6] Thus, we have to set the following coefficients s_i to zero,

$$s_1 = s_3 = s_4 = s_{11} = s_{13} = s_{14} = 0 \,. \qquad (2.3)$$

As we see below in section 2.2.2, this can be achieved globally, by blowing up $\mathbb{P}^3$ at three generic points.

For the moment, let us assume that (2.3) holds and determine P, Q, R, S. First we note

[6] In contrast, if we were considering an elliptic curve over an algebraically closed field, we could set some $s_i = 0$ by using the $\mathbb{P}GL(4)$ symmetries of $\mathbb{P}^3$ to eliminate some coefficients s_i. For example, $s_3 = 0$ can be achieved by making the transformation

$$u' \mapsto u' + kv' \,, \qquad \text{with } k \text{ obeying} \qquad (s_2 k^2 + s_6 k + s_3) = 0 \,. \qquad (2.2)$$

Solving this quadratic equation in k will, however, involve the square roots of s_i, which is only defined in an algebraically closed field. In particular, when considering elliptic fibrations the coefficients s_i will be represented by polynomials, of which a square root is not defined globally.

that the presentation (2.1) for the elliptic curve $\mathcal{E}$ now reads

$$\begin{aligned} s_2u'^2 + s_5u't' + s_6u'v' + s_7u'w' &= s_9v't' + s_{10}w't' - s_8v'w' \,, \\ s_{12}u'^2 + s_{15}u't' + s_{16}u'v' + s_{17}u'w' &= s_{19}v't' + s_{20}w't' - s_{18}v'w' \,, \end{aligned} \tag{2.4}$$

which is an intersection of two *non-generic* quadrics in $\mathbb{P}^3$. Setting $u' = 0$ we obtain

$$0 = s_9v't' + s_{10}w't' - s_8v'w' \,, \qquad 0 = s_{19}v't' + s_{20}w't' - s_{18}v'w' \,, \tag{2.5}$$

which has in the coordinates $[u' : v' : w' : t']$ the four solutions

$$\begin{aligned} P = [0:0:0:1] \,, \quad Q = [0:1:0:0] \,, \quad R = [0:0:1:0] \,, \\ S = [0 : |M_1^S||M_3^S| : -|M_1^S||M_2^S| : -|M_3^S||M_2^S|] \,. \end{aligned} \tag{2.6}$$

Here we introduced the determinants $|M_i^S|$ of all three 2×2-minors M_i^S reading

$$|M_1^S| = s_9s_{20} - s_{10}s_{19} \,, \qquad |M_2^S| = s_8s_{19} - s_9s_{18} \,, \qquad |M_3^S| = s_8s_{20} - s_{10}s_{18} \,, \tag{2.7}$$

that are obtained by deleting the $(4-i)$-th column in the matrix

$$M^S = \begin{pmatrix} s_9 & s_{10} & -s_8 \\ s_{19} & s_{20} & -s_{18} \end{pmatrix} , \tag{2.8}$$

where M^S is the matrix of coefficients in (2.5).

It is important to realize that the coordinates of the rational point S are products of determinants in (2.7), in particular when studying elliptic fibrations at higher codimension in the base B, cf. section 2.4. On the one hand, the vanishing loci of the determinant of a single determinant $|M_i^S|$ with $i = 1,2,3$ indicates the collisions of S with P, Q and R,

respectively, i.e.

$$|M_1^S| = 0 : \; S = P\,, \qquad |M_2^S| = 0 : \; S = Q\,, \qquad |M_3^S| = 0 : \; S = R\,. \tag{2.9}$$

On the other hand the simultaneous vanishing of all $|M_i^S|$ is equivalent to the two constraints in (2.4) getting linearly dependent. Then, the elliptic curve $\mathcal{E}$ degenerates to an I_2-curve, i.e. two $\mathbb{P}^1$'s intersecting at two points, see the discussion around (2.27), with the point S becoming the entire $\mathbb{P}^1 = \{u = s_9 v't' + s_{10} w't' - s_8 v'w' = 0\}$[7]. We note that this behavior of S indicates that in an elliptic fibration the point S will only give rise to a rational, not a holomorphic section of the fibration.

In summary, we have found that the general elliptic curve $\mathcal{E}$ with three rational points Q, R, S and a zero point P is embedded into $\mathbb{P}^3$ as the intersection of the two non-generic quadrics (2.4).

2.2.2 Resolved Elliptic Curve as Complete Intersection in $\mathbf{Bl}_3\mathbb{P}^3$

In this section we represent the elliptic curve $\mathcal{E}$ with a rank three Mordell-Weil group as a *generic* complete intersection Calabi-Yau in the ambient space $\mathrm{Bl}_3\mathbb{P}^3$. As we demonstrate here, the three blow-ups in $\mathrm{Bl}_3\mathbb{P}^3$ remove globally the coefficients in (2.3). In addition, the three blow-ups resolve all singularities of $\mathcal{E}$, that can appear in elliptic fibrations. Finally, we emphasize that the elliptic curve $\mathcal{E}$ is a complete intersection associated to the nef-partition of the polytope of $\mathrm{Bl}_3\mathbb{P}^3$, where we refer to appendix 2.7 for more details on nef-partitions.

First, we recall the polytope of $\mathbb{P}^3$ and its nef-partition describing a complete intersection of quadrics. The polytope $\nabla_{\mathbb{P}^3}$ of $\mathbb{P}^3$ is the convex hull $\nabla_{\mathbb{P}^3} = \langle \rho_1, \rho_2, \rho_3, \rho_4 \rangle$ of the four

[7] This curve can be seen to define a $\mathbb{P}^1$ either using adjunction or employing the Segre embedding of $\mathbb{P}^1 \times \mathbb{P}^1$ into $\mathbb{P}^3$.

vertices

$$\rho_1 = (-1,-1,-1)\,, \qquad \rho_2 = (1,0,0)\,, \qquad \rho_3 = (0,1,0)\,, \qquad \rho_4 = (0,0,1)\,, \tag{2.10}$$

corresponding to the homogeneous coordinates u', v', w' and t', respectively. The anti-canonical bundle of $\mathbb{P}^3$ is $K_{\mathbb{P}^3}^{-1} = \mathcal{O}(4H)$, where H denotes the hyperplane class of $\mathbb{P}^3$. Two generic degree two polynomials in the class $\mathcal{O}(2H)$ are obtained via (2.135) from the nef-partition of the polytope of $\mathbb{P}^3$ into ∇_1, ∇_2 reading

$$\nabla_{\mathbb{P}^3} = \langle \nabla_1 \cup \nabla_2 \rangle\,, \qquad \nabla_1 = \langle \rho_1, \rho_2 \rangle\,, \quad \nabla_2 = \langle \rho_3, \rho_4 \rangle\,, \tag{2.11}$$

where $\cup$ denotes the union of sets of a vector space. This complete intersection defines the elliptic curve in (2.1) with only the origin P.

Next, we describe the elliptic curve $\mathcal{E}$ as a generic complete intersection associated to a nef-partition of $\mathrm{Bl}_3\mathbb{P}^3$, the blow-up of $\mathbb{P}^3$ at three generic points, that we choose to be P, Q and R in (2.6). We first perform these blow-ups and determine the proper transform of $\mathcal{E}$ by hand, before we employ toric techniques and nef-paritions.

The blow-up from $\mathbb{P}^3$ to $\mathrm{Bl}_3\mathbb{P}^3$ is characterized by the blow-down map

$$u' = e_1 e_2 e_3 u\,, \qquad v' = e_2 e_3 v\,, \qquad w' = e_1 e_3 w\,, \qquad t' = e_1 e_2 t\,. \tag{2.12}$$

It maps the coordinates $[u:v:w:t:e_1:e_2:e_3]$ on $\mathrm{Bl}_3\mathbb{P}^3$ to the coordinates on $[u:v:w:t]$ on $\mathbb{P}^3$. Here the $e_i = 0$, $i = 1,2,3$, are the exceptional divisors E_i of the the blow-ups at the points Q, R and P, respectively. We summarize the divisor classes of all homogeneous coordinates on $\mathrm{Bl}_3\mathbb{P}^3$ together with the corresponding $\mathbb{C}^*$-actions that follow immediately

from (2.12) as

	divisor class	$\mathbb{C}^*$-actions			
u	$H-E_1-E_2-E_3$	1	1	1	1
v	$H-E_2-E_3$	1	0	1	1
w	$H-E_1-E_3$	1	1	0	1
t	$H-E_1-E_2$	1	1	1	0
e_1	E_1	0	−1	0	0
e_2	E_2	0	0	−1	0
e_3	E_3	0	0	0	−1

(2.13)

Here H denotes the pullback of the hyperplane class H on $\mathbb{P}^3$. The coordinates $[u:w:t]$, $[u:v:t]$ and $[u:v:w]$ are the homogeneous coordinates on each $E_i \cong \mathbb{P}^2$, respectively, and can not vanish simultaneously. Together with the pullback of the Stanley-Reissner ideal of $\mathbb{P}^3$ this implies the following Stanley Reisner ideal on $\mathrm{Bl}_3\mathbb{P}^3$,

$$SR = \{uvt, uwt, uvw, e_1v, e_2w, e_3t, e_1e_2, e_2e_3, e_1e_3\}. \tag{2.14}$$

This implies the following intersections of the four independent divisors on $\mathrm{Bl}_3\mathbb{P}^3$,

$$H^3 = E_i^3 = 1, \qquad E_i \cdot H = E_i \cdot E_j = 0, \quad i \neq j. \tag{2.15}$$

The proper transform under the map (2.12) of the constraints (2.4) describing $\mathcal{E}$ read

$$\begin{aligned} p_1 &:= s_2e_1e_2e_3u^2 + s_5e_1e_2ut + s_6e_2e_3uv + s_7e_1e_3uw - s_9e_2vt - s_{10}e_1wt + s_8e_3vw, \\ p_2 &:= s_{12}e_1e_2e_3u^2 + s_{15}e_1e_2ut + s_{16}e_2e_3uv + s_{17}e_1e_3uw - s_{19}e_2vt - s_{20}e_1wt + s_{18}e_3vw. \end{aligned} \tag{2.16}$$

We immediately see that this complete intersection defines a Calabi-Yau onefold in $\mathrm{Bl}_3\mathbb{P}^3$

employing (2.13), adjunction and noting that the anti-canonical bundle of $\mathrm{Bl}_3\mathbb{P}^3$ reads

$$K_{\mathrm{Bl}_3\mathbb{P}^3} = \mathcal{O}(4H - 2E_1 - 2E_2 - 2E_3)\,. \tag{2.17}$$

From (2.6), (2.12) and (2.16) we readily obtain the points in P, Q, R and S on $\mathrm{Bl}_3\mathbb{P}^3$. They are given by the intersection of (2.16) with the four inequivalent toric divisors on $\mathrm{Bl}_3\mathbb{P}^3$, the divisor $D_u := \{u = 0\}$ and the exceptional divisors E_i. Their coordinates read

$$\begin{aligned}
E_3 \cap \mathcal{E} \;:&\quad P = \left[s_{10}s_{19} - s_{20}s_9 : s_{10}s_{15} - s_{20}s_5 : s_{19}s_5 - s_{15}s_9 : 1 : 1 : 1 : 0\right],\\
E_1 \cap \mathcal{E} \;:&\quad Q = \left[s_{19}s_8 - s_{18}s_9 : 1 : -s_{19}s_6 + s_{16}s_9 : -s_{18}s_6 + s_{16}s_8 : 0 : 1 : 1\right],\\
E_2 \cap \mathcal{E} \;:&\quad R = \left[s_{10}s_{18} - s_{20}s_8 : -s_{10}s_{17} + s_{20}s_7 : 1 : s_{18}s_7 - s_{17}s_8 : 1 : 0 : 1\right],\\
D_u \cap \mathcal{E} \;:&\quad S = \left[0 : 1 : 1 : 1 : s_{19}s_8 - s_{18}s_9 : s_{10}s_{18} - s_{20}s_8 : s_{10}s_{19} - s_{20}s_9\right].
\end{aligned} \tag{2.18}$$

Here we made use of the Stanley-Reissner ideal (2.14) to set the coordinates to one that can not vanish simultaneously with $u = 0$, respectively, $e_i = 0$.

We emphasize that the coordinates (2.18) are again given by determinants of 2×2-minors. Indeed, we can write (2.18) as

$$\begin{aligned}
&P = \left[-|M_3^P| : |M_2^P| : -|M_1^P| : 1 : 1 : 1 : 0\right], \quad Q = \left[-|M_3^Q| : 1 : |M_2^Q| : -|M_1^Q| : 0 : 1 : 1\right],\\
&R = \left[|M_3^R| : -|M_2^R| : 1 : |M_1^R| : 1 : 0 : 1\right], \quad S = \left[0 : 1 : 1 : 1 : -|M_3^Q| : |M_3^R| : -|M_3^P|\right]
\end{aligned} \tag{2.19}$$

Here we defined the matrices

$$M^P = \begin{pmatrix} -s_5 & s_9 & s_{10} \\ -s_{15} & s_{19} & s_{20} \end{pmatrix}, \quad M^Q = \begin{pmatrix} -s_6 & -s_8 & s_9 \\ -s_{16} & -s_{18} & s_{19} \end{pmatrix}, \quad M^R = \begin{pmatrix} -s_7 & -s_8 & s_{10} \\ -s_{17} & -s_{18} & s_{20} \end{pmatrix} \tag{2.20}$$

with their 2×2-minors $M_i^{P,Q,R}$ defined by deleting the $(4-i)$-th column. We emphasize that the minors of the matrix M^S in (2.7) can be expressed by the minors of the matrices in (2.20) and, thus, M^S does not appear in (2.19). The matrices $M^{P,Q,R}$ describe the two linear equations that we obtain by setting $e_3 = 0$, $e_2 = 0$ and $e_1 = 0$ in (2.16), respectively.

It is important to realize that the points P, Q and R are always distinct, as can be seen from (2.19) and the Stanley-Reissner ideal (2.14) since the exceptional divisors do not mutually intersect. However, the point S can agree with all other points, if the appropriate minors in (2.19) vanish. In fact, we see the following pattern,

$$|M_3^P| = 0 : \; S = P\,, \qquad |M_3^Q| = 0 : \; S = Q\,, \qquad |M_3^R| = 0 : \; S = R\,, \tag{2.21}$$

which will be relevant to keep in mind for the study of elliptic fibrations.

We note that the elliptic curve $\mathcal{E}$ degenerates into an I_2-curve if, as explained before below (2.8), the rank of one of the matrices in (2.8) and (2.20) is one[8]. In addition, one particular intersection in (2.18) no longer yields a point in $\mathcal{E}$, but an entire $\mathbb{P}^1$. As discussed below in section 2.4 the points on $\mathcal{E}$, thus, will only lift to rational sections of an elliptic fibration of $\mathcal{E}$.

Finally, we show that the presentation of $\mathcal{E}$ as the complete intersection (2.16) can be obtained torically from a nef-partition of the $\mathrm{Bl}_3\mathbb{P}^3$. For this purpose we only have to realize that the blow-ups (2.12) can be realized torically by adding the following rays to the polytope of $\mathbb{P}^3$ in (2.10),

$$\rho_{e_1} = (-1,0,0)\,, \qquad \rho_{e_2} = (0,-1,0)\,, \qquad \rho_{e_3} = (0,0,-1)\,. \tag{2.22}$$

The rays of the polytope of $\mathrm{Bl}_3\mathbb{P}^3$ are illustrated in the center of figure (2.1).

[8]We emphasize that the complete intersection (2.4) in $\mathbb{P}^3$ degenerates into only one $\mathbb{P}^1$ and becomes singular if one matrices in (2.20) has rank one, in contrast to the smooth I_2-curve obtained from (2.16).

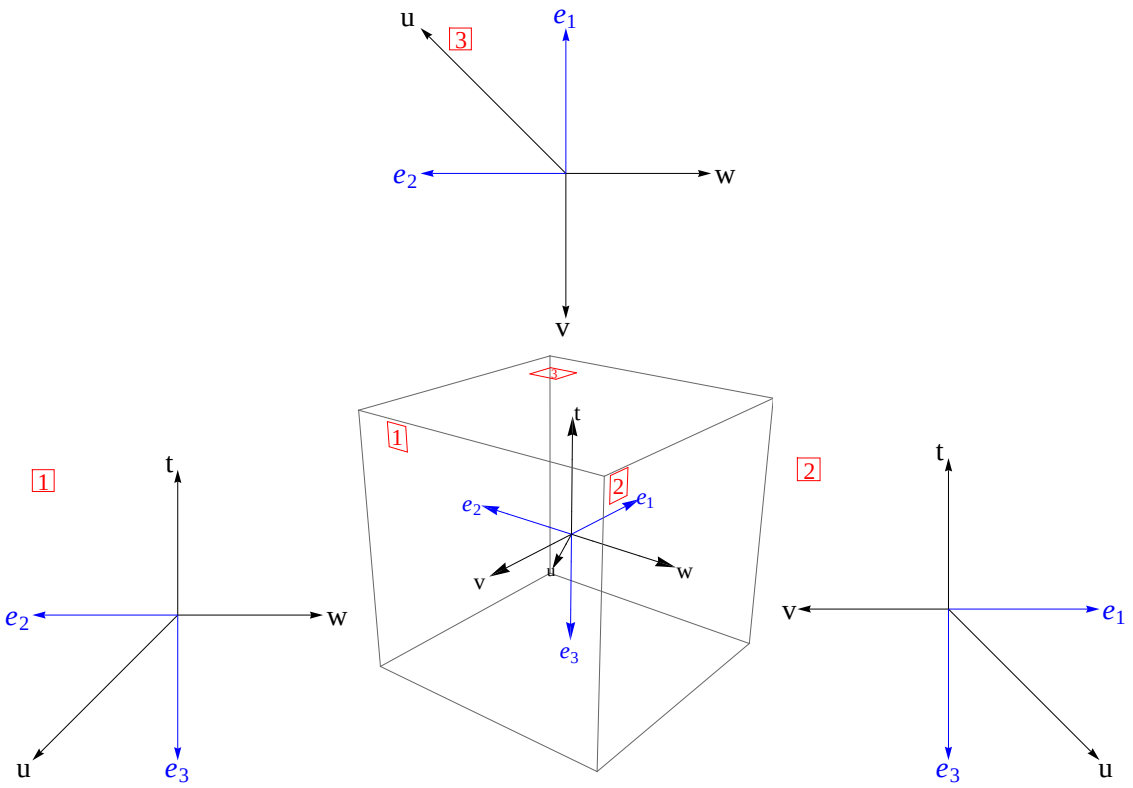

Figure 2.1: Toric fan of $\mathrm{Bl}_3\mathbb{P}^3$ and the 2D projections to the three coordinate planes, each of which yielding the polytope of dP_2.

Here the ray ρ_{e_i} precisely corresponds to the exceptional divisor $E_i = \{e_i = 0\}$. Then we determine the nef-partitions of this polytope $\nabla_{\mathrm{Bl}_3\mathbb{P}^3}$ of $\mathrm{Bl}_3\mathbb{P}^3$. We find that is admits a single nef-partition into ∇_1, ∇_2 reading

$$\nabla_{\mathrm{Bl}_3\mathbb{P}^3} = \langle \nabla_1 \cup \nabla_2 \rangle\,, \qquad \nabla_1 = \langle \rho_1, \rho_4, \rho_{e_1}, \rho_{e_2} \rangle \quad \nabla_2 = \langle \rho_2, \rho_3, \rho_{e_3} \rangle\,. \tag{2.23}$$

It is straightforward to check that the general formula (2.135) for the nef-partition at hand reproduces precisely the constraints (2.16).

2.2.3 Connection to the cubic in dP_2

In this section we construct three equivalent maps of the elliptic curve $\mathcal{E}$ given as the intersection (2.16) in $\mathrm{Bl}_3\mathbb{P}^3$ to the Calabi-Yau onefold in dP_2. The elliptic curve we obtain will not be the generic elliptic curve in dP_2 found in [155, 156] with rank two Mordell-Weil group, but non-generic with a rank three Mordell-Weil group with one *non-toric generator*. The map of the toric generator of the Mordell-Weil group in $\mathrm{Bl}_3\mathbb{P}^3$ to a non-toric generator in dP_2 will be manifest.

The presentation of $\mathcal{E}$ as a non-generic hypersurface in dP_2 with a non-toric Mordell-Weil group allows us to use the results of [156] from the analysis of the generic dP_2-curve. On the one hand, we can immediately obtain the birational map of $\mathcal{E}$ in (2.16) to the Weierstrass model by first using the map to dP_2 and then by the map from dP_2 to the Weierstrass form. We present this map separately in section 2.2.4. On the other hand, the study of codimension two singularities in section 2.4 will essentially reduce to the analysis of codimension two singularities in fibrations with elliptic fiber in dP_2. However, the additional non-toric Mordell-Weil generator as well as the non-generic hypersurface equation in dP_2 will give rise to a richer structure of codimension two singularities.

Mapping the Intersection of Two Quadrics in $\mathbb{P}^3$ to the Cubic in $\mathbb{P}^2$

As a preparation, we begin with a brief digression on the map of an elliptic curve with a single point P_0 given as a complete intersection of two quadrics in $\mathbb{P}^3$ to the cubic in $\mathbb{P}^2$, where we closely follow [124, 125].

Let us assume that there is a rational point P_0 on the complete intersection of two quadrics with coordinates $[x_0 : x_1 : x_2 : x_3] = [0 : 0 : 0 : 1]$ in $\mathbb{P}^3$.[9] This implies the quadrics

[9] We choose coordinates $[x_0 : x_1 : x_2 : x_3]$ on $\mathbb{P}^3$ in order to keep our discussion here general. We will identify the x_i with the coordinates used in sections 2.2.1 and (2.2.2) in section 2.2.3.

must have the form

$$Ax_3 + B = 0\,, \qquad Cx_3 + D = 0\,, \tag{2.24}$$

where A, C are linear and B, D are quadratic polynomials in the variables x_0, x_1, x_2. Assuming that A, C are generic, we obtain a cubic equation in $\mathbb{P}^2$ with coordinates $[x_0 : x_1 : x_2]$[10] by solving (2.24) for x_3,

$$AD - BC = 0\,, \tag{2.25}$$

Here we have to require that $[x_0 : x_1 : x_2] \neq [0,0,0]$, because $x_3 = -\frac{B}{A} = -\frac{D}{C}$ has to be well-defined. Then, the inverse map from the cubic in $\mathbb{P}^2$ to the complete intersection (2.24) reads

$$[x_0 : x_1 : x_2] \mapsto [x_0 : x_1 : x_2 : x_3 = -\tfrac{B}{A} = -\tfrac{D}{C}]\,. \tag{2.26}$$

The original point $P_0 = [0 : 0 : 0 : 1]$ is mapped to the rational point given by the intersection of the two lines $A = 0$, $C = 0$. This can be seen by noting that $A = C = 0$ in (2.24) implies also $B = D = 0$ which is only solved if $[x_0 : x_1 : x_2] = [0 : 0 : 0]$.

We note that the case when A and C are co-linear, i.e. $A \sim C$, is special because the curve (2.24) describes no longer a smooth elliptic curve, but a $\mathbb{P}^1$. Indeed, if $A = aC$ for a number a we can rewrite (2.24) as

$$B - aD = 0\,, \qquad Cx_3 + D = 0\,, \tag{2.27}$$

where we can solve the second constraint for x_3, given $C \neq 0$, so that we are left with the quadratic constraint $B - aD = 0$ in $\mathbb{P}^2$, which is a $\mathbb{P}^1$. This type of degeneration of the complete intersection (2.24) will be the prototype for the degenerations of the elliptic curve (2.16), that we find in section 2.4.

[10] We can think of this $\mathbb{P}^2$ as being obtained from $\mathbb{P}^3$ via a toric morphism defined by projection along one toric ray. In the case at hand this is the ray corresponding to $x_3 = 0$.

Mapping the Intersection in $\mathbf{Bl}_3\mathbb{P}^3$ to the Calabi-Yau Onefold in dP_2

Next we apply the map of section 2.2.3 to the elliptic curve $\mathcal{E}$ with three rational points. Since (2.4) is linear in all three coordinates v', w' and t' we will obtain according to the discussion below (2.24) three canonical maps to a cubic in $\mathbb{P}^2$. In fact, these maps lift to maps of the elliptic curve (2.16) in $\mathrm{Bl}_3\mathbb{P}^3$ to elliptic curves presented as Calabi-Yau hypersurfaces in dP_2, as we demonstrate in the following.

We construct the map from the complete intersection (2.16) to the elliptic curve in dP_2 explicitly for the point R in (2.6), i.e. we identify $P_0 \equiv R$ and $[x_0 : x_1 : x_2 : x_3] = [u' : v' : t' : w']$ in the coordinates on $\mathbb{P}^3$ before the blow-up for the discussion in section 2.2.3. Next, we compare (2.24) to the complete intersection (2.16). After the blow-up (2.12), the point R is mapped to $e_2 = 0$ as noted earlier in (2.18). This allows us to identify A, C in (2.24) as those terms in (2.16) that do not vanish, respectively, B, D as the terms that vanish for $e_2 = 0$. Thus we effectively rewrite (2.16) in the form (2.24) with $x_3 \equiv w$ after the blow-up, since $w = 1$ follows from (2.14) for $e_2 = 0$, and obtain

$$A = s_7 e_1 e_3 u + s_8 e_3 v - s_{10} e_1 t\,, \quad C = s_{17} e_1 e_3 u + s_{18} e_3 v - s_{20} e_1 t\,, \tag{2.28}$$
$$B = e_2\big(s_2 e_1 e_3 u^2 + s_5 e_1 u t + s_6 e_3 u v - s_9 v t\big)\,, \quad D = e_2\big(s_{12} e_1 e_3 u^2 + s_{15} e_1 u t + s_{16} e_3 u v - s_{19} v t\big)\,.$$

In particular, this identification implies that $R = \{e_2 = 0\}$ is mapped to $A = C = 0$ on dP_2 as required. Then, we solve both equations for w and obtain the hypersurface equation of the form

$$u\big(\tilde{s}_1 u^2 e_1^2 e_3^2 + \tilde{s}_2 u v e_1 e_3^2 + \tilde{s}_3 v^2 e_3^2 + \tilde{s}_5 u t e_1^2 e_3 + \tilde{s}_6 v t e_1 e_3 + \tilde{s}_8 t^2 e_1^2\big) + \tilde{s}_7 v^2 t e_3 + \tilde{s}_9 v t^2 e_1 = 0\,, \tag{2.29}$$

where we have set $e_2 = 1$ using one $\mathbb{C}^*$-action on $\mathrm{Bl}_3\mathbb{P}^3$ as $B, D \sim e_2$ and $e_2 = 0$ implies $w = -\frac{B}{A} = -\frac{D}{C} = 0$ which is inconsistent with the SR-ideal (2.14) . The coefficients $\tilde{s}_i$ in

(2.29) read

	coefficients in dP_2-curve projected along $[w : e_2]$
$\tilde{s}_1$	$-s_{17}s_2 + s_{12}s_7$
$\tilde{s}_2$	$-s_{18}s_2 - s_{17}s_6 + s_{16}s_7 + s_{12}s_8$
$\tilde{s}_3$	$-\lvert M_1^Q\rvert = s_{16}s_8 - s_{18}s_6$
$\tilde{s}_5$	$-s_{10}s_{12} + s_2s_{20} - s_{17}s_5 + s_{15}s_7$
$\tilde{s}_6$	$-s_{10}s_{16} - s_{18}s_5 + s_{20}s_6 - s_{19}s_7 + s_{15}s_8 + s_{17}s_9$
$\tilde{s}_7$	$\lvert M_3^Q\rvert = s_{18}s_9 - s_{19}s_8$
$\tilde{s}_8$	$-\lvert M_2^P\rvert = -s_{10}s_{15} + s_{20}s_5$
$\tilde{s}_9$	$-\lvert M_3^P\rvert = s_{10}s_{19} - s_{20}s_9$

(2.30)

Here we have used the minors introduced in (2.7) and in (2.19), (2.20).

We note that the ambient space of (2.29) is dP_2 with homogeneous coordinates $[u : v : w : t : e_1 : e_3]$. The relevant dP_2 is obtained from $\mathrm{Bl}_3\mathbb{P}^3$ by a toric morphism that is defined by projecting the polytope of $\mathrm{Bl}_3\mathbb{P}^3$ generated by (2.10), (2.22) onto the plane that is perpendicular to the line through the rays ρ_3 and ρ_{e_2}. The rays of the fan are shown in the figure on the right of 2.1 that is obtained by the projection of the rays on the face number two of the cube. This can also be seen from the unbroken $\mathbb{C}^*$-actions in (2.13) and the SR-ideal (2.14) for $e_2 = 1$ and $w = 0$, or $e_2 = 0$ and $w = 1$. Then, the cubic (2.29) is a section precisely of the anti-canonical bundle of this dP_2 surface.

The general elliptic curve in dP_2 was studied in [156, 155] and shown to have a rank two Mordell-Weil group. However, the elliptic curve (2.29) has by construction a rank three Mordell-Weil group. Indeed, we see that the coefficients $\tilde{s}_i$ are non-generic and precisely allow for a fourth rational point. This fourth point, however, does not descend from a divisor of the ambient space dP_2 and is not toric. In fact, the mapping of the four rational

points (2.18) in the coordinates on dP_2 reads

$$\begin{aligned} P = [-|M_3^P| : |M_2^P| : -|M_1^P| : 1 : 1 : 1 : 0] &\mapsto [|M_3^P| : -|M_2^P| : 1 : 1 : 0], \\ Q = [-|M_3^Q| : 1 : |M_2^Q| : -|M_1^Q| : 0 : 1 : 1] &\mapsto [-|M_3^Q| : 1 : -|M_1^Q| : 0 : 1], \\ R = [|M_3^R| : -|M_2^R| : 1 : |M_1^R| : 1 : 0 : 1] &\mapsto [|M_3^R| : -|M_2^R| : |M_1^R| : 1 : 1], \\ S = [0 : 1 : 1 : 1 : -|M_3^Q| : |M_3^R| : -|M_3^P|] &\mapsto [0 : 1 : 1 : -|M_3^Q| : -|M_3^P|]. \end{aligned} \tag{2.31}$$

We see, that the points P, Q and S are mapped to the three toric points on the elliptic curve in dP_2 studied in [156], whereas the points R is mapped to a non-toric point.

The map from the complete intersection in $\mathrm{Bl}_3\mathbb{P}^3$ to the elliptic curve (2.29) in dP_2 implies that the results from the analysis of [156], where the generic elliptic curve in dP_2 was considered, immediately apply. More precisely, renaming the coordinates $[u : v : t : e_1 : e_3]$ in (2.29) as $[u : v : w : e_1 : e_2]$ we readily recover equation (3.4) of [156]. Furthermore, the points P, Q and S in (2.31) immediately map to the origin and the two rational points of the rank two elliptic curve in dP_2, that we denote in the following as $\tilde{P}$, $\tilde{Q}$ and $\tilde{R}$. In the notation of [156] we thus rewrite (2.31) using (2.30) as

$$\begin{aligned} P \mapsto \tilde{P} := [-\tilde{s}_9 : \tilde{s}_8 : 1 : 1 : 0], \quad Q \mapsto \tilde{Q} := [-\tilde{s}_7 : 1 : \tilde{s}_3 : 0 : 1], \\ S \mapsto \tilde{R} := [0 : 1 : 1 : -\tilde{s}_7 : \tilde{s}_9]. \end{aligned} \tag{2.32}$$

We emphasize that the origin P in the complete intersection in (2.16) is mapped to the origin $\tilde{P}$, which implies that the Weierstrass form of the curve in dP_2 will agree with the Weierstrass form of the curve (2.16), cf. section 2.2.4.

As we mentioned before, the point R is mapped to a non-toric point in dP_2. This complicates the determination of the Weierstrass coordinates for R, for example. Fortunately, there are two other maps of the elliptic curve (2.16) to a curve in dP_2 in which the point R

is mapped to a toric point and another point, either Q or P, are realized non-torically. Thus, we construct in the following a second map to an elliptic curve in dP_2, where R is toric. Since the logic is completely analogous to the previous construction, we will be as brief as possible.

We choose $P_0 \equiv Q$ for the map to dP_2. We recall from (2.18) that Q is realized as $e_1 = 0$ on the elliptic curve in $\mathrm{Bl}_3\mathbb{P}^3$. Thus, we write (2.16) as

$$Av + B = 0\,, \qquad Cv + D = 0\,, \tag{2.33}$$

where, as before, A and C are obtained by setting $e_1 = 0$ and B, D are the terms proportional to e_1,

$$\begin{aligned} A &= -s_9 e_2 t + s_6 e_2 e_3 u + s_8 e_3 w\,, \quad C = -s_{19} e_2 t + s_{16} e_2 e_3 u + s_{18} e_3 w\,, \\ B &= e_1\big(s_2 e_2 e_3 u^2 + s_5 e_2 u t + s_7 e_3 u w - s_{10} w t\big)\,, \quad D = e_1\big(s_{12} e_2 e_3 u^2 + s_{15} e_2 u t + s_{17} e_3 u w - s_{20} w t\big)\,. \end{aligned} \tag{2.34}$$

Thus, we obtain an elliptic curve in dP_2 with homogeneous coordinates $[u : w : t : e_2 : e_3]$ by solving (2.33) for v and by setting $e_1 = 1$ as required by the SR-ideal (2.14). The hypersurface constraint (2.25) takes the form

$$u\big(\hat{s}_1 u^2 e_2^2 e_3^2 + \hat{s}_2 u w e_2 e_3^2 + \hat{s}_3 w^2 e_3^2 + \hat{s}_5 u t e_2^2 e_3 + \hat{s}_6 w t e_2 e_3 + \hat{s}_8 t^2 e_2^2\big) + \hat{s}_7 w^2 t e_3 + \hat{s}_9 w t^2 e_2 = 0\,, \tag{2.35}$$

with coefficients $\hat{s}_i$ defined as

	coefficients in dP_2-curve projected along $[v:e_1]$
$\hat{s}_1$	$-s_{16}s_2 + s_{12}s_6$
$\hat{s}_2$	$-s_{18}s_2 + s_{17}s_6 - s_{16}s_7 + s_{12}s_8$
$\hat{s}_3$	$-\lvert M_1^R\rvert = -s_{18}s_7 + s_{17}s_8$
$\hat{s}_5$	$s_{19}s_2 - s_{16}s_5 + s_{15}s_6 - s_{12}s_9$
$\hat{s}_6$	$s_{10}s_{16} - s_{18}s_5 - s_{20}s_6 + s_{19}s_7 + s_{15}s_8 - s_{17}s_9$
$\hat{s}_7$	$\lvert M_3^R\rvert = s_{10}s_{18} - s_{20}s_8$
$\hat{s}_8$	$-\lvert M_1^P\rvert = s_{19}s_5 - s_{15}s_9$
$\hat{s}_9$	$\lvert M_3^P\rvert = -\tilde{s}_9 = -s_{10}s_{19} + s_{20}s_9$

(2.36)

where we have used (2.30). Analogously to the previous map, the ambient space of the hypersurface (2.35) is the dP_2 with homogeneous coordinates $[u:w:t:e_2:e_3]$ that is obtained from $\mathrm{Bl}_3\mathbb{P}^3$ by the toric morphism induced by projecting along the line through the rays ρ_2 and ρ_{e_1}. The rays of the fan are shown in the left figure of 2.1 that corresponds to the projection of the rays on the face number one. Then, the three rational points on $\mathcal{E}$ and the origin get mapped, in the coordinates $[u:w:t:e_2:e_3]$ of dP_2, to

$$\begin{aligned}
P = [-\lvert M_3^P\rvert : \lvert M_2^P\rvert : -\lvert M_1^P\rvert : 1:1:1:0] &\mapsto [-\lvert M_3^P\rvert : -\lvert M_1^P\rvert : 1:1:0], \\
Q = [-\lvert M_3^Q\rvert : 1 : \lvert M_2^Q\rvert : -\lvert M_1^Q\rvert : 0:1:1] &\mapsto [-\lvert M_3^Q\rvert : \lvert M_2^Q\rvert : -\lvert M_1^Q\rvert : 1:1], \\
R = [\lvert M_3^R\rvert : -\lvert M_2^R\rvert : 1 : \lvert M_1^R\rvert : 1:0:1] &\mapsto [\lvert M_3^R\rvert : 1 : \lvert M_1^R\rvert : 0:1], \\
S = [0:1:1:1:-\lvert M_3^Q\rvert : \lvert M_3^R\rvert : -\lvert M_3^P\rvert] &\mapsto [0:1:1:\lvert M_3^R\rvert : -\lvert M_3^P\rvert].
\end{aligned} \tag{2.37}$$

As before, it is convenient to make contact to the notation of [156]. After the renaming $[u:w:t:e_2:e_3] \to [u:v:w:e_1:e_2]$ we obtain the hypersurface constraint (2.35) takes the standard form of eq. (3.4) in [156]. In addition, we see that the points P, R and S get

mapped to the toric points on dP_2, whereas Q maps to a non-toric point. Denoting the origin of the dP_2-curve by $\hat{P}$ and the two rational points by $\hat{Q}$, $\hat{R}$ in order to avoid confusion, we then write (2.37) as

$$P \;\mapsto\; \hat{P} := [-\hat{s}_9 : \hat{s}_8 : 1 : 1 : 0]\,, \quad R \;\mapsto\; \hat{Q} = [-\hat{s}_7 : 1 : \hat{s}_3 : 0 : 1]\,,$$
$$S \;\mapsto\; \tilde{R} = [0 : 1 : 1 : \hat{s}_7 : -\hat{s}_9]\,. \tag{2.38}$$

We note that there is a third map from (2.16) to dP_2 by solving for the variable t, respectively, e_3 (its fan would correspond to the upper figure in figure 2.1 that shows the projection of the rays in the face number three). Although this map is formally completely analogous to the above the maps, it is not very illuminating for our purposes since the chosen zero point P on $\mathcal{E}$ maps to a non-toric point in dP_2. In particular, the Weierstrass model with respect to P can not be obtained from this elliptic curve in dP_2 by simply applying the results of [156], where P by assumption has to be a toric point.

2.2.4 Weierstrass Form with Three Rational Points

Finally, we are prepared to obtain the Weierstrass model for the elliptic curve $\mathcal{E}$ in (2.16) with respect to the chosen origin P along with the coordinates in Weierstrass form for the three rational points Q, R and S. We present three maps to a Weierstrass model in this work, each of which yielding an identical Weierstrass form, i.e. identical f, g in $y^2 = x^3 + fxz^4 + gz^6$. The details of the relevant computations as well as the explicit results can be found in appendix 2.6.

The simplest two ways to obtain this Weierstrass from is by first exploiting the two presentations of the elliptic curve $\mathcal{E}$ as the hypersurfaces (2.29) and (2.35) in dP_2 constructed in section 2.2.3 and by then using the birational map of [156] of the general elliptic curve in dP_2 to the Weierstrass form in $\mathbb{P}^2(1,2,3)$. In summary, we find the following schematic

coordinates for the coordinates in Weierstrass form of the rational points Q, R and S

$$Q = [g_2^Q : g_3^Q : 1], \quad R = [g_2^R : g_3^R : 1], \qquad S = [g_2^S : g_3^S : (s_{10}s_{19} - s_9 s_{20})] \tag{2.39}$$

with the explicit expressions for $g_2^{Q,R,S}$ and $g_3^{Q,R,S}$ given in (2.127-2.131) in appendix 2.6. The explicit form for f and g, along with the discriminant follow from the formulas in [156] in combination with (2.30), respectively, (2.36). In fact, we obtain (2.39) for Q and S by using the presentation (2.29) along with the maps (2.32) of the rational points Q and S onto the two toric points in the dP_2-elliptic curve, denoted by $\tilde{Q}$ and $\tilde{R}$ in this context. Then, we apply Eqs. (3.11) and (3.12) of [156] for the coordinates in Weierstrass form of the two toric rational points on the elliptic curve in dP_2. For concreteness, for the curve (2.29) the coordinates in Weierstrass form of the two points read

$$[g_2^Q : g_3^Q : z_Q] = [\tfrac{1}{12}(\tilde{s}_6^2 - 4\tilde{s}_5\tilde{s}_7 + 8\tilde{s}_3\tilde{s}_8 - 4\tilde{s}_2\tilde{s}_9), \tfrac{1}{2}(\tilde{s}_3\tilde{s}_6\tilde{s}_8 - \tilde{s}_2\tilde{s}_7\tilde{s}_8 - \tilde{s}_3\tilde{s}_5\tilde{s}_9 + \tilde{s}_1\tilde{s}_7\tilde{s}_9) : 1] \tag{2.40}$$

for the point $\tilde{Q} = [-\tilde{s}_7 : 1 : \tilde{s}_3 : 0 : 1]$ and

$$\begin{aligned} g_2^S &= \tfrac{1}{12}(12\tilde{s}_7^2\tilde{s}_8^2 + \tilde{s}_9^2(\tilde{s}_6^2 + 8\tilde{s}_3\tilde{s}_8 - 4\tilde{s}_2\tilde{s}_9) + 4\tilde{s}_7\tilde{s}_9(-3\tilde{s}_6\tilde{s}_8 + 2\tilde{s}_5\tilde{s}_9)), \\ g_3^S &= \tfrac{1}{2}(2\tilde{s}_7^3\tilde{s}_8^3 + \tilde{s}_3\tilde{s}_9^3(-\tilde{s}_6\tilde{s}_8 + \tilde{s}_5\tilde{s}_9) + \tilde{s}_7^2\tilde{s}_8\tilde{s}_9(-3\tilde{s}_6\tilde{s}_8 + 2\tilde{s}_5\tilde{s}_9) \\ &\quad + \tilde{s}_7\tilde{s}_9^2(\tilde{s}_6^2\tilde{s}_8 + 2\tilde{s}_3\tilde{s}_8^2 - \tilde{s}_5\tilde{s}_6\tilde{s}_9 - \tilde{s}_2\tilde{s}_8\tilde{s}_9 + \tilde{s}_1\tilde{s}_9^2), \\ z_S &= \tilde{s}_9 \end{aligned} \tag{2.41}$$

for the point $\tilde{R} = [0 : 1 : 1 - \tilde{s}_7 : \tilde{s}_9]$, where we apply (2.30). The explicit result in terms of the coefficients s_i for both Q, S can be found in (2.127), respectively, (2.131).

In order to obtain the Weierstrass coordinates for the point R in (2.39) we invoke the map $R \mapsto \hat{Q}$ in (2.38) for the elliptic curve (2.35) in dP_2. Here, the coordinates of $R \mapsto \hat{Q}$ are again given by (2.40) after replacing $\tilde{s}_i \to \hat{s}_i$. The explicit form for these coordinates in

terms of the s_i is obtained using (2.36) and can be found in (2.129). We emphasize that the coordinates in Weierstrass form for S can also be obtained from the map $S \mapsto \hat{R}$ in (2.38) in combination with (2.36). They precisely agree with those in (2.131) deduced from the map $S \mapsto \tilde{R}$ and (2.30).

Alternatively, one can directly construct the birational map from (2.16) to the Weierstrass form by extension of the techniques of [154, 156], where x and y in $\mathbb{P}^2(1,2,3)$ are constructed as sections of appropriate line bundles that vanish with appropriate degrees at Q, R and S. However, the corresponding calculations are lengthy and the resulting Weierstrass model is identical to the one obtained from dP_2. Thus, we have opted to relegate this analysis to appendix 2.6.

2.3 Elliptic Fibrations with Three Rational Sections

In this section we construct resolved elliptically fibered Calabi-Yau manifolds $\mathcal{E} \to \hat{X} \stackrel{\pi}{\to} B$ over a base B with a rank three Mordell-Weil group. The map π denotes the projection to the base B and the general elliptic fiber $\mathcal{E} = \pi^{-1}(pt)$ over a generic point pt in B is the elliptic curve with rank three Mordell-Weil group of section 2.2. An elliptic Calabi-Yau manifold $\hat{X}$ with all singularities at higher codimension resolved is obtained by fibering $\mathcal{E}$ in the presentation (2.16). In addition, in this representation for $\mathcal{E}$ the generators of the Mordell-Weil group are given by the restriction to $\hat{X}$ of the toric divisors of the ambient space $\mathrm{Bl}_3\mathbb{P}^3$ of the fiber, i.e. the Mordell-Weil group of the generic $\hat{X}$ is toric.

We begin in section 2.3.1 with the construction of Calabi-Yau elliptic fibrations $\hat{X}$ with rank three Mordell-Weil group over a general base B with the elliptic curve (2.16) as the general elliptic fiber. We see that all these fibrations are classified by three divisors in the base B. Then in section 2.3.2 we compute the universal intersections on $\hat{X}$, that hold generically and are valid for any base B. Finally, in section 2.3.3 we classify all generic

Calabi-Yau manifolds $\hat{X}$ with elliptic fiber $\mathcal{E}$ in $\mathrm{Bl}_3\mathbb{P}^3$ over any base B. Each such F-theory vacua $\hat{X}$ is labeled by one point in a particular polytope, that we determine.

The techniques and results in the following analysis are a direct extension to the ones used in [156, 157, 159] for the case of a rank two Mordell-Weil group.

2.3.1 Constructing Calabi-Yau Elliptic Fibrations

Let us begin with the explicit construction of the Calabi-Yau manifold $\hat{X}$. Abstractly, a general elliptic fibration of the given elliptic curve $\mathcal{E}$ over a base B is given by defining the complete intersection (2.16) over the function field of B. In other words, we lift all coefficients s_i as well as the coordinates in (2.16) to sections of appropriate line bundles over B.

To each of the homogeneous coordinates on $\mathrm{Bl}_3\mathbb{P}^3$ we assign a different line bundle on the base B. However, we can use the $(\mathbb{C}^*)^4$-action in (2.13) to assign without loss of generality the following non-trivial line bundles

$$u \in \mathcal{O}_B(D_u)\,, \qquad v \in \mathcal{O}_B(D_v)\,, \qquad w \in \mathcal{O}_B(D_w)\,, \tag{2.42}$$

with all other coordinates $[t : e_1 : e_2 : e_3]$ transforming in the trivial bundle on B. Here K_B denotes the canonical bundle on B, $[K_B]$ the associated divisor and D_u, D_v and D_w are three, at the moment, arbitrary divisors on B. They will be fixed later in this section by the Calabi-Yau condition on the elliptic fibration. The assignment (2.42) can be described globally by constructing the fiber bundle

$$\begin{array}{ccc} \mathrm{Bl}_3\mathbb{P}^3 & \longrightarrow & \mathrm{Bl}_3\mathbb{P}^3_B(D_u, D_v, D_w) \\ & & \downarrow \\ & & B \end{array} \tag{2.43}$$

The total space of this fibration is the ambient space of the complete intersection (2.16), that defines the elliptic fibration of $\mathcal{E}$ over B.

Next, we require the complete intersection (2.16) to define a Calabi-Yau manifold in the ambient space (2.43). To this end, we first calculate the anti-canonical bundle of $\mathrm{Bl}_3\mathbb{P}^3_B(D_u, D_v, D_w)$ via adjunction. We obtain

$$K^{-1}_{\mathrm{Bl}_3\mathbb{P}^3_B} = 4H - 2E_1 - 2E_2 - 2E_3 + [K_B^{-1}] + D_u + D_v + D_w\,, \tag{2.44}$$

where we suppressed the dependence on the vertical divisors D_u, D_v and D_w for brevity of our notation and H as well as the E_i are the classes introduced in (2.13). For the complete intersection (2.16) to define a Calabi-Yau manifold $\hat{X}$ in (2.43) we infer again from adjunction that the sum of the classes of the two constraints p_1, p_2 has to be agree with $[K^{-1}_{\mathrm{Bl}_3\mathbb{P}^3_B}]$. Thus, the Calabi-Yau condition reads

$$[p_1] + [p_2] \stackrel{!}{=} 4H - 2E_1 - 2E_2 - 2E_3 + [K_B^{-1}] + D_u + D_v + D_w\,. \tag{2.45}$$

We see from (2.13) that both constraints in (2.16) are automatically in the divisor class $2H - E_1 - E_2 - E_3$ w.r.t. the classes on the fiber $\mathrm{Bl}_3\mathbb{P}^3$. Thus, (2.45) effectively reduces to a condition on the class of (2.16) in the homology of the base B. Denoting the part of the homology classes of the $[p_i]$ in the base B by $[p_1]^b$ and $[p_2]^b + D_v + D_w$, we obtain

$$[p_1]^b + [p_2]^b \stackrel{!}{=} [K_B^{-1}] + D_u\,. \tag{2.46}$$

Here we shifted the class $[p_2]^b \to D_v + D_w + [p_2^b]$ for reasons that will become clear in section 2.3.3.

Using this information we fix the line bundles on B in which the coefficients s_i take values. We infer from (2.16), (2.42) and the Calabi-Yau condition (2.46) the following

assignments of line bundles,

section	line-bundle	section	line-bundle
s_2	$\mathcal{O}([K_B^{-1}]-D_u-[p_2]^b)$	s_{12}	$\mathcal{O}(-2D_u+D_v+D_w+[p_2]^b)$
s_5	$\mathcal{O}([K_B^{-1}]-[p_2]^b)$	s_{15}	$\mathcal{O}(-D_u+D_v+D_w+[p_2]^b)$
s_6	$\mathcal{O}([K_B^{-1}]-[p_2]^b-D_v)$	s_{16}	$\mathcal{O}(-D_u+D_w+[p_2]^b)$
s_7	$\mathcal{O}([K_B^{-1}]-[p_2]^b-D_w)$	s_{17}	$\mathcal{O}(-D_u+D_v+[p_2]^b)$
s_8	$\mathcal{O}([K_B^{-1}]-[p_2]^b+D_u-D_v-D_w)$	s_{18}	$\mathcal{O}([p_2]^b)$
s_9	$\mathcal{O}([K_B^{-1}]-[p_2]^b+D_u-D_v)$	s_{19}	$\mathcal{O}(D_w+[p_2]^b)$
s_{10}	$\mathcal{O}([K_B^{-1}]-[p_2]^b+D_u-D_w)$	s_{20}	$\mathcal{O}(D_v+[p_2]^b)$

(2.47)

We also summarize the complete line bundles of the homogeneous coordinates on $\mathrm{Bl}_3\mathbb{P}^3$ by combining the classes in (2.13) and (2.42),

section	bundle
u	$\mathcal{O}(H-E_1-E_2-E_3+D_u)$
v	$\mathcal{O}(H-E_2-E_3+D_v)$
w	$\mathcal{O}(H-E_1-E_3+D_w)$
t	$\mathcal{O}(H-E_1-E_2)$
e_1	$\mathcal{O}(E_1)$
e_2	$\mathcal{O}(E_2)$
e_3	$\mathcal{O}(E_3)$

(2.48)

For later reference, we point out that the divisors associated to the vanishing of the coefficients $\tilde{s}_7$, $\hat{s}_7$ and $\tilde{s}_9 = -\hat{s}_9$, denoted as $\tilde{\mathcal{S}}_7$, $\hat{\mathcal{S}}_7$ respectively $\mathcal{S}_9$, in the two presentations

(2.29) and (2.35) in dP_2 of the elliptic curves $\mathcal{E}$ are given by

$$\tilde{\mathcal{S}}_7 := \left[-s_{19}s_8 + s_{18}s_9\right] = \left[K_B^{-1}\right] + D_u - D_v\,, \quad \hat{\mathcal{S}}_7 := \left[s_{10}s_{18} - s_{20}s_8\right] = \left[K_B^{-1}\right] + D_u - D_w\,,$$
$$\mathcal{S}_9 := \left[\tilde{s}_9\right] = \left[\hat{s}_9\right] = \left[-s_{10}s_{19} + s_{20}s_9\right] = D_u + \left[K_B^{-1}\right]. \tag{2.49}$$

Here we have used the definitions in (2.30), respectively, (2.36) together with (2.47) and denoted the divisor classes of a section s_i by $[\cdot]$.

It is important to notice that the line bundles of the s_i admit an additional degree of freedom due to the choice of the class $[p_2]^b$, the divisor class of the second constraint p_2 in the homology of B. This is due to the fact that the Calabi-Yau condition (2.46) is a partition problem, that only fixes the sum of the classes $[p_1]^b$, $[p_2]^b$ but leaves the individual classes undetermined. For example, in complete intersections in a toric ambient space (2.43) the freedom of the class $[p_2]^b$ is fixed by finding all nef-partitions of the toric polytope associated to (2.43) that are consistent with the nef-partition (2.23) of the $\mathrm{Bl}_3\mathbb{P}^3$-fiber. We discuss the freedom in $[p_2]^b$ further in section 2.3.3.

2.3.2 Basic Geometry of Calabi-Yau Manifolds with $\mathrm{Bl}_3\mathbb{P}^3$-elliptic Fiber

Let us next discuss the basic topological properties of the Calabi-Yau manifold $\hat{X}$.

We begin by constructing a basis D_A of the group of divisors $H^{(1,1)}(\hat{X})$ on $\hat{X}$ that is convenient for the study of F-theory on $\hat{X}$. A basis of divisors on the generic complete intersection $\hat{X}$ is induced from the basis of divisors of the ambient space $\mathrm{Bl}_3\mathbb{P}^3(\tilde{\mathcal{S}}_7, \hat{\mathcal{S}}_7, \mathcal{S}_9)$ by restriction to $\hat{X}$. There are the vertical divisors D_α that are obtained by pulling back divisors D_α^b on the base B as $D_\alpha = \pi^*(D_\alpha^b)$ under the projection map $\pi : \hat{X} \to B$. In addition, each point P, Q, R and S on the elliptic fiber $\mathcal{E}$ in (2.16) lifts to an in general rational section of the fibration $\pi : \hat{X} \to B$, that we denote by $\hat{s}_P$, $\hat{s}_Q$, $\hat{s}_R$ and $\hat{s}_S$, with $\hat{s}_P$ the zero

section. The corresponding divisor classes, denoted S_P, S_Q, S_R and S_S, then follow from (2.18) and (2.48) as

$$S_P = E_3\,, \qquad S_Q = E_1\,, \qquad S_R = E_2\,, \qquad S_S = H - E_1 - E_2 - E_3 + \mathcal{S}_9 + [K_B]\,, \tag{2.50}$$

where we denote, by abuse of notation, the lift of the classes H, E_1, E_2, E_3 of the fiber $\mathrm{Bl}_3\mathbb{P}^3$ in (2.13) to classes in $\hat{X}$ by the same symbol. For convenience, we collectively denote the generators of the Mordell-Weil group and their divisor classes as

$$\hat{s}_m = (\hat{s}_Q, \hat{s}_R, \hat{s}_S)\,, \qquad S_m = (S_Q, S_R, S_S) \quad m = 1,2,3\,. \tag{2.51}$$

The vertical divisors D_α together with the classes (2.50) of the rational points form a basis of $H^{(1,1)}(\hat{X})$. A basis that is better suited for applications to F-theory, however, is given by

$$D_A = (\tilde{S}_P, D_\alpha, \sigma(\hat{s}_m))\,, \quad A = 0, 1, \ldots, h^{(1,1)}(B) + 4\,, \tag{2.52}$$

where the Hodge number $h^{(1,1)}(B)$ of the base B counts the number of vertical divisors D_α in $\hat{X}$. Here we have introduced the class [126, 127]

$$\tilde{S}_P = S_P + \frac{1}{2}[K_B^{-1}]\,, \tag{2.53}$$

and have applied the Shioda map σ that maps the Mordell-Weil group of $\hat{X}$ to a certain subspace of $H^{(1,1)}(\hat{X})$. The map σ is defined as

$$\sigma(\hat{s}_m) := S_m - \tilde{S}_P - \pi(S_m \cdot \tilde{S}_P)\,, \tag{2.54}$$

where π, by abuse of notation, denotes the projection of $H^{(2,2)}(\hat{X})$ to the vertical homology

$\pi^* H^{(1,1)}(B)$ of the base B. For every $\mathcal{C}$ in $H^{(2,2)}(\hat{X})$ the map π is defined as

$$\pi(\mathcal{C}) = (\mathcal{C} \cdot \Sigma^\alpha) D_\alpha \,, \tag{2.55}$$

where we obtain the elements $\Sigma^\alpha = \pi^*(\Sigma_b^\alpha)$ in $H_4(\hat{X})$ as pullbacks from a dual basis Σ_b^α to the divisors D_α^b in B, i.e. $\Sigma_b^\alpha \cdot D_\beta^b = \delta_\beta^\alpha$.

Next, we list the fundamental intersections involving the divisors S_P, S_Q and S_R in (2.50), that will be relevant throughout this work:

Universal intersection:	$S_P \cdot F = S_m \cdot F = 1$ with general fiber $F \cong \mathcal{E}$, (2.56)
Rational sections:	$\pi(S_P^2 + [K_B^{-1}] \cdot S_P) = \pi(S_m^2 + [K_B^{-1}] \cdot S_m) = 0$, (2.57)
	$\tilde{\mathcal{S}}_7 = \pi(S_Q \cdot S_S)$, $\hat{\mathcal{S}}_7 = \pi(S_R \cdot S_S)$, $\mathcal{S}_9 = \pi(S_P \cdot S_S)$,
Holomorphic sections:	$S_P^2 + [K_B^{-1}] \cdot S_P = S_m^2 + [K_B^{-1}] \cdot S_m = 0$, (2.58)
Shioda maps:	$\sigma(\hat{s}_Q) = S_Q - S_P - [K_B^{-1}]$,
	$\sigma(\hat{s}_R) = S_R - S_P - [K_B^{-1}]$, (2.59)
	$\sigma(\hat{s}_R) = S_S - S_P - [K_B^{-1}] - \mathcal{S}_9$,

The first line (2.56) and the second line (2.57) are the defining property of a section of a fibration, whereas the fourth line only holds for a holomorphic section. The third line holds because the collision pattern of the points in (2.21) directly translates into intersections of their divisor classes S_m, where we made use of (2.30) and (2.36). In other words, (2.57) states that divisors $\tilde{\mathcal{S}}_7$, $\hat{\mathcal{S}}_7$, $\mathcal{S}_9$ are the codimension one loci where the sections collide with each other in the fiber $\mathcal{E}$. Finally, the result for the Shioda maps of

the sections follows from their definitions in (2.54) and the intersections in (2.57).

For later reference, we also compute the intersection matrix of the Shioda maps $\sigma(\hat{s}_m)$, i.e. the height pairing, as

$$\pi(\sigma(\hat{s}_m)\cdot\sigma(\hat{s}_n)) = \begin{pmatrix} 2[K_B] & [K_B] & -\mathcal{S}_9+\tilde{\mathcal{S}}_7+[K_B] \\ [K_B] & 2[K_B] & -\mathcal{S}_9+\hat{\mathcal{S}}_7+[K_B] \\ -\mathcal{S}_9+\hat{\mathcal{S}}_7+[K_B] & -\mathcal{S}_9+\hat{\mathcal{S}}_7+[K_B] & 2(-\mathcal{S}_9+[K_B]) \end{pmatrix}_{mn} . \quad (2.60)$$

which readily follows from (2.59) and (2.57).

We note that all the above intersections (2.56) , (2.57), (2.58), (2.59) and (2.60) are in completely analogous to the ones found in [120, 156, 157] for the case of an elliptic Calabi-Yau manifold with rank two Mordell-Weil group, see also [128, 154, 121, 129] for a discussion of intersections in the rank one case.

2.3.3 All Calabi-Yau manifolds $\hat{X}$ with $\mathrm{Bl}_3\mathbb{P}^3$-elliptic fiber over B

Finally, we are equipped to classify the generic Calabi-Yau manifolds $\hat{X}$ with elliptic fiber in $\mathrm{Bl}_3\mathbb{P}^3$ and base B. This task reduces to a classification of all possible assignments of line bundles to the sections s_i in (2.47) so that the Calabi-Yau manifold $\hat{X}$ is given by the generic complete intersection (2.16). Otherwise we expect additional singularities in $\hat{X}$, potentially corresponding to a minimal gauge symmetry in F-theory, either from non-toric non-Abelian singularities or from non-toric sections. We prove in the following that a generic Calabi-Yau manifold $\hat{X}$ over a base B corresponds to a point in a certain polytope, that is related to the single nef-partition of the polytope of $\mathrm{Bl}_3\mathbb{P}^3$ as explained below. The following discussion is similar in spirit to the one in [157, 155], that can agree with the toric classification of [123].

We begin with the basis expansion

$$D_u = n_u^\alpha D_\alpha\,, \quad D_v = n_v^\alpha D_\alpha\,, \quad D_w = n_w^\alpha D_\alpha\,, \tag{2.61}$$

into vertical divisors D_α, where the n_u^α, n_v^α and n_w^α are integer coefficients. For $\hat{X}$ to be generic these coefficients are bounded by the requirement that all the sections s_i in (2.47) are generic, i.e. that the line bundles of which the s_i are holomorphic sections admit holomorphic sections. This is equivalent to all divisors in (2.47) being effective.

First, we notice that effectiveness of the sum $[s_i] + [s_{i+10}] \geq 0$ in (2.47) is guaranteed if the vector of integers $\mathbf{n}^\alpha = (n_u^\alpha, n_v^\alpha, n_w^\alpha)$ is an integral point in the rescaled polytope of $\mathrm{Bl}_3\mathbb{P}^3$. Indeed, we can express the conditions of effectiveness of the divisors $[s_i] + [s_{i+10}]$ as the following set of inequalities in $\mathbb{R}^3$,

$$\frac{1}{-K^\alpha}\mathbf{n}^\alpha \cdot \nu_i \geq -1\,, \qquad i = 1, \ldots, 7\,, \tag{2.62}$$

where we also expand the canonical bundle K_B of the base B in terms of the vertical divisors D_α as

$$[K_B] = K^\alpha D_\alpha \tag{2.63}$$

with integer coefficients K^α. The entries of the vectors ν_i are extracted by first summing the rows of the two tables in (2.47), requiring the sum to be effective and then taking the coefficients of the the divisors D_u, D_v, D_w. The ν_i span the following polytope

$$\Delta_3 := \langle \nu_i \rangle = \left\langle \begin{pmatrix} -3 \\ 1 \\ 1 \end{pmatrix}, \begin{pmatrix} -1 \\ 1 \\ 1 \end{pmatrix}, \begin{pmatrix} -1 \\ -1 \\ 1 \end{pmatrix}, \begin{pmatrix} -1 \\ 1 \\ -1 \end{pmatrix}, \begin{pmatrix} 1 \\ -1 \\ -1 \end{pmatrix}, \begin{pmatrix} 1 \\ -1 \\ 1 \end{pmatrix} \begin{pmatrix} 1 \\ 1 \\ -1 \end{pmatrix} \right\rangle. \tag{2.64}$$

This is precisely the dual of the polytope $\nabla_{\mathrm{Bl}_3\mathbb{P}^3}$ of $\mathrm{Bl}_3\mathbb{P}^3$, where the latter polytope is the

convex hull of the following vertices,

$$\nabla_{\mathrm{Bl}_3\mathbb{P}^3} = \Big\langle -\rho_1, \rho_{e_1}, \rho_4, \rho_3, \rho_{e_2}, \rho_{e_3}, \rho_1 \Big\rangle . \tag{2.65}$$

We note that these vertices are related to the vertices in (2.10) and (2.22) by an $\mathrm{SL}(3,\mathbb{Z})$ transformation. Thus, we confirm that the solutions to (2.62), for which all divisors $[s_i] + [s_{i+10}]$ are effective, are precisely given by vectors $\mathbf{n}^\alpha$ that take values for all α in the polytope of $\mathrm{Bl}_3\mathbb{P}^3$ rescaled by the factor $-K^\alpha$.

Next we determine the conditions inferred from each individual class $[s_i]$ in (2.47) being effective. We obtain the following *two sets of conditions*, whose solutions, given also below, yield the set of all generic elliptic fibrations $\hat{X}$ with a general rank three Mordell-Weil group over a given base B:

$$\begin{aligned} &1) && 0 \le ([p_2]^b)^\alpha \le -K_B^\alpha , && (2.66)\\ &2) && \mathbf{n}^\alpha \cdot \nu_i \ge K^\alpha + ([p_2]^b)^\alpha , \quad \nu_i \in \nabla_1 , \qquad \mathbf{n}^\alpha \cdot \nu_i \ge -([p_2]^b)^\alpha , \quad \nu_i \in \nabla_2 . \end{aligned}$$

These conditions are solved by any $\mathbf{n}^\alpha$ being integral points in the following Minkowski sum of the polyhedra ∇_1, ∇_2 defined in (2.70),

$$\mathbf{n}^\alpha \in -(K^\alpha + ([p_2]^b)^\alpha)\nabla_1 + ([p_2]^b)^\alpha \nabla_2 , \qquad \forall \alpha = 1, \ldots, h^{(1,1)}(B) . \tag{2.67}$$

Here the two conditions for $[p_2]^b$ in the first line of (2.66) follow from $[s_5], [s_{18}] \ge 0$ and the first, respectively, second set of conditions in the second line follow from the first, respectively, second table in (2.47). In addition, we have expanded the class $[p_2]^b$ into a basis D_α as

$$[p_2]^b = ([p_2]^b)^\alpha D_\alpha \tag{2.68}$$

and have introduced the points ν_i that define two polytopes

$$\begin{aligned}\Delta_1 &:= \langle \nu_i \rangle_{0\le i\le 6} = \left\langle \begin{pmatrix}-1\\0\\0\end{pmatrix}, \begin{pmatrix}0\\-1\\0\end{pmatrix}, \begin{pmatrix}0\\0\\-1\end{pmatrix}, \begin{pmatrix}1\\-1\\-1\end{pmatrix}, \begin{pmatrix}1\\-1\\0\end{pmatrix}, \begin{pmatrix}1\\0\\-1\end{pmatrix} \right\rangle, \\ \Delta_2 &:= \langle \nu_i \rangle_{7\le i\le 12} = \left\langle \begin{pmatrix}-2\\1\\1\end{pmatrix}, \begin{pmatrix}-1\\1\\1\end{pmatrix}, \begin{pmatrix}-1\\0\\1\end{pmatrix}, \begin{pmatrix}-1\\1\\0\end{pmatrix}, \begin{pmatrix}0\\0\\1\end{pmatrix}, \begin{pmatrix}0\\1\\0\end{pmatrix} \right\rangle. \end{aligned} \tag{2.69}$$

Next, we show how we have constructed the solutions (2.67) to (2.66). To this end, it we only have to notice that the two polytopes Δ_1, Δ_2 are the duals in the sense of (2.134) of the following two polytopes ∇_1, ∇_2,

$$\nabla_1 = \left\langle -\rho_1, \rho_{e_1}, \rho_4, \rho_3 \right\rangle, \quad \nabla_2 = \left\langle \rho_{e_2}, \rho_{e_3}, \rho_1 \right\rangle, \tag{2.70}$$

where the vectors ρ_i, ρ_{e_i} were defined in (2.10), (2.22). These two polytopes correspond to the unique nef-partition of (2.65). Now, we first fix the class $[p_2]^b$ such that the first conditions in (2.66) are met. Second, for each allowed class for $[p_2]^b$ we solve the second set of conditions in (2.66) for the vectors $\mathbf{n}^\alpha$. However, these are just the duality relations between the Δ_i and ∇_j, rescaled by appropriate factors. Consequently, the solutions are precisely given by the integral points in the Minkowski sum of the polyhedra in (2.67). Here we emphasize again that both coefficients in (2.67) are positive integers by means of the first condition in (2.66).

In summary, we have shown that for a given base B a generic elliptically fibered Calabi-Yau manifold $\hat{X}$ with general elliptic fiber $\mathcal{E}$ given by (2.16) in $\mathrm{Bl}_3\mathbb{P}^3$ corresponds to an integral point $\mathbf{n}^\alpha$ in the polyhedron (2.67) for every α and for every class $[p_2]^b$ obeying $0 \le [p_2]^b \le [K_B^{-1}]$. The coordinates of the point $\mathbf{n}^\alpha$ are the coefficients of the divisors D_u,

D_v, D_w in the expansion (2.61) into vertical divisors D_α.

2.4 Matter in F-Theory Compactifications with a Rank Three Mordell-Weil Group

In this section we analyze the codimension two singularities of the elliptic fibration of $\hat{X}$ to determine the matter representations of corresponding F-theory compactifications to six and four dimensions. We find 14 different singlet representations in sections 2.4.1 and 2.4.2. Then, we determine the explicit matter multiplicities of these 14 matter fields in six-dimensional F-theory compactification on a Calabi-Yau threefold $\hat{X}_3$ with a general two-dimensional base B in section 2.4.3. The following discussion is based on techniques developed in [156, 157, 159] for the case of a rank two Mordell-Weil group, to which we refer for more background on some technical details.

We begin with an outline of the general strategy to determine matter in an F-theory compactification on a Calabi-Yau manifold with a higher rank Mordell-Weil group. First, we recall that in general rational curves c_{mat} obtained from resolving a singularity of the elliptic fibration at codimension two in the base B give rise to matter in F-theory due to the presence of light M2-brane states in the F-theory limit. In elliptically fibered Calabi-Yau manifolds with a non-Abelian gauge symmetry in F-theory, these codimension two singularities are located on the divisor in the base B, which supports the 7-branes giving rise to the non-Abelian gauge group. Technically, the discriminant of the elliptic fibration takes the form $\Delta = z^n(k + \mathcal{O}(z))$, where z vanishes along the 7-brane divisor and k is a polynomial independent of z. Then, the codimension two singularities are precisely given by the intersections of $z = 0$ and $k = 0$.

This is in contrast to elliptic fibrations with only a non-trivial Mordell-Weil group, i.e. only an Abelian gauge group, since the elliptic fibration over codimension one has

only I_1-singularities and the discriminant does not factorize in an obvious way. Thus, the codimension two codimension singularities are not contained in a simple divisor in B and have to be studied directly. In fact, the existence of a rational section, denoted by say $\hat{s}_Q$, means that there is a solution to the Weierstrass form (WSF) of the form $[x^Q : y^Q : z^Q] = [g_2^Q : g_3^Q : 1]$.[11] Here g_2^Q and g_3^Q are sections of K_B^{-2} and K_B^{-3}, respectively.[12]. Thus, the presence of $\hat{s}_Q$ implies the factorization

$$(y - g_3^Q z^3)(y + g_3^Q z^3) = (x - g_2^Q z^2)(x^2 + g_2^Q x z^2 + g_4^Q z^4) \tag{2.71}$$

for appropriate g_4^Q. Parametrizing the discriminant Δ in terms of the polynomials in (3.5), we see that it vanishes of order two at the codimension two loci in B reading

$$g_3^Q = 0\,, \qquad \hat{g}_4^Q := g_4^Q + 2(g_2^Q)^2 = 0\,. \tag{2.72}$$

These two conditions lead to a factorization of both sides of (3.5), so that a conifold singularity is developed at $y = (x - g_2^Q z^2) = 0$.

It is evident that the section $\hat{s}_Q$ passes automatically through the singular point of the elliptic curve. Thus, in the resolved elliptic curve $\mathcal{E}$ where the singular point $y = (x - g_2^Q z^2) = 0$ is replaced by a Hirzebruch-Jung sphere tree of intersecting $\mathbb{P}^1$'s,[13] the section $\hat{s}_Q$ automatically intersects at least one $\mathbb{P}^1$. This implies that the loci (2.72) in the base contain matter

[11] Sections with $z^Q = b$ for a section b of a line bundle $\mathcal{O}([b])$ on the base B and with g_2^Q, g_3^Q sections of $K_B^{-2} \otimes \mathcal{O}(2[b])$, respectively, $K_B^{-3} \otimes \mathcal{O}(3[b])$, can be studied similarly. We only have to assume that we are at a locus with $b \neq 0$. Then we can employ the $\mathbb{C}^*$-action to set $z^Q = 1$, $x^Q = \frac{g_2^Q}{b^2}$, $y^Q = \frac{g_3^Q}{b^3}$.

[12] For concreteness and for comparison to [154, 156], in the special case of the base $B = \mathbb{P}^2$, the sections $g_2^Q = g_6$, $g_3^Q = g_9$ are polynomials of degree 6, respectively, 9

[13] In F-theory compactifications with only Abelian groups the resolved elliptic fibers are expected to be I_2-curves, i.e. two $\mathbb{P}^1$'s intersecting at two points.

charged under $\mathrm{U}(1)_Q$ associated to $\hat{s}_Q$, as can be seen from the charge formula

$$q_Q = c_{\text{mat}} \cdot (S_Q - S_P)\,. \tag{2.73}$$

Here S_Q, S_P denote the divisor classes of $\hat{s}_Q$ and the zero section $\hat{s}_P$, respectively. In fact, the locus (2.72) contains the codimension two loci supporting *all* matter charged under $\mathrm{U}(1)_Q$, without distinguishing between matter with different $\mathrm{U}(1)_Q$-charges. The loci of the different matter representations correspond to the irreducible components of (2.72), that can in principle be obtained by finding all associated prime ideals of (2.72) of codimension two in B. Unfortunately, in many concrete setups this is computationally unfeasible and we have to pursue a different strategy to obtain the individual matter representations that has already been successful in the rank two case in [154, 156].

For the following analysis of codimension two singularities of $\hat{X}$ we identify the irreducible components of (2.72) corresponding to different matter representations in two qualitatively different ways:

1) One type of codimension two singularities corresponds to singularities of the sections $\hat{s}_m$ and $\hat{s}_P$. This analysis, see section 2.4.1, is performed in the presentation of $\mathcal{E}$ as the complete intersection (2.16) in $\mathrm{Bl}_3\mathbb{P}^3$, where the rational sections are given by (2.19). In fact, when a rational section $\hat{s}_m$ or the zero section $\hat{s}_P$ is ill-defined, the resolved elliptic curve splits into an I_2-curve with one $\mathbb{P}^1$ representing the original singular fiber and the other $\mathbb{P}^1$ representing the singular section.

2) The second type of codimension two singularities has to be found directly in the Weierstrass model. The basic idea is isolate special solutions to (2.72) by supplementing the two equations (2.72) by further constraints that have to vanish in addition in order for a certain matter representation to be present. We refer to section 2.4.2 for concrete examples. It is then possible to find the codimension two locus along

which all these constraints vanish simultaneously. We note that for the geometry $\hat{X}$ there are three rational sections, thus, three factorizations of the form (3.5) and loci (2.72), that have to be analyzed separately.

A complete analysis of codimension two singularities following the above two-step strategy should achieve a complete decomposition of (2.72) for all sections of $\hat{X}$ into irreducible components. It would be interesting to prove this mathematical for the codimension two singularities of $\hat{X}$ we find in this section. As a consistency check of our analysis of codimension two singularities we find, we determine the full spectrum, including multiplicities, of charged hypermultiplets of a six-dimensional F-theory compactification and check that six-dimensional anomalies are cancelled, cf. section 2.4.3.

2.4.1 Matter at the Singularity Loci of Rational Sections

Now that the strategy is clear, we will look for the first type of singularities in this subsection. These are the codimension two loci in the base where the rational sections are singular in $\text{Bl}_3\mathbb{P}^3$. This precisely happens when the coordinates (2.18), (2.19) of any of the rational sections take values in the Stanley-Reisner ideal (2.14) of $\text{Bl}_3\mathbb{P}^3$.

There are two reasons why codimension two loci with singular rational sections are good candidates for I_2-fibers. First, the elliptic fibration of $\hat{X}$ is smooth[14], thus, the indeterminacy of the coordinates of the sections in the fiber may imply that the section is not a point, but an entire $\mathbb{P}^1$. Second, as was remarked in [154] and [156], if we approach the codimension two singularity of the section along a line in the base B the section has a well defined coordinate given by the slope of the line. Thus, approaching the singularity along lines of all possible slopes the section at the singular point is identified with the $\mathbb{P}^1$ formed by all slopes. In fact, specializing the elliptic curve to each locus yielding a singularity of

[14]This is clear for toric bases B.

a rational section we observe a splitting of the elliptic curve into an I_2-curve. We note that it is crucial to work in $\mathrm{Bl}_3\mathbb{P}^3$, because only in this space the fiber is fully resolved space by the exceptional divisors E_i, in contrast to the curve (2.4) in $\mathbb{P}^3$.

The vanishing of two minors: special singularities of $\hat{s}_S$

In order to identify singularities of rational sections, let us take a close look at the Stanley-Reisner ideal (2.14). It contains monomials with two variables of the type $e_i e_j$ and monomials with three variables of the type uXY, where X and Y are two variables out of the set $\{v,w,t\}$. In this subsection we look for singular sections whose coordinates are forbidden by the elements $e_i e_j$.

From the coordinates (2.19) of the rational sections we infer that this type of singular behavior can only occur for the section $\hat{s}_S$, whose coordinates in the fiber $\mathcal{E}$ are

$$S = \left[0 : 1 : 1 : 1 : s_{19}s_8 - s_{18}s_9 : s_{10}s_{18} - s_{20}s_8 : s_{10}s_{19} - s_{20}s_9\right]. \tag{2.74}$$

There are three codimension two loci where S is singular, reading

$$\left\{s_8 = s_{18} = 0\right\}, \qquad \left\{s_9 = s_{19} = 0\right\}, \qquad \left\{s_{10} = s_{20} = 0\right\}. \tag{2.75}$$

It is important to note that the matrices (2.8), (2.20) retain rank two at these loci, since only two of their 2×2-minors, being identified with the coordinates (2.19), have vanishing determinant. Next, we inspect the constraint (2.16) of the elliptic curve at these loci.

At all these three codimension two loci, we see that the elliptic curve in (2.16) takes the common form

$$Au + BY = 0\,, \quad Cu + DY = 0\,. \tag{2.76}$$

Here Y is one of the variables $\{v,w,t\}$ and the polynomials B, D are chosen to be indepen-

dent of u and Y, which fixes the polynomials A, C uniquely. This complete intersection describes a reducible curve. This can be seen by rewriting it as

$$(AD-BC)u=0\,,\qquad Au+BY=Cu+DY=0\,, \tag{2.77}$$

which we obtained by solving for the variable Y in the first equation of (2.76) and requiring consistency with the second equation.

Now, we directly see that one solution to (2.77) is given by $\{u=0,Y=0\}$. This is a $\mathbb{P}^1$ as is clear from the remaining generators of the SR-ideal after setting the coordinates that are not allowed to vanish to one using the $\mathbb{C}^*$-actions. The second solution, which also describes a $\mathbb{P}^1$, is given by the vanishing of the determinant in the first equation in (2.77), which implies that the two constraint in the second equation become dependent. Thus, the two $\mathbb{P}^1$'s of the I_2-curve are given by

$$c_1=\{u=0,Y=0\}\,,\qquad c_2=\{AD-BC=0,Cu+DY=0\}\,. \tag{2.78}$$

As an example, let us look at the loci $\{s_8=s_{18}=0\}$ in (2.75) in detail. In this case the elliptic curve $\mathcal{E}$ given in (2.16) takes the form

$$\begin{aligned} u\big(s_2e_1e_2e_3u+s_5e_1e_2t+s_6e_2e_3v+s_7e_1e_3w\big)&=t\big(s_9e_2v+s_{10}e_1w\big)\,,\\ u\big(s_{12}e_1e_2e_3u+s_{15}e_1e_2t+s_{16}e_2e_3v+s_{17}e_1e_3w\big)&=t\big(s_{19}e_2v+s_{20}e_1w\big)\,. \end{aligned} \tag{2.79}$$

This complete intersection is in the form (2.76) by identifying $Y=t$ and setting

$$\begin{aligned} A&=\big(s_2e_1e_2e_3u+s_5e_1e_2t+s_6e_2e_3v+s_7e_1e_3w\big)\,,\qquad B=-\big(s_9e_2v+s_{10}e_1w\big)\,,\\ C&=\big(s_{12}e_1e_2e_3u+s_{15}e_1e_2t+s_{16}e_2e_3v+s_{17}e_1e_3w\big),\qquad D=-\big(s_{19}e_2v+s_{20}e_1w\big)\,. \end{aligned} \tag{2.80}$$

Then the two $\mathbb{P}^1$'s of the I_2-curve are given by c_1, c_2 in (2.78).

Equipped with the equations for the individual curves c_1, c_2 we can now calculate the intersections with the sections and the charge of the hypermultiplet that is supported there. The intersections of the curve defined c_1 can be readily obtained from the toric intersections of $\mathrm{Bl}_3\mathbb{P}^3$. It has intersection -1 with the section S_S, intersection one with the sections S_Q, S_R and zero with S_P, where the last intersection is clear from the existence of the term $e_3 t$ in the Stanley-Reisner ideal (2.14). The intersections with c_2 can be calculated either directly from (2.78) or from the fact, that the intersections of a section with the total class $F = c_1 + c_2$ have to be one.

We summarize our findings as:

Loci	Curve	$\cdot S_P$	$\cdot S_Q$	$\cdot S_R$	$\cdot S_S$
$s_8 = s_{18} = 0$	$c_1 = \{u = t = 0\}$	0	1	1	-1
	c_2	1	0	0	2
$s_9 = s_{19} = 0$	$c_1 = \{u = w = 0\}$	1	1	0	-1
	c_2	0	0	1	2
$s_{10} = s_{20} = 0$	$c_1 = \{u = v = 0\}$	1	0	1	-1
	c_2	0	1	0	2

(2.81)

Here we denoted the intersection pairing by '$\cdot$' and we also computed the intersections of the sections with the I_2-curves at the other two codimension two loci in (2.75). In these cases, we identified $Y = w$, respectively, $Y = v$.

We proceed with the calculation of the charges in each case employing the charge formula (2.73). We note that the isolated curve c_{mat} is always the curve in the I_2-fiber that that

does not intersect the zero section S_P. We obtain the charges:

Loci	q_Q	q_R	q_S
$s_8 = s_{18} = 0$	1	1	-1
$s_9 = s_{19} = 0$	0	1	2
$s_{10} = s_{20} = 0$	1	0	2

(2.82)

The vanishing of three minors: singularities of all sections

The remaining singularities of the rational sections occur if the three of the determinants of the minors of the matrices (2.8), (2.20) vanish. This implies that three coordinates (2.19) of a section are forbidden by the SR-ideal (2.14), which happens also for the sections $\hat{s}_P$, $\hat{s}_Q$, $\hat{s}_R$, in addition to $\hat{s}_S$, due to the elements uXY with X, Y in $\{v,w,t\}$.

Before analyzing these loci, we emphasize that the three vanishing conditions are a codimension two phenomenon because the vanishing of the determinants of three minors of the same matrix is not independent. In fact, these codimension two loci can be viewed as determinantal varieties describing the loci where the rank of each of the matrices in (2.8), (2.20) jump from two to one, which is clearly a codimension two phenomenon.

Concretely, for the section $\hat{s}_P$ to be singular, the three minors that have to vanish are $|M_3^P| = |M_2^P| = |M_1^P| = 0$, which implies the conditions

$$\frac{s_5}{s_{15}} = \frac{s_{10}}{s_{20}} = \frac{s_9}{s_{19}}\,. \tag{2.83}$$

Similarly, for $\hat{s}_Q$ to be singular, we impose $|M_3^Q| = |M_2^Q| = |M_1^Q| = 0$, which yields

$$\frac{s_6}{s_{16}} = \frac{s_8}{s_{18}} = \frac{s_9}{s_{19}}\,. \tag{2.84}$$

For a singular section $\hat{s}_R$, we require $|M_3^R| = |M_2^R| = |M_1^R| = 0$, which is equivalent to

$$\frac{s_{10}}{s_{20}} = \frac{s_8}{s_{18}} = \frac{s_7}{s_{17}}\,. \tag{2.85}$$

Finally, the section $\hat{s}_S$ is singular at $|M_3^Q| = |M_3^R| = |M_3^P| = 0$, or equivalently at

$$\frac{s_{10}}{s_{20}} = \frac{s_8}{s_{18}} = \frac{s_9}{s_{19}}\,. \tag{2.86}$$

We remark that the vanishing of the three minors in all these cases excludes the loci (2.75) of the previous subsection.

All these singularities imply a reducible curve of a form similar to (2.27), however, adapted to the ambient space $\mathrm{Bl}_3\mathbb{P}^3$. In fact, at each of the loci (2.83)-(2.86) the complete intersection (2.16) takes the form

$$AX + BY = 0\,, \qquad CX + DY = 0\,, \tag{2.87}$$

for appropriate polynomials A, B, C, D with A and C collinear, that is $A = aC$, and the pair of coordinates $[X : Y]$ forming a $\mathbb{P}^1$.[15] Then, we can multiply the second equation by a and subtract from the first equation, to obtain

$$(B - aD)Y = 0\,, \qquad AX + BY = 0\,. \tag{2.88}$$

From this we see that the two solutions are given by

$$c_1 = \{Y = A = 0\}\,, \qquad c_2 = \{B - aD = AX + BY = 0\}\,, \tag{2.89}$$

[15] When $\hat{s}_S$ becomes singular, we identify $Y = u$ and $X = 1$. However, A, C still become collinear and the argument applies.

that describe two $\mathbb{P}^1$'s intersecting at two points. Thus the complete intersection (2.88) is an I_2-curve.

One example in detail

Let us focus on the locus in (2.84) where the section $\hat{s}_Q$ is singular. The complete intersection (2.16) then takes the form

$$v(-e_2 s_9 t + e_2 e_3 s_6 u + e_3 s_8 w) + e_1(e_2 s_5 t u + e_2 e_3 s_2 u^2 - s_{10} t w + s_7 e_3 u w) = 0\,,$$
$$v(-e_2 s_{19} t + e_2 e_3 s_{16} u + e_3 s_{18} w) + e_1(e_2 s_{15} t u + e_2 e_3 s_{12} u^2 - s_{20} t w + e_3 s_{17} u w) = 0\,.$$

This is of the form (2.87) as we see by identifying $X = v$ and $Y = e_1$ and by setting

$$A = -e_2 s_9 t + e_2 e_3 s_6 u + e_3 s_8 w\,, \quad B = e_2 s_5 t u + e_2 e_3 s_2 u^2 - s_{10} t w + s_7 e_3 u w\,, \tag{2.90}$$
$$C = -e_2 s_{19} t + e_2 e_3 s_{16} u + e_3 s_{18} w\,, \quad D = e_2 s_{15} t u + e_2 e_3 s_{12} u^2 - s_{20} t w + e_3 s_{17} u w$$

with $A = (s_8/s_{18})C$ collinear at the locus (2.84) . Then, the two $\mathbb{P}^1$'s in this I_2-curve are given by (2.89) with the identifications (2.90).

Next, we obtain the intersections of the curves c_1, c_2 with the rational sections, that follow directly from the toric intersections of $\mathrm{Bl}_3\mathbb{P}^3$. We find the intersections

Loci	Curve	$\cdot S_P$	$\cdot S_Q$	$\cdot S_R$	$\cdot S_S$
$\lvert M_3^Q\rvert = \lvert M_2^Q\rvert = \lvert M_1^Q\rvert = 0$	c_1	0	-1	0	1
	c_2	1	2	1	0

(2.91)

As expected, the total fiber $F = c_1 + c_2$ has intersections $S_m \cdot F = 1$ with all sections.

Repeating the procedure with the other codimension two loci (2.83), (2.85) and (2.86),

we obtain the intersections of the split elliptic curve with the sections as

Loci	Curve	$\cdot S_P$	$\cdot S_Q$	$\cdot S_R$	$\cdot S_S$
$\lvert M_3^R\rvert = \lvert M_2^R\rvert = \lvert M_1^R\rvert = 0$	c_1	0	0	-1	1
	c_2	1	1	2	0
$\lvert M_3^P\rvert = \lvert M_2^P\rvert = \lvert M_1^P\rvert = 0$	c_1	-1	0	0	1
	c_2	2	1	1	0
$\lvert M_3^Q\rvert = \lvert M_3^R\rvert = \lvert M_3^P\rvert = 0$	c_1	1	1	1	-1
	c_2	0	0	0	2

(2.92)

With these intersection numbers and the charge formula (2.73) we obtain the charges

Loci	q_Q	q_R	q_S
$\lvert M_3^Q\rvert = \lvert M_2^Q\rvert = \lvert M_1^Q\rvert = 0$	-1	0	1
$\lvert M_3^R\rvert = \lvert M_2^R\rvert = \lvert M_1^R\rvert = 0$	0	-1	1
$\lvert M_3^P\rvert = \lvert M_2^P\rvert = \lvert M_1^P\rvert = 0$	-1	-1	-2
$\lvert M_3^Q\rvert = \lvert M_3^R\rvert = \lvert M_3^P\rvert = 0$	0	0	2

(2.93)

Relation to dP_2

In section 2.2.3 we saw that the elliptic curve $\mathcal{E}$ can be mapped to two[16] non-generic anti-canonical hypersurfaces in dP_2. It is expected that some of the singularities we just found map to the singularities in the dP_2-elliptic curve. We recall from [156, 155], that the Calabi-Yau hypersurfaces (2.29), (2.35) in dP_2 have singular sections at the codimension two loci given by $\tilde{s}_3 = \tilde{s}_7 = 0$ ($\hat{s}_3 = \hat{s}_7 = 0$), $\tilde{s}_8 = \tilde{s}_9 = 0$ ($\hat{s}_8 = \hat{s}_9 = 0$) and $\tilde{s}_7 = \tilde{s}_9 = 0$ ($\hat{s}_7 = \hat{s}_9 = 0$), respectively.

In tables (2.30) and (2.36) we readily identified the minors of the matrices in (2.20)

[16]There are actually three dP_2 maps if we are willing to give up the zero point as a toric point. See section 2.2.3 for more details.

with the some of the coefficients $\tilde{s}_i$ and $\hat{s}_j$. This implies a relationship between the singular codimension two loci of the elliptic curves in $\mathrm{Bl}_3\mathbb{P}^3$ and in the two dP_2-varieties, that we summarize in the following table:

$\mathrm{Bl}_3\mathbb{P}^3$-singularity	Singularity of curve in (2.29)	Singularity of curve in (2.35)
$\lvert M_3^Q\rvert = \lvert M_2^Q\rvert = \lvert M_1^Q\rvert = 0$	$\tilde{s}_3 = \tilde{s}_7 = 0$	Q non-toric
$\lvert M_3^R\rvert = \lvert M_2^R\rvert = \lvert M_1^R\rvert = 0$	R non-toric	$\hat{s}_3 = \hat{s}_7 = 0$
$\lvert M_3^P\rvert = \lvert M_2^P\rvert = \lvert M_1^P\rvert = 0$	$\tilde{s}_8 = \tilde{s}_9 = 0$	$\hat{s}_8 = \hat{s}_9 = 0$
$\lvert M_3^Q\rvert = \lvert M_3^R\rvert = \lvert M_3^P\rvert = 0$	$\tilde{s}_7 = \tilde{s}_9 = 0$	$\hat{s}_7 = \hat{s}_9 = 0$

(2.94)

In each case, three out of the four singular loci (2.93) yield singularities of the toric sections in the dP_2-elliptic curve. The other singular locus in the curve in $\mathrm{Bl}_3\mathbb{P}^3$ is not simply given by the vanishing of two coefficients $\tilde{s}_i$, respectively $\hat{s}_j$, because the non-toric rational sections becomes singular. Nevertheless, the elliptic curve in dP_2 admits a factorization at the singular locus of the non-toric section, i.e. it splits into an I_2-curve, due to the non-genericity of the corresponding coefficients $\tilde{s}_i$ or $\hat{s}_j$.

2.4.2 Matter from Singularities in the Weierstrass Model

As mentioned in the introduction of this subsection, *all* the loci of matter charged under a section $\hat{s}_m$ satisfy the equations $g_3^m = 0$ and $\hat{g}_4^m = 0$. Since we have three rational sections $\hat{s}_m$, the WSF admits three possible factorizations of the form (3.5), each of which implying a singular elliptic fiber at the loci $g_3^{Q,R,S} = \hat{g}_4^{Q,R,S} = 0$ with $\hat{g}_4^{R,S}$ defined analogous to (2.72). In this subsection we separate solutions to these equations by requiring additional constraints to vanish.

We can isolate matter with simultaneous U(1)-charges. The idea is the following. If the

matter is charged under two sections, both sections have to pass through the singularity in the WSF. This requires the x-coordinates $g_2^{m_1}$, $g_2^{m_2}$ of the sections to agree[17],

$$\delta g_2^{m_1,m_2} := g_2^{m_1} - g_2^{m_2} \stackrel{!}{=} 0, \tag{2.95}$$

for any two sections $\hat{s}_{m_1}$ and $\hat{s}_{m_2}$. The polynomial (2.95) has a smaller degree than the other two conditions (2.72) and in fact it will be one of the two polynomials of the complete intersection describing the codimension two locus. The other constraint will be $g_3^m = 0$ for m either m_1 or m_2.

If we solve for two coefficients in these two polynomials and insert the solution back into the elliptic curve (2.16) we observe a reducible curve of the form (2.88). In this I_2-curve, one $\mathbb{P}^1$ is automatically intersected once by both sections $\hat{s}_{m_1}$ and $\hat{s}_{m_2}$. This means that a generic solution of equations (2.72), (2.95) support matter with charges one under $\mathrm{U}(1)_{m_1}\times\mathrm{U}(1)_{m_2}$.

Let us be more specific for matter charged under the sections $\hat{s}_Q$ and $\hat{s}_R$, that is matter transforming under $\mathrm{U}(1)_Q\times\mathrm{U}(1)_R$. The conditions (2.72) and (2.95) read

$$\delta g_2^{QR} := g_2^Q - g_2^R \stackrel{!}{=} 0\,, \qquad g_3^Q = 0\,, \qquad \hat{g}_4^Q = 0\,, \tag{2.96}$$

and the codimension to locus is given by the complete intersection $\delta g_2^{QR} = g_3^Q = 0$. In fact the constraint $\hat{g}_4^Q$, $\hat{g}_4^R$ are in the ideal generate by $\langle \delta g_2^{QR}, g_3^Q\rangle$.

We proceed to look for matter charged under $\mathrm{U}(1)_Q\times\mathrm{U}(1)_S$. In this case, because of the section $\hat{s}_S$ having a non-trivial z-component, the right patch of the WSF is $z \equiv \tilde{z}^S = s_{10}s_{19} - s_{20}s_9$, c.f. (2.39). Thus, the constrains (2.72) and (2.95) take the form

$$\delta g_2^{QS} := g_2^S - (\tilde{z}^S)^2 g_2^Q \stackrel{!}{=} 0\,, \qquad g_3^S = 0\,, \qquad \hat{g}_4^S = 0\,. \tag{2.97}$$

[17]Here we assume that the z−-coordinates of both sections are $z = 1$, for simplicity.

Instead of using these polynomials, we will use two slightly modified polynomials that generate the same ideal. They were defined in [156] where they were denoted by $\delta g_6'$ and g_9' and defined as

$$\delta(g_2^{QS})' := \tilde{s}_7\tilde{s}_8^2 + \tilde{s}_9(-\tilde{s}_6\tilde{s}_8 + \tilde{s}_5\tilde{s}_9) = 0, \qquad (g_3^{QS})' := \tilde{s}_3\tilde{s}_8^2 - \tilde{s}_2\tilde{s}_8\tilde{s}_9 + \tilde{s}_1\tilde{s}_9^2 = 0\,, \tag{2.98}$$

Here we have to use the map (2.30) to obtain these polynomials in terms of the coefficients s_i. We will see in section 2.4.3 that these polynomials are crucial to obtain the matter multiplicities of this type of charged matter fields.

Similarly, for matter charged under $\mathrm{U}(1)_R\times\mathrm{U}(1)_S$ we demand

$$\delta g_2^{RS} := g_2^S - (\tilde{z}^S)^2 g_2^R \stackrel{!}{=} 0\,, \qquad g_3^S = 0\,, \qquad \hat{g}_4^S = 0\,. \tag{2.99}$$

For this type of locus we will also use the modified polynomials $\delta(g_2^{RS})'$ and $\delta(g_3^{RS})'$ that can be obtained from (2.98) by replacing all the coefficients $\tilde{s}_i \to \hat{s}_i$ and by using (2.36).

Next, we look for matter charged under all U(1) factors $\mathrm{U}(1)_Q\times\mathrm{U}(1)_R\times\mathrm{U}(1)_S$. This requires the three sections to collide and pass through the singular point $y = 0$ in the WSF, at codimension two. The four polynomials that are required to vanish simultaneously are

$$\delta g_2^{QS} = 0\,, \qquad (\tilde{z}^S)^2\delta g_2^{RS} = 0\,, \qquad g_3^S = 0\,, \qquad \hat{g}_4^S = 0\,, \tag{2.100}$$

where the first two conditions enforce a collision of the three sections in the elliptic fiber. In order for a codimension two locus to satisfy all these constraints simultaneously, all the polynomials (2.100) should factor as

$$p = h_1 p_1 + h_2 p_2\,, \tag{2.101}$$

where h_1 and h_2 are the polynomials whose zero-locus defines the codimension two locus in question. To obtain the polynomials we use the Euclidean algorithm twice. We first divide all polynomials in (2.100) by the lowest order polynomial available, which is δg_2^{QR} and take the biggest common factor from all residues. This is the polynomial h_1 and it reads

$$\begin{aligned} h_1 \;=\; & \big(s_{10}^2 s_{15} s_{16} s_{19} + s_{10}^2 s_{12} s_{19}^2 + s_{10} s_{15} s_{18} s_{19} s_5 + s_{10} s_{17} s_{19}^2 s_5 - s_{10} s_{16} s_{19} s_{20} s_5 \\ & - s_{18} s_{19} s_{20} s_5^2 - s_{10} s_{15}^2 s_{18} s_9 - s_{10} s_{15} s_{17} s_{19} s_9 - s_{10} s_{15} s_{16} s_{20} s_9 - 2 s_{10} s_{12} s_{19} s_{20} s_9 \\ & + s_{15} s_{18} s_{20} s_5 s_9 - s_{17} s_{19} s_{20} s_5 s_9 + s_{16} s_{20}^2 s_5 s_9 + s_{15} s_{17} s_{20} s_9^2 + s_{12} s_{20}^2 s_9^2 \big) . \end{aligned} \tag{2.102}$$

The knowledge of h_1 allows us to repeat the Euclidean algorithm. We reduce the polynomials (2.100) by (2.102) and again obtain the second common factor from the residues of all polynomials reading

$$\begin{aligned} h_2 \;=\; & s_{10}^2 s_{19} \big(s_{15} s_{16} + s_{12} s_{19}\big) - s_{10} \Big[s_{15}^2 s_{18} s_9 + s_{19} \big(-s_{17} s_{19} s_5 + s_{16} s_{20} s_5 + 2 s_{12} s_{20} s_9\big) \\ & + s_{15} \big(-s_{18} s_{19} s_5 + s_{17} s_{19} s_9 + s_{16} s_{20} s_9\big) \Big] + s_{20} \Big[s_{18} s_5 \big(-s_{19} s_5 + s_{15} s_9\big) \\ & + s_9 \big(-s_{17} s_{19} s_5 + s_{16} s_{20} s_5 + s_{15} s_{17} s_9 + s_{12} s_{20} s_9\big) \Big] . \end{aligned} \tag{2.103}$$

To confirm that these polynomials define the codimension two locus we were looking for, we check that all the constraints (2.100) are in the ideal generated by $\langle h_1, h_2 \rangle$.

Finally, if there are no more smaller ideals, i.e. special solutions, of $g_3^m = \hat{g}_4^m = 0$ we expect its remaining solutions to be generic and to support matter charged under only the section $\hat{s}_m$, i.e. matter with charges $q_m = 1$, and $q_n = 0$ for $n \neq m$. In summary, we find that

matter at a generic point of the following loci has the following charges,

Generic point in locus	q_Q	q_R	q_S
$g_2^{QR} = g_3^Q = 0$	1	1	0
$(g_2^{QS})' = (g_3^S)' = 0$	1	0	1
$(g_2^{RS})' = (g_3^S)' = 0$	1	0	1
$h_1 = h_2 = 0$	1	1	1
$g_3^Q = \hat{g}_4^Q = 0$	1	0	0
$g_3^R = \hat{g}_4^R = 0$	0	1	0
$g_3^S = \hat{g}_4^S = 0$	0	0	1

(2.104)

In each of these six cases we checked explicitly the factorization of the complete intersection (2.27) for $\mathcal{E}$ into an I_2-curve, then computed the intersections of the sections $\hat{s}_P$, $\hat{s}_m$, $m = Q, R, S$ and obtained the charges by applying the charge formula (2.73).

2.4.3 6D Matter Muliplicities and Anomaly Cancellation

In this section we specialize to six-dimensional F-theory compactifications on an elliptically fibered Calabi-Yau threefolds $\hat{X}_3$ over a general two-dimensional base B with generic elliptic fiber given by (2.16). We work out the spectrum of charged hypermultiplets, that transform in the 14 different singlet representations found in sections 2.4.1 and 2.4.2. To this end, we compute the explicit expressions for the multiplicities of these 14 hypermultiplets. We show consistency of this charged spectrum by checking anomaly-freedom.

The matter multiplicities are given by the homology class of the irreducible locus that supports a given matter representation. As discussed above, some of these irreducible matter loci can only be expressed as prime ideals, of which we can not directly compute the homology classes. Thus, we have to compute matter multiplicities successively, starting

from the complete intersections Loc_{CI} in (2.104) that support multiple matter fields of different type. We found, that at the generic point of the complete intersection Loc_{CI} one type of matter is supported, but at special points Loc_s^i different matter fields are located. We summarize this as

$$\cup_i \text{Loc}_s^i \subset \text{Loc}_{\text{CI}} \,. \tag{2.105}$$

Thus, first we calculate all multiplicities of matter located at all these special loci Loc_s^i and then subtract them from the complete intersection Loc_{CI} in which they are contained with a certain degree. This degree is given by the order of vanishing of resultant, that has already been used in a similar context in [156]. It is defined as follows. Given two polynomials (r,s) in the variables (x,y), if $(0,0)$ is a zero of both polynomials, its degree is given by the order of vanishing of the resultant $h(y) \coloneqq \text{Res}_x(r,s)$ at $y = 0$.

This is a straightforward calculation when the variables (x,y) are pairs of the coefficients s_i. However, for more complicated loci we will need to treat full polynomials (p_1, p_2) as these variables, for example $x = \tilde{s}_7$, $y = \tilde{s}_9$ or $x = \delta g_6$, $y = g_9$. In this case we have to solve for two coefficients s_i, s_j from $\{p_1 = x, p_2 = y\}$, then replace them in (r,s) and finally proceed to take the resultant in x and y.

There is one technical caveat, when we are considering polynomials (p_1, p_2) that contain multiple different matter multiplets. We choose the coefficients s_i, s_j in such a way that the variables (x,y) only parametrize the locus of the hypermultiplets we are interested in. This is achieved by choosing s_i, s_j we are solving for so that the polynomials of the locus we are *not* interested in appear as denominators and are, thus, forbidden. For example, let us look at the loci $|M_3^Q| = |M_3^P| = 0$. This complete intersection contains the loci of the hypermultiplets with charges $(0,0,2)$ at the generic point and with charges $(0,1,2)$ at the special locus $s_9 = s_{19} = 0$, c.f. (2.82), respectively, (2.93). Let us focus on the former

hypermultiplets. We set

$$|M_3^Q| = s_{18}s_9 - s_{19}s_8 \equiv x\,, \qquad |M_3^P| = s_{10}s_{19} - s_{20}s_9 \equiv y\,, \tag{2.106}$$

and solve for s_8 and s_{20} to obtain

$$s_8 = \frac{(s_{18}s_9 - x)}{s_{19}}\,, \qquad s_{20} = \frac{(s_{10}s_{19} + y)}{s_9}\,. \tag{2.107}$$

From this, it is clear the locus $s_9 = s_{19} = 0$ corresponding to hypermultiplets with charges $(0,1,2)$ is excluded because of the denominators. Thus, (x,y) indeed parametrize the locus of the hypermultiplets of charges $(0,0,2)$.

We begin the computation of multiplicities with the simplest singularities in 2.4.1 located at the vanishing-loci of two coefficients $s_i = s_j = 0$. Their multiplicities are directly given by their homology classes, that are simply the product of the classes $[s_i]$, $[s_j]$. We obtain

Loci	q_Q	q_R	q_S	Multiplicity
$s_8 = s_{18} = 0$	1	1	-1	$[s_8]\cdot[s_{18}]$
$s_9 = s_{19} = 0$	0	1	2	$[s_9]\cdot[s_{19}]$
$s_{10} = s_{20} = 0$	1	0	2	$[s_{10}]\cdot[s_{20}]$

(2.108)

Next we proceed to calculate the multiplicities of the loci given by the vanishing of three minors given in (2.93). The most direct way of obtaining these multiplicities is by using the Porteous formula to obtain the first Chern class of a determinantal variety. However, we will use here a simpler approach that yields the same results.

It was noted in section 2.4.1, that the locus described by the vanishing of the three minors can be equivalently represented as the vanishing of only two minors, after excluding the zero locus from the vanishing of the two coefficients s_i, s_j that appear in both two minors. Thus, the multiplicities can be calculated by multiplying the homology classes of

the two minors and subtracting the homology class $[s_i]\cdot[s_j]$ of the locus $s_i = s_j = 0$.

For example the multiplicity of the locus $|M_3^Q| = |M_2^Q| = |M_1^Q| = 0$ can be obtained from multiplying the classes of $|M_3^Q| = |M_1^Q| = 0$ and subtracting the multiplicity of the locus $s_8 = s_{18} = 0$ that satisfies these two equations, but not $M_2^Q = -s_6 s_{19} + s_9 s_{16}$:

$$\begin{aligned} x_{(-1,0,1)} &= [|M_3^Q|]\cdot[|M_1^Q|] - [s_8]\cdot[s_{18}] \\ &= ([p_2]^b)^2 + [p_2]^b\cdot(\hat{\mathcal{S}}_7 + \cdot\tilde{\mathcal{S}}_7 - 3\tilde{\mathcal{S}}_9) + [K_B^{-1}]\cdot\tilde{\mathcal{S}}_7 + \tilde{\mathcal{S}}_7^2 - \hat{\mathcal{S}}_7\cdot\mathcal{S}_9 - 2\tilde{\mathcal{S}}_7\cdot\mathcal{S}_9 + 2\mathcal{S}_9^2\,, \end{aligned} \tag{2.109}$$

Here we denote the multiplicity of hypermultiplets with charge (q_Q, q_R, q_S) by $x_{(q_Q,q_R,q_S)}$, indicate homology classes of sections of line bundles by $[\cdot]$, as before, and employ (2.47), (2.30) and the divisors defined in (2.49) to obtain the second line. Calculating the other multiplicities in a similarly we obtain

Charges	Loci	Multiplicity
$(-1,0,1)$	$\|M_3^Q\| = \|M_2^Q\| = \|M_1^Q\| = 0$	$x_{(-1,0,1)} = [\|M_1^Q\|]\cdot[\|M_3^Q\|] - [s_8]\cdot[s_{18}]$
$(0,-1,1)$	$\|M_3^R\| = \|M_2^R\| = \|M_1^R\| = 0$	$x_{(0,-1,1)} = [\|M_1^R\|]\cdot[\|M_3^R\|] - [s_8]\cdot[s_{18}]$
$(-1,-1,-2)$	$\|M_3^P\| = \|M_2^P\| = \|M_1^P\| = 0$	$x_{(-1,-1,-2)} = [\|M_2^P\|]\cdot[\|M_3^P\|] - [s_{10}]\cdot[s_{20}]$
$(0,0,2)$	$\|M_3^P\| = \|M_3^Q\| = \|M_3^R\| = 0$	$x_{(0,0,2)} = [\|M_3^Q\|]\cdot[\|M_3^P\|] - [s_{19}][s_9]$

(2.110)

It is straightforward but a bit lengthy to use (2.47) in combination with (2.30), (2.36) to obtain, as demonstrated in (2.109), the expressions for the multiplicities of all these matter fields explicitly. We have shown one possible way of calculating the multiplicities in (2.110), i.e. choosing one particular pair of minors. We emphasize that the same results for the multiplicities can be obtained by picking any other the possible pairs of minors.

Finally we calculate the hypermultiplets of the matter found in the WSF, as discussed in section 2.4.2. In each case, in order to calculate the multiplicity of the matter located at a generic point of the polynomials (2.104) we need to first identify all the loci, which

solve one particular constraint in (2.104), but support other charged hypermultiplets. Then, we have to find the respective orders of vanishing of the polynomial in (2.104) at these special loci using the resultant technique explained below (2.105). Finally, we compute the homology class of the complete intersection under consideration in (2.104) subtract the homology classes of the special loci with their appropriate orders.

We start with the matter with charges $(1,1,1)$ in (2.104) which is located at a generic point of the locus $h_1 = h_2 = 0$. In this case, the degree of vanishing of the other loci are given by

Charge	$x_{(1,1,-1)}$	$x_{(0,1,2)}$	$x_{(1,0,2)}$	$x_{(-1,0,1)}$	$x_{(0,-1,1)}$	$x_{(-1,-1,-2)}$	$x_{(0,0,2)}$
$(1,1,1)$	0	1	1	0	0	4	0

(2.111)

Here we labeled the loci that are contained in $h_1 = h_2 = 0$ by the multiplicity of matter which supported on them. We note that the other six matter fields in (2.104) do not appear in this table, because the matter with charges $(1,1,1)$ is contained in their loci, as we demonstrate next. This implies that the multiplicity of the hypermultiplets with charge $(1,1,1)$ is given by

$$\begin{aligned} x_{(1,1,1)} &= [h_1]\cdot[h_2] - x_{(0,1,2)} - x_{(1,0,2)} - 4x_{(-1,-1,-2)}\,, \\ &= 4[K_B^{-1}]^2 - 3([p_2]^b)^2 - 2[K_B^{-1}]\hat{\mathcal{S}}_7 - 3([p_2]^b)\cdot\hat{\mathcal{S}}_7 - 2[K_B^{-1}]\cdot\tilde{\mathcal{S}}_7 - 3([p_2]^b)\cdot\tilde{\mathcal{S}}_7 \\ &\quad -2\hat{\mathcal{S}}_7\cdot\tilde{\mathcal{S}}_7 + 2[K_B^{-1}]\mathcal{S}_9 + 9([p_2]^b)\mathcal{S}_9 + 5\hat{\mathcal{S}}_7\cdot\mathcal{S}_9 + 5\tilde{\mathcal{S}}_7\cdot\mathcal{S}_9 - 8\mathcal{S}_9^2\,, \end{aligned} \tag{2.112}$$

where the first term is the class of the complete intersection $h_1 = h_2 = 0$ and the three following terms are the necessary subtractions that follow from (2.111). The homology classes of h_1, h_2 can be obtained by determining the class of one term in (2.102), respectively, (2.103) using (2.47).

Proceeding in a similar way for the hympermultiplets with charges $(1,0,1)$, $(0,1,1)$

and $(1,1,0)$ we get the following orders of vanishing of the loci supporting the remaining matter fields:

Charges	$x_{(1,1,-1)}$	$x_{(0,1,2)}$	$x_{(1,0,2)}$	$x_{(-1,0,1)}$	$x_{(0,-1,1)}$	$x_{(-1,-1,-2)}$	$x_{(0,0,2)}$	$x_{(1,1,1)}$
$(1,0,1)$	0	0	4	0	0	4	0	1
$(0,1,1)$	0	4	0	0	0	4	0	1
$(1,1,0)$	1	0	0	0	0	1	0	1

(2.113)

We finally obtain the multiplicities of these matter fields by computing the homology class of the corresponding complete intersection in (2.104) and subtracting the multiplicities the matter fields contained in these complete intersections with the degrees determined in (2.113). We obtain

$$\begin{aligned}
x_{(1,0,1)} &= 2[K_B^{-1}]^2 + 3([p_2]^b)^2 + 2[K_B^{-1}]\hat{\mathcal{S}}_7 + 3([p_2]^b)\hat{\mathcal{S}}_7 - 3[K_B^{-1}]\tilde{\mathcal{S}}_7 + 3([p_2]^b)\tilde{\mathcal{S}}_7 \\
&\quad + 2\hat{\mathcal{S}}_7\tilde{\mathcal{S}}_7 + \tilde{\mathcal{S}}_7^2 + 2[K_B^{-1}]\mathcal{S}_9 - 9([p_2]^b)\mathcal{S}_9 - 5\hat{\mathcal{S}}_7\mathcal{S}_9 - 4\tilde{\mathcal{S}}_7\mathcal{S}_9 + 6\mathcal{S}_9^2\,, \\
x_{(0,1,1)} &= 2[K_B^{-1}]^2 + 3([p_2]^b)^2 - 3[K_B^{-1}]\hat{\mathcal{S}}_7 + 3([p_2]^b)\hat{\mathcal{S}}_7 + \hat{\mathcal{S}}_7^2 + 2[K_B^{-1}]\tilde{\mathcal{S}}_7 \\
&\quad + 3([p_2]^b)\tilde{\mathcal{S}}_7 + 2\hat{\mathcal{S}}_7\tilde{\mathcal{S}}_7 + 2[K_B^{-1}]\mathcal{S}_9 - 9([p_2]^b)\mathcal{S}_9 - 4\hat{\mathcal{S}}_7\mathcal{S}_9 - 5\tilde{\mathcal{S}}_7\mathcal{S}_9 + 6\mathcal{S}_9^2\,, \\
x_{(1,1,0)} &= 2[K_B^{-1}]^2 + 3([p_2]^b)^2 + 2[K_B^{-1}]\hat{\mathcal{S}}_7 + 3([p_2]^b)\hat{\mathcal{S}}_7 + 2[K_B^{-1}]\tilde{\mathcal{S}}_7 + 3([p_2]^b)\tilde{\mathcal{S}}_7 \\
&\quad + \hat{\mathcal{S}}_7\tilde{\mathcal{S}}_7 - 3[K_B^{-1}]\mathcal{S}_9 - 9([p_2]^b)\mathcal{S}_9 - 4\hat{\mathcal{S}}_7\mathcal{S}_9 - 4\tilde{\mathcal{S}}_7\mathcal{S}_9 + 7\mathcal{S}_9^2\,.
\end{aligned} \tag{2.114}$$

Finally for the hypermultiplets of charges $(1,0,0)$, $(0,1,0)$ and $(0,0,1)$ we obtain the following degrees of vanishing of the loci supporting the other matter fields:

Charges	$x_{(1,1,-1)}$	$x_{(0,1,2)}$	$x_{(1,0,2)}$	$x_{(-1,0,1)}$	$x_{(0,-1,1)}$	$x_{(-1,-1,-2)}$	$x_{(0,0,2)}$	$x_{(1,0,1)}$	$x_{(0,1,1)}$	$x_{(1,1,0)}$	$x_{(1,1,1)}$
$(1,0,0)$	1	0	1	1	0	1	0	1	0	1	1
$(0,1,0)$	1	1	0	0	1	1	0	0	1	1	1
$(0,0,1)$	1	16	16	1	1	16	16	1	1	0	1

(2.115)

Again we first computing the homology class of the complete intersection in (2.104) supporting the hypermultiplets with charges $(1,0,0)$, $(0,1,0)$, respectively, $(0,0,1)$ and subtracting the multiplicities the matter fields contained in these complete intersections with the degrees determined in (2.115). We obtain

$$\begin{aligned}
x_{(1,0,0)} &= 4[K_B^{-1}]^2 - 3([p_2]^b)^2 - 2[K_B^{-1}]\hat{\mathcal{S}}_7 - 3([p_2]^b)\hat{\mathcal{S}}_7 + 2[K_B^{-1}]\tilde{\mathcal{S}}_7 - 3([p_2]^b)\tilde{\mathcal{S}}_7 \\
&\quad -\hat{\mathcal{S}}_7\tilde{\mathcal{S}}_7 - 2\tilde{\mathcal{S}}_7^2 - 2[K_B^{-1}]\mathcal{S}_9 + 9([p_2]^b)\mathcal{S}_9 + 4\hat{\mathcal{S}}_7\mathcal{S}_9 + 5\tilde{\mathcal{S}}_7\mathcal{S}_9 - 6\mathcal{S}_9^2\,, \\
x_{(0,1,0)} &= 4[K_B^{-1}]^2 - 3([p_2]^b)^2 + 2[K_B^{-1}]\hat{\mathcal{S}}_7 - 3([p_2]^b)\hat{\mathcal{S}}_7 - 2\hat{\mathcal{S}}_7^2 - 2[K_B^{-1}]\tilde{\mathcal{S}}_7 \\
&\quad -3([p_2]^b)\tilde{\mathcal{S}}_7 - \hat{\mathcal{S}}_7\tilde{\mathcal{S}}_7 - 2[K_B^{-1}]\mathcal{S}_9 + 9([p_2]^b)\mathcal{S}_9 + 5\hat{\mathcal{S}}_7\mathcal{S}_9 + 4\tilde{\mathcal{S}}_7\mathcal{S}_9 - 6\mathcal{S}_9^2\,, \\
x_{(0,0,1)} &= 4[K_B^{-1}]^2 - 4([p_2]^b)^2 + 2[K_B^{-1}]\hat{\mathcal{S}}_7 - 4([p_2]^b)\hat{\mathcal{S}}_7 - 2\hat{\mathcal{S}}_7^2 + 2[K_B^{-1}]\tilde{\mathcal{S}}_7 - 4([p_2]^b)\tilde{\mathcal{S}}_7 \\
&\quad -2\hat{\mathcal{S}}_7\tilde{\mathcal{S}}_7 - 2\tilde{\mathcal{S}}_7^2 + 2[K_B^{-1}]\mathcal{S}_9 + 12([p_2]^b)\mathcal{S}_9 + 6\hat{\mathcal{S}}_7\mathcal{S}_9 + 6\tilde{\mathcal{S}}_7\mathcal{S}_9 s - 10\mathcal{S}_9^2\,.
\end{aligned}$$

We conclude by showing that the spectrum of the theory we have calculated is anomaly-free, which serves also as a physically motivated consistency check for the completeness of analysis of codimension two singularities presented in sections 2.4.1 and 2.4.2. We refer to [130, 131] for a general account on anomaly cancellation and to [128, 154, 156] for the explicit form of the anomaly cancellation conditions adapted to the application to F-theory, c.f. for example Eq. (5.1) in [156]. Indeed, we readily check that the spectrum (2.108), (2.110), (2.112), (2.114) and (2.116) together with the height pairing matrix b_{mn} reading

$$b_{mn} = -\pi(\sigma(\hat{s}_m)\cdot\sigma(\hat{s}_n)) = \begin{pmatrix} -2[K_B] & -[K_B] & \mathcal{S}_9 - \tilde{\mathcal{S}}_7 - [K_B] \\ -[K_B] & -2[K_B] & \mathcal{S}_9 - \hat{\mathcal{S}}_7 - [K_B] \\ \mathcal{S}_9 - \hat{\mathcal{S}}_7 - [K_B] & \mathcal{S}_9 - \hat{\mathcal{S}}_7 - [K_B] & 2(\mathcal{S}_9 - [K_B]) \end{pmatrix}_{mn} \tag{2.116}$$

with $m,n = 1,2,3$ all mixed gravitational-Abelian and purely-Abelian anomalies in Eq. (5.1) of [156] are canceled.

2.5 Conclusions

In this work we have analyzed F-theory compactifications with U(1)×U(1)×U(1) gauge symmetry that are obtained by compactification on the most general elliptically fibered Calabi-Yau manifolds with a rank three Mordell-Weil group. We have found that the natural presentation of the resolved elliptic fibration with three rational sections is given by a Calabi-Yau complete intersection $\hat{X}$ with general elliptic fiber given by the unique Calabi-Yau complete intersection in $\mathrm{Bl}_3\mathbb{P}^3$. We have shown that all F-theory vacua obtained by compactifying on a generic $\hat{X}$ over a given general base B are classified by certain reflexive polytopes related to the nef-partition of $\mathrm{Bl}_3\mathbb{P}^3$.

We have analyzed the geometry of these elliptically fibered Calabi-Yau manifolds $\hat{X}$ in detail, in particular the singularities of the elliptic fibration at codimension two in the base B. This way we could identify the 14 different matter representations of F-theory compactifications on $\hat{X}$ to four and six dimensions. We have found three matter representations that are simultaneously charged under all three U(1)-factors, most notably a tri-fundamental representation. This unexpected representation is present because of the presence of a codimension two locus in B, along which all the four constraints in (2.100), δg_2^{QR}, δg_2^{QS}, g_3^Q and $\hat{g}_4^Q$, miraculously vanish simultaneously. We could explicitly identify the two polynomials describing this codimension two locus algebraically in (2.102), (2.103) by application of the Euclidean algorithm. These results point to an intriguing structure of codimension two singularities encoded in the elliptic fibrations with higher rank Mordell-Weil groups.

We also determined the multiplicities of the massless charged hypermultiplets in six-dimensional F-theory compactifications with general two-dimensional base B. The key to this analysis was the identification of the codimension two loci of all matter fields, which required a two-step strategy where first the singularities of the rational sections in the resolved fibration with $\mathrm{Bl}_3\mathbb{P}^3$-elliptic fiber have to be determined and then the remaining

singularities that are visible in the singular Weierstrass form. We note that the loci of the former matter are determinantal varieties, whose homology classes we determine in general. The completeness of our strategy has been cross-checked by verifying 6D anomaly cancellation.

We would like to emphasize certain technical aspects in the analysis of the elliptic fibration. Specifically, we constructed three birational maps of the elliptic curve $\mathcal{E}$ in $\mathrm{Bl}_3\mathbb{P}^3$ to three different elliptic curves in dP_2. On the level of the toric ambient spaces $\mathrm{Bl}_3\mathbb{P}^3$ and dP_2 these maps are toric morphisms. The general elliptic curves in these toric varieties are isomorphic, whereas the map breaks down for the degenerations of $\mathcal{E}$ in section 2.4.1. Besides loop-holes of this kind, we expect the degeneration of $\mathrm{Bl}_3\mathbb{P}^3$-elliptic fibrations to be largely captured by the degenerations of the non-generic dP_2-fibrations.

It would be important for future works to systematically add non-Abelian gauge groups to the rank three Abelian sector of F-theory on $\hat{X}$. This requires to classify the possible ways to engineer appropriate codimension one singularities of the elliptic fibration of $\hat{X}$. A straightforward way to obtain many explicit constructions of non-Abelian gauge groups is to employ the aforementioned birational maps to dP_2, because every codimension one singularity of the dP_2-elliptic fibration automatically induces an according singularity of the $\mathrm{Bl}_3\mathbb{P}^3$-elliptic fibration. In particular, many concrete I_4-singularities, i.e. SU(5) groups, can be obtained by application of the constructions of I_4-singularities of dP_2-elliptic fibrations in [155, 156, 121]. However, it would be important to analyze whether all codimension one singularities of $\hat{X}$ are induced by singularities of the corresponding dP_2-elliptic fibrations. For phenomenological applications, it would then be relevant to determine the matter representations for all possible SU(5)-GUT sectors that can be realized in Calabi-Yau manifolds $\hat{X}$ with $\mathrm{Bl}_3\mathbb{P}^3$-elliptic fiber. Compactifications with $\mathrm{Bl}_3\mathbb{P}^3$-elliptic fiber might lead to new implications for for particle physics: e.g., the appearance of **10**-representations with different U(1)-factors, which does not seem to appear in the rank-two Mordell-Weil construc-

tions, and the intriguing possibility for the appearance of **5**-representations charged under all three U(1)-factors, i.e. quadruple-fundamental representations, which are not present in perturbative Type II compactifications.

Furthermore, for explicit 4D GUT-model building, it would be necessary to combine the analysis of this work with the techniques of [157] to obtain chiral four-dimensional compactifications of F-theory. The determination of chiral indices of 4D matter requires the determination of all matter surfaces as well as the construction of the general G_4-flux on Calabi-Yau fourfolds $\hat{X}$ with general elliptic fiber in $\mathrm{Bl}_3\mathbb{P}^3$, most desirable in the presence of an interesting GUT-sector. Furthermore the structure of Yukawa couplings should to be determined by an analysis of codimension three singularities of the fibration.

Acknowledgments

We gratefully acknowledge discussions and correspondence with Lasha Berezhiani,Yi-Zen Chu, Thomas Grimm and in particular Antonella Grassi and Albrecht Klemm. M.C. thanks CERN Theory Division and Aspen Center for Physics for hospitality. D.K. thanks the Bethe Center for Theoretical Physics Bonn and the Mitchell Institute at Texas A&M University for hospitality. The research is supported by the DOE grant DE-SC0007901 (M.C., H.P., D.K.), the NSF String Vacuum Project Grant No. NSF PHY05-51164 (H.P.), Dean's Funds for Faculty Working Group (M.C., D.K.), the Fay R. and Eugene L.Langberg Endowed Chair (M.C.) and the Slovenian Research Agency (ARRS) (M.C.).

2.6 The Weierstrass Form of the Elliptic Curve with Three Rational Points

The main text made extensive use of the mapping of the elliptic curve $\mathcal{E}$ with Mordell-Weil rank three to the Calabi-Yau hypersurface in dP_2. Specifically, the calculation of

the coordinates of the rational points, the Weierstrass form and the discriminant were all performed employing the results for the dP_2-elliptic curve in [156]. Following [154, 156], that we refer when needed, in this appendix we calculate the Weierstrass form and the coordinates of the three ratinal points directly from the three elliptic curve $\mathcal{E}$.

In order to motivate the approach below, we briefly summarize how to obtain the Tate form of an elliptic curve with the zero point P. Given an elliptic curve with one marked point P, we can obtain the Tate equation with respect to this point by finding the sections of $\mathcal{O}(kP)$, $k = 1,...,6$. The coordinate z will be the only section of $\mathcal{O}(P)$, the coordinate x is a section of $\mathcal{O}(2P)$ independent of z^2, and y is a section of $\mathcal{O}(3P)$ independent of z^3 and xz. The Tate equation is obtained from the linear relation between the sections of $\mathcal{O}(6P)$.

Coordinates x, y and z

To obtain the birational map from the complete intersection (2.4) in $\mathbb{P}^3$ to the Tate form, we need to construct the Weierstrass coordinates x, y and z as sections of the line bundles $\mathcal{O}(kP)$ on $\mathcal{E}$ with $k = 1,2,3$. In section 2.2.1 we found a basis for the bundle $\mathcal{M} = \mathcal{O}(P+Q+R+S)$, as well as a basis for $\mathcal{M}^2$ and a choice of basis for $\mathcal{M}^3$. The sections of $\mathcal{O}(kP)$ are obtained from linear combinations of $\mathcal{O}(kM)$ that vanish with degree k at the points Q, R and S.

From the discussion in section 2.2.1, the section z can be taken to be $z := u'$. To find x, we take an eight-dimensional basis of $H^0(\mathcal{E},\mathcal{M}^2)$ and construct the most general linear combination. The coefficient of u'^2 is set to zero in order for x to be independent of z^2. Thus, the ansatz for the variable x reduces to

$$x := at'^2 + cv'^2 + dw'^2 + et'u' + fu'v' + gu'w' + hv'w' . \tag{2.117}$$

Six out of the seven coefficients are fixed by imposing zeroes of order two at the three

points Q, R and S. The last coefficient can be eliminated by an overall scaling. Solving the constraints but keeping h as the overall scaling coefficient, we obtain

$$a = \frac{h(s_{10}s_{19}-s_{20}s_9)^2}{(s_{10}s_{18}-s_{20}s_8)(-s_{19}s_8+s_{18}s_9)}, \qquad c = d = 0, \qquad f = h\frac{(s_{19}s_6-s_{16}s_9)}{s_{19}s_8-s_{18}s_9}, \qquad g = h\frac{(s_{10}s_{17}-s_{20}s_7)}{s_{10}s_{18}-s_{20}s_8},$$

$$\begin{aligned} e \;=\; & -hs_{10}\frac{s_{18}s_{19}s_5 - s_{19}s_{20}s_6 + s_{19}^2 s_7 + s_{15}s_{19}s_8 - 2s_{15}s_{18}s_9 - s_{17}s_{19}s_9 - s_{16}s_{20}s_9}{(s_{10}s_{18}-s_{20}s_8)(-s_{19}s_8+s_{18}s_9)} \\ & -h\frac{s_{10}^2 s_{16}s_{19} + s_{20}\big[s_9(s_{18}s_5+s_{20}s_6+s_{15}s_8+s_{17}s_9) - s_{19}(2s_5s_8+s_7s_9)\big]}{(s_{10}s_{18}-s_{20}s_8)(-s_{19}s_8+s_{18}s_9)}. \end{aligned}$$

Finally consider $y \in \mathcal{O}(3P)$ as a section linearly independent of u^3 and ux. We make the ansatz

$$y := \tilde{a}t'^3 + \tilde{c}v'^3 + \tilde{d}w'^3 + \tilde{f}t'u'^2 + \tilde{g}u'^2v' + \tilde{h}u'^2w' + \tilde{i}u'v'^2 + \tilde{j}u'w'^2 + \tilde{k}u'v'w' + \tilde{l}v'^2w', \quad (2.118)$$

where again, all but one of the coefficients can be fixed by demanding y to have zeroes of degree three at Q, R and S and the free coefficient is an overall scaling. The solutions of these coefficients are long and not illuminating, thus we will not be presented here but can be provided on request.

Tate equations and Weierstrass form

Once the sections x, y and z are known, we impose the Tate form

$$y^2 + a_1yxz + a_3yz^3 = x^3 + a_4x^2z^4 + a_6z^6 \quad (2.119)$$

to hold in the ideal generated by the complete intersection (2.4). First we exploit the free scalings of x and y to obtain coefficients equal to one in front of the monomials x^3 and y^2 in (2.117) and (2.118). Then we compute all the monomials in equation (2.119) after inserting

$z = u'$, (2.117) and (2.118) and reduce by the ideal generated by the polynomials (2.4). Finally, from a comparison of coefficient, we obtain 23 equations that can be solved uniquely for the five Tate coefficients a_i. Unfortunately the results are long and not illuminating and are again provided on request.

From the Tate form (2.119), the Weierstrass form

$$y^2 = x^3 + fxz^4 + gz^6 \tag{2.120}$$

is obtained by the variable transformation

$$x \mapsto x + \tfrac{1}{12} b_2 z^2 , \qquad y \mapsto y + \tfrac{1}{2} a_1 xz + \tfrac{1}{2} a_3 z^3 \tag{2.121}$$

with the following definitions

$$\begin{aligned} f &= -\tfrac{1}{48}(b_2^2 - 24 b_4) , \qquad g = -\tfrac{1}{864}(-b_2^3 + 36 b_2 b_4 - 216 b_6) , \\ b_2 &= a_1^2 + 4a_2 , \qquad b_4 = a_1 a_3 + 2a_4 , \qquad b_6 = a_3^2 + 4a_6 , \\ \Delta &= -16(4f^3 + 27g^2) = -8b_4^3 + \tfrac{1}{4} b_2^2 b_4^2 + 9 b_2 b_4 b_6 - \tfrac{1}{4} b_6 b_2^3 - 27 b_6 . \end{aligned} \tag{2.122}$$

Rational points in the Weierstrass form

Equipped with the Weierstrass form (2.120) of the curve, we calculate the coordinates $[x^m : y^m : z^m] = [g_2^m : g_3^m : b^m]$ of all the rational points $m = P, Q, R, S$. By construction the point P is mapped to the zero section, that is the point $[\lambda^2 : \lambda^3 : 0]$.

The coordinates of the other points are all obtained through the following procedure: Let us call the generic point N with Tate coordinates $[x^N : y^N : z^N]$. First, we find a section of degree two, denoted x', that vanishes with degree three at the point N. In this case we need to make use of the full basis of $\mathcal{O}(2M)$ that includes u^2. The vanishing at degree two

already fixes most of the coefficients as in (2.117). The condition of vanishing at degree three fixes the new coefficient of u^2. Restoring the variables x and z we obtain

$$x'|_N = x + \tilde{g}_m z^2 \,. \tag{2.123}$$

Then, the coordinate x^N of N is given in terms of z^N by requiring $x'|_N = 0$. The coordinate y^N is determined by inserting the values for z^N, x^N into the Tate form (2.119). Finally, the coordinates in Weierstrass form are obtained by the transformations (2.121).

We summarize our results for the coordinates of the rational points Q, R and S in the following. We obtain the coordinates of the form

$$\begin{aligned}
\left[x^Q, y^Q, z^Q\right] &= \left[g_2^Q : g_3^Q : 1\right], &(2.124)\\
\left[x^R, y^R, z^R\right] &= \left[g_2^R : g_3^R : 1\right], &(2.125)\\
\left[x^S, y^S, z^S\right] &= \left[g_2^S : g_3^S : (s_{10}s_{19} - s_{20}s_9)\right], &(2.126)
\end{aligned}$$

where we have made the following definitions:

$$\begin{aligned}
g_2^Q &= \frac{1}{12}\Big[8(s_{10}s_{15} - s_{20}s_5)(s_{18}s_6 - s_{16}s_8) + (s_{10}s_{16} + s_{18}s_5 - s_{20}s_6 + s_{19}s_7 - s_{15}s_8 - s_{17}s_9)^2 \\
&\quad -4(s_{10}s_{12} - s_2 s_{20} + s_{17}s_5 - s_{15}s_7)(s_{19}s_8 - s_{18}s_9) \\
&\quad +4(s_{18}s_2 + s_{17}s_6 - s_{16}s_7 - s_{12}s_8)(s_{10}s_{19} - s_{20}s_9)\Big], &(2.127)\\
g_3^Q &= \frac{1}{2}\Big[(-s_{10}s_{15} + s_{20}s_5)(-s_{18}s_6 + s_{16}s_8)(-s_{10}s_{16} - s_{18}s_5 + s_{20}s_6 - s_{19}s_7 + s_{15}s_8 + s_{17}s_9) \\
&\quad -(s_{10}s_{15} - s_{20}s_5)(s_{18}s_2 + s_{17}s_6 - s_{16}s_7 - s_{12}s_8)(-s_{19}s_8 + s_{18}s_9) \\
&\quad -(s_{10}s_{12} - s_2 s_{20} + s_{17}s_5 - s_{15}s_7)(s_{18}s_6 - s_{16}s_8)(s_{10}s_{19} - s_{20}s_9) \\
&\quad +(s_{17}s_2 - s_{12}s_7)(s_{19}s_8 - s_{18}s_9)(s_{10}s_{19} - s_{20}s_9)\Big], &(2.128)
\end{aligned}$$

$$
\begin{aligned}
g_2^R &= \frac{1}{12}\Big[-4(s_{10}s_{18}-s_{20}s_8)(s_{19}s_2-s_{16}s_5+s_{15}s_6-s_{12}s_9) \\
&\quad +8(-s_{18}s_7+s_{17}s_8)(s_{19}s_5-s_{15}s_9)+(s_{10}s_{16}-s_{18}s_5-s_{20}s_6+s_{19}s_7+s_{15}s_8-s_{17}s_9)^2 \\
&\quad -4(s_{18}s_2-s_{17}s_6+s_{16}s_7-s_{12}s_8)(s_{10}s_{19}-s_{20}s_9)\Big], \qquad (2.129) \\
g_3^R &= \frac{1}{2}\Big[(s_{18}s_2-s_{17}s_6+s_{16}s_7-s_{12}s_8)(s_{10}s_{18}-s_{20}s_8)(s_{19}s_5-s_{15}s_9) \\
&\quad +(s_{18}s_7-s_{17}s_8)(s_{19}s_5-s_{15}s_9)(-s_{10}s_{16}+s_{18}s_5+s_{20}s_6-s_{19}s_7-s_{15}s_8+s_{17}s_9) \\
&\quad +(s_{16}s_2-s_{12}s_6)(s_{10}s_{18}-s_{20}s_8)(s_{10}s_{19}-s_{20}s_9) \\
&\quad -(s_{18}s_7-s_{17}s_8)(s_{19}s_2-s_{16}s_5+s_{15}s_6-s_{12}s_9)(s_{10}s_{19}-s_{20}s_9)\Big], \qquad (2.130)
\end{aligned}
$$

$$
\begin{aligned}
g_2^S &= \frac{1}{12}\Big\{12(s_{10}s_{18}-s_{20}s_8)^2(s_{19}s_5-s_{15}s_9)^2 \\
&\quad +(s_{10}s_{19}-s_{20}s_9)^2\Big[8(-s_{18}s_7+s_{17}s_8)(s_{19}s_5-s_{15}s_9) \\
&\quad +(s_{10}s_{16}-s_{18}s_5-s_{20}s_6+s_{19}s_7+s_{15}s_8-s_{17}s_9)^2 \\
&\quad -4(s_{18}s_2-s_{17}s_6+s_{16}s_7-s_{12}s_8)(s_{10}s_{19}-s_{20}s_9)\Big] \\
&\quad +4(s_{10}s_{18}-s_{20}s_8)(-s_{10}s_{19}+s_{20}s_9)\times\Big[\\
&\quad -3(s_{19}s_5-s_{15}s_9)(s_{10}s_{16}-s_{18}s_5-s_{20}s_6+s_{19}s_7+s_{15}s_8-s_{17}s_9) \\
&\quad +2(s_{19}s_2-s_{16}s_5+s_{15}s_6-s_{12}s_9)(-s_{10}s_{19}+s_{20}s_9)\Big]\Big\}, \qquad (2.131)
\end{aligned}
$$

$$
\begin{aligned}
g_3^S \;=\; & \frac{1}{2}\Big\{2(s_{10}s_{18}-s_{20}s_8)^3(s_{19}s_5-s_{15}s_9)^3 \qquad (2.132)\\
& +(s_{10}s_{18}-s_{20}s_8)(s_{10}s_{19}-s_{20}s_9)^2\big[2(-s_{18}s_7+s_{17}s_8)(s_{19}s_5-s_{15}s_9)^2\\
& +(s_{19}s_5-s_{15}s_9)(s_{10}s_{16}-s_{18}s_5-s_{20}s_6+s_{19}s_7+s_{15}s_8-s_{17}s_9)^2\\
& -(s_{18}s_2-s_{17}s_6+s_{16}s_7-s_{12}s_8)(s_{19}s_5-s_{15}s_9)(s_{10}s_{19}-s_{20}s_9)\\
& +(s_{19}s_2-s_{16}s_5+s_{15}s_6-s_{12}s_9)(s_{10}s_{16}-s_{18}s_5-s_{20}s_6+s_{19}s_7+s_{15}s_8-s_{17}s_9)\times\\
& (s_{10}s_{19}-s_{20}s_9)+(-s_{16}s_2+s_{12}s_6)(s_{10}s_{19}-s_{20}s_9)^2\big]\\
& +(-s_{18}s_7+s_{17}s_8)(-s_{10}s_{19}+s_{20}s_9)^3\times\\
& \big[-(s_{19}s_5-s_{15}s_9)(s_{10}s_{16}-s_{18}s_5-s_{20}s_6+s_{19}s_7+s_{15}s_8-s_{17}s_9)\\
& +(s_{19}s_2-s_{16}s_5+s_{15}s_6-s_{12}s_9)(-s_{10}s_{19}+s_{20}s_9)\big]\\
& +(s_{10}s_{18}-s_{20}s_8)^2(s_{19}s_5-s_{15}s_9)(-s_{10}s_{19}+s_{20}s_9)\times\\
& \big[-3(s_{19}s_5-s_{15}s_9)(s_{10}s_{16}-s_{18}s_5-s_{20}s_6+s_{19}s_7+s_{15}s_8-s_{17}s_9)\\
& +2(s_{19}s_2-s_{16}s_5+s_{15}s_6-s_{12}s_9)(-s_{10}s_{19}+s_{20}s_9)\big]\Big\}. \qquad (2.133)
\end{aligned}
$$

2.7 Nef-partitions

Here we recall the very basic definitions and results about nef-Partitions. We refer for example to [132] for a detailed mathematical account.

Definition Let $X = \mathbb{P}_\nabla$ be a toric variety with a corresponding polytope ∇, a normal fan of the polytope ∇ and rays $\rho \in \Sigma(1)$ with associated divisors D_ρ. Given a partition of $\Sigma(1) = I_1 \cup \cdots \cup I_k$, into k disjoint subsets, there are divisors $E_j = \sum_{\rho\in I_j} D_\rho$ such that $-K_X = E_1 + \cdots + E_k$. This decomposition is called a nef-partition if for each j, E_j is a a Cartier divisor spanned by its global sections.

We denote the convex hull of the rays in I_j as ∇_j and their dual polytopes by Δ_j, which

are defined as

$$\Delta_j = \{m \in \mathbb{Z}^3 | \langle m, \rho_i \rangle \geq -\delta_{ij} \text{ for } \rho_i \in \nabla_j\}. \tag{2.134}$$

The generic global sections, h_j of D_j are computed according to the expression

$$h_j = \sum_{m \in \Delta_j \cap \mathbb{Z}^3} a_m \prod_{j=1}^{k} \prod_{\rho_i \in \nabla_j} x_i^{\langle m, \rho^i \rangle + \delta_{ij}}, \qquad \delta_{ij} = \begin{cases} 1 \text{ for } \rho_i \in \nabla_j \\ 0 \text{ else.} \end{cases} \tag{2.135}$$

Chapter 3

Origin of abelian gauge symmetries in heterotic/F-theory duality

3.1 Introduction and Summary of Results

The study of effective theories of string theory in lower dimensions with minimal supersymmetry are both of conceptual and phenomenological relevance. Two very prominent avenues to their construction are Calabi-Yau compactifications of the $E_8 \times E_8$ heterotic string and of F-theory, respectively. The defining data of the two compactifications are seemingly very different. While a compactification to $10-2n$ dimensions is defined in the heterotic string by a complex n-dimensional Calabi-Yau manifold Z_n and a holomorphic, semi-stable vector bundle V [133, 134], in F-theory one needs to specify a complex $(n+1)$-dimensional elliptically-fibered Calabi-Yau manifold X_{n+1} [135, 136, 137]. For an elliptic K3-fibered X_{n+1} and an elliptically fibered Z_n, however, both formulations of compactifications of string theory are physically equivalent. The defining data of both sides are related to each other by heterotic/F-theory duality [135, 136, 137]. Most notably, this duality allows making statements about the heterotic vector bundle V in terms of the controllable

geometry of the Calabi-Yau manifold X_{n+1} on the F-theory side. Studying the structure of the heterotic vector bundle V is crucial for understanding the gauge theory sector of the resulting effective theories. In this note, we present key steps towards developing the geometrical duality map between heterotic and F-theory compactifications with Abelian gauge symmetries in their effective theories.

Since the advent of F-theory, the matching of gauge symmetry and the matter content in the effective theories has been studied in heterotic/F-theory duality [135, 136, 137]. Mathematically, the duality astonishingly allows to use the data of singular Calabi-Yau manifolds X_{n+1} in F-theory to efficiently construct vector bundles V on the heterotic side, which is typically very challenging. The duality can be precisely formulated in the so-called stable degeneration limit of X_{n+1} [138], in which its K3-fibration degenerates into two half K3-fibrations $X^{\pm}_{n+1}$,

$$X_{n+1} \;\to\; X^{+}_{n+1} \cup_{Z_n} X^{-}_{n+1}\,, \tag{3.1}$$

that intersect in the heterotic Calabi-Yau manifold, $X^{+}_{n+1} \cap X^{-}_{n+1} = Z_n$. It can be shown that $X^{\pm}_{n+1}$ naturally encode the heterotic vector bundle V on elliptically fibered Calabi-Yau manifolds Z_n [139]. The most concrete map between the data of X_{n+1} in stable degeneration and the heterotic side is realized if V is described by a spectral cover employing the Fourier-Mukai transform [139, 140] (for more details see e.g. [141] and references therein). Heterotic/F-theory duality has been systematically applied using toric geometry for the construction of vector bundles V with non-Abelian structure groups described both via spectral covers and half K3 fibrations, see e.g. [142, 143] for representative works. More recently, heterotic/F-theory duality has been used to study the geometric constraints on both sides of the duality in four-dimensional compactifications and to characterize the arising low-energy physics [144], see also [145]. Furthermore, computations of both vector bundle and M5-brane superpotentials could be performed by calculation of the F-theory su-

perpotential using powerful techniques from mirror symmetry [146, 147, 148]. In addition, the heterotic/F-theory duality has been recently explored for studies of moduli-dependent prefactor of M5-instanton corrections to the superpotential in F-theory compactifications [149, 150]. The focus of all these works has been on vector bundles V with non-Abelian structure groups, see however [151, 152] for first works on aspects of heterotic/F-theory duality with U(1)'s.

In this work, we will apply the simple and unifying description on the F-theory side in terms of elliptically fibered Calabi-Yau manifolds X_{n+1} to study explicitly, using stable degeneration, the structure of spectral covers yielding heterotic vector bundles that give rise to U(1) gauge symmetry in the lower-dimensional effective theory, continuing the analysis explained in the 2010 talk [153].[1]

Abelian gauge symmetries are desired ingredients for controlling the phenomenology both of extensions of the standard model as well as of GUT theories. Recently, there has been tremendous progress on the construction of F-theory compactifications with Abelian gauge symmetries based on the improved understanding of elliptically fibered Calabi-Yau manifold X_{n+1} with higher rank Mordell-Weil group of rational sections, see the representative works [154, 155, 156, 157, 158, 159, 160, 161, 162, 163]. In contrast, it has been long known that Abelian gauge symmetries in the heterotic theory can for example be constructed by considering background bundle V with line bundle components [133]. The setup we are studying in this work is the duality map between the concrete and known geometry of the Calabi-Yau manifold X_{n+1} with a rank one Mordell-Weil group in [154] on the F-theory side and the data of the Calabi-Yau manifold Z_n and the vector bundle V defining the dual heterotic compactification. We will demonstrate, at the hand of a number of concrete examples, the utility of the F-theory Calabi-Yau manifold X_{n+1} for the construction of vector bundles with non-simply connected structure groups that arise naturally in

[1] We have recently learned that A. Braun and S. Schäfer-Nameki have been working on similar techniques.

this duality. In particular, the F-theory side will guide us to the physical interpretation of less familiar or novel structures in the heterotic vector bundle.

There are numerous key advancements in this direction presented in this work:

- We rigorously perform the stable degeneration limit of a class of F-theory Calabi-Yau manifolds X_{n+1} with U(1) Abelian gauge symmetry using toric geometry, applying and extending the techniques of [164]. We explicitly extract the data of the two half-K3 surfaces inside $X^{\pm}_{n+1}$, the spectral covers and the heterotic Calabi-Yau manifold Z_n. We point out the non-commutativity of the stable degeneration limit and birational maps, such as the one to the Weierstrass model. The stable degeneration limit we perform, which we denote as "toric stable degeneration", preserves the structure of the Mordell-Weil group of rational sections before and after the limit, which is, in contrast, obscured in the stable degeneration limit performed in the Weierstrass model. We apply our general techniques to Calabi-Yau manifolds with elliptic fiber in $\mathrm{Bl}_1\mathbb{P}^2(1,1,2)$, which yield one U(1) in F-theory [154].

- We illuminate the systematics in the mapping under heterotic/F-theory duality between F-theory with a Mordell-Weil group and heterotic vector bundles with non-simply connected structure groups leading to U(1)'s in their effective theories. We find that a single type of F-theory geometry X_{n+1} can be dual to a whole range of different phenomena in the heterotic string, at the hand of numerous concrete examples. We find three different classes of examples of how a U(1) gauge group is obtained in the heterotic string: one class of examples has a split spectral cover, which is a well-known ingredient for obtaining U(1) gauge groups in the heterotic literature starting with [165] and the F-theory literature, see e.g. [166, 167, 168]; another class of models have a spectral cover containing a torsional section of the heterotic Calabi-Yau manifold Z_n, where, duality suggests that this should describe zero-size instantons of

discrete holonomy, as considered in [169]; in a last set of examples, the U(1) arises as the commutant inside E_8 of vector bundles with purely non-Abelian structure groups. We analyze the emerging spectral covers by explicit computations in the group law on the elliptic curve in Z_n. In the first two classes of examples, it is crucial that the heterotic elliptic fibration Z_n exhibits rational sections, as also found in [170]. In addition, in certain examples, the U(1) is only visible in the half K3 fibration (and in Z_n), but not in the spectral cover.

- Whereas the number of massless U(1)'s on the F-theory side equals the Mordell-Weil rank of X_{n+1}, it is on the heterotic side a mixture of geometry and effective field theory effects: while the analysis of the spectral cover can be performed already in 8D, in 6D and lower dimensions U(1)'s can be lifted from the massless spectrum by a Stückelberg effect, i.e. gaugings of axions [133]. We understand explicitly in all three classes of examples how these gaugings arise and what is the remaining number of massless U(1) fields.

We note that although our analysis is performed in 8D and 6D, it is equally applicable also to heterotic/F-theory duality for compactifications to 4D.

This paper is organized in the following way: In Section 3.2, we provide a brief review of the key points of heterotic/F-theory duality as well as a discussion of the new insights gained in this work into spectral covers and half K3-fibrations for vector bundles with non-simply connected structure groups. We review and discuss heterotic/F-theory duality in eight and six dimensions, the spectral cover construction for SU(N) bundles, specializations thereof giving rise to U(1) factors in the heterotic string and the Stückelberg mechanism rendering certain U(1) gauge fields massive. Section 3.3 contains the toric description of a class of F-theory models X_{n+1} for which we describe a toric stable degeneration limit. We specialize to the toric fiber $\mathrm{Bl}_1\mathbb{P}^2(1,1,2)$ and obtain the half K3-fibrations as well as the

dual heterotic geometry and spectral cover polynomial. In Section 3.4, we present selected examples of F-theory/heterotic dual compactifications. We illustrate the three different classes of examples with heterotic vector bundles of structure groups $\mathrm{S}(\mathrm{U}(n)\times\mathrm{U}(1))$ and $\mathrm{S}(\mathrm{U}(n)\times\mathbb{Z}_k)$, as well as purely non-Abelian ones having a centralizer in E_8 with one U(1) factor. There we also illustrate the utility of the Stückelberg mechanism to correctly match the number of geometrically massless U(1)'s on both sides of the duality. In Section 3.5, we conclude and discuss possibilities for future works. This work has four Appendices: we present the birational map of the quartic in $\mathbb{P}^2(1,1,2)$ to Tate and Weierstrass form in Appendix 3.6); Appendix 3.7 contains examples with no U(1) factor, consistently reproducing [136]; in Appendix 3.8 we state the condition for the existence of two independent rational sections and Appendix 3.9 illustrates explicitly the non-commutativity of the stable degeneration limit and the birational map to Weierstrass form.

3.2 Heterotic/F-theory Duality and U(1)-Factors

The aim of this section is two-fold: On the one hand, we review those aspects of heterotic/F-theory duality in eight and six dimensions that are relevant for the analyses performed in this work. On the other hand, we point out subtleties and new insights into heterotic/F-theory duality with Abelian U(1) factors. In particular, we discuss in detail split spectral covers for heterotic vector bundles with non-simply connected gauge groups and the heterotic Stückelberg mechanism.

In Section 3.2.1, we discuss the fundamental duality in 8d, the standard stable degeneration limit in Weierstrass form and the principal matching of gauge groups and moduli. There, we also discuss a subtlety in performing the stable degeneration limit of F-theory models with U(1) factors due to the non-commutativity of this limit with the map to the Weierstrass model. Section 3.2.2 contains a discussion of the spectral cover construction

for SU(N) bundles as well as of split spectral covers giving rise to $\mathrm{S}(\mathrm{U}(N-1)\times\mathrm{U}(1))$ and $\mathrm{S}(\mathrm{U}(N-1)\times\mathbb{Z}_k)$ bundles. In Section 3.2.3 we briefly review heterotic/F-theory duality in 6d, before we discuss the Stückelberg effect in the effective theory of heterotic compactifications with U(1) bundles as well as the relation to gluing condition of rational sections in Section 3.2.4.

In the review part, we mainly follow [171, 139, 141], to which we refer for further details.

3.2.1 Heterotic/F-Theory duality in eight dimensions

The basic statement of heterotic/F-Theory duality is that the heterotic String (in the following, we always concentrate on the $E_8\times E_8$ string) compactified on a torus, which we denote by Z_1, is equivalent to F-Theory compactified on an elliptically fibered K3 surface X_2. The first evidence is that the moduli spaces $\mathcal{M}$ of these two theories coincide and are parametrized by

$$\mathcal{M} = \mathrm{SO}(18,2,\mathbb{Z})\backslash\mathrm{SO}(18,2,\mathbb{R})/(\mathrm{SO}(18)\times\mathrm{SO}(2))\times\mathbb{R}^+. \tag{3.2}$$

From a heterotic perspective this is just the parametrization of the complex and Kähler structure of the torus Z_1 as well as of the 24 Wilson lines. On the F-Theory side it corresponds to the moduli space of algebraic K3 surfaces X_2 with Picard number two. The last factor corresponds to the vacuum expectation value of the dilaton and the size of the base $\mathbb{P}^1$ of X_2, respectively.

Lower-dimensional dualities are obtained, applying the adiabatic argument [172], by fibering the eight-dimensional duality over a base manifold B_{n-1} of complex dimension $n-1$ that is common to both theories of the duality.

The standard stable degeneration limit

In order to match the moduli on both sides of the duality, the K3 surface X_2 has to undergo the so-called stable degeneration limit. In this limit it splits into two half K3 surfaces X_2^+, X_2^- as

$$X_2 \to X_2^+ \cup_{Z_1} X_2^- . \tag{3.3}$$

Each of these are an elliptic fibration $\pi_\pm : X_2^\pm \longrightarrow \mathbb{P}^1$ over a $\mathbb{P}^1$. These two $\mathbb{P}^1$ intersect in precisely one point so that the two half K3 surfaces intersect in a common elliptic fiber which is identified with the heterotic elliptic curve, $X_2^+ \cap X_2^- = Z_1$. On the heterotic side, the stable degeneration limit corresponds to the large elliptic fiber limit of Z_1.

Matching the gauge groups

The F-theory gauge group is given by the singularities of the elliptic fibration of X_2, determining the non-Abelian part G, and its rational sections, which correspond to Abelian gauge fields [135, 137, 173]. In stable degeneration the non-Abelian gauge group of F-theory is distributed into the two half K3 surfaces $X_2^\pm$ and matched with the heterotic side as follows.

It is a well-known fact that the homology lattice of a half K3 surface $X_2^\pm$ is given in general by

$$H_2(X_2^\pm, \mathbb{Z}) = \Gamma_8 \oplus U \tag{3.4}$$

Here, U contains the classes of the elliptic fiber as well as of the zero section. Γ_8 equals the root lattice of E_8 and splits into a direct sum of two contributions: the first contribution is given by the Mordell-Weil group of the rational elliptic surface while the second contribution is given by a sub-lattice which forms, for the half K3 surfaces $X_2^\pm$ at hand, the root-lattice of the part $G_\pm$ of the non-Abelian F-theory gauge group $G = G_+ \times G_-$ that is of ADE type. In the F-Theory limit all fiber components are shrunken to zero size and the half

K3 surface develops a singularity of type $G_{\pm}$. The possible ADE-singularities in the case of complex surfaces have been classified by Kodaira [174]. Thus, one can always read off the corresponding gauge group from the order of vanishings of f, g and Δ once the half K3 has been brought into affine Weierstrass normal form

$$y^2 z = x^3 + f x z^2 + g z^3, \qquad \Delta = f^3 + 27 g^2, \tag{3.5}$$

with f and g in $\mathcal{O}(4)$ and $\mathcal{O}(6)$ of $\mathbb{P}^1$, respectively. For convenience of the reader, we reproduce Kodaira's classification in Table 3.1.

order (f)	order (g)	order (Δ)	singularity
≥ 0	≥ 0	0	none
0	0	n	A_{n-1}
≥ 1	1	2	none
1	≥ 2	3	A_1
≥ 2	2	4	A_2
2	≥ 3	$n+6$	D_{n+4}
≥ 2	3	$n+6$	D_{n+4}
≥ 3	4	8	E_6
3	≥ 5	9	E_7
≥ 4	5	10	E_8

Table 3.1: The Kodaira classification of singular fibers. Here f and g are the coefficients of the Weierstrass normal form, Δ is the discriminant as defined in (3.95) and order refers to their order of vanishing at a particular zero.

In contrast, the gauge group on the heterotic side is encoded in two vector bundles V_1, V_2 that generically carry the structure group E_8. Their respective commutants inside the two ten-dimensional E_8 gauge groups of the heterotic string are to be identified with the F-theory gauge group. As observed in [139], the moduli space of semi-stable E_8-bundles on an elliptic curve E corresponds to the complex structure moduli space of a half K3 surface S whose anti-canonical class is given by E. Furthermore, if S has an ADE singularity of type $\tilde{G}_{\pm}$ then the structure group of V_1, V_2 is reduced to the centralizer $H_{\pm}$ of

$\tilde{G}_\pm$ within E_8, respectively. In heterotic/F-theory duality, a matching of the gauge group is then established by identifying $S \equiv X_2^\pm$ yielding $\tilde{G}_\pm \equiv G_\pm$.

Notice that the full eight-dimensional gauge group is given by $G \times \mathrm{U}(1)^{16-\mathrm{rk}(G)} \times \mathrm{U}(1)^4$. Here, the last factor accounts for the reduction of the metric and the Kalb Ramond B-field along the two one-cycles of the torus in the heterotic string. From the F-theory perspective, all U(1) factors arise from the reduction of the C_3 field along those 2-forms in the full K3 surface X_2 that are orthogonal to the zero section and the elliptic fiber. In particular, the $\mathrm{U}(1)^{16-\mathrm{rk}(G)}$ arises from the generators of the Mordell-Weil group of the half K3 surfaces. For a derivation in Type IIB string theory, see the recent work [175].

Matching complex structure and bundle moduli

In this section, we discuss how the heterotic moduli can be recovered from the data of the F-theory K3 surface [136, 176]. Here we restrict the discussion to the moduli of the heterotic torus Z_1 and the vector bundle (i.e. Wilson line) moduli, ignoring the heterotic dilaton modulus.

So far, this discussion has been restricted to the case that the elliptic fibration of the K3 surface is described by a Weierstrass model. In this case, the standard stable degeneration procedure applies. Given the Weierstrass form (3.5) for X_2 with f, g sections of $\mathcal{O}(8)$ and $\mathcal{O}(12)$ on $\mathbb{P}^1$, respectively, we can expand these degree eight and twelve polynomials in the affine $\mathbb{P}^1$-coordinate u as

$$f = \sum_{i=0}^{8} f_i u^i, \qquad g = \sum_{i=0}^{12} g_i u^i. \tag{3.6}$$

Then, the two half K3 surfaces $X_2^\pm$ arising in the stable degeneration limit, given as the Weierstrass models

$$X^\pm : \qquad y^2 z = x^3 + f^\pm z + g^\pm z^3, \tag{3.7}$$

can be obtained from (3.6) by the split

$$f^+ = \sum_{i=0}^{4} f_i u^i\,, \quad f^- = \sum_{i=4}^{8} f_i u^i\,, \qquad g^+ = \sum_{i=0}^{6} g_i u^i\,, \quad g^- = \sum_{i=6}^{12} g_i u^i\,, \tag{3.8}$$

The "middle" polynomials f_4 and g_6 correspond to the heterotic elliptic curve, which then reads

$$y^2 z = x^3 + f_4 x z^2 + g_6 z^3, \tag{3.9}$$

while the "upper" and "lower" coefficients correspond to the moduli of the two E_8-bundles.

Stable degeneration with other elliptic fiber types

The focus of the present work are F-theory compactifications with one U(1) gauge group arising from elliptically fibered Calabi-Yau manifolds with two rational sections. These are naturally constructed using the fiber ambient space $\mathrm{Bl}_1\mathbb{P}^{(1,1,2)}$ [154]. More precisely, we will consider K3 surfaces given as sections χ of the anti-canonical bundle $-K_{\mathbb{P}^1\times\mathrm{Bl}_1\mathbb{P}^{(1,1,2)}}$ of $\mathbb{P}^1\times\mathrm{Bl}_1\mathbb{P}^{(1,1,2)}$ reading

$$\chi = \sum_i s_i \chi^i\,. \tag{3.10}$$

Here s_i and χ^i are sections of the anti-canonical bundles $-K_{\mathbb{P}^1} = \mathcal{O}(2)$ and $-K_{\mathrm{Bl}_1\mathbb{P}^{(1,1,2)}}$, respectively.

Then, analogously to the above construction, one can perform a stable degeneration limit for these hypersurfaces as well. However, it is crucial to note here that we can perform the stable degeneration limit in *two* possible ways, as shown in Figure 3.1: one way is to first take the Weierstrass normal form W_χ (upper horizontal arrow) of the full $\mathrm{Bl}_1\mathbb{P}^{(1,1,2)}$-model and then apply the split (3.8) to obtain two half K3 surfaces (right vertical arrow); a second way is to first perform stable degeneration (left vertical arrow), yielding two half K3 surfaces $\chi^\pm$ with elliptic fibers in $\mathrm{Bl}_1\mathbb{P}^{(1,1,2)}$, and then compute their Weierstrass normal

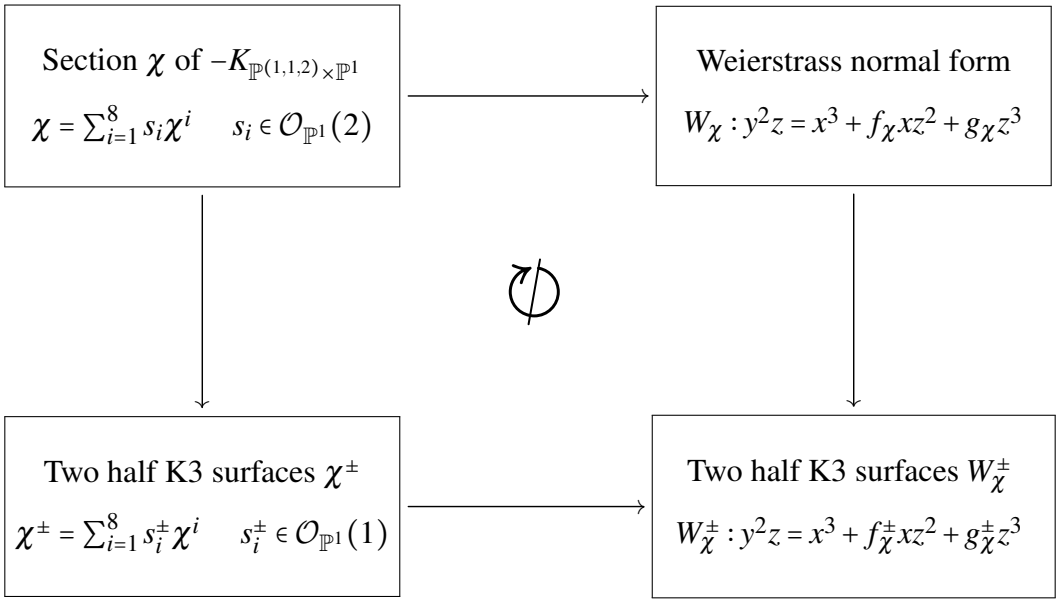

Figure 3.1: Computing the Weierstrass normal form (horizontal arrows) and taking the stable degeneration limit (vertical arrows) does not commute.

forms $W_\chi^\pm$ (lower horizontal arrow). It is important to realize, however, that these two possible paths in the diagram 3.1 do not commute, as explicitly shown in Appendix 3.9.

We propose and demonstrate in Section 3.3 that the natural order to perform heterotic/F-theory duality for models with U(1) factors and different elliptic fiber types than the Weierstrass model is to first perform stable degeneration with the other fiber type (left vertical arrow) and then compute the Weierstrass model of the resulting half K3-fibrations (lower horizontal arrow) in order to analyze the physics of the model.

3.2.2 Constructing SU(N) bundles on elliptic curves and fibrations

While the description of the structure group of the vector bundle via half K3 surfaces as reviewed above is of high conceptual importance, it is in practice often easier to construct vector bundles with the desired structure group directly. In the following section, we review

this construction for SU(N) bundles and specializations thereof which has been studied first in [177] and was further developed in [140, 139, 178].

In this section E always denotes an elliptic curve with a marked point p. The curve is defined over a general field K, which does not necessarily have to be algebraically closed. It is well-known that an elliptic curve with a point p has a representation in the Weierstrass normal form (3.5), where p reads $[x:y:z] = [0:1:0]$. In general, a degree zero line bundle $\mathcal{L} \longrightarrow E$, i.e. a U(1)-bundle, takes the form

$$\mathcal{L} = \mathcal{O}(q) \otimes \mathcal{O}(p)^{-1} = \mathcal{O}(q-p)\,, \tag{3.11}$$

where q denotes another arbitrary rational point on E (note that over $K = \mathbb{C}$ every point is rational). Furthermore, we note that there is a bijective map ϕ from the elliptic curve E onto its Picard group of degree zero which is defined by

$$\phi : E \longrightarrow \mathrm{Pic}^0(E)\,, \qquad q \mapsto q - p\,. \tag{3.12}$$

In particular, this extends to an isomorphism from the space of line bundles onto $\mathrm{Pic}^0(E)$, defined by $\mathrm{div}(\mathcal{L}) = q - p$. To be more precise, the divisor map 'div' is to be applied to a meromorphic section[2] of $\mathcal{L}$. For later purposes, we also recall that the addition law in $\mathrm{Pic}^0(E)$ can be identified with the group law on E, which we denote by $\boxplus$, via this isomorphism.

A semi-stable SU(N) vector bundle of degree zero V is then given as the sum[3] of N holomorphic line bundles $\mathcal{L}_i$, i.e. we have $V = \oplus_{i=1}^N \mathcal{L}_i = \oplus_{i=1}^N \mathcal{O}(q_i - p)$, such that the

[2] This map is independent of the section chosen.

[3] If two or more points coincide, the situation is a bit more subtle. In this case the bundle is given by $\oplus_{i=1}^N \mathcal{O}(q_i - p) I_{r_i}$, where r_i denotes the multiplicity of the point q_i and I_r is inductively defined by the extension sequence $0 \longrightarrow \mathcal{O} \longrightarrow I_{r-1} \longrightarrow \mathcal{O} \longrightarrow 0$. However, one usually only considers bundles up to S-equivalence which identifies I_r with $\mathcal{O}^{\oplus r}$.

determinant of V is trivial. The latter implies that

$$\otimes_{i=1}^{N} \mathcal{O}(q_i - p) = \mathcal{O} \qquad \Leftrightarrow \qquad \boxplus_{i=1}^{N} q_i = 0\,. \tag{3.13}$$

An $\mathrm{SU}(N)$ vector bundle is therefore determined by the choice of N points on E that sum up to zero. Any such N-tupel is determined by a projectively unique element of $H^0(E, \mathcal{O}(Np))$, i.e. a function with N zeros and a pole of order N at p. Thus, the moduli space of $\mathrm{SU}(N)$ vector bundles is given by

$$\mathcal{M}_{\mathrm{SU}(N)} = \mathbb{P}H^0(E, \mathcal{O}(Np))\,. \tag{3.14}$$

In the affine Weierstrass form of E, given by (3.5), the coordinates x, y have a pole of order two and three at p, respectively. Accordingly, any element of $\mathbb{P}H^0(E, \mathcal{O}(Np))$ enjoys an expansion

$$w = c_0 + c_1 x + c_2 y + c_3 x^2 + \ldots + \begin{cases} c_N x^{\frac{N}{2}} & \text{if } N \text{ is even}\,, \\ c_N x^{\frac{N-3}{2}} y & \text{if } N \text{ is odd}\,, \end{cases} \tag{3.15}$$

with $c_i \in K$. The section w is called the spectral cover polynomial and has N common points with E, called the *spectral cover*, which define the desired $\mathrm{SU}(N)$ bundle. Counting parameters of (3.15), one is lead to the conclusion that

$$\mathcal{M}_{\mathrm{SU}(N)} = \mathbb{P}^{N-1}\,. \tag{3.16}$$

Finally, a comment on rational versus non-rational points is in order. Generically, p is the only point on E over a general field K. However, in such a situation, it is possible to mark N points in a rational way by the polynomial $w = 0$ which give rise to an $\mathrm{SU}(N)$ bundle in the way just described. Nevertheless, under the circumstances that there are additional rational points on E and the spectral cover polynomial $w = 0$ specializes appropriately, the

structure group reduces in a certain way, as discussed next.

Vector bundles with reduced structure groups

As described in the previous section, the choice of N points on E describes an $\mathrm{SU}(N)$ bundle. If we consider just an elliptic curve E over $\mathbb{C}$, which is the geometry relevant for the construction of heterotic compactifications to eight dimensions, the spectral cover (3.15) can be factorized completely. This corresponds to the 16 possible Wilson lines on T^2.

In contrast, if we consider an elliptic curve over a function field, as it arises in elliptic fibrations Z_n of E over a base B_{n-1} used for lower-dimensional heterotic compactifcations, the N points are the zeros of (3.15), which defines an N-section of the fibration. In non-generic situations, where subsets of the N sheets of this N-section are well-defined globally, i.e. are monodromy invariant, the structure group of the vector bundle is reduced. For example, a separation into two sets of k and l sheets (with $k+l=N$), respectively, results in the structure group $\mathrm{S}(\mathrm{U}(k)\times\mathrm{U}(l))$. The spectral cover defined by (3.15) is called "split" and defines a reducible variety inside Z_n, see e.g. [165, 166, 167, 168]. In the most extreme case, one could have $k=1$ and $l=N-1$. In this case, the elliptic fibration of Z_n has to necessarily have another well-defined section in addition to the section induced by the rational point p: it is the one marked by the component of the spectral cover $w=0$ with just one sheet [170]. Thus, the fiber E has a rational point, which we denote by q and one can, as discussed above, define a U(1) line bundle $\mathcal{L}$ via (3.11). As this fiberwise well-defined line bundle is also well-defined globally, it will induce a line bundle on Z_n, whose first Chern class is given, up to vertical components, by the difference of the sections induced by q and p, cf. [179]. The structure group H of the vector bundle is in this case given by

$$H = \mathrm{S}(\mathrm{U}(N-1)\times\mathrm{U}(1))\,. \tag{3.17}$$

We will see later that this situation will be relevant situation for the construction of U(1) gauge groups in the heterotic string.

We emphasize that for a U(1)-bundle alone there is no spectral cover polynomial (3.15) that would be able to detect this additional rational point. This is due to the fact that there is no function that has only one zero on an elliptic curve E . However, if the rational point is accompanied by further points, rational or non-rational points over the field K, it can very well be seen by the spectral cover. For instance, one could construct a spectral cover from q and $-q$, which would describe a bundle of structure group $\mathrm{S}(\mathrm{U}(1)\times\mathrm{U}(1))$.

Finally, it needs to be discussed what interpretation should be given to the case that the rational point q on the curve E happens to be torsion of order k. In this case the structure group H reduces further to $\mathrm{S}(\mathrm{U}(N)\times\mathbb{Z}_k)$. To argue for this, we invoke again a fiberwise argument. The fiber at a generic point in B_{n-1} admits a line bundle $\mathcal{L} = \mathcal{O}(q-p)$ with the property that $\mathcal{L}^k = \mathcal{O}$. This is clear as the transition functions g_{ij} will be subject to $g_{ij}^k = 1$ in Čech cohomology as k times the Poincaré dual of its first Chern class is trivial. However, this is just the statement that the fiberwise structure group of $\mathcal{L}$ is contained in $\mathbb{Z}_k$. Employing that p and q are globally well-defined sections then suggests that this argument also holds on Z_n.

3.2.3 Heterotic/F-Theory duality in six dimensions

Six-dimensional heterotic/F-Theory duality arises by fibering the eight-dimensional duality over a common base $B_1 = \mathbb{P}^1$, employing the adiabatic argument [172]. Thus, the heterotic string gets compactified on an elliptically fibered K3 surface Z_2 while F-Theory is compactified on an elliptically fibered Calabi-Yau threefold X_3 over a Hirzebruch surface $\mathbb{F}_n$. Our presentation will be brief and focused on the later applications in this work. For a more detailed discussion we refer to the classical reference [137, 136, 139] or the reviews [171, 141].

On the F-theory side, the non-Abelian gauge content originates from the codimension one singularities of the elliptic fibration $\pi : X_3 \to \mathbb{F}_n$. The singularity is generically of type G', which gets broken down to $G \subset G'$ by monodromies corresponding to outer automorphisms of the Dynkin diagram of G' [173]. The resulting gauge symmetry is encoded in the order of vanishing of the coefficients $a_0, a_1, a_2, a_3, a_4, a_6$ in the Tate form of the elliptic fibration

$$y^2 + a_1 xy + a_2 = x^3 + a_3 x^2 + a_4 x + a_6 \,. \tag{3.18}$$

In addition, we introduce the *Tate vector* $\vec{t}_X$ which encodes the orders of vanishing of the coefficients a_i along the divisor defined by the local coordinate X:

$$\vec{t}_X = \left(\mathrm{ord}_X\left(a_0\right), \mathrm{ord}_X\left(a_1\right), \mathrm{ord}_X\left(a_2\right), \mathrm{ord}_X\left(a_3\right), \mathrm{ord}_X\left(a_4\right), \mathrm{ord}_X\left(a_6\right), ord_X\left(\Delta\right)\right). \tag{3.19}$$

The results of the analysis of singularities, known as Tate's algorithm, are summarized in Table 3.2 [180, 173], see, however, [181] for subtleties.

On the heterotic side, the gauge theory content is encoded in a vector bundle V where the following discussion restricts itself to the case of $\mathrm{SU}(N)$ bundles. The six-dimensional bundle is defined in terms of two pieces of data, the spectral cover curve C as well as a line bundle $\mathcal{N}$ which is defined on C. Here, the spectral curve C is the 6d analog of the points defined by the section of $\mathbb{P}H^0(E, \mathcal{O}(np))$ which has been discussed in 3.2.2. In six dimensions, the elliptic curve $Z_1 \cong E$ gets promoted to an elliptic fibration, which can again be described by a Weierstrass form (3.5) with coordinates x, y,z being sections of $\mathcal{L}^2$, $\mathcal{L}^2$, $\mathcal{O}$, respectively, for $\mathcal{L} = K_{\mathbb{P}^1}^{-1} = \mathcal{O}(-2)$ and coefficients f, g being in $\mathcal{L}^4$, $\mathcal{L}^6$, respectively. Accordingly, the coefficients c_i entering the spectral cover (3.15) are now sections of $\mathcal{M} \otimes \mathcal{L}^{-i}$, $\mathcal{M}$ being an arbitrary line bundle on $\mathbb{P}^1$ and C is defined as the zero locus of the section of (3.15). Thus, C defines an N-sheeted ramified covering of $\mathbb{P}^1$, i.e. a Riemann surface. The spectral cover C defines the isomorphism class of a semi-stable

vector bundle above each fiber. The line bundle $\mathcal{N}$ describes the possibility to twist the vector bundle without changing its isomorphism class. It is usually fixed, up to a twisting class γ, by the condition $c_1(V) = 0$ for an $\mathrm{SU}(N)$ bundle, see [139] for more details.

3.2.4 Massless U(1)-factors in heterotic/F-theory duality

As previously discussed, the perturbative heterotic gauge group is obtained by commuting the structure group H of the vector bundle V within the two E_8-bundles. We propose three possibilities, how U(1) gauge groups can arise from this perspective:

- H contains a U(1) factor, i.e. it is of the form $H = H_1 \times \mathrm{U}(1)$, or $\mathrm{S}(\mathrm{U}(M) \times \mathrm{U}(1))$,
- H contains a discrete piece, i.e. a part taking values in $\mathbb{Z}_k$,
- or H is non-Abelian and is embedded such that its centralizer in E_8 necessarily contains a U(1)-symmetry.

The construction of a vector bundle for these three different cases employing spectral covers has been discussed in Section 3.2.2.

In general, we emphasize that U(1)-factor which arises from a split spectral cover is usually massive due to a Stückelberg mass term which is induced by the first Chern class of the U(1) background bundle, as we review next. However, if the U(1) term originates from a background bundle with non-Abelian structure group there is tautologically no U(1) background factor which could produce a mass term and therefore the six-dimensional U(1) field is expected to be massless. Finally, we propose, for consistency with heterotic/F-theory duality, that a six-dimensional torsional section gives rise to a point-like instanton with discrete holonomy, as introduced in [169]. Indeed, we will show in several examples in Section 3.4 that all three cases naturally appear in heterotic duals of F-theory compactifications with one U(1) and that a matching of the corresponding gauge groups is only possible if the arising spectral covers are interpreted as suggested here.

The heterotic Stückelberg mechanism

In six and lower dimensions, it is well-known that a geometric Stückelberg effect can render a U(1) gauge field massive [133]. To identify the mass term of the six- (or lower-) dimensional U(1), one considers the modified ten-dimensional kinetic term of the Kalb-Ramond field B_2 which reads, up to some irrelevant proportionality constant, as

$$\mathcal{L}^{10d}_{\text{kin}} = H \wedge \star_{10d} H, \qquad H = dB_2 - \frac{\alpha'}{4}\left(\omega_{3Y}(A) - \omega_{3L}(\Omega)\right). \tag{3.20}$$

Here, $\star_{10d}$ is the ten-dimensional Hodge-star and ω_{3Y}, ω_{3L} denote the Chern-Simons terms of the gauge field and the spin connection, respectively. The physical effect we want to discuss here arises from the former one, which is given explicitly by

$$\omega_{3Y} = \text{Tr}\left(A \wedge dA + \frac{2}{3} A \wedge A \wedge A\right). \tag{3.21}$$

Now, we perform a dimensional reduction of the kinetic term (3.20) in the background of a U(1) vector bundle on the heterotic compactification manifold Z_n, ignoring possible additional non-Abelian vector bundles for simplicity. On such a background, we can expand the ten-dimensional field strength $F^{10d}_{U(1)}$ of the U(1) gauge field as

$$F^{10d}_{U(1)} = F_{U(1)} + \mathcal{F} = F_{U(1)} + k_\alpha \omega^\alpha. \tag{3.22}$$

Here $\mathcal{F} = \frac{1}{2\pi i} c_1(\mathcal{L})$ is the background field strength, i.e. the first Chern class $c_1(\mathcal{L})$ of the corresponding U(1) line bundle $\mathcal{L}$, and $F_{U(1)}$ is the lower-dimensional gauge field. We have also introduced a basis ω^α, $\alpha = 1, \ldots, b_2(Z_n)$, of harmonic two-forms in $H^{(2)}(Z_n)$, where $b_2(Z_n)$ is the second Betti number of Z_n, along which we have expanded $\mathcal{F}$ into the flux

quanta k_α. We also expand the ten-dimensional Kalb-Ramond field as

$$B_2 = b_2 + \rho_\alpha \omega^\alpha \,, \tag{3.23}$$

where b_2 is a lower-dimensional two-form and ρ_α are lower-dimensional axionic scalars . We readily insert this reduction ansatz into the ten-dimensional field strength H in (3.20), where we only take into account the gauge part, to arrive, dropping unimportant prefactors, at the lower-dimensional kinetic term for the axions ρ_α of the form

$$\mathcal{L}_{\text{Stück.}} = G^{\alpha\beta} \left(d\rho_\alpha + k_\alpha A_{U(1)} \right) \wedge \star \left(d\rho_\beta + k_\beta A_{U(1)} \right) . \tag{3.24}$$

Here we introduced the kinetic metric

$$G^{\alpha\beta} = \int_{Z_n} \omega^\alpha \wedge \star \omega^\beta \,. \tag{3.25}$$

It is clear from (3.24) that a single U(1) gauge field will be massive if we have a non-trivial $c_1(\mathcal{L}) \neq 0$. However, we note that in the presence of multiple massive U(1) gauge fields, appropriate linear combinations of them in the kernel of the mass matrix can remain massless U(1) fields. A computation similar to the one above has appeared in e.g. [165], where also the case of multiple U(1)'s is systematically discussed.

U(1)-factors from gluing conditions in half K3-fibrations

We conclude this section by discussing the connection between the previous field theoretic considerations that lead to a massive U(1) via the Stückelberg action (3.24) on the heterotic side and geometric glueing conditions of the sections of half K3 surfaces to global sections of the two half K3-fibrations $X_n^\pm$ that arise in stable degeneration as well as of the full Calabi-Yau manifold X_n. We illustrate this in six dimensions for concreteness, i.e. for F-

theory on a Calabi-Yau threefold X_3 and the heterotic string on a K3 surface Z_2, although the arguments hold more generally.

It is well known that the number of U(1) factors in F-theory is given by the rank of the Mordell-Weil group, i.e. by the number of independent global rational sections of the elliptic fibration X_3 in addition to the zero section. As discussed in Section 3.2.1, a half K3 surface with ADE singularity of rank r has an $(8-r)$-dimensional Mordell-Weil group. Promoting the half K3 surface to a fibration of half K3 surfaces over the base $\mathbb{P}^1$, such as the threefolds $X_3^{\pm}$, these sections need not necessarily give rise to sections of the arising three-dimensional elliptic fibrations. Considering the half K3 surfaces arising in the stable degeneration limit of F-theory, there are those sections which also give rise to sections of e.g. the full half K3 fibration X_3^+. These sections will induce a U(1)-factor on the heterotic side which is embedded into one E_8-bundle and which is generically massive with a mass arising via the Stückelberg action (3.24). If there is also a globally well-defined section of the other half K3 fibration X_3^- and this section glues with the section in the first half K3 fibration X_3^+, then there is a linear combination of U(1)'s that remains massless in the Stückelberg mechanism on the heterotic side. This is clear from the F-theory perspective, as these two sections can then be glued along the heterotic two-fold Z_2 to a section of the full Calabi-Yau threefold X_3, i.e. give rise to an element in its Mordell-Weil group and a massless U(1).

3.3 Dual Geometries with Toric Stable Degeneration

In this section, we describe a toric method in order to study the stable degeneration limit of an elliptically fibered K3 surface. This stable degeneration limit will be at the heart of the analysis of the examples of heterotic/F-theory dual geometries in Section 3.4. In a first step in Section 3.3.1, we construct an elliptically fibered K3 surface. Afterwards in Section

3.3.2, we fiber this K3 surface over another $\mathbb{P}^1$ which is used to investigate the splitting of the K3 surface into two rational elliptic surfaces, as discussed in Section 3.3.3. In the concluding Section 3.3.4, we prove that the surfaces arising in the stable degeneration of the K3 surface indeed define rational elliptic surfaces, i.e. half K3 surfaces.

3.3.1 Constructing an elliptically fibered K3 surface

We start by constructing a three-dimensional reflexive polytope Δ_3° given as the convex hull of vertices that are the rows of the following matrix:

$$\left(\begin{array}{ccc|c} a_1 & b_1 & 0 & x_1 \\ \vdots & & 0 & x_i \\ a_n & b_n & 0 & x_n \\ 0 & 0 & 1 & U \\ 0 & 0 & -1 & V \end{array}\right). \tag{3.26}$$

Here $(a_i\, b_i)$ denote the points of a two-dimensional reflexive polytope Δ_2°, which will specify the geometry of the elliptic fiber E. It is embedded into Δ_3° in the xy-plane, see the first picture in Figure 3.2. The last column contains the homogeneous coordinate associated to a given vertex. We label the rays of the two-dimensional polytope counter-clockwise by the coordinates $x_1, \ldots x_n$. In addition, we assign the coordinates U, V to the points $(0\,0\,1)$ and $(0\,0\,-1)$ which correspond to the rays of the fan of the $\mathbb{P}^1$-base. We use the shorthand notation $\mathbb{P}^1_{[U:V]}$ to indicate its homogeneous coordinates. Finally, we use the notation ρ_H for the ray with corresponding homogeneous coordinate H. We denote by Σ_3 the natural simplicial fan associated to Δ_3° and denote the corresponding toric variety over the fan of Δ° as $\mathbb{P}_{\Sigma_3}$. Provided a fine triangulation of the polytope Δ_3° has been chosen, the toric ambient space $\mathbb{P}_{\Sigma_3}$ will be Gorenstein and terminal.

A general section χ of the anti-canonical bundle $\mathcal{O}_{\mathbb{P}_{\Sigma_3}}(-K_{\mathbb{P}_{\Sigma_3}})$ defines a smooth elliptically fibered K3 surface X_2. The ambient space of its elliptic fiber E is the toric variety $\mathbb{P}_{\Sigma_2}$ that is constructed from the fan Σ_2 of the polytope Δ_2° induced by Σ_3. As the toric fibration of Σ_2 over $\Sigma_{\mathbb{P}^1}$ is direct, the section χ takes the form

$$\chi = s_i \eta^i \qquad \text{for} \qquad s_i = s_i^0 U^2 + s_i^1 UV + s_i^2 V^2. \tag{3.27}$$

Here η^i are the sections of the anti-canonical bundle of $\mathcal{O}_{\mathbb{P}_{\Sigma_2}}(-K_{\mathbb{P}_{\Sigma_2}})$, i.e. the range of the index i is given by the number of integral points in Δ_2, and s_i^k, $k = 1,2,3$, are constants. Note that, for a very general[4] X_2, the dimension $h^{(1,1)}(X)$, of the cohomology group $H^{(1,1)}(X_2,\mathbb{C})$ can be computed combinatorically from the pair of reflexive polyhedra Δ_3, Δ_3° by a generalization of the Batyrev's formula [182]:

$$h^{(1,1)}(X) \;=\; l(\Delta^\circ) - n - 1 - \sum_{\Gamma^\circ} l^*(\Gamma^\circ) + \sum_{\Theta^\circ} l^*(\Theta^\circ) l^*(\hat{\Theta}^\circ)\,. \tag{3.28}$$

Here $l(\Delta)$ ($l^*(\Delta)$) denote the number of (inner) points of the n-dimensional polytope Δ. In addition, Γ (Γ°) denote the codimension one faces of Δ (Δ°), while Θ denotes a codimension two face with $\hat{\Theta}$ being its dual.

3.3.2 Constructing K3 fibrations

As a next step, we fiber this ambient space over a second $\mathbb{P}^1_{[\lambda_1,\lambda_2]}$ with homogeneous coordinates λ_1, λ_2. The following construction is such that the generic fiber consists of a smooth K3 surface X_2 over a generic point of $\mathbb{P}^1_{[\lambda_1,\lambda_2]}$ and a split fiber, i.e. a splitting into two half K3 surfaces, over a distinguished point of $\mathbb{P}^1_{[\lambda_1,\lambda_2]}$, as explained below.

[4] A point is very general if it lies outside a countable union of closed subschemes of positive codimension

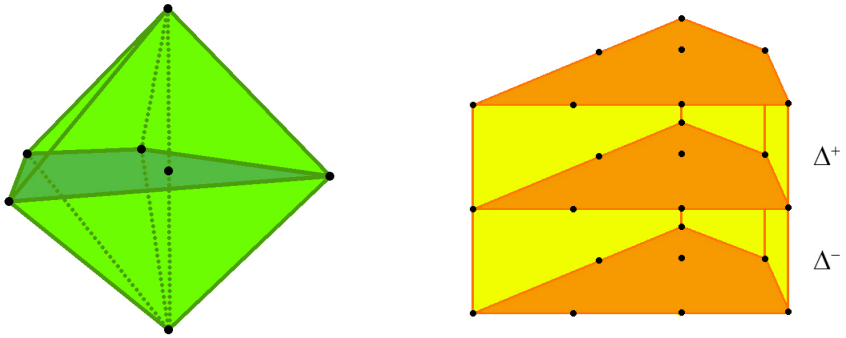

Figure 3.2: On the left we show the reflexive polytope Δ_3°, while its dual Δ_3 is shown on the right. In this example, the ambient space for the elliptic fiber, specified by Δ_2°, is given by $\mathrm{Bl}_1\mathbb{P}^{(1,1,2)}$.

The four-dimensional polytope which describes this construction is given by

$$\Delta_4 = \left\{ (m_1,m_2,m_3,m_4) \in \mathbb{Z}^4 \,\middle|\, (m_1,m_2,m_3) \in \Delta_3,\ -1 \le m_4 \le 1, \begin{cases} m_4 \ge -1 \text{ if } m_3 \le 0\,, \\ m_4 \ge m_3 - 1 \text{ if } m_3 \ge 0\,. \end{cases} \right\}. \tag{3.29}$$

Here, Δ_3 denotes the dual polytope of Δ_3°, cf. the second picture in Figure 3.2. The faces of Δ_4 are given by the (intersection of the) hyperplanes

$$m_4 = 1\,, \qquad m_4 = -1\,, \qquad m_4 = -1 + m_3\,, \qquad m_3 = -1\,, \quad m_3 = 1\,, \qquad \sum_{j=0}^{2} a_i^j m_j = 1\,, \tag{3.30}$$

where the last expression is given by the the defining hyperplanes of Δ_2, the dual of Δ_2°. We denote by Σ_4 the fan associated to the dual polytope Δ_4° of Δ_4. In particular, the normal vectors of the facets of Δ_4 give the rays of Σ_4. To be explicit, the rays of Σ_4 are given by

the rows of the matrix

$$\left(\begin{array}{cccc|c} a_1 & b_1 & 0 & 0 & x_1 \\ \vdots & & 0 & 0 & x_i \\ a_n & b_n & 0 & 0 & x_n \\ 0 & 0 & 1 & 0 & U \\ 0 & 0 & 0 & 1 & \lambda_1 \\ 0 & 0 & -1 & 1 & \mu \\ 0 & 0 & -1 & 0 & V \\ 0 & 0 & 0 & -1 & \lambda_2 \end{array}\right). \tag{3.31}$$

We note that the coordinates assigned to its rays as displayed in (3.31) transform as follows under the $\mathbb{C}^*$-actions

$$(U:\lambda_1:\mu:V:\lambda_2) \sim \left(a^{-1}U : ab^{-1}\lambda_1 : a^{-1}bc^{-1}\mu : b^{-1}cV : c^{-1}\lambda_2\right) \tag{3.32}$$

with $a, b, c \in \mathbb{C}^*$.

In analogy to the discussion in the previous section, a section χ_4 of the anti-canonical bundle $-K_{\mathbb{P}_{\Sigma_4}}$ of the toric variety $\mathbb{P}_{\Sigma_4}$ defines a three-dimensional smooth Calabi-Yau manifold $\mathfrak{X}$. In particular, the Calabi-Yau constraint (3.27) generalizes as

$$\chi_4 = s_i \eta^i, \tag{3.33}$$

where the η^i are given as before and the coefficients s_i now read

$$\begin{aligned} s_i(U,V,\lambda_1,\lambda_2,\mu) \;=\; & s_i^1\lambda_1\lambda_2U^2 + s_i^2\lambda_1^2\mu U^2 + s_i^3\lambda_2^2UV + s_i^4\lambda_1\lambda_2\mu UV + s_i^5\lambda_1^2\mu^2UV \\ & + s_i^6\lambda_2^2\mu V^2 + s_i^7\lambda_1\lambda_2\mu^2V^2 + s_i^8\lambda_1^2\mu^3V^2 \end{aligned} \tag{3.34}$$

with constants $s_i^j \in \mathbb{C}$.

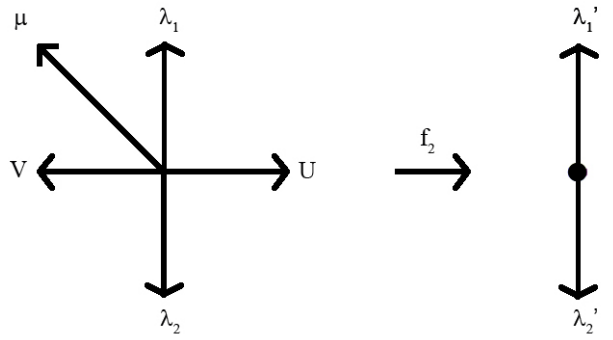

Figure 3.3: The toric morphism f_2.

We proceed by observing that the projection on the last two columns in (3.31) yields the polytope $\Delta^\circ_{dP_2}$ of the toric variety dP_2, cf. Figure 3.3. Denoting the fan of $\Delta^\circ_{dP_2}$ by Σ_{dP_2} this projection gives rise to a toric map

$$f_1 : \Sigma_4 \longrightarrow \Sigma_{dP_2} . \tag{3.35}$$

In addition, dP_2 is fibered over the $\mathbb{P}^1_{[\lambda_1':\lambda_2']}$ as can be seen by projecting onto the fourth column of Δ_4, cf. Figure 3.3, i.e. there is a toric map

$$f_2 : \Sigma_{dP_2} \longrightarrow \Sigma_{\mathbb{P}^1} , \tag{3.36}$$

where $\Sigma_{\mathbb{P}^1}$ is the fan of $\mathbb{P}^1_{[\lambda_1':\lambda_2']}$. Note that this $\mathbb{P}^1$ is isomorphic to $\mathbb{P}^1_{[\lambda_1:\lambda_2]}$. We denote the composition map of the two by $f = f_2 \circ f_1$.

In summary, we have the following diagram of toric morphisms and induced maps on

$\mathfrak{X}$:

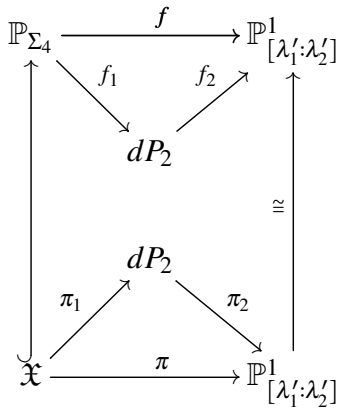

Here we denote the toric maps f_1, f_2, f and their induced morphisms of toric varieties by the same symbol, respectively. Note that for a generic point, the fiber of π is given by a smooth K3 surface X_2.

In order to prepare for the discussion of the stable degeneration limit, we proceed by discussing the fibration map in more detail. For this purpose, we note the correspondence of facets and rays as displayed in Table 3.3. The dual Δ_{dP_2} of $\Delta^\circ_{dP_2}$ with associated monomials is shown in Figure 3.4. These monomials are the global sections of K_{dP_2} and are constructed according to [183]

$$\chi_{dP_2} = \sum_{P\in\Delta_{dP_2}} \prod_{P^*\in\Delta^*_{dP_2}} a_P x_{P^*}^{\langle P|,P^*|+\rangle 1} \,. \tag{3.37}$$

Here x_{P^*} denotes the coordinate which is associated to the corresponding ray of the toric diagram and a_P are constants.

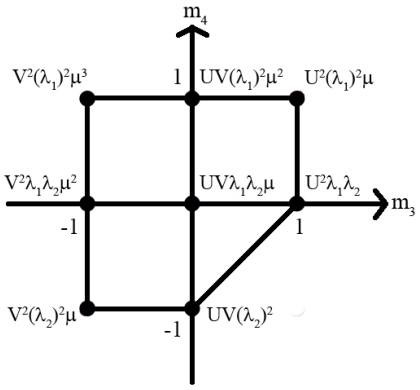

Figure 3.4: The dual polytope Δ_{dP_2} and the associated monomials.

By the correspondence between cones of $\Delta^{\circ}_{dP_2}$ and vertices of Δ_{dP_2} the vertex corresponding to the monomial $V^2\lambda_2^2\mu$ is dual to the cone spanned by the rays ρ_U and ρ_{λ_1}. We denote the coordinates associated to the two rays of $\mathbb{P}^1_{[\lambda_1:\lambda_2]}$ inside $\Delta^0_{dP_2}$ appearing in (3.36) by $\rho_{\lambda_1'}$ and $\rho_{\lambda_2'}$. Note that $f_2^{-1}(\rho_{\lambda_1'}) = \{\rho_{\lambda_1}, \rho_\mu\}$, while $f_2^{-1}(\rho_{\lambda_2'}) = \{\rho_{\lambda_2}\}$.

3.3.3 The toric stable degeneration limit

In the following, we aim to show that the general fiber of the map π gives rise to a smooth K3 surface while the pre-image of the point $[\lambda_1' : \lambda_2'] = [1:0]$ gives rise to a degeneration into two half K3 surfaces $X_2^{\pm}$ that intersect in the elliptic fiber Z_1 over the point of intersection of the two $\mathbb{P}^1$ which are the respective bases of their elliptic fibrations.

Let us first consider the toric variety $f_2^{-1}(\lambda_2' = 0)$ corresponding to the pre-image in $\Delta^0_{dP_2}$ of $\rho_{\lambda_2'}$. It is given by the star of ρ_{λ_2} in $\Delta^0_{dP_2}$ which is just the generic fiber of f_2. Indeed, if $\lambda_2 = 0$, the coordinates μ and λ_1 are non-vanishing due to the Stanley-Reisner ideal. Two of the scaling relations (3.32) can be used in order to eliminate the latter two variables while the remaining (linear combination) endows the coordinates U, V with the well-known scaling relations of $\mathbb{P}^1_{[U,V]}$. In addition, the monomials associated to the vertices of the dual

facet of ρ_{λ_2} give rise to the following sections

$$s_{\lambda_2} := s_i^2 U^2 + s_i^5 UV + s_i^8 V^2 \,, \tag{3.38}$$

as follows from (3.34) by setting $\lambda_2 = 0$. These provide precisely the global sections of $O_{\mathbb{P}^1}(2)$ that are needed for the Veronese embedding, i.e. the embedding of $\mathbb{P}^1_{[U,V]}$ into $\mathbb{P}^2$ as a conic

$$[U:V] \longmapsto [U^2 : UV : V^2] \,. \tag{3.39}$$

In contrast, the preimage of $\rho_{\lambda_1'}$ consists of the two divisors $\lambda_1 = 0$ and $\mu = 0$. In this case the Stanley-Reisner ideal forbids the vanishing of the coordinates V, λ_2 and U, λ_2 respectively. Taking again into account the scaling relations (3.32), one observes that the pre-image of the divisor $\lambda_1' = 0$ consists of two $\mathbb{P}^1$'s that are given by

$$D_{\lambda_1} = [U:0:\mu:1:1], \qquad D_{\mu} = [1:\lambda_1:0:V:1] \,. \tag{3.40}$$

These intersect in precisely one point given by $[1:0:0:1:1]$. One identifies the dual facets of ρ_{λ_1} and ρ_{μ} as $m_4 = -1$ and $m_4 = m_3 - 1$. In this case the global sections are given by

$$s_{\lambda_1} := s_i^3 U + s_i^6 \mu \,, \qquad s_{\mu} := s_i^1 \lambda_1 + s_i^3 V \,, \tag{3.41}$$

as follows again from (3.34). This induces in this case only the trivial embedding via the identity map. Note that the union of the two divisors D_{λ_1} and D_{μ} is given by a degenerate conic

$$z_1 z_3 = z_2^2 \lambda_1 \mu \,, \qquad \text{with} \qquad (V^2\mu, UV, U^2\lambda_1) \mapsto [z_1 : z_2 : z_3] \in \mathbb{P}^2 \,, \tag{3.42}$$

which splits as just observed into the two lines $z_1 = 0$, $z_3 = 0$ at $\lambda_1 = 0$ and $\mu = 0$.

A similar reasoning applies to the pre-image of $\rho_{\lambda_1'}$ under the composite map f. As

noted above, we have $f^{-1}(\rho_{\lambda_1'}) = \{\rho_\mu, \rho_{\lambda_1}\}$, which implies that the pre-image is given by the two divisors $\mathbb{P}_{\Sigma_3^+} = \{\mu = 0\}$ and $\mathbb{P}_{\Sigma_3^-} = \{\lambda_1 = 0\}$ in $\mathbb{P}_{\Sigma_4}$. They are obtained as the star of ρ_μ and ρ_{λ_1} in Δ_4^0, respectively, with their fans $\Sigma_3^\pm$ induced by Σ_4. The corresponding respective dual facets are given by the three-dimensional facets $m_4 = -1$ and $m_4 = m_3 - 1$ in Δ_4. In addition, this gives rise to a splitting of Δ_3 as

$$\Delta_3^+ = \left\{(m_1, m_2, m_3) \in \mathbb{Z}^3 \,|\, (m_1, m_2) \in \Delta_2,\ m_3 \in \{0, 1\}\right\}, \tag{3.43}$$

$$\Delta_3^- = \left\{(m_1, m_2, m_3) \in \mathbb{Z}^3 \,|\, (m_1, m_2) \in \Delta_2,\ m_3 \in \{-1, 0\}\right\}, \tag{3.44}$$

which is also referred to as the top and bottom splitting [142], c.f. Figure 3.2. Thus, the section of the anti-canonical bundle $\mathcal{O}(-K_{\mathbb{P}_{\Sigma_3}})$ in (3.27) in the limit becomes the sum of

$$\begin{aligned} \chi_{X_2^+} &:= s_i^+ \eta^i, \qquad \text{with} \qquad s_i^+ = {s^+}_i^0 V + {s^+}_i^1 \lambda_1, \\ \chi_{X_2^-} &:= s_i^- \eta^i, \qquad \text{with} \qquad s_i^- = {s^-}_i^0 U + {s^-}_i^1 \mu, \end{aligned} \tag{3.45}$$

so that we can define the two surfaces $X_2^\pm$ as

$$X_2^+ = X_2|_{\mathbb{P}_{\Sigma_3^+}} = \Big\{\chi = \mu = 0\Big\}, \qquad X_2^- = X_2|_{\mathbb{P}_{\Sigma_3^-}} = \Big\{\chi = \lambda_1 = 0\Big\}. \tag{3.46}$$

As we will prove in the next subsection, X_2^+ and X_2^- are two rational elliptic surfaces (half K3 surfaces).

In contrast, the pre-image of $\rho_{\lambda_2'}$ is given by the whole three-dimensional fan Σ_3 as it is also for a generic point in $\mathbb{P}^1_{[\lambda_1:\lambda_2]}$. To justify the latter statement inspect the fiber above the origin 0 of the fan $\Sigma_{\mathbb{P}^1}$ corresponding to a generic point in $\mathbb{P}^1_{[\lambda_1:\lambda_2]}$.

Finally, we remark that the two rational elliptic surfaces X_2^+, X_2^- that arise at the loci $\{\mu = 0\}$ and $\{\mu = 0\}$, respectively, are independent of the K3 surface which appears over the locus $\{\lambda_2 = 0\}$. In the following, we explain how the half K3 surfaces can be obtained

from the data of the K3 surface X_2 directly. As the notation used so far is rather heavy, which is unfortunately necessary, we introduce a slightly easier notation that will be used in the discussion of explicit examples in section 3.4. We rewrite a general hypersurface constraint as

$$\chi = s_i \eta^i, \qquad s_i = s^0_{i1} U^2 + s^1_{i2} UV + s^2_{i3} V^2 , \tag{3.47}$$

which requires, depending on the situation at hand, the following identifications between the coefficients of (3.47) and of (3.34):

$$\begin{aligned} & s_{i1} \equiv s^2_i , \qquad s_{i2} \equiv s^5_i , \qquad s_{i3} \equiv s^8_i , \\ \text{or} \qquad & s_{i1} \equiv s^1_i , \qquad s_{i2} \equiv s^3_i , \qquad s_{i3} \equiv s^6_i . \end{aligned} \tag{3.48}$$

However, it is crucial to note that the pair of coordinates U, V is only suited to describe the base $\mathbb{P}^1$ of the K3 surface X_2, while the base coordinates $\mathbb{P}^1$'s of X_2^+ and X_2^- are given by λ_1, V and U, μ, respectively.

3.3.4 Computing the canonical classes of the half K3 surfaces $X_2^\pm$

In this subsection, we discuss how the half K3 surfaces $X_2^\pm$ can be re-discovered in the toric stable degeneration limit. Note that the two components $\mathbb{P}_{\Sigma_3^+}$ and $\mathbb{P}_{\Sigma_3^-}$ of the degenerate fiber, as divisors in $\mathbb{P}_{\Sigma_4}$, should equal the generic fiber $\mathbb{P}_{\Sigma_3}$:

$$\mathbb{P}_{\Sigma_3^+} + \mathbb{P}_{\Sigma_3^-} \cong \mathbb{P}_{\Sigma_3} . \tag{3.49}$$

In addition, we have

$$\mathbb{P}_{\Sigma_3} \cdot \mathbb{P}_{\Sigma_3^\pm} = 0 \tag{3.50}$$

as the generic fiber can be moved away from the locus $\lambda_1' = 0$, cf. Figure 3.3. This allows us to compute the canonical bundle of $\mathbb{P}_{\Sigma_3^\pm}$ using adjunction in $\mathbb{P}_{\Sigma_4}$ as

$$K_{\mathbb{P}^\pm_{\Sigma_3}} = \left(K_{\mathbb{P}_{\Sigma_4}} \otimes \mathcal{O}_{\mathbb{P}_{\Sigma_4}}(\mathbb{P}_{\Sigma_3^\pm})\right)\Big|_{\mathbb{P}^\pm_{\Sigma_3}} = K_{\mathbb{P}_{\Sigma_4}}\Big|_{\mathbb{P}^\pm_{\Sigma_3}} \otimes \mathcal{O}_{\mathbb{P}^\pm_{\Sigma_3}}\left(-\mathbb{P}_{\Sigma_3^\pm}\cdot\mathbb{P}_{\Sigma_3^\mp}\right), \tag{3.51}$$

where we used (3.49) and (3.50). Note that the divisor corresponding to the last term equals the class of the ambient space $\mathbb{P}_{\Sigma_2}$ of elliptic fiber of X_2, i.e. $\mathbb{P}_{\Sigma_3^+}\cdot\mathbb{P}_{\Sigma_3^-} = \mathbb{P}_{\Sigma_2}$. Making one more time use of the adjunction formula, one finally arrives at

$$\begin{aligned} K_{X_2^\pm} &= \left(K_{\mathbb{P}_{\Sigma_3^\pm}} \otimes \mathcal{O}_{\mathbb{P}_{\Sigma_3^\pm}}(X_2^\pm)\right)\Big|_{X_2^\pm} = \left(K_{\mathbb{P}_{\Sigma_4}}\Big|_{\mathbb{P}^\pm_{\Sigma_3}} \otimes \mathcal{O}_{\mathbb{P}^\pm_{\Sigma_3}}\left(-\mathbb{P}_{\Sigma_2}\right) \otimes \mathcal{O}_{\mathbb{P}_{\Sigma_3^\pm}}(X_2^\pm)\right)\Big|_{X_2^\pm} \\ &= \mathcal{O}_{\mathbb{P}^\pm_{\Sigma_3}}\left(-\mathbb{P}_{\Sigma_2}\right)\Big|_{X^\pm} = \mathcal{O}_{X_2^\pm}\left(-\mathcal{E}\right), \end{aligned}$$

where we used (3.51) in the second equality and $K_{\mathbb{P}_{\Sigma_4}}|_{\mathbb{P}^\pm_{\Sigma_3}} = \mathcal{O}_{\mathbb{P}_{\Sigma_3^\pm}}(X_2^\pm)$. Thus, the anti-canonical class of $X_2^\pm$ is given by that of the elliptic fiber E which leads to the conclusion that $X_2^\pm$ is indeed a rational elliptic surface.

3.4 Examples of Heterotic/F-Theory Duals with U(1)'s

In the section, we use the tools of Section 3.3 to construct explicit elliptically fibered Calabi-Yau two- and threefolds whose stable degeneration limit is well under control. Our geometries have generically two sections, which give rise to a U(1)-factor in the corresponding F-Theory compactification. Performing the toric symplectic cut allows us to explicitly track these sections through the stable degeneration limit and to make non-trivial statements about the vector bundle data on the heterotic side in which the U(1)-factor in the effective theory is encoded. Finally, after having performed the stable degeneration limit as discussed in section 3.3.3, we split the resulting half K3 surfaces into the spectral

cover polynomial and the constraint for the heterotic elliptic curve. Then, we determine the common solutions of the latter two constraints which encode the data of a (split) spectral cover. The general geometries we consider as well as the procedure we apply their analysis is discussed in Section 3.4.1. Despite the fact that we do not determine the embedding of the structure group into E_8 directly, we are able to match the spectral cover with the resulting gauge group in all cases. In particular, we consider three different classes of examples. In subsection 3.4.2 we investigate a number of examples whose heterotic dual gives rise to a split spectral cover. This class of examples has generically one U(1) factor embedded into both E_8-bundles of which only a linear combination is massless. The next class of examples considered in subsection 3.4.3 displays torsional points in its spectral cover. There is one example with a U(1)-factor on the F-theory side which is found to be only embedded into one E_8-bundle while the other E_8-bundle is kept intact. Finally, in the last subsection 3.4.4 we consider an example where the structure group reads SU(2) $\times$ SU(3). However, we argue that it is embedded in such a way that its centralizer necessarily contains a U(1) factor.

3.4.1 The geometrical set-up: toric hypersurfaces in $\mathbb{P}^1 \times \mathbf{Bl}_1\mathbb{P}^{(1,1,2)}$

For convenience, we recall the three-dimensional polyhedron Δ_3° for the resolved toric ambient space $\mathbb{P}_{\Sigma_3} = \mathbb{P}^1 \times \mathrm{Bl}_1\mathbb{P}^{(1,1,2)}$. It is given by the points

$$\left(\begin{array}{ccc|c} -1 & 1 & 0 & x_1 \\ -1 & -1 & 0 & x_2 \\ 1 & 0 & 0 & x_3 \\ 0 & 1 & 0 & x_4 \\ -1 & 0 & 0 & x_5 \\ 0 & 0 & 1 & U \\ 0 & 0 & -1 & V \end{array}\right). \tag{3.52}$$

Here, $x_1, \ldots x_5$ are homogeneous coordinates on the resolved variety $\mathrm{Bl}_1\mathbb{P}^{(1,1,2)}$, while U, V denote the two homogeneous coordinates of $\mathbb{P}^1$. In particular, x_5 resolves the A_1-singularity of the space $\mathrm{Bl}_1\mathbb{P}^{(1,1,2)}$.

A generic section of the anti-canonical bundle of the ambient space $\mathbb{P}_{\Sigma_3}$ takes the form

$$\begin{aligned} \chi \coloneqq\ & s_1 x_1^4 x_4^3 x_5^2 + s_2 x_1^3 x_2 x_4^2 x_5^2 + s_3 x_1^2 x_2^2 x_4 x_5 + s_4 x_1 x_2^3 x_5^2 + s_5 x_1^2 x_3 x_4^2 x_5 \\ & + s_6 x_1 x_2 x_3 x_4 x_5 + s_7 x_2^2 x_3 x_5 + s_8 x_3^2 x_4 = 0\,, \end{aligned} \tag{3.53}$$

where the coefficients s_i are homogeneous quadratic polynomials in U, V. An elliptically fibered K3 surface is defined by $X_2 = \{\chi = 0\}$. As can be seen for example its Weierstrass form, the K3 surface generically has a Kodaira fiber of type I_2 at the locus $s_8 = 0$. It is resolved by the divisor $\{x_5 = 0\} \cap X_2$ as mentioned above.[5] In addition, X_2 generically has a Mordell-Weil group of rank one. A choice of zero section S_0 and generator of the Mordell-

[5] As the details of the resolution are not important, we can set $x_5 = 1$ in most computations performed here.

Weil group S_1 are given by

$$S_0 = X_2 \cap \{x_1 = 0\}, \qquad S_1 = X_2 \cap \{x_4 = 0\}\,. \tag{3.54}$$

Explicitly, their coordinates read

$$S_0 = \begin{cases} [0:1:1:s_7:-s_8] & \text{generically}\,, \\ [0:1:1:0:1] & \text{if } s_7 = 0\,, \\ [0:1:1:1:0] & \text{if } s_8 = 0\,, \end{cases} \qquad S_1 = \begin{cases} [s_7:1:-s_4:0:1] & \text{generically}\,, \\ [0:1:1:0:1] & \text{if } s_7 = 0\,, \\ [1:1:0:0:1] & \text{if } s_4 = 0\,. \end{cases} \tag{3.55}$$

Here we distinguished the special cases with $s_7 = 0$ and $s_8 = 0$, respectively, from the generic situation. Using the fact that the generic K3 surface X_2 has $h^{(1,1)} = 5$ [182], we, hence, conclude that the full F-theory gauge group G_{X_2} is[6]

$$G_{X_2} = \mathrm{SU}(2) \times \mathrm{SU}(2) \times \mathrm{U}(1)\,. \tag{3.56}$$

We note that if $s_7 = 0$, one observes that the two sections coincide, as was also employed in [184]. That the converse is true is shown in Appendix 3.8. This is expected as the vanishing of s_7 can be interpreted as a change of the toric fibre ambient space from $\mathrm{Bl}_1\mathbb{P}^{(1,1,2)}$ to $\mathbb{P}^{(1,2,3)}$, which has a purely non-Abelian gauge group [162].

[6]We note that $s_8 = 0$ has two solutions on $\mathbb{P}^1$. If we consider higher dimensional bases of the elliptic fibration, we will just have one SU(2) factor as $s_8 = 0$ is in general an irreducible divisor.

Engineering gauge symmetry: specialized sections of $-K_{\mathbb{P}^1 \times \mathbf{Bl}_1 \mathbb{P}^{(1,1,2)}}$

In order to construct examples with higher rank gauge groups, we tune the coefficients of χ^{sing} further. To be concrete, every s_i in (3.53) takes the form

$$s_i = s_{i1}U^2 + s_{i2}UV + s_{i3}V^2 \tag{3.57}$$

and a specialization corresponds to the identical vanishing of some s_{ij}. This specialization of coefficients implies that Δ, the dual polyhedron of $\mathbb{P}^1 \times \text{Bl}_1\mathbb{P}^{(1,1,2)}$, gets replaced by the Newton polytope $\Delta_{\text{spec.}}$ of the specialized constraint,compare also Figure 3.5. As a technical side-remark we note that we strictly speaking refer with $\Delta_{\text{spec.}}$ to the convex hull of the points defined by the non-vanishing monomials in (3.57) respectively (3.53). As a consequence, also Δ° changes to the dual of $\Delta^\circ_{\text{spec.}}$. Thus, we have secretly changed the toric ambient space by this specialization of coefficients. It is crucial to note that only those polyhedra $\Delta_{\text{spec.}}$ give rise to consistent geometries which are reflexive.

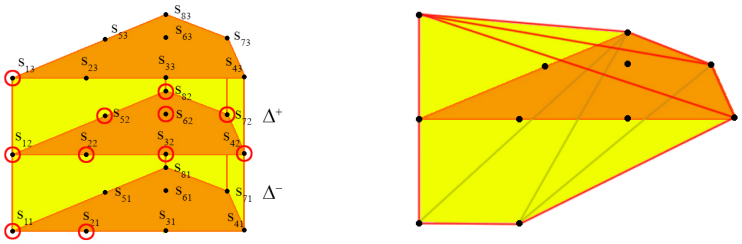

Figure 3.5: This figure illustrates a specialization of the coefficients of the hypersurface $\chi = 0$ such that the resulting gauge group is enhanced to $E_7 \times E_6 \times U(1)$, see also the discussion in Section 3.4.2. In the left picture, the non-vanishing coefficients are marked by a circle in the polytope Δ_3. In the right figure the new polytope, i.e. the Newton polytope of the specialized constraint $\chi = 0$, is shown.

In order to determine the gauge group of this specialized hypersuface, we need to transform $\chi = 0$ into its corresponding model into Tate or Weierstrass normal form. For conve-

nience, we provide the Weierstrass as well as the Tate form of the most general hypersurface in Appendix 3.6.

Stable degeneration and the spectral cover polynomial

As a next step, we show how the K3 surface X_2 defined via (3.53) can be decomposed into the two half K3 surfaces $X_2^{\pm}$ and the heterotic elliptic curve as well as the two spectral cover polynomials, respectively. First, we write the Calabi-Yau hypersurface equation (3.54) for X_2 as

$$\chi = p^+(x_i, s_{j1})U^2 + p_0(x_i, s_{j2})UV + p^-(x_i, s_{j3})V^2, \tag{3.58}$$

for appropriate polynomials p^+, p_0 and p^- depending on the fiber coordinates. By the results of the previous section, the K3 surface X_2 in the semistable degeneration limit can be described by the half K3 surfaces $X_2^{\pm}$ with defining equations

$$X_2^+ : \quad p^+(x_i, s_{j1})U + p_0(x_i, s_{j2})V = 0, \qquad X_2^- : \quad p^-(x_i, s_{j3})V + p_0(x_i, s_{j2})U = 0\,. \tag{3.59}$$

It follows that generically the two linearly independent sections (3.55) of the K3 become independent sections in the half K3s, which we denote, by abuse of notation, by the same symbols. They intersects along the common (heterotic) elliptic curve. This is a novel property of our toric degeneration.

In addition, the heterotic elliptic curve is given as $p_0(x_i, s_j) = 0$ while the data of the two background bundles are given by the spectral cover polynomials $p^+(x_i, s_{j1}) = 0$ and $p^-(x_i, s_{j3}) = 0$. The structure group of the two heterotic bundles is then determined by the common solutions of $p_0(x_i, s_j) = 0$ with $p^{\pm}(x_i, s_{j1/3}) = 0$ using the results and techniques from Section 3.2.2.

Promotion to elliptically fibered threefolds

Eventually, we are interested in examples of six-dimensional heterotic/F-Theory duality. In order to promote the K3 surfaces X_2 constructed above to elliptically fibered threefolds we promote the coefficients s_{ij}, defined in (3.57), to sections of a line bundle of another $\mathbb{P}^1$ with homogeneous coordinates R, T. The base of the previously considered K3 surface and the new $\mathbb{P}^1$ form a Hirzebruch surface $\mathbb{F}_n$. At this point, we only consider base geometries which are Fano and restrict our discussion to $\mathbb{F}_0$ and $\mathbb{F}_1$ for simplicity, avoiding additional singularities in the heterotic elliptic fibration. For these two geometries, the explicit form of the s_{ij} reads

$$s_{ij} = s_{ij1}R^2 + s_{ij2}RT + s_{ij3}T^2\,, \tag{3.60}$$

for $\mathbb{F}_0$ and

$$s_i = s_{i11}R + s_{i12}T + s_{i21}R^2 + s_{i22}RT + s_{i23}T^2 + s_{i31}R^3 + s_{i32}R^2T + s_{i33}RT^2 + s_{i34}T^3\,, \tag{3.61}$$

for the geometry $\mathbb{F}_1$.

Next, we observe that the explicit expression of the discriminant of the heterotic Calabi-Yau manifold Z_n, which is given by $p_0 = 0$, contains a factor of s_{82}^2. While this is certainly not a problem in eight dimensions, as s_{82} is just a constant there, it gives rise to an SU(2)-singularity at co-dimension one in the heterotic K3 surface Z_2. This can be cured by a resolution of this singularity through an exceptional divisor E, which is the analog of x_5 in (3.52). In particular, the solutions to the spectral cover constraint will pass through the singular point in the fiber. Thus, one expects that the spectral cover curve will pick up contributions from the class E in general. A similar situation has been analyzed in [185] where it has been argued that the introduction of this exceptional divisor will not change the structure of the spectral cover as an N-sheeted branched cover of the base except for a finite

number of points where it wraps a whole new fiber component over the base. As discussed in [185], this introduces more freedom in the construction of the heterotic vector bundle V. As this work focuses on the mapping of $\mathrm{U}(1)$-factors under the heterotic/F-theory duality, we only concentrate on the generic structure of the spectral cover and leave the resolution of this singularity as well as an exploration of the freedom in the construction of V to future works.

3.4.2 $\mathrm{U}(1)$'s arising from $\mathrm{U}(1)$ factors in the heterotic structure group

In this section, we consider examples that have an additional rational section in the dual heterotic geometry. We consider K3 surfaces in F-theory, which are given as hypersurfaces in $\mathrm{Bl}_1\mathbb{P}^{(1,1,2)} \times \mathbb{P}^1$ with appropriately specialized coefficients generating a corresponding gauge symmetry. Elliptic K3 fibered Calabi-Yau threefolds are constructed straightforwardly as described in section 3.4.1. Thus, our following discussion will be equally valid in six dimensions, although, in order to avoid confusion, we present our geometric discussions in eight dimensions. Having this in mind we, therefore, drop here in the rest of this work the subscripts on all considered manifolds X_{n+1}, $X^{\pm}_{n+1}$ and Z_n, respectively, . In the following, we discuss the main geometric properties of the Calabi-Yau manifold X, demonstrate heterotic/F-theory duality and relations among different examples by a chain of Higgsings.

We begin by a summary of key results and by setting some notation. As we will see, all considered examples have the same heterotic Calabi-Yau manifold Z in common. It is given by the most generic section of the anti-canonical bundle in $\mathrm{Bl}_1\mathbb{P}^{(1,1,2)}$ reading

$$Z: \; s_{12}x_1^4 + s_{22}x_1^3x_2 + s_{32}x_1^2x_2^2 + s_{42}x_1x_2^3 + s_{52}x_1^2x_3 + s_{62}x_1x_2x_3 + s_{72}x_2^2x_3 + s_{82}x_3^2 = 0\,. \quad (3.62)$$

The examples considered here only differ among each other by the spectral covers, i.e. by

the choice of the coefficients s_{i1} and s_{i3} in (3.47), which will be different in each case. Generically, all examples will have a U(1)-factor embedded into the structure groups of both heterotic vector bundles V_1, V_2. Thus, the maximal non-Abelian gauge group determining any chain of Higgsings is given by $\mathrm{E}_7 \times \mathrm{E}_7$. For later reference we also note the Weierstrass normal form of (3.62) is given by

$$\begin{aligned} W_Z:\ y^2 \;=\;& x^3 + \Big(-\frac{1}{48}s_{62}^4 + \frac{1}{6}s_{52}s_{62}^2s_{72} - \frac{1}{3}s_{52}^2s_{72}^2 - \frac{1}{2}s_{42}s_{52}s_{62}s_{82} + \frac{1}{6}s_{32}s_{62}^2s_{82} \\ &+ \frac{1}{3}s_{32}s_{52}s_{72}s_{82} - \frac{1}{2}s_{22}s_{62}s_{72}s_{82} + s_{21}s_{72}^2s_{82} - \frac{1}{3}s_{32}^2s_{82}^2 + s_{22}s_{42}s_{82}^2\Big)x \\ &+ \Big(\frac{1}{864}s_{62}^6 - \frac{1}{72}s_{52}s_{62}^4s_{72} + \frac{1}{18}s_{52}^2s_{62}^2s_{72}^2 - \frac{2}{27}s_{52}^3s_{72}^3 + \frac{1}{24}s_{42}s_{52}s_{62}^3s_{82} \\ &- \frac{1}{72}s_{32}s_{62}^4s_{82} - \frac{1}{6}s_{42}s_{52}^2s_{62}s_{72}s_{82} + \frac{1}{36}s_{32}s_{52}s_{62}^2s_{72}s_{82} + \frac{1}{24}s_{22}s_{62}^3s_{72}s_{82} \\ &+ \frac{1}{9}s_{32}s_{52}^2s_{72}^2s_{82} - \frac{1}{6}s_{22}s_{52}s_{62}s_{72}^2s_{82} - \frac{1}{12}s_{21}s_{62}^2s_{72}^2s_{82} + \frac{1}{3}s_{21}s_{52}s_{72}^3s_{82} \\ &+ \frac{1}{4}s_{42}^2s_{52}^2s_{82}^2 - \frac{1}{6}s_{32}s_{42}s_{52}s_{62}s_{82}^2 + \frac{1}{18}s_{32}^2s_{62}^2s_{82}^2 - \frac{1}{12}s_{22}s_{42}s_{62}^2s_{82}^2 \\ &+ \frac{1}{9}s_{32}^2s_{52}s_{72}s_{82}^2 - \frac{1}{6}s_{22}s_{42}s_{52}s_{72}s_{82}^2 - \frac{1}{6}s_{22}s_{32}s_{62}s_{72}s_{82}^2 + s_{21}s_{42}s_{62}s_{72}s_{82}^2 \\ &+ \frac{1}{4}s_{22}^2s_{72}^2s_{82}^2 - \frac{2}{3}s_{21}s_{32}s_{72}^2s_{82}^2 - \frac{2}{27}s_{32}^3s_{82}^3 + \frac{1}{3}s_{22}s_{32}s_{42}s_{82}^3 - s_{21}s_{42}^2s_{82}^3\Big). \end{aligned} \tag{3.63}$$

Also, the two generic sections of the heterotic geometry Z, denoted by S_0^Z and S_1^Z read in Weierstrass normal form as

$$S_0^Z = [1:1:0], \tag{3.64}$$

$$\begin{aligned} S_1^Z \;=\;& \Big[\frac{1}{12}\big(s_{62}^2s_{72}^2 - 4s_{52}s_{72}^3 - 12s_{42}s_{62}s_{72}s_{82} + 8s_{32}s_{72}^2s_{82} + 12s_{42}^2s_{82}^2\big) : \frac{1}{2}s_{82}\big(s_{42}s_{62}^2s_{72}^2 \\ &- s_{42}s_{52}s_{72}^3 - s_{32}s_{62}s_{72}^3 + s_{22}s_{72}^4 - 3s_{42}^2s_{62}s_{72}s_{82} + 2s_{32}s_{42}s_{72}^2s_{82} + 2s_{42}^3s_{82}^2\big) : s_7\Big]. \end{aligned} \tag{3.65}$$

Here, the first section S_0^Z is the point at infinity, while the second section S_1^Z can be seen also

in the affine chart. We note that S_0^Z can be obtained by a simple coordinate transformation[7] from S_0 defined in (3.54), while S_1^Z needs to be constructed using the procedure of Deligne applied in [154].

Structure group $\mathbf{U}(1)\times\mathbf{U}(1)$: $\mathbf{E}_7\times\mathbf{E}_7\times\mathbf{U}(1)$ gauge symmetry

We start with a model which has a heterotic vector bundle of structure group $\mathrm{U}(1)\times\mathrm{U}(1)$. Upon commutation within the group $\mathrm{E}_8\times\mathrm{E}_8$, the centralizer is given as $\mathrm{E}_7\times\mathrm{U}(1)\times\mathrm{E}_7\times\mathrm{U}(1)$. On the heterotic side, the two U(1) factors acquire a mass term so that only a linear combination of them is massless. This matches the F-theory gauge group given by $\mathrm{E}_7\times\mathrm{E}_7\times\mathrm{U}(1)$.

Our example is specified by the following non-vanishing coefficients:

Coefficient	X	X^-	X^+
s_1	$s_{11}U^2+s_{12}UV+s_{13}V^2$	$s_{12}U+s_{13}\mu$	$s_{11}\lambda_1+s_{12}V$
s_2	$s_{22}UV$	$s_{22}U$	$s_{22}V$
s_3	$s_{32}UV$	$s_{32}U$	$s_{32}V$
s_4	$s_{42}UV$	$s_{42}U$	$s_{42}V$
s_5	$s_{52}UV$	$s_{52}U$	$s_{52}V$
s_6	$s_{62}UV$	$s_{62}U$	$s_{62}V$
s_7	$s_{72}UV$	$s_{72}U$	$s_{72}V$
s_8	$s_{82}UV$	$s_{82}U$	$s_{82}V$

Here, the first columns denotes the coefficient in the Calabi-Yau constraint (3.27), the second column indices the chosen specialization and the third as well as fourth column contain the resulting coefficient in the half K3 fibrations $X^\pm$, respectively.

Using the identities (3.41) and (3.46), we readily write down the defining equations for

[7] To be more precise, we refer in this case to (3.54) as a section of the heterotic geometry.

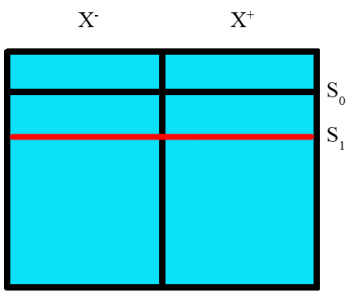

Figure 3.6: This figure shows the stable degeneration limit of a K3 surface which has $\mathrm{E}_7 \times \mathrm{E}_7 \times \mathrm{U}(1)$ gauge symmetry. There are the two half K3 surfaces, X^+ and X^- which have both an E_7 singularity and intersect in a common elliptic curve. Both have two sections, S_0 and S_1 which meet in the common elliptic curve. Thus, there are two global sections in the full K3 surface and therefore a $\mathrm{U}(1)$ factor.

the half K3 surfaces $X_2^{\pm}$ obtained via stable degeneration explicitly. They read

$$\begin{aligned} X^+ : \quad & (s_{11}\lambda_1 + s_{12}V)x_1^4 + s_{22}Vx_1^3x_2 + s_{32}Vx_1^2x_2^2 + s_{42}Vx_1x_2^3 \\ & + s_{52}Vx_1^2x_3 + s_{62}Vx_1x_2x_3 + s_{72}Vx_2^2x_3 + s_{82}Vx_3^2 = 0, \\ X^- : \quad & (s_{12}U + s_{13}\mu)x_1^4 + s_{22}Ux_1^3x_2 + s_{32}Ux_1^2x_2^2 + s_{42}Ux_1x_2^3 \\ & + s_{52}Ux_1^2x_3 + s_{62}Ux_1x_2x_3 + s_{72}Ux_2^2x_3 + s_{82}Ux_3^2 = 0. \end{aligned} \tag{3.66}$$

By explicitly evaluating the Tate coefficients (3.92), one obtains the following orders of vanishing for the Tate vector at the loci $U = 0$ and $V = 0$ for the full K3 surface,

$$\vec{t}_U = \vec{t}_V = (1,2,3,3,5,9)\,, \tag{3.67}$$

which reveal two E_7 singularities. Also, the two half K3 surfaces inherit an E_7 singularity each, which are located at $U = 0$, $V = 0$, respectively. Thus, the non-Abelian part of the gauge group is given by $\mathrm{E}_7 \times \mathrm{E}_7$. Both half K3 surfaces have two rational sections given by $S_0^{X^\pm} = [0:1:0]$ and $S_1^{X^+} = [0 : s_{82}V : -s_{72}s_{82}V^2]$ and $S_1^{X^-} = [0 : s_{82}U : -s_{72}s_{82}U^2]$, respectively.

In the intersection point of the two half K3's given by $[U : \lambda_1 : \mu : V : \lambda_2] = [1 : 0 : 0 : 1 : 1]$, the sections $S_0^{X^\pm}$ from both half K3's intersect and meet each other, and similarly the sections $S_1^{X^\pm}$ from both half K3's intersect and meet each other, cf. Figure 3.6. Thus, the six-dimensional gauge group contains a $\mathrm{U}(1)$ factor.

However, if one evaluates the spectral cover, as described in section 3.4.1, one obtains[8]

$$p_+ = s_{11} x_1^4, \qquad p_- = s_{13} x_1^4 . \tag{3.68}$$

which is mapped by use of the transformations (3.98) onto

$$p_+^W = s_{11} z^4, \qquad p_-^W = s_{13} z^4 . \tag{3.69}$$

These expressions gives rise to a constant spectral cover in affine Weierstrass coordinates x, y defined by $z = 1$. However, on an elliptic curve there does not exist any function which has exactly one zero at a single point, in this case S_1.[9] Nevertheless, one can use the two points S_0^Z and S_1^Z on the heterotic elliptic curve in order to construct the bundle $\mathcal{L} = \mathcal{O}(S_1^Z - S_0^Z)$ fiberwise, which is symmetrically embedded into both E_8-bundles. As argued in [179], this bundle promotes to a bundle $\mathcal{L}^{6d}$ in six dimensions whose first Chern class is given by the difference of the two sections $c_1(\mathcal{L}^{6d}) = \sigma_{S_1^Z} - \sigma_{S_0^Z}$, up to fiber contributions. Thus, the heterotic gauge group is given by $\mathrm{E}_7 \times \mathrm{E}_7 \times \mathrm{U}(1) \times \mathrm{U}(1)$. Due to the background bundle $\mathcal{L}^{6d}$, these two $\mathrm{U}(1)$'s seem both massive according to the Stückelberg mechanism discussed in Section 3.2.4. However, due to the symmetric embedding into both E_8's their sum remains massless. Thus, one obtains a perfect match with the F-theory gauge group.

We conclude with the remark that one can interpret this model also as a Higgsing of a model with $\mathrm{E}_8 \times \mathrm{E}_8$ gauge symmetry as presented in the Appendix 3.7.1. Here, the Hig-

[8] Here, and in the following we set $x_4 \to 1$, $x_5 \to 1$ for convenience.

[9] However, note that the homogeneous expression x_1^4 vanishes indeed at the loci of S_0^Z and of S_1^Z.

gsing corresponds to a geometrical transition from the ambient space geometry $\mathbb{P}^{(1:2:3)}$ to $\mathrm{Bl}_1\mathbb{P}^{(1,1,2)}$ where the vacuum expectation value of the Higgs corresponds to the non-vanishing coefficient s_{72}.

Structure group $\mathbf{S(U(2)\times U(1))}$: $\mathbf{E_7 \times E_6 \times U(1)}$ gauge symmetry

As a next step, we investigate an example which has $\mathrm{E}_7 \times \mathrm{E}_6 \times \mathrm{U}(1)$ gauge symmetry. On the heterotic side we find an $\mathrm{U}(1) \times \mathrm{SU}((2) \times \mathrm{U}(1))$ structure group which directly matches the non-Abelian gauge group and gives rise to one massless as well as one massive $\mathrm{U}(1)$. The model is specified by the following non-vanishing coefficients:

Coefficient	X	X^-	X^+
s_1	$s_{11}U^2 + s_{12}UV + s_{13}V^2$	$s_{12}U + s_{13}\mu$	$s_{11}\lambda_1 + s_{12}V$
s_2	$s_{21}U^2 + s_{22}UV$	$s_{22}U$	$s_{21}\lambda_1 + s_{22}V$
s_3	$s_{32}UV$	$s_{32}U$	$s_{32}V$
s_4	$s_{42}UV$	$s_{42}U$	$s_{42}V$
s_5	$s_{52}UV$	$s_{52}U$	$s_{52}V$
s_6	$s_{62}UV$	$s_{62}U$	$s_{62}V$
s_7	$s_{72}UV$	$s_{72}U$	$s_{72}V$
s_8	$s_{82}UV$	$s_{82}U$	$s_{82}V$

The evaluation of the order of vanishing of the Tate coefficients is summarized in the two Tate vectors

$$\vec{t}_V = (1,2,2,3,5,8) \qquad \vec{t}_U = (1,2,3,3,5,9)\,. \tag{3.70}$$

It signal one E_6 singularity at $V = 0$ and one E_7 singularity at $U = 0$. The E_7 singularity is inherited by the half K3 surface X^- while the E_6 singularity is contained in the half K3 surface X^+ after stable degeneration.

Next, we turn to the heterotic side. Here, the analysis of sections and $\mathrm{U}(1)$ symmetries

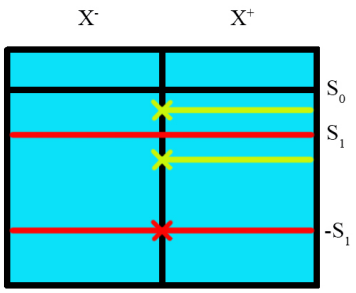

Figure 3.7: The interpretation of this figure is similar to Figure 3.6. The additional structure arises from two sections shown in yellow which form together with $\ominus S_1$ the zeros of the spectral cover.

from the perspective of the gluing condition is completely analogous to the geometry with $E_7 \times E_7 \times U(1)$ gauge symmetry discussed in the previous Section 3.4.2. The situation at hand is summarized in Figure 3.7. However, there is a crucial difference in the evaluation of the spectral cover which we discuss next.

The corresponding split of the two half K3 surfaces into a spectral cover polynomial and the heterotic elliptic curve results in

$$p^+ = s_{11}x_1^4 + s_{21}x_1^3x_2\,, \qquad p^- = s_{13}x_1^4\,. \tag{3.71}$$

Again, in order to evaluate the spectral cover information, one needs to transform both constraints into Weierstrass normal form. p^- is again just a constant and its interpretation is along the lines of the previous example in Section 3.4.2. However, in the case of p^+

something non-trivial happens. Its transform into Weierstrass coordinates reads explicitly

$$\begin{aligned} p_W^+ \;=\; & \big(s_{21}s_{62}^3 s_{72} - 4s_{21}s_{52}s_{62}s_{72}^2 - 2s_{11}s_{62}^2 s_{72}^2 + 8s_{11}s_{52}s_{72}^3 - 2s_{21}s_{42}s_{62}^2 s_{82} \\ & -4s_{21}s_{42}s_{52}s_{72}s_{82} - 4s_{21}s_{32}s_{62}s_{72}s_{82} + 24s_{11}s_{42}s_{62}s_{72}s_{82} + 12s_{21}s_{22}s_{72}^2 s_{82} \\ & -16s_{11}s_{32}s_{72}^2 s_{82} + 8s_{21}s_{32}s_{42}s_{82}^2 - 24s_{11}s_{42}^2 s_{82}^2 - 12s_{21}s_{62}s_{72}x \\ & +24s_{11}s_{72}^2 x + 24s_{21}s_{42}s_{82}x + 24s_{21}s_{72}y\big) / \big(2\big(-s_{62}^2 s_{72}^2 + 4s_{52}s_{72}^3 \\ & +12s_{42}s_{62}s_{72}s_{82} - 8s_{32}s_{72}^2 s_{82} - 12s_{42}^2 s_{82}^2 + 12s_{72}^2 x\big)\big)\,. \end{aligned} \tag{3.72}$$

In contrast to the well-known case of the spectral cover in the $\mathbb{P}^{(1,2,3)}$-model which takes only poles at infinity, one observes that the denominator of (3.72) has two zeros at S_1^Z and at $\ominus S_1^Z$, the negative of S_1^Z in the Mordell-Weil group of Z. In addition, the numerator has zeros at two irrational points Q_1, Q_2 and at $\ominus S_1$. Finally, there is a pole of order one at S_0^Z. Here, S_0^Z and S_1^Z refer to the two sections (3.64), (3.65). Thus, the divisor of p_W^- is given by

$$\mathrm{div}\,(p_W^+) = Q_1 + Q_2 - S_1 - S_0\,. \tag{3.73}$$

Clearly, in order to promote the points defined by the spectral cover polynomial in eight dimensions to a curve in six dimensions, the current form of p_W^- is not suitable due to its non-trivial denominator. However, one observes that the polynomial given by the numerator of p_W^+ gives rise to the divisor

$$\mathrm{div}\,(\mathrm{Numerator}\,(p_W^+)) = Q_1 + Q_2 + \ominus S_1 - 3S_0 \tag{3.74}$$

which is, however, linearly equivalent[10] to the divisor (3.73). Consequently, a spectral cover, valid also for the construction of lower-dimensional compactifications, is defined by

[10]To see this, one notices that the element $-S_1 + S_0$ in $\mathrm{Pic}^0(E)$ is equivalent to $-S_1 + S_0 + f$ where f is defined as $x - x_{S_1}$ on E with x_{S_1} denoting the x-coordinate of S_1. It holds that $\mathrm{div}(f) = S_1 + \ominus S_1 - 2S_0$. Thus, $-S_1 + S_0$ maps to $\ominus S_1$ on E under the map (3.12).

the numerator of (3.72).

Thus, the three zeros Q_1, Q_2 and $\boxminus S_1$ form, following Section 3.2.2, a split SU(3) spectral cover, i.e. an S(U(2)×U(1)) spectral cover. All three points extend as sections into the half K3 surface X^+, cf. Figure 3.7. Two of these sections are linearly independent and are in eight dimensions the generators of the rank two Mordell-Weil group corresponding to a rational elliptic surface with an E_6 singularity. However, due to monodromies of Q_1 and Q_2 only $\boxminus S_1$ survives in six dimensions as a rational section.

In conclusion, this spectral cover gives rise to an $S(U(2) \times U(1))$ background bundle which is embedded into the E_8 factor corresponding to X^+. The centralizer of this is given by $E_6 \times U(1)$. The latter factor seems again massive due to the $U(1)$ background bundle. However, this $U(1)$ forms together with the seemingly massive $U(1)$ of the half K3 surface X^- a massless linear combination. In conclusion, there is a perfect match with the F-theory analysis of the low energy gauge group. Analogously to the previous case in Section 3.4.2, this model can be understood as arising by Higgsing the non-Abelian model 3.7.2 with gauge symmetry $E_8 \times E_7$. Here, a (massive) $U(1)$ factor is embedded minimally into both factors. Again, the vacuum expectation value of the Higgs corresponds to the coefficient s_{72}. In addition, we can view this model also as arising by a Higgsing process from a compactification with $E_7 \times E_7 \times U(1)$ gauge group where a vacuum expectation value of the Higgs corresponds to s_{21}.

Structure group $\mathbf{SU}(2) \times \mathbf{SU}(2) \times \mathbf{U}(1)$: $\mathbf{E}_7 \times \mathbf{SO}(9) \times \mathbf{U}(1)$ gauge symmetry

The final example in this chain of Higgsings is given by a model with $E_7 \times SO(9) \times U(1)$ gauge symmetry. On the heterotic side we find an $U(1) \times (SU(2) \times SU(2) \times U(1))$ structure group which matches the non-Abelian gauge content. Also in this case we find one massless as well as one massive $U(1)$ on the heterotic side.

As before, we define the model by the following choice of coefficients in X:

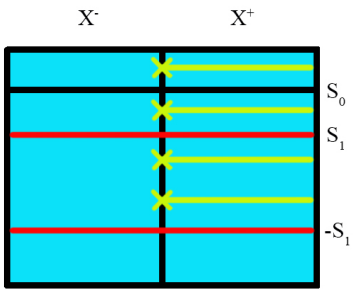

Figure 3.8: The half K3 surface X^- only exhibits the section S^1 in addition to the zero section. In contrast, X^+ gives rise to a spectral cover polynomial that has two pairs of irrational solutions Q_1, Q_2, R_1, R_2 that sum up to S_1^Z each.

Coefficient	X	X^-	X^+
s_1	$s_{11}U^2 + s_{12}UV + s_{13}V^2$	$s_{12}U + s_{13}\mu$	$s_{11}\lambda_1 + s_{12}V$
s_2	$s_{21}U^2 + s_{22}UV$	$s_{22}U$	$s_{21}\lambda_1 + s_{22}V$
s_3	$s_{31}U^2 + s_{32}UV$	$s_{32}U$	$s_{31}\lambda_1 + s_{32}V$
s_4	$s_{42}UV$	$s_{42}U$	$s_{42}V$
s_5	$s_{52}UV$	$s_{52}U$	$s_{52}V$
s_6	$s_{62}UV$	$s_{62}U$	$s_{62}V$
s_7	$s_{72}UV$	$s_{72}U$	$s_{72}V$
s_8	$s_{82}UV$	$s_{82}U$	$s_{82}V$

Once again we begin the analysis on the F-theory side with the evaluation of the order of vanishing of the Tate coefficients. We obtain the Tate vectors

$$\vec{t}_V = (1,1,2,3,4,7), \qquad \vec{t}_U = (1,2,3,3,5,9), \tag{3.75}$$

which signal one SO(9) singularity at $V = 0$ and one E_7 singularity at $U = 0$, each of which being inherited by one half K3 surface.

For the analysis of the heterotic side, we split the two half K3 surfaces into a spectral

cover polynomial and the heterotic elliptic curve. We obtain

$$p^+ = s_{11}x_1^4 + s_{21}x_1^3x_2 + s_{31}x_1^2x_2^2\,, \qquad p^- = s_{11}x_1^4\,, \tag{3.76}$$

from which we see that p^- is again a trivial spectral cover. Again, in order to evaluate the non-trivial spectral cover p^+, one needs to transform both constraints into Weierstrass normal form. The interpretation of p^+ is as in the previous cases. We again obtain a Weierstrass form p_W^+ with a denominator. The explicit expression is rather lengthy and can be provided upon request. Its divisor is given by

$$\mathrm{div}\,(p_W^+) = Q_1 + Q_2 + R_1 + R_2 - 2S_1 - 2S_0\,, \tag{3.77}$$

Here Q_1, Q_2 and R_1, R_2 are two pairs of irrational points which obey $Q_1 \boxplus Q_2 \boxminus S_1 = 0$ and $R_1 \boxplus R_2 \boxminus S_1 = 0$. The divisor of p_W^+ is again equivalent to the divisor of its numerator reading

$$\mathrm{div}\,(\mathrm{Numerator}\,(p_W^+)) = Q_1 + Q_2 + R_1 + R_2 + 2 \boxminus S_1 - 6S_0\,. \tag{3.78}$$

By a similar token as before, we thus drop the denominator and just work with the numerator of p_W^+.

All the points appearing here extend to sections of the half K3 surface X^+. However, while Q_1, Q_2, R_1, R_2 extend to rational sections of the half K3 surface they do not lift to rational sections of the fibration of the rational elliptic surface over $\mathbb{P}^1$. Altogether, we obtain as in the previous examples two rational sections in both half K3 surfaces which glue to global sections and therefore give rise to a $\mathrm{U}(1)$ factor. Besides that the spectral cover is split and describes a vector bundle with structure group $\mathrm{S}(\mathrm{U}(2)\times\mathrm{U}(1))\times\mathrm{S}(\mathrm{U}(2)\times\mathrm{U}(1))$, where the $\mathrm{U}(1)$ part in both factors needs to be identified. This is due to the fact that in both cases the same point, $\boxminus S_1^Z$, splits off. Thus, the spectral cover is isomorphic

to $\mathrm{SU}(2)\times\mathrm{SU}(2)\times\mathrm{U}(1)$ whose centralizer[11] within E_8 is given by $\mathrm{SO}(9)\times\mathrm{U}(1)$. Thus we obtain again two seemingly massive $\mathrm{U}(1)$'s which give rise to one massless linear combination.

This model can be understood by a Higgsing mechanism. Either it can be viewed as arising from the non-Abelian model in Section 3.7.3 with $\mathrm{E}_8\times\mathrm{SO}(11)$ gauge symmetry, by giving a vacuum expectation value to a Higgs corresponding to s_{72}, or from the previous example in Section 3.4.2, by giving a vacuum expectation value to a Higgs associated to s_{31}.

Example with only one massive $\mathrm{U}(1)$: $\mathbf{S}(\mathbf{U}(1)\times\mathbf{U}(1))$ structure group

Finally, we conclude the list of examples with a model which has only one $\mathrm{U}(1)$-bundle embedded into one of its E_8 factors while the other E_8 stays untouched. Accordingly there is only one massive $\mathrm{U}(1)$ symmetry. On the F-theory side we obtain an $\mathrm{E}_8\times\mathrm{E}_6\times\mathrm{SU}(2)$ gauge symmetry which matches the findings on the heterotic side.

The model is defined by the following specialization of the coefficients in the constraint (3.53):

Coefficient	X	X^-	X^+
s_1	$s_{13}V^2$	$s_{13}\mu$	0
s_2	$s_{22}UV$	$s_{22}U$	$s_{22}V$
s_3	$s_{32}UV$	$s_{32}U$	$s_{32}V$
s_4	$s_{41}U^2+s_{42}UV$	$s_{42}U$	$s_{42}V+s_{41}\lambda_1$
s_5	$s_{52}UV$	$s_{52}U$	$s_{52}V$
s_6	$s_{62}UV$	$s_{62}U$	$s_{62}V$
s_7	0	0	0
s_8	$s_{82}UV$	$s_{82}U$	$s_{82}V$

[11] We employ here the breaking $\mathrm{E}_8\longrightarrow\mathrm{SO}(9)\times\mathrm{SU}(2)\times\mathrm{SU}(2)\times\mathrm{SU}(2)$.

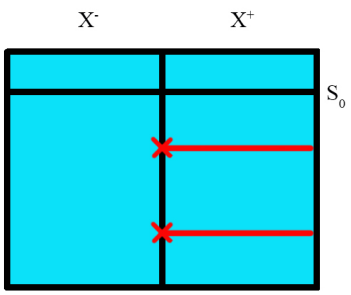

Figure 3.9: The half K3 surface X^- has only one section $S_0^{X^-}$ which merges with the section $S_0^{X^+}$ from the other half K3 surface X^+. X^+ has in addition also the section S^{X^+} which does not merge with a section of X^-. Thus, there is no U(1)-factor on the F-theory side.

First of all, we note that the coefficient s_7 vanishes identically. Thus, we have changed the ambient space of the fiber from $\mathrm{Bl}_1\mathbb{P}^{(1,1,2)}$ to $\mathbb{P}^{(1,2,3)}$. Therefore, we do not expect to see another section besides the zero section on the F-theory side and therefore no $\mathrm{U}(1)$, cf. Appendix 3.8.

First, we determine the gauge group on the F-theory. As before, we evaluate the Tate coefficients along the singular fibers which are in the case at hand located at $U = 0$, $V = 0$ and $s_{41}U + s_{42}V = 0$. One obtains the Tate vectors

$$\vec{t}_U = (1,2,3,4,5,10)\,, \qquad \vec{t}_V = (1,2,2,3,5,8)\,, \qquad \vec{t}_{s_{41}U+s_{42}V} = (0,0,1,1,2,2)\,. \tag{3.79}$$

Clearly, these signal an $\mathrm{E}_8 \times \mathrm{E}_6 \times \mathrm{SU}(2)$ gauge group in F-Theory. Also, after the stable degeneration limit, one obtains one half K3 surface X^- with an E_8 singularity and one, X^+, with an $\mathrm{E}_6 \times \mathrm{SU}(2)$ singularity.

For the further analysis we remark that there is the zero section $S_0 = [0:1:0]$ in the K3 surface only. Here and in the following, we refer to the $\mathbb{P}^{(1,1,2)}$ coordinates $[x_1 : x_2 : x_3]$ only, i.e. we work in the limit $x_4 \to 1$, $x_5 \to 1$. For the two half K3s one finds that X^- has only a zero section. In contrast, one observes the sections[12] $S^{X^+} = [1:0:0]$ and $\boxminus S^{X^+} =$

[12] Clearly, as the rank of the Mordell Weil group of X^+ is positive, there are in fact infinitely many sections.

$[s_{82}V : 0 : -s_{52}s_{82}V^2]$ in the other half K3 surface X^+. However, these sections do not glue with another section of X^- and therefore do not give rise to a $\mathrm{U}(1)$ symmetry from the F-theory perspective. However, from the heterotic perspective they should give rise to a *massive* $\mathrm{U}(1)$ which upon commutation within E_8 leaves an $\mathrm{E}_6 \times \mathrm{SU}(2)$ gauge symmetry.

This result is in agreement with the spectral cover analysis. One evaluates the spectral cover polynomials as

$$p^- = s_{13}x_1^4 \qquad p^+ = s_{41}x_1x_2^3 . \tag{3.80}$$

As observed already before, the Weierstrass transform p_W^- of p_W^- does not have any common solution with the heterotic elliptic curve and therefore the E_8-symmetry does not get broken. For the half K3 surface X^+, the common solutions to p_W^+ and the heterotic elliptic curve are given in Weierstrass coordinates $[x : y : z]$ as

$$\begin{aligned} S_W^Z &= \left[\frac{1}{12}(s_{62}^2 - 4s_{32}s_{82}) : -\frac{1}{2}s_{42}s_{52}s_{82} : 1\right], \\ \boxminus S_W^Z &= \left[\frac{1}{12}(s_{62}^2 - 4s_{32}s_{82}) : \frac{1}{2}s_{42}s_{52}s_{82} : 1\right]. \end{aligned} \tag{3.81}$$

Here, S_W^Z and $\boxminus S_W^Z$ denote the intersections of S^{X^+} and $\boxminus S^{X^+}$ with the heterotic geometry Z respectively, in Weierstrass coordinates. Thus, we observe a split spectral cover pointing towards the structure group $S(\mathrm{U}(1) \times \mathrm{U}(1))$. Using the breaking $\mathrm{E}_8 \longrightarrow \mathrm{E}_6 \times \mathrm{SU}(2) \times \mathrm{U}(1)$, this spectral cover matches with the observed gauge group. The U(1) is decoupled from the massless spectrum via the Stückelberg effect of Section 3.2.4.

3.4.3 Split spectral covers with torsional points

In the following, we discuss examples which exhibit a torsional section in their spectral covers. As mentioned before, heterotic/F-theory duality suggests that the structure group of the heterotic vector bundle should contain a discrete part.

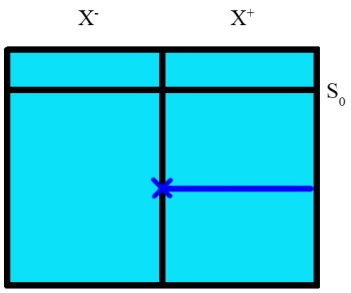

Figure 3.10: The stable degeneration limit of a K3 surface with $\mathrm{E}_8 \times (\mathrm{E}_7 \times \mathrm{SU}(2))/\mathbb{Z}_2$. The half K3 surface X^- has trivial Mordell-Weil group, while the half K3 surface X^+ has a torsional Mordell-Weil group $\mathbb{Z}_2$.

Structure group $\mathbb{Z}_2$: $\mathbf{E}_8 \times \mathbf{E}_7 \times \mathbf{SU}(2)$ gauge symmetry

We consider a model which arises by the following specialization of coefficients in (3.53):

Coefficient	X	X^-	X^+
s_1	$s_{13}V^2$	$s_{13}\mu$	0
s_2	$s_{22}UV$	$s_{22}U$	$s_{22}V$
s_3	$s_{32}UV$	$s_{32}U$	$s_{32}V$
s_4	$s_{41}U^2 + s_{42}UV$	$s_{42}U$	$s_{42}V + s_{41}\lambda_1$
s_5	0	0	0
s_6	$s_{62}UV$	$s_{62}U$	$s_{62}V$
s_7	0	0	0
s_8	$s_{82}UV$	$s_{82}U$	$s_{82}V$

We start the analysis with the gauge group on the F-theory side first. There are three singular loci of the fibration at $U = 0$, $V = 0$ and $s_{41}U + s_{42}V$. The evaluation of the Tate coefficients reveals the Tate vectors

$$\vec{t}_U = (1,2,\infty,4,5,10)\,, \qquad t_V = (1,2,\infty,3,5,9)\,, \qquad \vec{t}_{s_{41}U+s_{42}V} = (0,0,\infty,1,2,2)\,. \quad (3.82)$$

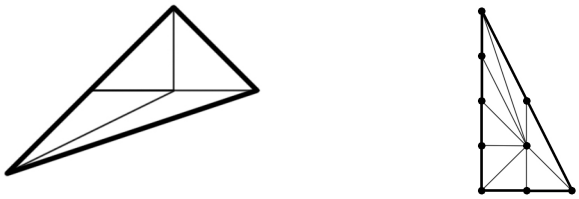

Figure 3.11: The left picture shows the specialized two-dimensional polytope Δ_2 corresponding to the half K3 surface X^+. The right figure shows its dual, Δ_2°, which specifies the ambient space of the elliptic fiber of X^+.

Thus, there are an E_8 singularity as well as an E_7 and an SU(2) singularity. The E_8 singularity is inherited by the half K3 surface X^- while X^+ gets endowed with an E_7 and an SU(2) singularity.

As a next step, we observe that there is only one section given by $[1:0:0]$ in the half K3 surface X^- and two sections given by $[x_1:x_2:x_3] = [0:1:0]$ and $[x_1:x_2:x_3] = [1:0:0]$ in the half K3 surface X^+. Here, we work again in the limit $x_4 = x_5 = 1$. In contrast, the full K3 surface has only one section namely the point at infinity. Moreover, a transformation into Weierstrass coordinates shows that the generic section $S_1^{X^+}$ has specialized into a torsional section of order two as can be checked using the results of [169]. This is expected, as the centralizer of the gauge algebra[13] $E_7 \times SU(2)$ within E_8 is given by $\mathbb{Z}_2$, which is also expected from the general analysis of [186]. In contrast, the full K3 surface X does not seem to exhibit a torsional section of order two.

Finally, we turn towards the analysis of the gauge group from the heterotic side. Here, the spectral cover is given by

$$p^- = s_{13}x_1^4, \qquad p^+ = s_{41}x_1x_2^3. \tag{3.83}$$

After transformation to Weierstrass normal coordinates p_W^- is given by a constant which

[13] To be precise, E_8 only contains the group $(E_7 \times SU(2))/\mathbb{Z}_2$ as a subgroup.

has no common solution with the elliptic curve. In contrast, the transformed quantity p_W^+ gives rise to the point

$$[x:y:z] = \left[\frac{1}{3}\left(\frac{s_{62}^2}{4} - s_{32}s_{82}\right) : 0 : 1\right]. \tag{3.84}$$

which is a torsion point of order two. In other words we see that the spectral cover is just given by a torsional point.

In [169] it has been suggested that an F-theory compactification with a torsional section in an elliptically fibered Calabi-Yau manifold and its stable degeneration limit should be dual to pointlike instantons with discrete holonomy on the heterotic side. Due to the similarity to the considered example, we propose that the spectral cover p_W^+ is to be interpreted as describing such a pointlike instanton with discrete holonomy. In addition, as pointed out above, the matching of gauge symmetry on both sides of the duality only works if the spectral cover p_W^+ is interpreted in this way. It would be important to confirm this proposal further by a more detailed analysis of the spectral cover, computation of the heterotic tadpole, or an analysis of codimension two singularities in F-theory.

Structure group S(U(2) $\times\mathbb{Z}_2$): $\mathbf{E}_8 \times \mathbf{E}_6 \times \mathbf{U}(1)$ gauge symmetry

In this section we present another example whose spectral cover polynomial containing a torsional point and leading to an $\mathrm{E}_8 \times \mathrm{E}_6 \times \mathrm{U}(1)$ gauge symmetry. As one E_8 factor is left intact, the $\mathrm{U}(1)$ factor needs to be embedded solely into one E_8 bundle.

The starting point of our analysis is the following specialization of coefficients in (3.53):

Coefficient	X	X^-	X^+
s_1	$s_{13}V^2$	$s_{13}\mu$	0
s_2	$s_{22}UV$	$s_{22}U$	$s_{22}V$
s_3	$s_{32}UV$	$s_{32}U$	$s_{32}V$
s_4	$s_{41}U^2 + s_{42}UV$	$s_{42}U$	$s_{42}V + s_{41}\lambda_1$
s_5	0	0	0
s_6	$s_{62}UV$	$s_{62}U$	$s_{62}V$
s_7	$s_{71}U^2$	0	$s_{71}\lambda_1$
s_8	$s_{82}UV$	$s_{82}U$	$s_{82}V$

As in the previous cases, we compute the orders of vanishing of the Tate coefficients in order to determine the gauge group on the F-theory side. The computed Tate vectors signal an E_8 symmetry at $U = 0$ and an E_6 symmetry at $V = 0$. As a next step, we investigate the rational sections of X. As the coefficient s_7 does not vanish for the full K3 surface, there are the two generic sections S_0, S_1 realized in this model. However, the half K3 surface X^- only has the zero section S_0. In contrast, the half K3 surface X^+ has two sections given by S_0, S_1, which unify in the heterotic elliptic curve and continue as one section into the other half K3 surface, see Figure 3.12. This behavior of rational sections explains the origin of the $\mathrm{U}(1)$-factor from the gluing condition discussed in Section 3.2.4.

As a further step, we investigate how this $\mathrm{U}(1)$ factor is reflected in the spectral cover on the heterotic side. The spectral cover polynomials computed by stable degeneration read

$$p^- = s_{13}x_1^4, \qquad p^+ = s_{41}x_1x_2^3 + s_{71}x_2^2x_3\,. \tag{3.85}$$

The interpretation of p^- is as in all the other cases just a trivial spectral cover. The common solution to p^+ and the heterotic Calabi-Yau manifold Z is given by a pair of irrational points

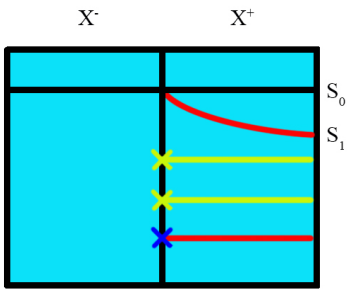

Figure 3.12: The half K3 surface X^- exhibits only the zero section, while the half K3 surface X^+ has also the section $S_1^{X^+}$ which merges with the section $S_0^{X^-}$ along the heterotic geometry. Thus there are two independent sections in the full K3 surface giving rise to a U(1) gauge group factor. In addition, the inverse of $S_1^{X^+}$ becomes a torsion point of order two when hitting the heterotic geometry.

R_1, R_2 as well as a further point T_t which has in Weierstrass normal form coordinates

$$T_t = \left[\frac{1}{3}\left(\frac{1}{4}s_{62}^2 - s_{32}s_{82}\right) : 0 : 1\right]. \tag{3.86}$$

Thus, it is a torsion point of order two. However, it does not extend as a full torsional section into the half K3 surface X^+. The corresponding section is rather the inverse of S_1.

Again we see that the split spectral cover p^+ contains a torsional section. Let us comment on the interpretation of this for the structure group of the heterotic vector bundle. Heterotic/F-theory duality implies that the low-energy effective theory contains a massless U(1)-symmetry. However, as we have seen in Section 3.2.4, a U(1) background bundle in the heterotic theory has a non-trivial field strength and thus a non-vanishing first Chern class, which would yield a massive U(1) in the effective field theory. Thus, we can not interpret the torsional component T_t to the spectral cover as a U(1) background bundle. By the arguments of Section 3.2.2 and the similarity to the setups considered in [169], it is tempting to identify this torsional component T_t as a pointlike heterotic instanton with discrete holonomy. In order to justify this statement, it would be necessary to compute

the first Chern class of a heterotic line bundle that is defined in terms of components to the cameral cover given by rational sections of the half K3 fibrations arising in stable degeneration. In [179], it has been argued that the first Chern class is given, up to vertical components, by the difference of the rational section and the zero section. If the first Chern class were completed into the Shioda map of the rational section, which we conjecture to be the case, it would be zero precisely for a torsional section [187]. Consequently, the U(1) in the commutant of E_8 would remain massless as the gauging in (3.24) would be absent. It would be important to confirm this conjecture by working out the missing vertical part in the formula for the first Chern class of a U(1) vector bundle.

3.4.4 $\mathrm{U}(1)$ factors arising from purely non-Abelian structure groups

In this final section, we present an example in which the heterotic vector bundle has only purely non-Abelian structure group, while the F-Theory gauge group analysis clearly signals a $\mathrm{U}(1)$ factor.

As in the previous cases, we start by specifying the specialization of the coefficients in the defining hypersurface equation for X:

Coefficient	X	X^-	X^+
s_1	$s_{12}UV + s_{13}V^2$	$s_{12}U + s_{13}\mu$	$s_{12}V$
s_2	$s_{22}UV$	$s_{22}U$	$s_{22}V$
s_3	$s_{32}UV$	$s_{32}U$	$s_{32}V$
s_4	$s_{42}UV$	$s_{42}U$	$s_{42}V$
s_5	$s_{52}UV$	$s_{52}U$	$s_{52}V$
s_6	$s_{62}UV$	$s_{62}U$	$s_{62}V$
s_7	$s_{71}U^2$	0	$s_{71}\lambda_1$
s_8	$s_{82}UV$	$s_{82}U$	$s_{82}V$

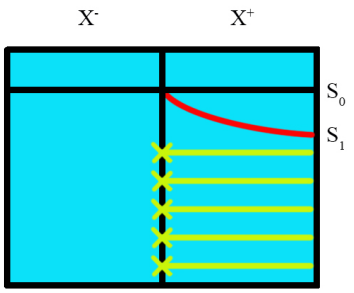

Figure 3.13: The half K3 surface X^- exhibits only the zero section, while the half K3 surface X^+ has also the section $S_1^{X^+}$ which merges with the section $S_0^{X^-}$ in the heterotic geometry. Thus, there are two independent sections in the full K3 surface giving rise to a U(1) gauge group factor.

We determine the gauge symmetry of the F-theory side by analysis of the Tate coefficients. We obtain the Tate vectors

$$\vec{t}_U = (1,2,3,4,5,10) \qquad \vec{t}_V = (1,1,2,2,4,6)\,, \tag{3.87}$$

which reveals an E_8 singularity at $U = 0$ and an SO(7) singularity at $V = 0$. We note that it is not directly possible to distinguish an SO(7) singularity from an SO(8) singularity using the Tate table 3.2 only. To confirm that the type of singularity is indeed SO(7) we have to investigate the monodromy cover [188] which is for an I_0^* fiber given by

$$A: \qquad \psi^3 + \left(\frac{f}{v^2}\bigg|_{v=0}\right)\psi + \left(\frac{g}{v^3}\bigg|_{v=0}\right). \tag{3.88}$$

Here, v is the affine coordinate V/U and f, g are the Weierstrass coefficients. An I_0^* fiber is SO(7) if the monodromy cover A factors into a quadratic and a linear constraint, which is indeed the case for the example at hand.

The stable degeneration limit yields two half K3 surfaces, X^+ and X^-, cf. Figure 3.13. There only exists the zero section in X^-. In contrast, X^+ has two sections which are given

by $S_0^{X^+}$ and $S_1^{X^+}$. As in the previously considered case in Section 3.4.3, $S_1^{X^+}$ unifies with $S_0^{X^-}$ on the heterotic elliptic curve. Thus, there are two global sections in the full K3 surface and therefore a $\mathrm{U}(1)$ factor in the F-theory compactification.

Turning towards the discussion of the heterotic gauge bundles, one finds that the $\mathrm{U}(1)$ factor is encoded in the data of the spectral cover polynomial as follows. We observe that the spectral covers following X^+ and X^-, respectively, are given by

$$p^- = s_{13}x_1^4\,, \qquad p^+ = s_{71}x_2^2x_3\,. \tag{3.89}$$

The intersection of its Weierstrass transform p_W^+ with the heterotic elliptic curve gives five irrational points R_1, R_2, T_1, T_2, T_3 with $R_1 \oplus R_2 = 0$ and $T_1 \oplus T_2 \oplus T_3 = 0$. Thus we have a heterotic vector bundle with SU(2) × SU(3). As the spectral cover p^+ has one free parameter only, namely s_{71}, this model does not seem to have any moduli.

As our understanding of the precise embedding of the structure group into E_8 is limited, we have checked all possible ways to embed the group SO(7) × SU(2) × SU(3) into E_8. Independently of the chosen embedding, there is always a $\mathrm{U}(1)$ in all possible breakings. Thus, we are led to conclude that the centralizer of SU(2) × SU(3) necessarily produces a $\mathrm{U}(1)$ factor which matches with the F-theoric analysis.

3.5 Conclusions and Future Directions

In this paper we have presented a first explicit analysis of the origin of Abelian gauge symmetries for string theory compactifications within the duality between the $\mathrm{E}_8 \times \mathrm{E}_8$ heterotic string and F-theory. Here we summarize the framework of the analysis, highlight the key advancements, and conclude with future directions.

Framework

We have focused on F-theory compactifcations with a rank one Mordell-Weil group of rational sections both for compactifications to D=8 and D=6. We have systematically studied a broad class F-theory compactifications on elliptically fibered Calabi-Yau $(n+1)$-folds (with $n = 1,2$, respectively) with rational sections and rigorously performed the stable degeneration limit to dual heterotic compactifications on elliptically fibered Calabi-Yau n-folds. All considered examples are toric hypersurfaces and the stable degeneration limit is performed as a toric symplectic cut.

The key aspects of the analysis are the following:

- We have carefully investigated the solutions of the spectral cover polynomial and the hypersurface for the heterotic elliptically fibered Calabi-Yau manifold. We have used the group law of the elliptic curve in Weierstrass normal form in order to determine the structure group of the heterotic background bundle.

- We have analyzed the origin of the resulting gauge group. In D=6 this involves incorporation of the massive $\mathrm{U}(1)$ gauge symmetries, due to the heterotic Stückelberg mechanism, that are not visible in F-theory.

Key Results

While the F-theory side provides a unifying treatment of Abelian gauge symmetries, as encoded in the Mordell-Weil group of elliptically fibered Calabi-Yau $(n+1)$-folds, a detailed analysis of a broad classes of toric F-theory compactifications has resulted in the proposal of three different classes of heterotic duals that give rise to $\mathrm{U}(1)$ gauge group factors:

- Split spectral covers describing bundles with $\mathrm{S}(\mathrm{U}(m)\times\mathrm{U}(1))$ structure group. Examples of this type have been discussed in Section 3.4.2.

- Spectral covers containing torsional sections giving rise to bundles with $\mathrm{SU}(m) \times \mathbb{Z}_n$ structure group. Classes of examples with this structure group have been presented in Section 3.4.3.

- The appearance of bundles with structure groups of the type $\mathrm{SU}(m) \times \mathrm{SU}(n)$ whose commutants inside E_8 contain a $\mathrm{U}(1)$-factor. Explicit examples of this form can be found in Section 3.4.4.

Future Directions

While the work presents a pioneering effort, addressing comprehensively the origin of Abelian gauge group factors in heterotic/F-theory duality for a class of compactifications, the analysis provides a stage for further studies, both by extending the systematics of the analysis and by further detailed studies of the dual heterotic geometry and vector bundle data.

- It would be important to extend the studies to examples within larger classes of pairs of dual toric varieties as well as of more general elliptically fibered Calabi-Yau manifolds, respectively. In particular, this would allow to account for studies of dual geometries with broader classes of complex structure moduli spaces, and thus for an analysis of more general spectral covers of dual heterotic vector bundles. In D=6 our analysis has been limited to a specific elliptically fibered Calabi-Yau $(n+1)$-folds, which has resulted in constrained appearances of non-Abelian gauge symmetries and additional $\mathrm{U}(1)$'s. In particular, it would be illuminating to elaborate on the stable degeneration limit for general toric fibrations of two-dimensional polyhedra over $\mathbb{P}^1$ in eight dimensions and, in addition, over Hirzebruch surfaces in six dimensions.

- It would be interesting to have the tools to study the spectral cover directly in the $\mathrm{Bl}_1\mathbb{P}^{(1,1,2)}$ model or more generally for fiber geometries which are given by the sixteen two-dimensioal reflexive polyhedra. This would require in particular a notion of the group law for these representations of elliptic curves.

- The study of the properties of the spectral cover was primarily confined to the derivation of the resulting gauge symmetries and the structure groups of the heterotic vector bundles. Further analysis of the spectral cover in compactifications to D=6 (and extensions to D=4) is needed; it should shed light on the further spectral cover data,

which enter Chern classes, anomaly cancellation and matter spectrum calculations. This study is complicated by the resolution of singularities of the heterotic geometry that may have to be performed, resulting in spectral covers, which are not finite [185].

- Our analysis has been primarily constrained to studies of Abelian gauge symmetries in the language of a perturbative heterotic dual. Although we have encountered spectral covers which seem to describe small instantons, i.e. non-perturbative M5-branes, with discrete holonomy, we have not systematically analyzed their effect. In F-theory, M5-branes are visible as non-minimal singularities which occur at co-dimension two loci that have to be blown up. It would be interesting to thoroughly perform this geometric analysis. We expect in addition rich structures of Abelian gauge symmetry factors in F-theory whose heterotic duals are due to other types of non-perturbative M5-branes. Furthermore, it would be interesting to study the geometric transitions between F-theory geometries with different numbers of tensor multiplets, whose discussion is again related to this resolution process.

Acknowledgments

We thank L. Anderson, R. Donagi, J. Gray, T. Grimm, A. Klemm, D. Morrison, R. Pardini, S. Schäfer-Nameki, V. Perduca and W. Taylor for useful discussions. We are grateful to the Theory Division of CERN (M.C. and M.P.), the 2015 Summer Program on "F-Theory at the interface of particle physics and mathematics" at the Aspen Center for Physics (M.C., A.G., D.K. and M. P.) and the UPenn (D.K.) for hospitality during the course of the project. This research is supported in part by the DOE Grant Award DE-SC0013528, (M.C., M.P., P.S.), UPenn School of Arts and Sciences Funds for Faculty Working Group (A.G. and M.C.), the Fay R. and Eugene L. Langberg Endowed Chair (M.C.) and the Slovenian Research Agency (ARRS) (M.C.).

3.6 Weierstrass and Tate form of the hypersurface χ^{sing}

In this appendix, we summarize the Weierstrass normal form as well as the Tate coefficients of the χ^{sing} model. For convenience, we recall the most general form of the hypersurface χ^{sing} which reads

$$\chi^{\text{sing}} := s_1 x_1^4 + s_2 x_1^3 x_2 + s_3 x_1^2 x_2^2 + s_4 x_1 x_2^3 + s_5 x_1^2 x_3 + s_6 x_1 x_2 x_3 + s_7 x_2^2 x_3 + s_8 x_3^2 = 0, \quad s_i \in \mathcal{O}_{\mathbb{P}^1}(2)\,. \tag{3.90}$$

This can be brought in the so-called Tate form

$$y^2 + a_1 xy + a_3 y = x^3 + a_2 + a_4 x + a_6\,. \tag{3.91}$$

The Tate coefficients are explicitly given as [162]

$$\begin{aligned} a_1 &= s_6\,, \\ a_2 &= -s_5 s_7 - s_3 s_8\,, \\ a_3 &= -s_4 s_5 s_8 - s_2 s_7 s_8\,, \\ a_4 &= s_3 s_5 s_7 s_8 + s_1 s_7^2 s_8 + s_2 s_4 s_8^2\,, \\ a_6 &= -s_1 s_3 s_7^2 s_8^2 - s_1 s_4^2 s_8^3 + s_4 s_7 \left(-s_2 s_5 s_8^2 + s_1 s_6 s_8^2\right). \end{aligned} \tag{3.92}$$

In addition, it is useful, to introduce the quantities

$$\begin{aligned} b_2 &= a_1^2 + 4a_2\,, \\ b_4 &= a_1 a_3 + 2a_4\,, \\ b_6 &= a_3^2 + 4a_6\,. \end{aligned} \tag{3.93}$$

The Weierstrass normal form of χ^{sing} reads

$$
\begin{aligned}
f &= \Big(-\frac{1}{48}s_{62}^4+\frac{1}{6}s_{52}s_{62}^2s_{72}-\frac{1}{3}s_{52}^2s_{72}^2-\frac{1}{2}s_{42}s_{52}s_{62}s_{82}+\frac{1}{6}s_{32}s_{62}^2s_{82}\\
&\quad+\frac{1}{3}s_{32}s_{52}s_{72}s_{82}-\frac{1}{2}s_{22}s_{62}s_{72}s_{82}+s_{21}s_{72}^2s_{82}-\frac{1}{3}s_{32}^2s_{82}^2+s_{22}s_{42}s_{82}^2\Big).\\
\\
g &= \Big(\frac{1}{864}s_{62}^6-\frac{1}{72}s_{52}s_{62}^4s_{72}+\frac{1}{18}s_{52}^2s_{62}^2s_{72}^2-\frac{2}{27}s_{52}^3s_{72}^3+\frac{1}{24}s_{42}s_{52}s_{62}^3s_{82}\\
&\quad-\frac{1}{72}s_{32}s_{62}^4s_{82}-\frac{1}{6}s_{42}s_{52}^2s_{62}s_{72}s_{82}+\frac{1}{36}s_{32}s_{52}s_{62}^2s_{72}s_{82}+\frac{1}{24}s_{22}s_{62}^3s_{72}s_{82}\\
&\quad+\frac{1}{9}s_{32}s_{52}^2s_{72}^2s_{82}-\frac{1}{6}s_{22}s_{52}s_{62}s_{72}^2s_{82}-\frac{1}{12}s_{21}s_{62}^2s_{72}^2s_{82}+\frac{1}{3}s_{21}s_{52}s_{72}^3s_{82}\\
&\quad+\frac{1}{4}s_{42}^2s_{52}^2s_{82}^2-\frac{1}{6}s_{32}s_{42}s_{52}s_{62}s_{82}^2+\frac{1}{18}s_{32}^2s_{62}^2s_{82}^2-\frac{1}{12}s_{22}s_{42}s_{62}^2s_{82}^2\\
&\quad+\frac{1}{9}s_{32}^2s_{52}s_{72}s_{82}^2-\frac{1}{6}s_{22}s_{42}s_{52}s_{72}s_{82}^2-\frac{1}{6}s_{22}s_{32}s_{62}s_{72}s_{82}^2+s_{21}s_{42}s_{62}s_{72}s_{82}^2\\
&\quad+\frac{1}{4}s_{22}^2s_{72}^2s_{82}^2-\frac{2}{3}s_{21}s_{32}s_{72}^2s_{82}^2-\frac{2}{27}s_{32}^3s_{82}^3+\frac{1}{3}s_{22}s_{32}s_{42}s_{82}^3-s_{21}s_{42}^2s_{82}^3\Big). \qquad (3.94)
\end{aligned}
$$

In particular, the discriminant reads

$$\Delta = 4f^3+27g^2 = \frac{1}{48}s_{82}^2(\dots). \qquad (3.95)$$

where the expression in the bracket denotes a generic polynomial.

3.6.1 The map to Weierstrass normal form

In this subsection we discuss the bi-rational map of (3.90) to Weierstrass normal form. As a first step, we transform (3.53) into the form

$$\tilde{s}_1x_1^4+\tilde{s}_2x_1^3x_2+\tilde{s}_3x_1^2x_2^2+\tilde{s}_4x_1x_2^3+s_7x_2^2x_3+x_3^2=0. \qquad (3.96)$$

Here, we have introduced the new quantities

$$\tilde{s}_1 = -\frac{1}{4}s_5^2 + S_0 s_8, \quad \tilde{s}_2 = -\frac{1}{2}s_5 s_6 + S_1 s_8, \quad \tilde{s}_3 = -\frac{1}{4}s_6^2 - \frac{1}{2}s_5 s_7 + s_3 s_8, \quad \tilde{s}_4 = -\frac{1}{2}s_6 s_7 + s_4 s_8 \tag{3.97}$$

Next, one uses the transformations provided in [154]

$$\begin{aligned}
x_1 &\longmapsto z \\
x_2 &\longmapsto \frac{6s_7 y + 6\tilde{s}_4 xz + 2\tilde{s}_3\tilde{s}_4 z^3 + 3\tilde{s}_2 s_7^2 z^3}{2\left(3s_7^2 x - 3\tilde{s}_4^2 z^2 - 2\tilde{s}_3 s_7^2 z^2\right)} \\
x_3 &\longmapsto \Big(108s_7^3 x^3 - 108s_7^3 y^2 - 108\tilde{s}_4 s_7^2 xyz - 216\tilde{s}_4^2 s_7 x^2 z^2 - 108\tilde{s}_3 s_7^3 x^2 z^2 - 108\tilde{s}_4^3 yz^3 \\
&\quad -144\tilde{s}_3\tilde{s}_4 s_7^2 yz^3 - 108\tilde{s}_2 s_7^4 yz^3 - 36\tilde{s}_3\tilde{s}_4^2 s_7 xz^4 - 54\tilde{s}_2\tilde{s}_4 s_7^3 xz^4 + 12\tilde{s}_3^2\tilde{s}_4^2 s_7 z^6 \\
&\quad -54\tilde{s}_2\tilde{s}_4^3 s_7 z^6 + 16\tilde{s}_3^3 s_7^3 z^6 - 72\tilde{s}_2\tilde{s}_3\tilde{s}_4 s_7^3 z^6 - 27\tilde{s}_2^2 s_7^5 z^6\Big) \Big/ \\
&\quad 12\left(3s_7^2 x - 3\tilde{s}_4^2 z^2 - 2\tilde{s}_3 s_7^2 z^2\right)^2
\end{aligned} \tag{3.98}$$

in order to finally bring (3.96) into Weierstrass normal form in $\mathbb{P}^{(1,2,3)}$. We also note that the transformations (3.98) simplify in the case $s_7 = 0$, in particular their denominators loose their dependence on x, y.

3.7 Spectral Cover Examples with no U(1)

For convenience and to demonstrate how our formalism works in a well-understood situation, we analyze several examples with pure non-Abelian gauge content only. These are related to the examples 3.4.2, 3.4.2 and 3.4.2 by a Higgsing process which gives s_{72} a vacuum expectation value.

3.7.1 Trivial structure group: $E_8 \times E_8$ gauge symmetry

As described in the previous section, we can obtain examples with higher rank gauge symmetry by specializing the coefficients of chi_{sing}. Aiming for a model with $E_8 \times E_8$ gauge symmetry, one obtains the following coefficients.

Coefficient	K3	X^-	X^+
s_1	$s_{11}U^2 + s_{12}UV + s_{13}V^2$	$s_{12}U + s_{13}\mu$	$s_{12}V + s_{11}\lambda_1$
s_2	$s_{22}UV$	$s_{22}U$	$s_{22}V$
s_3	$s_{32}UV$	$s_{32}U$	$s_{32}V$
s_4	$s_{42}UV$	$s_{42}U$	$s_{42}V$
s_5	$s_{52}UV$	$s_{52}U$	$s_{52}V$
s_6	$s_{62}UV$	$s_{62}U$	$s_{62}V$
s_7	0	0	0
s_8	$s_{82}UV$	$s_{82}U$	$s_{82}V$

Here the second row displays the coefficients of the full K3 surface while the coefficients of the two half K3 surfaces are displayed in row three and four. In particular, one notices that the coefficient s_7 is missing which means that one is passing from the toric ambient space $Bl_1\mathbb{P}^{(1,1,2)} \times \mathbb{P}^1$ to the ambient space $\mathbb{P}^{(1,2,3)} \times \mathbb{P}^1$. Clearly, a generic section of the anti-canonical bundle of $\mathbb{P}^{(1,2,3)}$ does not have a second section, so there is also no reason to expect any $\mathrm{U}(1)$.

We proceed by analyzing the F-Theory gauge group. The analysis of the Tate vectors reveals that

$$\vec{t}_U = \vec{t}_V = (1,2,3,4,5,10) \tag{3.99}$$

and thus there is an $E_8 \times E_8$ gauge symmetry. After the stable degeneration limit, both half K3 surfaces X^+ and X^- obtain one E_8 singularity each.

Finally, we turn to the Heterotic side. The splitting of the two half K3's into the Heterotic elliptic curve and the spectral cover contributions reveals that

$$p^+ = s_{11}x_1^4, \qquad p^- = s_{13}x_1^4. \tag{3.100}$$

After transforming these expression into the affine Weierstrass coordinates x, y, one obtains

$$p_W^+ = s_{11}, \qquad p_W^- = s_{13} \tag{3.101}$$

In both cases,one obtains an $\mathrm{SU}(1)$ spectral cover. However, the centralizer of the identity in E_8 is E_8 and one obtains a perfect match with the F-theory calculation.

3.7.2 Structure group SU(1) × SU(2): $\mathrm{E}_8 \times \mathrm{E}_7$ gauge symmetry

We consider the following model which is specified by the following coefficients in (3.53).

Coefficient	K3	X^-	X^+
s_1	$s_{11}U^2 + s_{12}UV + s_{13}V^2$	$s_{12}U + s_{13}\mu$	$s_{12}V + s_{11}\lambda_1$
s_2	$s_{21}U^2 + s_{22}UV$	$s_{22}U$	$s_{22}V + s_{21}\lambda_1$
s_3	$s_{32}UV$	$s_{32}U$	$s_{32}V$
s_4	$s_{42}UV$	$s_{42}U$	$s_{42}V$
s_5	$s_{52}UV$	$s_{52}U$	$s_{52}V$
s_6	$s_{62}UV$	$s_{62}U$	$s_{62}V$
s_7	0	0	0
s_8	$s_{82}UV$	$s_{82}U$	$s_{82}V$

This time, we obtain the following Tate vectors

$$\vec{t}_V = (1,2,3,3,5,9), \qquad \vec{t}_U = (1,2,3,4,5,10) \tag{3.102}$$

which signal an E_7 singularity at $V = 0$ as well as an E_8 singularity at $U = 0$. The former one is inherited by the half K3 surface X^- while the latter one moves into X^+.

The spectral cover is in this case given by

$$p^+ = x_1^3 \left(s_{11} x_1 + s_{21} x_2 \right), \qquad p^- = s_{11} x_1^4 . \tag{3.103}$$

We only comment on the non-trivial spectral cover. After applying the transformation (3.98), it reads

$$p_W^+ = c_0 + c_1 x \tag{3.104}$$

which defines an SU(2) spectral cover and is precisely what is expected. Explicitly, the a_i's read

$$c_0 = s_{21} s_{62}^2 - 4 s_{21} s_{32} s_{82} + 12 s_{11} s_{42} s_{82} \qquad c_1 = -s_{21} \tag{3.105}$$

Note that the a_i are indeed proportional to s_{11}, s_{21} which define the spectral cover. Thus, we obtain an SU(2) spectral cover in the case of X^+ and a trivial structure group for the case of X^-. In conclusion, there is a perfect match with the F-theory analysis.

3.7.3 Example with gauge group $E_8 \times SO(11)$

We consider the following model which is specified by the following coefficients in (3.53).

Coefficient	K3	X^-	X^+
s_1	$s_{11}U^2+s_{12}UV+s_{13}V^2$	$s_{12}U+s_{13}\mu$	$s_{12}V+s_{11}\lambda_1$
s_2	$s_{21}U^2+s_{22}UV$	$s_{22}U$	$s_{22}V+s_{21}\lambda_1$
s_3	$s_{31}U^2+s_{32}UV$	$s_{32}U$	$s_{32}V+s_{31}\lambda_1$
s_4	$s_{42}UV$	$s_{42}U$	$s_{42}V$
s_5	$s_{52}UV$	$s_{52}U$	$s_{52}V$
s_6	$s_{62}UV$	$s_{62}U$	$s_{62}V$
s_7	0	0	0
s_8	$s_{82}UV$	$s_{82}U$	$s_{82}V$

This time, we obtain the following Tate vectors

$$\vec{t}_V = (1,1,3,3,5,8), \qquad \vec{t}_U = (1,2,3,4,5,10) \tag{3.106}$$

which signal an SO(11) singularity at $V=0$ as well as an E_8 singularity at $U=0$. The former one is inherited by the half K3 surface X^+ while the latter one moves into X^-.

The spectral cover is in this case given by

$$p^+ = x_1^2\left(s_{11}x_1^2+s_{21}x_1x_2+s_{31}x_2^2\right), \qquad p^- = s_{11}x_1^4. \tag{3.107}$$

We only comment on the non-trivial spectral cover. After applying the transformation (3.98), it reads

$$p_W^+ = c_0+c_1x+c_2x^2 \tag{3.108}$$

which defines an $\mathrm{Sp}(2)\cong\mathrm{SO}(5)$ spectral cover[14] [139] and is precisely what is expected. Thus, we obtain an Sp(2) spectral cover in the case of X^+ and a trivial structure group for the case of X^-. The commutant of SO(5) within E_8 is given by SO(11).

[14] Sometimes, Sp(N) is denoted by Sp($2N$).

3.8 Tuned models without rational sections

In this appendix we reproduce [154, 184] the following

Lemma 10. *The two sections denoted by* $x_1 = 0$ *and* $x_4 = 0$ *in* (3.54) *merge into a single section if and only if* $s_7 = 0$ *in* (3.53). *Furthermore, the single section is given by* $[x_1 : x_2 : x_3 : x_4 : x_5] = [0 : 1 : 1 : 0 : 1]$.

Proof. Suppose the two sections $x_1 = 0$ and $x_4 = 0$ merge into a single section. Then this single section obeys both $x_1 = 0$ and $x_4 = 0$, everywhere. Thus the Stanley-Reisner ideal requires $x_2 \neq 0$, $x_3 \neq 0$ and $x_5 \neq 0$ everywhere. Making use of the skaling relations of the resolved space $\mathrm{Bl}_1\mathbb{P}^{(1,1,2)}$, one obtains that this section is indeed given by $[x_1 : x_2 : x_3 : x_4 : x_5] = [0 : 1 : 1 : 0 : 1]$.

Suppose now that $s_7 = 0$. Setting x_1 in (3.53) to zero, results in the equation $s_8 x_3^2 x_4 = 0$. As $x_3 \neq 0$ due to the Stanley Reisner ideal, x_4 has to vanish as well resulting in the merging of the two sections. Similarly, $x_4 = 0$ requires that $s_4 x_1 x_2^3 x_5^2 = 0$. The Stanley Reisner ideal requires x_2 and x_5 to be non-vanishing. Thus, there is also in this case only one section given by $[x_1 : x_2 : x_3 : x_4 : x_5] = [0 : 1 : 1 : 0 : 1]$.

□

3.9 Non-commutativity of the semi-stable degeneration limit and the map to Weierstrass form

We illustrate the non-commutativity of the diagram (3.1) using the above example with gauge group $\mathrm{E}_7 \times \mathrm{SO}(9) \times \mathrm{U}(1)$. To be precise, on the top left corner of the diagram, the section χ of $-K_{\mathbb{P}^{(1,1,2)}\times\mathbb{P}^1}$ is given by

$$\begin{aligned}
\chi: \quad & s_1 x_1^4 + s_2 x_1^3 x_2 + s_3 x_1^2 x_2^2 + s_4 x_1 x_2^3 + s_5 x_1^2 x_3 + s_6 x_1 x_2 x_3 + s_7 x_2^2 x_3 + s_8 x_3^2 = 0\,, \\
\text{where} \quad & s_1 = s_{11} U^2 + s_{12} UV + s_{13} V^2\,, \quad s_i = s_{i1} U^2 + s_{i2} UV \text{ for } 2 \le i \le 3\,, \\
& s_i = s_{i2} UV \text{ for } 4 \le i \le 8\,. \qquad (3.109)
\end{aligned}$$

Under the stable degeneration limit, denoted by the left map in the diagram (3.1), χ is split into $\chi^{\pm}$, which are in turn defined by

$$\begin{aligned}
\chi^{\pm}: \quad & s_1^{\pm} x_1^4 + s_2^{\pm} x_1^3 x_2 + s_3^{\pm} x_1^2 x_2^2 + s_4^{\pm} x_1 x_2^3 + s_5^{\pm} x_1^2 x_3 + s_6^{\pm} x_1 x_2 x_3 + s_7^{\pm} x_2^2 x_3 + s_8^{\pm} x_3^2 = 0\,, \\
\text{where} \quad & s_1^{+} = s_{12} U + s_{13} \mu\,, \quad s_1^{-} = s_{11} \lambda_1 + s_{12} V\,, \\
& s_i^{+} = s_{i2} U \text{ and } s_i^{-} = s_{i1} \lambda_1 + s_{i2} V \text{ for } 2 \le i \le 3\,, \\
& s_i^{+} = s_{i2} U \text{ and } s_i^{-} = s_{i2} V \text{ for } 4 \le i \le 8\,. \qquad (3.110)
\end{aligned}$$

We further map $\chi^{\pm}$, under the bottom map of the diagram (3.1), into their respective Weierstrass forms

$$W_{\chi}^{\pm}: y^2 = x^3 + f_{\chi}^{\pm} x z^4 + g_{\chi}^{\pm} z^6\,. \qquad (3.111)$$

We can show that $W_{\chi}^{\pm}$ obtained in this way is different compared to $W_{\chi}^{'\pm}$ obtained by taking the other route in diagram (3.1), namely start from χ on the top left corner of the diagram, first map χ into its Weierstrass form W_{χ} using the map on top of (3.1), and then use the map on the right of (3.1) to split W_{χ} into

$$W_{\chi}^{'\pm}: y^2 = x^3 + f_{\chi}^{'\pm} x z^4 + g_{\chi}^{'\pm} z^6\,. \qquad (3.112)$$

Indeed,

$$W_\chi^+ \neq W_\chi^{\prime +}, \qquad W_\chi^- \neq W_\chi^{\prime -}. \tag{3.113}$$

To be precise,

$$f_\chi^\pm = f_\chi^{\prime \pm} \quad \text{but} \quad g_\chi^\pm \neq g_\chi^{\prime \pm}, \quad g_\chi^+ - g_\chi^{\prime +} = \frac{2}{3} U^6 s_{13} s_{31} s_{72}^2 s_{82}^2, \quad g_\chi^- - g_\chi^{\prime -} = \frac{2}{3} V^6 s_{13} s_{31} s_{72}^2 s_{82}^2. \tag{3.114}$$

Type	Group	a_1	a_2	a_3	a_4	a_6	Δ
I_0	$\{\mathrm{e}\}$	0	0	0	0	0	0
I_1	$\{\mathrm{e}\}$	0	0	1	1	1	1
I_2	SU(2)	0	0	1	1	2	2
I_3	SU(3)	0	1	1	2	3	3
$I_{2k}, k \geq 2$	Sp(k)	0	0	k	k	$2k$	$2k$
$I_{2k+1}, k \geq 1$	Sp(k)	0	0	$k+1$	$k+1$	$2k+1$	$2k+1$
$I_n, n \geq 4$	SU(n)	0	1	$\left\lfloor \frac{n}{2} \right\rfloor$	$\left\lceil \frac{n+1}{2} \right\rceil$	n	n
II	$\{\mathrm{e}\}$	1	1	1	1	1	2
III	SU(2)	1	1	1	1	2	3
IV	Sp(1)	1	1	1	2	2	4
IV	SU(3)	1	1	1	2	3	4
I_0^*	G_2	1	1	2	2	3	6
I_0^*	Spin(7)	1	1	2	2	4	6
I_0^*	Spin(8)	1	1	2	2	4	6
I_1^*	Spin(9)	1	1	2	3	4	7
I_1^*	Spin(10)	1	1	2	3	5	7
I_2^*	Spin(11)	1	1	3	3	5	8
I_2^*	Spin(12)	1	1	3	3	5	8
$I_{2k-3}^*, k \geq 3$	SO($4k+1$)	1	1	k	$k+1$	$2k$	$2k+3$
$I_{2k-3}^*, k \geq 3$	SO($4k+2$)	1	1	k	$k+1$	$2k+1$	$2k+3$
$I_{2k-2}^*, k \geq 3$	SO($4k+3$)	1	1	$k+1$	$k+1$	$2k+1$	$2k+4$
$I_{2k-2}^*, k \geq 3$	SO($4k+4$)	1	1	$k+1$	$k+1$	$2k+1$	$2k+4$
IV^*	F_4	1	2	2	3	4	8
IV^*	E_6	1	2	2	3	5	8
III^*	E_7	1	2	3	3	5	9
II^*	E_8	1	2	3	4	5	10
non-min	-	1	2	3	4	6	12

Table 3.2: Results from Tate's algorithm.

ray	facet	constraint
ρ_{λ_1}	$m_4 = -1$	$s_{\lambda_1} = s_i^3 U + s_i^6 \mu$
ρ_μ	$m_4 = m_3 - 1$	$s_\mu = s_i^1 \lambda_1 + s_i^3 V$
ρ_{λ_2}	$m_4 = 1$	$s_{\lambda_2} = s_i^2 U^2 + s_i^5 UV + s_i^8 V^2$

Table 3.3: The correspondence between the rays of $\Delta_{dP_2}^\circ$ and the facets of Δ_{dP_2}. The last column displays the global sections that embed the associated divisor into $\mathbb{P}^1$ and $\mathbb{P}^2$, respectively. The coefficients on the right-hand side refer to equation (3.34).

Chapter 4

Conclusion

Finally, we summarize the main results of this dissertation.

In chapter 1 of this dissertation, I proved finiteness of a region of the string landscape in Type IIB compactifications. I showed, using a mathematical proof, that Type IIB theories when compactified on elliptically fibered Calabi-Yau threefolds $\pi : X \to B$ whose base B satisfy a few easily-checked conditions (summarized in chapter 1 of this dissertation), only give rise to a finite number of four-dimensional $N = 1$ supergravity theories, and that these theories only have finitely many gauge sectors with finitely many chiral spectra. Some examples of the bases B includes the del Pezzo surfaces dP_n for $n = 0, 1, ..., 8$, and the Hirzebruch surfaces $\mathbb{F}_0 = \mathbb{P}^1 \times \mathbb{P}^1, \mathbb{F}_1 = dP_1, \mathbb{F}_2$. My proof also allowed us to derive the explicit and computable bounds on all flux quanta and on the number of D5-branes. These bounds only depends on the topology of the base B and are independent on the continuous moduli of the compactification, in particular the Kähler moduli, as long as the supergravity approximation is valid.

In chapter 2 of this dissertation, I constructed general F-theory compactifications with U(1) × U(1) × U(1) abelian gauge symmetry. I showed that in the case with three U(1) factors, the general elliptic fiber is a complete intersection of two quadrics in $\mathbb{P}^3$, and

the general elliptic fiber in the fully resolved elliptic fibration is embedded as the generic Calabi-Yau complete intersection into $Bl_3\mathbb{P}^3$, the blow-up of $\mathbb{P}^3$ at three generic points. This eventually leads to our analysis of representations of massless matter at codimension two singularities of these compactifications. Interestingly, we obtained a tri-fundamental representation which is unexpected from perturbative Type II compactifications, further illustrating the power of F-theory.

In chapter 3 of this dissertation, I study abelian gauge symmetries in the duality between F-theory and $E_8 \times E_8$ heterotic string theory. We found that in general, there are three ways in which U(1)-s can arise on the heterotic side: the case where the heterotic theory admits vector bundles with $S(U(1) \times U(m))$ structure group, the case where the heterotic theory admits vector bundles with $SU(m) \times \mathbb{Z}_n$ structure group, as well as the case where the heterotic theory admits vector bundles with structure groups having a centralizer in E_8 which contains a U(1) factor. Another important achievement was my discovery of the non-commutativity of the semi-stable degeneration map which splits a K3 surface into two half K3 surfaces, and the map to Weierstrass form, which was not previously known in the literature.

Bibliography

[1] S. Kachru, R. Kallosh, A. D. Linde, and S. P. Trivedi, *De Sitter Vacua in String Theory*, Phys. Rev. **D68** (2003) 046005, [hep-th/0301240].

[2] V. Balasubramanian, P. Berglund, J. P. Conlon, and F. Quevedo, *Systematics of Moduli Stabilisation in Calabi-Yau Flux Compactifications*, JHEP **0503** (2005) 007, [hep-th/0502058].

[3] J. Louis, M. Rummel, R. Valandro, and A. Westphal, *Building an explicit de Sitter*, JHEP **1210** (2012) 163, [arXiv:1208.3208].

[4] D. Martinez-Pedrera, D. Mehta, M. Rummel, and A. Westphal, *Finding all flux vacua in an explicit example*, JHEP **1306** (2013) 110, [arXiv:1212.4530].

[5] M. Cicoli, D. Klevers, S. Krippendorf, C. Mayrhofer, F. Quevedo, et. al., *Explicit de Sitter Flux Vacua for Global String Models with Chiral Matter*, arXiv:1312.0014.

[6] R. Bousso and J. Polchinski, *Quantization of Four Form Fluxes and Dynamical Neutralization of the Cosmological Constant*, JHEP **0006** (2000) 006, [hep-th/0004134].

[7] F. Denef and M. R. Douglas, *Computational Complexity of the Landscape. I*, Annals Phys. **322** (2007) 1096–1142, [hep-th/0602072].

[8] M. Cvetič, I. Garcia-Etxebarria, and J. Halverson, *On the Computation of Non-Perturbative Effective Potentials in the String Theory Landscape – Iib/F-Theory Perspective*, arXiv:1009.5386.

[9] F. Denef and M. R. Douglas, *Distributions of flux vacua*, JHEP **0405** (2004) 072, [hep-th/0404116].

[10] F. Denef and M. R. Douglas, *Distributions of nonsupersymmetric flux vacua*, JHEP **0503** (2005) 061, [hep-th/0411183].

[11] R. Donagi and M. Wijnholt, *Model Building with F-Theory*, arXiv:0802.2969.

[12] C. Beasley, J. J. Heckman, and C. Vafa, *Guts and Exceptional Branes in F-Theory - I*, JHEP **01** (2009) 058, [arXiv:0802.3391].

[13] C. Vafa, *The String Landscape and the Swampland*, hep-th/0509212.

[14] A. M. Uranga, *D-Brane Probes, Rr Tadpole Cancellation and K-Theory Charge*, Nucl. Phys. **B598** (2001) 225–246, [hep-th/0011048].

[15] G. Aldazabal, S. Franco, L. E. Ibanez, R. Rabadan, and A. M. Uranga, *D = 4 chiral string compactifications from intersecting branes*, J. Math. Phys. **42** (2001) 3103–3126, [hep-th/0011073].

[16] L. E. Ibanez, F. Marchesano, and R. Rabadan, *Getting just the standard model at intersecting branes*, JHEP **0111** (2001) 002, [hep-th/0105155].

[17] M. Cvetič, G. Shiu, and A. M. Uranga, *Chiral four-dimensional N=1 supersymmetric type 2A orientifolds from intersecting D6 branes*, Nucl.Phys. **B615** (2001) 3–32, [hep-th/0107166].

[18] J. Halverson, *Anomaly Nucleation Constrains SU(2) Gauge Theories*, arXiv:1310.1091.

[19] M. Cvetič, T. W. Grimm, and D. Klevers, *Anomaly Cancellation And Abelian Gauge Symmetries In F-theory*, arXiv:1210.6034.

[20] W. Lerche, D. Lüst, and A. Schellekens, *Chiral Four-Dimensional Heterotic Strings from Selfdual Lattices*, Nucl.Phys. **B287** (1987) 477.

[21] F. Gmeiner, R. Blumenhagen, G. Honecker, D. Lust, and T. Weigand, *One in a billion: MSSM-like D-brane statistics*, JHEP **0601** (2006) 004, [hep-th/0510170].

[22] S. H. Katz and C. Vafa, *Matter from Geometry*, Nucl.Phys. **B497** (1997) 146–154, [hep-th/9606086].

[23] O. DeWolfe and B. Zwiebach, *String Junctions for Arbitrary Lie Algebra Representations*, Nucl. Phys. **B541** (1999) 509–565, [hep-th/9804210].

[24] A. Grassi and D. R. Morrison, *Group representations and the Euler characteristic of elliptically fibered Calabi-Yau threefolds*, math/0005196.

[25] A. Grassi and D. R. Morrison, *Anomalies and the Euler Characteristic of Elliptic Calabi-Yau Threefolds*, arXiv:1109.0042.

[26] D. R. Morrison and W. Taylor, *Matter and Singularities*, JHEP **1201** (2012) 022, [arXiv:1106.3563].

[27] A. Grassi, J. Halverson, and J. L. Shaneson, *Matter from Geometry without Resolution*, arXiv:1306.1832.

[28] H. Hayashi, C. Lawrie, D. R. Morrison, and S. Schafer-Nameki, *Box Graphs and Singular Fibers*, arXiv:1402.2653.

[29] A. Grassi, J. Halverson, and J. L. Shaneson, *Non-Abelian Gauge Symmetry and the Higgs Mechanism in F-theory*, arXiv:1402.5962.

[30] M. Esole, S.-H. Shao, and S.-T. Yau, *Singularities and Gauge Theory Phases*, arXiv:1402.6331.

[31] D. R. Morrison and D. S. Park, *F-Theory and the Mordell-Weil Group of Elliptically-Fibered Calabi-Yau Threefolds*, JHEP **1210** (2012) 128, [arXiv:1208.2695].

[32] J. Borchmann, C. Mayrhofer, E. Palti, and T. Weigand, *Elliptic fibrations for SU(5) x U(1) x U(1) F-theory vacua*, Phys.Rev. **D88** (2013) 046005, [arXiv:1303.5054].

[33] M. Cvetič, D. Klevers, and H. Piragua, *F-Theory Compactifications with Multiple U(1)-Factors: Constructing Elliptic Fibrations with Rational Sections*, JHEP **1306** (2013) 067, [arXiv:1303.6970].

[34] T. W. Grimm, A. Kapfer, and J. Keitel, *Effective action of 6D F-Theory with U(1) factors: Rational sections make Chern-Simons terms jump*, JHEP **1307** (2013) 115, [arXiv:1305.1929].

[35] V. Braun, T. W. Grimm, and J. Keitel, *Geometric Engineering in Toric F-Theory and GUTs with U(1) Gauge Factors*, arXiv:1306.0577.

[36] M. Cvetič, A. Grassi, D. Klevers, and H. Piragua, *Chiral Four-Dimensional F-Theory Compactifications With SU(5) and Multiple U(1)-Factors*, arXiv:1306.3987.

[37] J. Borchmann, C. Mayrhofer, E. Palti, and T. Weigand, *SU(5) Tops with Multiple U(1)s in F-theory*, arXiv:1307.2902.

[38] M. Cvetič, D. Klevers, and H. Piragua, *F-Theory Compactifications with Multiple U(1)-Factors: Addendum*, arXiv:1307.6425.

[39] M. Cvetič, D. Klevers, H. Piragua, and P. Song, *Elliptic Fibrations with Rank Three Mordell-Weil Group: F-theory with U(1) x U(1) x U(1) Gauge Symmetry*, arXiv:1310.0463.

[40] M. R. Douglas and W. Taylor, *The Landscape of Intersecting Brane Models*, JHEP **0701** (2007) 031, [hep-th/0606109].

[41] R. Blumenhagen, M. Cvetič, P. Langacker, and G. Shiu, *Toward realistic intersecting D-brane models*, Ann.Rev.Nucl.Part.Sci. **55** (2005) 71–139, [hep-th/0502005].

[42] R. Blumenhagen, B. Kors, D. Lust, and S. Stieberger, *Four-dimensional String Compactifications with D-Branes, Orientifolds and Fluxes*, Phys.Rept. **445** (2007) 1–193, [hep-th/0610327].

[43] M. Cvetič and J. Halverson, *TASI Lectures: Particle Physics from Perturbative and Non-perturbative Effects in D-braneworlds*, arXiv:1101.2907.

[44] R. Blumenhagen, F. Gmeiner, G. Honecker, D. Lust, and T. Weigand, *The Statistics of supersymmetric D-brane models*, Nucl.Phys. **B713** (2005) 83–135, [hep-th/0411173].

[45] M. Cvetič, G. Shiu, and A. M. Uranga, *Three family supersymmetric standard - like models from intersecting brane worlds*, Phys.Rev.Lett. **87** (2001) 201801, [hep-th/0107143].

[46] M. Cvetič, T. Li, and T. Liu, *Supersymmetric patiSalam models from intersecting D6-branes: A Road to the standard model*, Nucl.Phys. **B698** (2004) 163–201, [hep-th/0403061].

[47] L. B. Anderson and W. Taylor, *Geometric constraints in dual F-theory and heterotic string compactifications*, to appear.

[48] R. Blumenhagen, G. Honecker, and T. Weigand, *Supersymmetric (Non-)Abelian Bundles in the Type I and SO(32) Heterotic String*, JHEP **0508** (2005) 009, [hep-th/0507041].

[49] C. Bachas, *A Way to Break Supersymmetry*, hep-th/9503030.

[50] D. Honda and T. Okuda, *Exact Results for Boundaries and Domain Walls in 2D Supersymmetric Theories*, arXiv:1308.2217.

[51] S. Sugishita and S. Terashima, *Exact Results in Supersymmetric Field Theories on Manifolds with Boundaries*, JHEP **1311** (2013) 021, [arXiv:1308.1973].

[52] K. Hori and M. Romo, *Exact Results in Two-Dimensional (2,2) Supersymmetric Gauge Theories with Boundary*, arXiv:1308.2438.

[53] J. Halverson, H. Jockers, J. M. Lapan, and D. R. Morrison, *Perturbative Corrections to Kähler Moduli Spaces*, arXiv:1308.2157.

[54] R. Friedman, J. Morgan, and E. Witten, *Vector bundles and F theory*, Commun.Math.Phys. **187** (1997) 679–743, [hep-th/9701162].

[55] D. R. Morrison and C. Vafa, *Compactifications of F theory on Calabi-Yau threefolds. 2.*, Nucl.Phys. **B476** (1996) 437–469, [hep-th/9603161].

[56] M.-X. Huang, A. Klemm, and M. Poretschkin, *Refined stable pair invariants for E-, M- and $[p,q]$-strings*, JHEP **1311** (2013) 112, [arXiv:1308.0619].

[57] M.-x. Huang, A. Klemm, J. Reuter, and M. Schiereck, *Quantum geometry of del Pezzo surfaces in the Nekrasov-Shatashvili limit*, arXiv:1401.4723.

[58] M. Demazure, H. C. Pinkham, and B. Teissier, *Séminaire sur les singularités des surfaces*, Lecture Notes in Mathematics, Berlin Springer Verlag **777** (1980).

[59] R. Donagi, Y.-H. He, B. A. Ovrut, and R. Reinbacher, *The Particle spectrum of heterotic compactifications*, JHEP **0412** (2004) 054, [hep-th/0405014].

[60] A. Klemm, J. Manschot, and T. Wotschke, *Quantum Geometry of Elliptic Calabi-Yau Manifolds*, arXiv:1205.1795.

[61] W. Stein et. al., Sage Mathematics Software (Version 6.0). The Sage Development Team, 2013. http://www.sagemath.org.

[62] F. Gmeiner and G. Honecker, *Mapping an Island in the Landscape*, JHEP **0709** (2007) 128, [arXiv:0708.2285].

[63] G. Honecker, M. Ripka, and W. Staessens, *The Importance of Being Rigid: D6-Brane Model Building on T^6/Z_2xZ_6' with Discrete Torsion*, Nucl.Phys. **B868** (2013) 156–222, [arXiv:1209.3010].

[64] T. W. Grimm, D. Klevers, and M. Poretschkin, *Fluxes and Warping for Gauge Couplings in F-theory*, JHEP **1301** (2013) 023, [arXiv:1202.0285].

[65] I. Garcia-Etxebarria, H. Hayashi, R. Savelli, and G. Shiu, *On quantum corrected Kahler potentials in F-theory*, JHEP **1303** (2013) 005, [arXiv:1212.4831].

[66] T. W. Grimm, R. Savelli, and M. Weissenbacher, *On α'-corrections in N=1 F-theory compactifications*, Phys.Lett. **B725** (2013) 431–436, [arXiv:1303.3317].

[67] T. W. Grimm, J. Keitel, R. Savelli, and M. Weissenbacher, *From M-theory higher curvature terms to α'-corrections in F-theory*, arXiv:1312.1376.

[68] C. Vafa, "Evidence for F theory," Nucl.Phys. **B469** (1996) 403–418, arXiv:hep-th/9602022 [hep-th].

[69] D. R. Morrison and C. Vafa, "Compactifications of F theory on Calabi-Yau threefolds. 1," Nucl.Phys. **B473** (1996) 74–92, arXiv:hep-th/9602114 [hep-th].

[70] D. R. Morrison and C. Vafa, "Compactifications of F theory on Calabi-Yau threefolds. 2.," Nucl.Phys. **B476** (1996) 437–469, arXiv:hep-th/9603161 [hep-th].

[71] R. Donagi and M. Wijnholt, "Model Building with F-Theory," arXiv:0802.2969 [hep-th].

[72] C. Beasley, J. J. Heckman, and C. Vafa, "GUTs and Exceptional Branes in F-theory - I," JHEP **01** (2009) 058, arXiv:0802.3391 [hep-th].

[73] C. Beasley, J. J. Heckman, and C. Vafa, "GUTs and Exceptional Branes in F-theory - II: Experimental Predictions," JHEP **01** (2009) 059, arXiv:0806.0102 [hep-th].

[74] R. Donagi and M. Wijnholt, "Breaking GUT Groups in F-Theory," Adv.Theor.Math.Phys. **15** (2011) 1523–1604, arXiv:0808.2223 [hep-th].

[75] R. Blumenhagen, T. W. Grimm, B. Jurke, and T. Weigand, "Global F-theory GUTs," Nucl.Phys. **B829** (2010) 325–369, arXiv:0908.1784 [hep-th].

[76] J. Marsano, N. Saulina, and S. Schafer-Nameki, "Compact F-theory GUTs with U(1) (PQ)," JHEP **1004** (2010) 095, arXiv:0912.0272 [hep-th].

[77] C.-M. Chen, J. Knapp, M. Kreuzer, and C. Mayrhofer, "Global SO(10) F-theory GUTs," JHEP **1010** (2010) 057, arXiv:1005.5735 [hep-th].

[78] T. W. Grimm, S. Krause, and T. Weigand, "F-Theory GUT Vacua on Compact Calabi-Yau Fourfolds," JHEP **1007** (2010) 037, arXiv:0912.3524 [hep-th].

[79] J. Knapp and M. Kreuzer, "Toric Methods in F-theory Model Building," Adv.High Energy Phys. **2011** (2011) 513436, arXiv:1103.3358 [hep-th].

[80] J. J. Heckman, "Particle Physics Implications of F-theory," Ann.Rev.Nucl.Part.Sci. **60** (2010) 237–265, arXiv:1001.0577 [hep-th].

[81] T. Weigand, "Lectures on F-theory compactifications and model building," Class.Quant.Grav. **27** (2010) 214004, arXiv:1009.3497 [hep-th].

[82] A. Maharana and E. Palti, "Models of Particle Physics from Type IIB String Theory and F-theory: A Review," arXiv:1212.0555 [hep-th].

[83] M. Bershadsky, K. A. Intriligator, S. Kachru, D. R. Morrison, V. Sadov, et al., "Geometric singularities and enhanced gauge symmetries," Nucl.Phys. **B481** (1996) 215–252, arXiv:hep-th/9605200 [hep-th].

[84] K. Kodaira, "On compact analytic surfaces: Ii," The Annals of Mathematics **77** no. 3, (1963) 563–626.

[85] J. Tate, "Algorithm for determining the type of a singular fiber in an elliptic pencil," Modular functions of one variable IV (1975) 33–52.

[86] P. Candelas and A. Font, "Duality between the webs of heterotic and type II vacua," Nucl.Phys. **B511** (1998) 295–325, arXiv:hep-th/9603170 [hep-th].

[87] P. Candelas, E. Perevalov, and G. Rajesh, "Toric geometry and enhanced gauge symmetry of F theory / heterotic vacua," Nucl.Phys. **B507** (1997) 445–474, arXiv:hep-th/9704097 [hep-th].

[88] V. Bouchard and H. Skarke, "Affine Kac-Moody algebras, CHL strings and the classification of tops," Adv.Theor.Math.Phys. **7** (2003) 205–232, arXiv:hep-th/0303218 [hep-th].

[89] S. H. Katz and C. Vafa, "Matter from geometry," Nucl.Phys. **B497** (1997) 146–154, arXiv:hep-th/9606086 [hep-th].

[90] M. Esole and S.-T. Yau, "Small resolutions of SU(5)-models in F-theory," arXiv:1107.0733 [hep-th].

[91] J. Marsano and S. Schafer-Nameki, "Yukawas, G-flux, and Spectral Covers from Resolved Calabi-Yau's," JHEP **1111** (2011) 098, arXiv:1108.1794 [hep-th].

[92] C. Lawrie and S. Schafer-Nameki, "The Tate Form on Steroids: Resolution and Higher Codimension Fibers," arXiv:1212.2949 [hep-th].

[93] A. Grassi, J. Halverson, and J. L. Shaneson, "Matter From Geometry Without Resolution," arXiv:1306.1832 [hep-th].

[94] M.-x. Huang, A. Klemm, and M. Poretschkin, "Refined stable pair invariants for E-, M- and [p,q]-strings," arXiv:1308.0619 [hep-th].

[95] P. S. Aspinwall and D. R. Morrison, "Nonsimply connected gauge groups and rational points on elliptic curves," JHEP **9807** (1998) 012, arXiv:hep-th/9805206 [hep-th].

[96] P. S. Aspinwall, S. H. Katz, and D. R. Morrison, "Lie groups, Calabi-Yau threefolds, and F theory," Adv.Theor.Math.Phys. **4** (2000) 95–126, arXiv:hep-th/0002012 [hep-th].

[97] A. Néron, "Modeles minimaux des variétés abéliennes sur les corps locaux et globaux," Publications Mathématiques de L'IHÉS **21** no. 1, (1964) 5–125.

[98] T. Shioda, "On the Mordell-Weil lattices," Comment. Math. Univ. St. Paul **39** no. 2, (1990) 211–240.

[99] T. Shioda, "Mordell-Weil lattices and Galois representation. I," Proc. Japan Acad. **65A** (1989) 268–271.

[100] R. Wazir, "Arithmetic on Elliptic Threefolds," arXiv:math/0112259 [math.NT].

[101] J. H. Silverman, The arithmetic of elliptic curves, vol. 106. Springer, 2009.

[102] D. R. Morrison and D. S. Park, "F-Theory and the Mordell-Weil Group of Elliptically-Fibered Calabi-Yau Threefolds," JHEP **1210** (2012) 128, arXiv:1208.2695 [hep-th].

[103] E. P. J. Borchmann, C. Mayrhofer and T. Weigand, "Elliptic fibrations for SU(5) x U(1) x U(1) F-theory vacua," arXiv:1303.5054 [hep-th].

[104] M. Cvetic, D. Klevers, and H. Piragua, "F-Theory Compactifications with Multiple U(1)-Factors: Constructing Elliptic Fibrations with Rational Sections," arXiv:1303.6970 [hep-th].

[105] M. Cvetic, D. Klevers, and H. Piragua, "F-Theory Compactifications with Multiple U(1)-Factors: Addendum," arXiv:1307.6425 [hep-th].

[106] M. Cvetič, A. Grassi, D. Klevers, and H. Piragua, "Chiral Four-Dimensional F-Theory Compactifications With SU(5) and Multiple U(1)-Factors," arXiv:1306.3987 [hep-th].

[107] J. Borchmann, C. Mayrhofer, E. Palti, and T. Weigand, "SU(5) Tops with Multiple U(1)s in F-theory," arXiv:1307.2902 [hep-th].

[108] R. Donagi and M. Wijnholt, "Higgs Bundles and UV Completion in F-Theory," arXiv:0904.1218 [hep-th].

[109] J. Marsano, N. Saulina, and S. Schafer-Nameki, "Monodromies, Fluxes, and Compact Three-Generation F-theory GUTs," JHEP **0908** (2009) 046, arXiv:0906.4672 [hep-th].

[110] E. Dudas and E. Palti, "Froggatt-Nielsen models from E(8) in F-theory GUTs," JHEP **1001** (2010) 127, arXiv:0912.0853 [hep-th].

[111] M. Cvetic, I. Garcia-Etxebarria, and J. Halverson, "Global F-theory Models: Instantons and Gauge Dynamics," JHEP **1101** (2011) 073, arXiv:1003.5337 [hep-th].

[112] E. Dudas and E. Palti, "On hypercharge flux and exotics in F-theory GUTs," JHEP **1009** (2010) 013, arXiv:1007.1297 [hep-ph].

[113] M. J. Dolan, J. Marsano, N. Saulina, and S. Schafer-Nameki, "F-theory GUTs with U(1) Symmetries: Generalities and Survey," Phys.Rev. **D84** (2011) 066008, arXiv:1102.0290 [hep-th].

[114] J. Marsano, H. Clemens, T. Pantev, S. Raby, and H.-H. Tseng, "A Global SU(5) F-theory model with Wilson line breaking," JHEP **1301** (2013) 150, arXiv:1206.6132 [hep-th].

[115] C. Mayrhofer, E. Palti, and T. Weigand, "U(1) symmetries in F-theory GUTs with multiple sections," arXiv:1211.6742 [hep-th].

[116] T. W. Grimm and T. Weigand, "On Abelian Gauge Symmetries and Proton Decay in Global F-theory GUTs," Phys.Rev. **D82** (2010) 086009, arXiv:1006.0226 [hep-th].

[117] A. P. Braun, A. Collinucci, and R. Valandro, "G-flux in F-theory and algebraic cycles," Nucl.Phys. **B856** (2012) 129–179, arXiv:1107.5337 [hep-th].

[118] S. Krause, C. Mayrhofer, and T. Weigand, "G_4 flux, chiral matter and singularity resolution in F-theory compactifications," Nucl.Phys. **B858** (2012) 1–47, arXiv:1109.3454 [hep-th].

[119] T. W. Grimm and H. Hayashi, "F-theory fluxes, Chirality and Chern-Simons theories," JHEP **1203** (2012) 027, arXiv:1111.1232 [hep-th].

[120] M. Cvetic, T. W. Grimm, and D. Klevers, "Anomaly Cancellation And Abelian Gauge Symmetries In F-theory," JHEP **1302** (2013) 101, arXiv:1210.6034 [hep-th].

[121] V. Braun, T. W. Grimm, and J. Keitel, "New Global F-theory GUTs with U(1) symmetries," arXiv:1302.1854 [hep-th].

[122] A. Grassi and V. Perduca, "Weierstrass models of elliptic toric K3 hypersurfaces and symplectic cuts," arXiv:1201.0930 [math.AG].

[123] V. Braun, T. W. Grimm, and J. Keitel, "Geometric Engineering in Toric F-Theory and GUTs with U(1) Gauge Factors," arXiv:1306.0577 [hep-th].

[124] J. W. S. Cassels, LMSST: 24 Lectures on Elliptic Curves, vol. 24. Cambridge University Press, 1991.

[125] I. Connell, "Elliptic curve handbook," Preprint (1996) .

[126] T. W. Grimm and R. Savelli, "Gravitational Instantons and Fluxes from M/F-theory on Calabi-Yau fourfolds," Phys.Rev. **D85** (2012) 026003, arXiv:1109.3191 [hep-th].

[127] F. Bonetti and T. W. Grimm, "Six-dimensional (1,0) effective action of F-theory via M-theory on Calabi-Yau threefolds," JHEP **1205** (2012) 019, arXiv:1112.1082 [hep-th].

[128] D. S. Park, "Anomaly Equations and Intersection Theory," JHEP **1201** (2012) 093, arXiv:1111.2351 [hep-th].

[129] T. W. Grimm, A. Kapfer, and J. Keitel, "Effective action of 6D F-Theory with U(1) factors: Rational sections make Chern-Simons terms jump," arXiv:1305.1929 [hep-th].

[130] J. Erler, "Anomaly cancellation in six-dimensions," J.Math.Phys. **35** (1994) 1819–1833, arXiv:hep-th/9304104 [hep-th].

[131] G. Honecker, "Massive U(1)s and heterotic five-branes on K3," Nucl.Phys. **B748** (2006) 126–148, arXiv:hep-th/0602101 [hep-th].

[132] D. A. Cox and S. Katz, Mirror symmetry and algebraic geometry, vol. 68. AMS Bookstore, 1999.

[133] M. B. Green, J. H. Schwarz, and E. Witten, Superstring theory: volume 2, Loop amplitudes, anomalies and phenomenology. Cambridge university press, 2012.

[134] J. Polchinski, String Theory, vol. 1& 2. Cambridge University Press, 1998.

[135] C. Vafa, "Evidence for F theory," Nucl.Phys. **B469** (1996) 403–418, arXiv:hep-th/9602022 [hep-th].

[136] D. R. Morrison and C. Vafa, "Compactifications of F theory on Calabi-Yau threefolds. 2.," Nucl.Phys. **B476** (1996) 437–469, arXiv:hep-th/9603161 [hep-th].

[137] D. R. Morrison and C. Vafa, "Compactifications of F theory on Calabi-Yau threefolds. 1," Nucl.Phys. **B473** (1996) 74–92, arXiv:hep-th/9602114 [hep-th].

[138] P. S. Aspinwall and D. R. Morrison, "Point - like instantons on K3 orbifolds," Nucl.Phys. **B503** (1997) 533–564, arXiv:hep-th/9705104 [hep-th].

[139] R. Friedman, J. Morgan, and E. Witten, "Vector bundles and F theory," Commun. Math. Phys. **187** (1997) 679–743, arXiv:hep-th/9701162 [hep-th].

[140] R. Y. Donagi, "Principal bundles on elliptic fibrations," Asian J. Math. **1** (1997) 214–223, arXiv:alg-geom/9702002 [alg-geom].

[141] B. Andreas, "N=1 heterotic / F theory duality," Fortsch. Phys. **47** (1999) 587–642, arXiv:hep-th/9808159 [hep-th].

[142] P. Candelas and A. Font, "Duality between the webs of heterotic and type II vacua," Nucl.Phys. **B511** (1998) 295–325, arXiv:hep-th/9603170 [hep-th].

[143] P. Berglund and P. Mayr, "Heterotic string / F theory duality from mirror symmetry," Adv. Theor. Math. Phys. **2** (1999) 1307–1372, arXiv:hep-th/9811217 [hep-th].

[144] L. B. Anderson and W. Taylor, "Geometric constraints in dual F-theory and heterotic string compactifications," JHEP **08** (2014) 025, arXiv:1405.2074 [hep-th].

[145] H. Hayashi, R. Tatar, Y. Toda, T. Watari, and M. Yamazaki, "New Aspects of Heterotic–F Theory Duality," Nucl.Phys. **B806** (2009) 224–299, arXiv:0805.1057 [hep-th].

[146] T. W. Grimm, T.-W. Ha, A. Klemm, and D. Klevers, "Computing Brane and Flux Superpotentials in F-theory Compactifications," JHEP **1004** (2010) 015, arXiv:0909.2025 [hep-th].

[147] T. W. Grimm, T.-W. Ha, A. Klemm, and D. Klevers, "Five-Brane Superpotentials and Heterotic / F-theory Duality," Nucl. Phys. **B838** (2010) 458–491, arXiv:0912.3250 [hep-th].

[148] H. Jockers, P. Mayr, and J. Walcher, "On N=1 4d Effective Couplings for F-theory and Heterotic Vacua," Adv. Theor. Math. Phys. **14** (2010) 1433–1514, arXiv:0912.3265 [hep-th].

[149] M. Cvetic, I. Garcia Etxebarria, and J. Halverson, "Three Looks at Instantons in F-theory – New Insights from Anomaly Inflow, String Junctions and Heterotic Duality," JHEP **11** (2011) 101, arXiv:1107.2388 [hep-th].

[150] M. Cvetic, R. Donagi, J. Halverson, and J. Marsano, "On Seven-Brane Dependent Instanton Prefactors in F-theory," JHEP **11** (2012) 004, arXiv:1209.4906 [hep-th].

[151] G. Aldazabal, A. Font, L. E. Ibanez, and A. M. Uranga, "New branches of string compactifications and their F theory duals," Nucl. Phys. **B492** (1997) 119–151, arXiv:hep-th/9607121 [hep-th].

[152] A. Klemm, P. Mayr, and C. Vafa, "BPS states of exceptional noncritical strings," arXiv:hep-th/9607139 [hep-th].

[153] A. Grassi, "Toric Weierstrass models," I.P.M.U. 2010 talk (2010) http://www.ipmu.jp/node/552.

[154] D. R. Morrison and D. S. Park, "F-Theory and the Mordell-Weil Group of Elliptically-Fibered Calabi-Yau Threefolds," JHEP **1210** (2012) 128, arXiv:1208.2695 [hep-th].

[155] E. P. J. Borchmann, C. Mayrhofer and T. Weigand, "Elliptic fibrations for SU(5) x U(1) x U(1) F-theory vacua," arXiv:1303.5054 [hep-th].

[156] M. Cvetič, D. Klevers, and H. Piragua, "F-Theory Compactifications with Multiple U(1)-Factors: Constructing Elliptic Fibrations with Rational Sections," arXiv:1303.6970 [hep-th].

[157] M. Cvetič, A. Grassi, D. Klevers, and H. Piragua, "Chiral Four-Dimensional F-Theory Compactifications With SU(5) and Multiple U(1)-Factors," arXiv:1306.3987 [hep-th].

[158] J. Borchmann, C. Mayrhofer, E. Palti, and T. Weigand, "SU(5) Tops with Multiple U(1)s in F-theory," arXiv:1307.2902 [hep-th].

[159] M. Cvetič, D. Klevers, and H. Piragua, "F-Theory Compactifications with Multiple U(1)-Factors: Addendum," JHEP **1312** (2013) 056, arXiv:1307.6425 [hep-th].

[160] M. Cvetič, D. Klevers, H. Piragua, and P. Song, "Elliptic fibrations with rank three Mordell-Weil group: F-theory with U(1) x U(1) x U(1) gauge symmetry," JHEP **1403** (2014) 021, arXiv:1310.0463 [hep-th].

[161] V. Braun, T. W. Grimm, and J. Keitel, "Complete Intersection Fibers in F-Theory," JHEP **03** (2015) 125, arXiv:1411.2615 [hep-th].

[162] D. Klevers, D. K. Mayorga Pena, P.-K. Oehlmann, H. Piragua, and J. Reuter, "F-Theory on all Toric Hypersurface Fibrations and its Higgs Branches," JHEP **1501** (2015) 142, arXiv:1408.4808 [hep-th].

[163] M. Cvetič, D. Klevers, H. Piragua, and W. Taylor, "General U(1)xU(1) F-theory Compactifications and Beyond: Geometry of unHiggsings and novel Matter Structure," arXiv:1507.05954 [hep-th].

[164] A. Grassi and V. Perduca, "Weierstrass models of elliptic toric K3 hypersurfaces and symplectic cuts," arXiv:1201.0930 [math.AG].

[165] R. Blumenhagen, G. Honecker, and T. Weigand, "Loop-corrected compactifications of the heterotic string with line bundles," JHEP **06** (2005) 020, arXiv:hep-th/0504232 [hep-th].

[166] J. Marsano, N. Saulina, and S. Schafer-Nameki, "Monodromies, Fluxes, and Compact Three-Generation F-theory GUTs," JHEP **08** (2009) 046, arXiv:0906.4672 [hep-th].

[167] R. Blumenhagen, T. W. Grimm, B. Jurke, and T. Weigand, "Global F-theory GUTs," Nucl.Phys. **B829** (2010) 325–369, arXiv:0908.1784 [hep-th].

[168] T. W. Grimm and T. Weigand, "On Abelian Gauge Symmetries and Proton Decay

in Global F-theory GUTs," Phys.Rev. **D82** (2010) 086009, arXiv:1006.0226 [hep-th].

[169] P. S. Aspinwall and D. R. Morrison, "Nonsimply connected gauge groups and rational points on elliptic curves," JHEP **9807** (1998) 012, arXiv:hep-th/9805206 [hep-th].

[170] K.-S. Choi and H. Hayashi, "U(n) Spectral Covers from Decomposition," JHEP **06** (2012) 009, arXiv:1203.3812 [hep-th].

[171] P. S. Aspinwall, "K3 surfaces and string duality," in Fields, strings and duality. Proceedings, Summer School, Theoretical Advanced Study Institute in Elementary Particle Physics, TASI'96, Boulder, USA, June 2-28, 1996, pp. 421–540. 1996. arXiv:hep-th/9611137 [hep-th].

[172] C. Vafa and E. Witten, "Dual string pairs with N = 1 and N = 2 supersymmetry in four dimensions," Nucl. Phys. Proc. Suppl. **46** (1996) 225–247, arXiv:hep-th/9507050.

[173] M. Bershadsky, K. A. Intriligator, S. Kachru, D. R. Morrison, V. Sadov, et al., "Geometric singularities and enhanced gauge symmetries," Nucl.Phys. **B481** (1996) 215–252, arXiv:hep-th/9605200 [hep-th].

[174] K. Kodaira, "On compact analytic surfaces: Ii," The Annals of Mathematics **77** no. 3, (1963) 563–626.

[175] M. R. Douglas, D. S. Park, and C. Schnell, "The Cremmer-Scherk Mechanism in F-theory Compactifications on K3 Manifolds," JHEP **05** (2014) 135, arXiv:1403.1595 [hep-th].

[176] R. Donagi, "Heterotic / F theory duality: ICMP lecture," in Mathematical physics. Proceedings, 12th International Congress, ICMP'97, Brisbane, Australia, July 13-19, 1997. 1998. arXiv:hep-th/9802093 [hep-th]. http://alice.cern.ch/format/showfull?sysnb=0270001.

[177] M. F. Atiyah, "Vector bundles over an elliptic curve," Proceedings of the London Mathematical Society **s3-7** no. 1, (1957) 414–452, http://plms.oxfordjournals.org/content/s3-7/1/414.full.pdf+html. http://plms.oxfordjournals.org/content/s3-s7/1/414.short.

[178] R. Friedman, J. W. Morgan, and E. Witten, "Vector bundles over elliptic fibrations," arXiv:alg-geom/9709029 [alg-geom].

[179] P. S. Aspinwall, "An analysis of fluxes by duality," arXiv:hep-th/0504036 [hep-th].

[180] J. Tate, "Algorithm for determining the type of a singular fiber in an elliptic pencil," Modular functions of one variable IV (1975) 33–52.

[181] S. Katz, D. R. Morrison, S. Schafer-Nameki, and J. Sully, "Tate's algorithm and F-theory," JHEP **1108** (2011) 094, arXiv:1106.3854 [hep-th].

[182] U. Bruzzo and A. Grassi, "Picard group of hypersurfaces in toric 3-folds," ArXiv e-prints (Nov., 2010) , arXiv:1011.1003 [math.AG].

[183] V. V. Batyrev, "Dual polyhedra and mirror symmetry for Calabi-Yau hypersurfaces in toric varieties," J.Alg.Geom. **3** (1994) 493–545, arXiv:alg-geom/9310003 [alg-geom].

[184] D. R. Morrison and W. Taylor, "Sections, multisections, and U(1) fields in F-theory," arXiv:1404.1527 [hep-th].

[185] R. Donagi, B. A. Ovrut, T. Pantev, and D. Waldram, "Standard models from heterotic M theory," Adv. Theor. Math. Phys. **5** (2002) 93–137, arXiv:hep-th/9912208 [hep-th].

[186] T. Shioda and K. Oguiso, "The Mordell-Weil lattice of a rational elliptic surface," Comment. Math. Univ. St. Paul **40** (1991) 83–99.

[187] C. Mayrhofer, D. R. Morrison, O. Till, and T. Weigand, "Mordell-Weil Torsion and the Global Structure of Gauge Groups in F-theory," arXiv:1405.3656 [hep-th].

[188] A. Grassi and D. R. Morrison, "Anomalies and the Euler characteristic of elliptic Calabi-Yau threefolds," arXiv:1109.0042 [hep-th].